Role of inducible Nitric Oxide Synthase and Histone Deacetylase in Human Lung Epithelial Cell Model of Inflammation and Steroid Insensitivity

DISSERTATION

zur
Erlangung des akademischen Grades des
Doktors der Naturwissenschaften (Dr. rer. nat.)
des Fachbereichs für Biologie
an der Universität Konstanz

vorgelegt von

Dan Liu

Tag der mündlichen Prüfung: 16.11.2009
1. Referent: Prof. Dr. Alexander Buerkle
2. Referent: Prof. Dr. Michael Arand

Konstanzer Online-Publikations-System (KOPS)
URN: http://nbn-resolving.de/urn:nbn:de:bsz:352-opus-108436
URL: http://kops.ub.uni-konstanz.de/volltexte/2010/10843/

Acknowledgments

The present dissertation was performed from May 2006 - September 2009 in the Department of In Vitro Biology 2 (RDP/B2) at Nycomed GmbH, Konstanz. For the encouragement and extensive support that I received during the study I would like to express my sincere gratitude and respect. Especially I thank:

Dr. Christian Hesslinger for offering the attractive project in his lab, for critical surveillance and support of the study, and for the outstanding scientific expertise, for his excellent supervision, the friendly atmosphere and excellent team-work in his group, the helpful advices for the progress of the study, but also for facilitating self-directed work, especially for making it possible for me to finish writing my thesis at home so that I can take care of my small son.
Prof. Dr. Alexander Buerkle for being my Doktorvater, for the continuous evaluation of the study and inspiring ideas for the scientific concept and also for his always-encouraging attitude.
Prof. Dr. Michael Arand for taking the responsibility to be in my thesis committee and giving critical and helpful suggestions for the study.
Prof. Dr. Marcel Leist for being ready to be responsible for my doctoral examination.
Ilka Gruhler, Elisabeth Herrmann, Thomas Reinberg, Waltraud Burckhardt-Boer, Bernd Brun and Bettina Eidmann for the cordially teamwork and always friendly help in the lab and all other colleagues from the biochemistry departments for appreciated help in various concerns.
Dr. Gereon Lauer and Christina Guetze for the great support of Luminex assay.
Dr. Gianluca Quintini for many scientific advises concerning the transfection. Britta Voland for support with PCR and transfection experiments.
Dr. Elisa May for helpful advices and supports for the GR translocation study.
Prof. Dr. Albrecht Wendel, Prof. Dr. Marcel Leist and Prof. Dr. Klaus Schaefer for having organized graduate program IRTG and Dr. Jutta Schlepper-Schaefer and Josefa Ittner for having coordinated the IRTG-program during my dissertation.

I would like to thank all colleagues and friends from work and social life, who altogether multifariously contributed to transform challenging ‘everyday’ work into a pleasant and motivating activity.

I am deeply thankful to my husband Martin for his encouragement.
Finally, I thank my parents, who always supported me on my way and gave me faith in what I was doing.

Some parts of this thesis have been already published:

Liu, D., Lauer, G., Hatzelmann, A., and Hesslinger, C., *"The role of inducible NO synthase (iNOS) in a cell model of steroid resistance in chronic obstructive pulmonary disease"* Abstract and poster presented at annual congress of ERS (2008)

Hesslinger, C., Lehner, M.L., Strub, A., Boer, R., Ulrich, W.-R., Külzer, R., Lauer, G., Liu, D., Spicer, D., Fitzgerald, M., Wollin, L., Weidenbach, A. *"The highly selective iNOS inhibitor BYK402750 exerts potent anti-inflammatory effects in a mouse model of cigarette smoke induced inflammation"* Abstract and poster presented at international NO-meeting 2008 and annual congress of ERS (2008)

TABLE OF CONTENTS

LIST OF ABBREVIATIONS

Abbreviation	Full name
AMT	2-amino-5,6-dihydro-6-methyl-4*H*-1,3-thiazine
AP-1	Activator protein 1
BAL	Bronchoalveolar lavage
BALF	Bronchoalveolar lavage fluid
BH4	(6R)-5,6,7,8-tetrahydro-biopterin
Bp	Base pair
cAMP	Adenosine 3'-5' cyclic monophosphate
CBP	CREB-binding protein
CM	Cytokine mix
COPD	Chronic obstructive pulmonary disease
COX	Cyclo-oxygenase
CRE	cAMP response element
CREB	CRE-binding protein
ELISA	Enzyme- linked immunosorbent assay
FAD	Flavine-adenine dinucleotide
FCS	Fetal calf serum
FMN	Flavine mononucleotide
GC	Glucocorticoids
G-CSF	Granulocyte colony-stimulating factor
GM-CSF	Granulocyte/macrophage colony-stimulating factor
GMP	3`,5`-cyclic guanosine monophosphate
GR	Glucocorticoid receptor
GREs	GC response elements
H_2O_2	Hydrogen peroxide
HAT	Acetyltranferase
HC	Hydrocortisone
HDAC	Histone deacetylase
HDACi	Histone deacetylase inhibtiors
HRP	Horseradish peroxidase
ICS	Inhaled corticosteroids
IFN	Interferon
IKK	Inhibitor of NF- kinase
IL	Interleukin
iNOS	Inducible nitric oxide synthase
IP-10	Interferon-inducible protein-10
IRF-1	IFN regulatory factor 1
L-NAME	NG-nitro-L-arginine methyl ester
L-NMMA	*N*G-monomethyl-L-arginine
LPS	Lipopolysaccharide
MMP-9	Matrix metalloproteinase- 9
NFκB	Nuclear factor κB
NHBE	Normal human bronchial epithelial cells
NO	Nitric oxide
NOS	Nitric oxide synthase
O_2^-	Superoxide
P/S	Penicillin/streptomycin

PCAF	p300/CBP-activating factor
PI3K	Phosphoinositol-3-kinase
poly(I:C)	Poly-riboinosinic-ribocytidylic acid
RANTES	Regulated on activation, normal T cell expressed, and secreted
rHDAC	Recombinant histone deacetylase
RNS	Reactive nitrogen species
ROS	Reactive oxygen species
SAHA	Superoylanilide hydoxamic acid
sGC	soluble guanylyl cyclase
SIN-1	3-morpholinosyndnonimine
SOD	Superoxide dismutase
STAT	Signal transducer and activator of transcription proteins
TLRs	Toll Like Receptors
TNFα	Tumour necrosis factor
TNS	Trypsin neutralization solution
TSA	Trichostatin A

1 Introduction

1.1 Chronic obstructive pulmonary disease (COPD)

Chronic obstructive pulmonary disease (COPD) was recently defined as a collection of disorders sharing the common physiological feature of progressively worsening expiratory airflow limitation (Pauwels et al. 2001). This disease is characterized by chronic local and systemic inflammation, destruction of the lung epithelial layer leading to emphysema, and remodelling of both airways and vasculature resulting in lung fibrosis and pulmonary hypertension, respectively. Importantly, the reduced expiratory airflow that defines COPD results both from inflammatory exudates containing mucus which occludes the airway lumen and from the abnormal tissue-repair process which thickens the walls and narrows the lumen of the conducting airways. Figure 1-1 demonstrates the obstruction in small conducting airways.

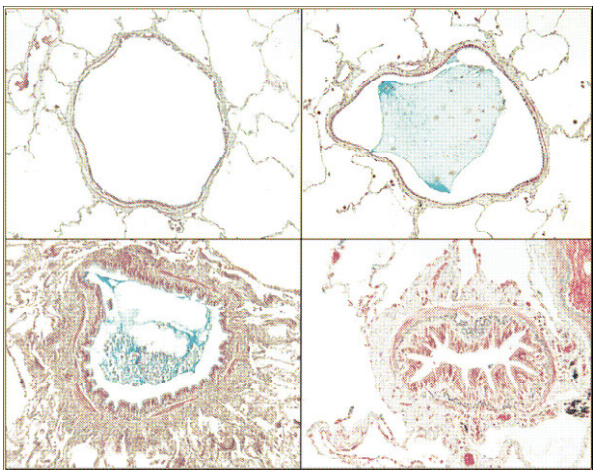

Figure 1-1 Obstruction in small conducting airways (Hogg and Timens 2008)

(*a*) An airway with an empty lumen shown for comparison. (*b*) An airway with lumen partially filled with a bland mucus plug containing a few epithelial cells. (*c*) An airway with an active inflammatory process, where the exudate extends into the lumen. (*d*) An airway that has been narrowed by the deposition in the peribronchiolar space.

COPD has become a major global epidemic that is increasing throughout the world, particularly in developing countries (Barnes 2007), and is now one of the leading causes of death and disability in most countries (Mannino and Buist 2007). Although COPD has an enormous global impact, there are no drug therapies that have been shown to prevent disease progression or reduce mortality. Moreover, insensitivity to

inhaled corticosteroids (ICS) has been shown for the majority of COPD patients, thus leaving this serious disease without adequate therapy.

1.1.1 Pathogenesis of COPD

The current hypothesis for the pathogenesis of COPD focuses on an abnormal response to the inhalation of toxic particles and gases, which include a range of both occupational and environmental fumes and dusts, as well as cigarette smoke (Pauwels et al. 2001). Cigarette smoke, a complex mixture of oxidants/free radicals and different chemical compounds which include reactive aldehydes and semiquinones known to cause oxidative stress in the lungs (Pryor and Stone 1993; Rahman and Adcock 2006), is the primary risk factor for the pathogenesis of COPD (Rahman and Adcock 2006). However, smoke on its own has minimal effects on lung function in the majority of smokers (Wright et al. 1984; Hogg et al. 1994). Not every smoker develops COPD and not every COPD patient is or was smoker. One explanation for this difference may be a genetically determined predisposition to develop this disease. Regarding the complex disorders in COPD and the intension of this study the following discussion will focus on the inflammation-related aspect of its pathogenetic mechanism.

The inhalation of noxious agents initiates a local and systemic responses generated by both innate and adaptive immune systems. *In vitro* studies have shown that important pro-inflammatory cytokines and chemokines are released from alveolar macrophages as they phagocytose carbon particles of similar size to those suspended in the atmosphere (Mukae et al. 2000). Moreover, incubation of human airway epithelial cells and/or alveolar macrophages with well-characterized particles from the air has shown paracrine interactions between these two cell types that amplify the release of pro-inflammatory cytokines (Fujii et al. 2001; Fujii et al. 2002). More importantly, tobacco smoking is well known to elevate the circulating leukocyte count in a manner consistent with chronic stimulation of the bone marrow (van Eeden and Hogg 2000) which are responsible for the systemic inflammation. Collectively, these data suggest that smoking and breathing polluted air induces a local inflammatory process in the airways by producing pro-inflammatory cytokines and chemokines and recruitment of inflammatory cells and stimulates a systemic inflammatory response that elevates the circulating leukocyte count. An increased level of the circulating leukocytes is also an important predictor of both excessive decline in lung function (Chan-Yeung et al. 1988) and increased mortality in COPD(Weiss et al. 1995).

The activation of inflammatory processes is caused by a variety of mechanisms. A variety of cell types within the lung can be activated to produce pro-inflammatory cytokines, including alveolar macrophages and lung epithelial cells (Mio et al. 1997). Moreover, activated complement can produce pro-inflammatory cytokines (Robbins et al. 1991). As a result, cigarette smoke can lead to the accumulation of activated inflammatory cells, including neutrophils, alveolar macrophages and T cells, in the lung where they release more pro-inflammatory cytokines and chemokines as well as mediators capable of damaging lung structures, such as proteases and oxidants. Furthermore, damage induced by this way may further potentiate the inflammation by releasing chemotactic peptides from the extracellular matrix (Senior et al. 1980), which is critical for structure and function of the lung. Cigarette smoke may also exacerbate lung damage by impairing lung defence mechanism. Such effects could contribute to an excessive inflammatory response.

In fact, in the susceptible smokers who develop COPD the inflammatory process is amplified and persists extensively after smoking cessation (Retamales et al. 2001). Damage to lung structures in COPD results both from the exposures and more essentially, from the chronic inflammatory responses. The chronic inflammation in COPD is characterized through enhanced infiltration of inflammatory cells, such as neutrophils, alveolar macrophages and T lymphocytes, into lung tissue, and linked to an abnormal tissue-repair and -remodeling process that enlarges the bronchial mucus glands and increases the mucus content of epithelium lining the airways lumen, the proliferative activity of the epithelial cells, and a both mucous and squamous cell metaplasia (Hogg and Timens 2008). Mucus hypersecretion, accompanied by disturbed cilia beating, causes further injuries of the lung, which on one hand lead to the emphysematous destruction of the lung, and on the other hand activate repair responses. However, individuals, either on a genetic or developmental basis, differ in their sensitivity to inflammation and in their ability to repair the injuries. A disordered tissue-repair process causes abnormal proliferation of fibroblasts and smooth muscle cells, which are responsible for thickening the small conducting airways, which in turn, causes airflow limitation. A multivariate analysis of the overall tissue response indicates that the remodeling of the small-airway-wall tissue explains more of the variance in the association between changes in histology and decline in lung function than does the infiltration of the airways by any particular type of inflammatory cell

(Hogg et al. 2004). Therefore, it seems likely that disordered repair processes can lead to tissue remodeling with altered structure and loss of function in COPD.

Taken together, the inflammatory process in the lung caused by cigarette smoke initiates an abnormal change of the structure and function of the lung, which promotes the chronic inflammation and development of a collection of disorders in COPD.

1.1.2 Airway epithelial cells in lung inflammation

Airway epithelial cells are not only simple structural cells of the lung but also serve as a barrier to invading allergens, produce enzymes and mediators that maintain normal airway homeostasis and have important role in airway diseases. The structure and function of airway epithelium is characteristically altered in COPD. Mucus hypersecretion by hyperplastic airway goblets cells is a hallmark of COPD. Airway epithelial cells also play a critical role in lung inflammation by releasing a lot of inflammatory mediators and may act as important as inflammatory cells like neutrophils, macrophages and T lymphocytes in COPD (Riffo-Vasquez et al. 2000).

The supernatants of cultured airway epithelial cells contain detectable amounts of chemokines and cytokines such as IL-1, IL-6, IL-8, GM-CSF and G-CSF (Takizawa 1998). On epithelial cell stimulation, the expression and release of these molecules is increased, e. g. TNFα, which was originally identified as a product of activated macrophages, is also produced by the airways epithelium upon stimulation (Abdelaziz et al. 1995). Cigarette smoke is capable of activating both macrophages and airway epithelial cells to release inflammatory mediators including IL-8 (Kraft et al. 1998).

The epithelium is both a target for factors released by infiltrating inflammatory cells and a major effector of inflammation (Martin et al. 1997). On encountering inflammatory factors, the epithelium produces mediators, such as IFNγ and TNFα, that provoke epithelial cells and inflammatory cells to produce secondary mediators including lipid mediators, reactive oxygen species (ROS), reactive nitrogen species (RNS), and cytokines and chemokines like IL-8 and GM-CSF (Becker et al. 1993). IL-8 in turn stimulates the infiltration of neutrophils into the respiratory tract and GM-CSF may increase their survival. These secondary mediators can also further affect pathophysiologic alterations such as hypersecretion of mucus (Adler et al. 1992). In the present study, IL-8 and GM-SCF release was generally used to assess the

stimulation of inflammation. Importantly, ROS and RNS, which will be detailed in the next section, are potent effectors of intracellular signalling of inflammatory gene expression and are involved in many mechanisms related to the development of COPD, like tissue destruction.

The human airway epithelium appears also to be the primary site of inducible nitric oxide synthase (iNOS) expression in lung inflammation, in which the iNOS-derived nitric oxide (NO) regulates various signaling pathways involved in airway inflammation. iNOS-derived NO and peroxynitrite is also an important source of nitrative stress in lung inflammation. Details about the induction and the role of iNOS and iNOS-derived NO in lung inflammation will be explained in section 1.3.

The mechanisms underlying inflammation in epithelial cells are well studied. The induction of inflammatory responses in epithelial cells causes activation of transcription factors nuclear factor κB (NF-κB) and activator protein 1 (AP-1) (Remacle et al. 1995). Stimuli known to activate the NF-κB complex include TNFα, IL-1β, LPS, ultraviolet light, ROS/RNS, and a number of viruses (Maestrelli et al. 1996). IL-1β and TNFα activate AP-1 in lung tissues (Barnes 1994). These transcription factors are implicated in the increased expression of many cytokines and mediators involved in the inflammatory response of the airway epithelium (Baldwin 1996).

1.1.3 Role of oxidative and nitrative stress in COPD

Increased oxidative and nitrative stress is seen in many inflammatory diseases, including COPD. Oxidative and nitrative stress represents an imbalance with an increase in ROS/RNS and/or a defect in endogenous or exogenous antioxidants. Generally, the definition oxidative stress includes the oxidative effects from ROS and RNS. However, in COPD lung increased nitrative stress both from cigarette smoke and iNOS-derived NO and peroxynitrite has been demonstrated in various studies and especially tyrosine nitration by peroxynitrite contribute to the development of the disease. This chapter will mainly focus on the effect of general oxidative stress in COPD and details about nitrative stress from iNOS-derived NO and peroxynitrite will be discussed in chapter 1.3.

ROS is enzymatically produced by inflammatory and epithelial cells within the lung as part of a defensive immune response towards a pathogen or irritant (Rochelle et al.

1998). Several sources for production of superoxide (O_2^-) and other ROS exist within a cell and include mitochondrial respiration, NADPH oxidase and the xanthine/xanthine oxidase system, of which the principal ROS generator is NADPH oxidase. Importantly, it has also been shown that nitric oxide synthase can generate both O_2^- and NO (Stuehr et al. 2001). This O_2^- can either react with NO to form highly reactive peroxynitrite or, alternatively, be rapidly converted into hydrogen peroxide (H_2O_2) under the influence of superoxide dismutase (SOD). However, H_2O_2 in the presence of Fe^{2+} can also produce the more damaging hydroxide radical (•OH) through Fenton chemistry (Halliwell and Gutteridge 1990). Once produced, ROS can interact with a wide variety of molecules, such as phospholipids, DNA and enzyme residues, through electron donation in biological systems.

Cigarette smoke is the most important source of exogenous oxidative stress in COPD. Cigarette smoke contains over 4700 chemical compounds and high concentrations of oxidants (Church and Pryor 1985). The nature of ROS/RNS found within cigarette smoke varies from short-lived oxidants, such as O_2^- and the NO molecule, to long-lived organic radicals, such as semiquinones which can undergo redox-cycling, a process that may continue as a chain reaction, within the epithelial lining fluid of smokers for some considerable period of time (Zang et al. 1995).

ROS and RNS, especially when generated close to cell membranes, oxidize membrane phospholipids (lipid peroxidation). This can impair membrane function, inactivate membrane-bound receptors and enzymes and increase tissue permeability and these processes have been implicated in the pathogenesis of many forms of tissue injury. Intracellularly, oxidative and nitrative stress can also have a major impact on redox-sensitive signalling pathways as well as act as a second messenger itself (Garg and Aggarwal 2002; Poli et al. 2004). As discussed above, the activation of redox-sensitive transcription factors, such as transcription factors NF-κB and AP-1, is necessary for induction of pro-inflammatory gene expression. However, at another level of gene regulation, chromatin topology also plays an important role, through which ROS/RNS can have a major impact. Histone acetylation by histone acetyltranferase (HAT) is generally correlated with gene activation and histone deacetylation by histone deacetylase (HDAC) with gene inactivation. For example, ROS/RNS has been shown to inactivate HDAC2 and this is achieved through increased nitration or carbonylation (Marwick et al. 2004). Coupled with ROS/RNS-

induced activation of transcription factors NF-κB and AP-1, this has the net effect of promoting pro-inflammatory gene expression (Rahman and Adcock 2006). More details about this complex regulatory mechanism will be discussed in section 1.4. Furthermore, the impact of ROS and RNS on histone deacetylase 2 (HDAC-2) is particularly important as it has also been shown to be required not only for inflammation regulation but also for corticosteroid-mediated inhibition of the inflammatory response and reduced HDAC2 has been hypothesized to result in corticosteroid insensitivity in COPD (Rahman and Adcock 2006). This point will be detailed in the next chapter.

Taken together, oxidative and nitrative stress from exogenous (cigarette smoke/pollution) and endogenous (activated inflammatory cells) sources is believed to have a major contribution to the lung injury and the progression of chronic inflammation and it may also contribute to the development of chronic inflammation and reduced steroid insensitivity in COPD.

1.2 Steroid insensitivity in COPD

Glucocorticoids (GCs) are highly effective in treating many inflammatory diseases and, for example, asthma is controlled in the majority of patients by therapy with inhaled corticosteroids (ICS), either alone or in combination with long-acting β_2 -agonists (LABAs), with minimal side effects (Ito et al. 2006a). Nevertheless, there is a small proportion of asthmatic patients, including present cigarette smokers and former cigarette smokers, and patients with COPD that fail to respond to both inhaled and oral corticosteroids (Chaudhuri et al. 2006). Even high doses of GCs have a minimal effect on the rapid decline in lung function in COPD patients and have only a small effect in reducing COPD exacerbations (Barnes 2007). The efficacy of ICSs is partially due to a reduction of the eosinophilic and lymphocytic inflammation in the airway wall and in suppressing the expression of multiple inflammatory genes in the airways (Ito et al. 2006a). It has been demonstrated that therapy with ICSs or oral corticosteroids fails to reduce the numbers of inflammatory cells including alveolar macrophages, cytokines, chemokines, or proteases in induced sputum or airway biopsy specimens from COPD patients (Barnes 2007). This insensitivity may also be seen at the level of single cells, as it has been shown that GCs are also ineffective in suppressing inflammatory proteins, such as TNFα, IL-8, and matrix metalloproteinase-9 (MMP-9), in alveolar

macrophages from COPD patients compared to cells from healthy smokers and non-smokers (Barnes 2007). This appears to result from a defect in the anti-inflammatory effect of GCs, since other anti-inflammatory therapies, such as theophylline and resveratrol, have inhibitory effects (Barnes 2007). Therefore, steroid insensitivity presents a profound management problem in patients with steroid-insensitive asthma and patients with COPD.

1.2.1 Mechanism of glucocorticoid receptor function in inflammation

Corticosteroids act by binding to the glucocorticoid receptor (GR), which, under resting conditions, is located in the cytosol of cells and is bound to chaperons such as heat shock protein-90. These chaperones protect the receptor and maintain them in a state of readiness for activation. GR is a member of the nuclear receptor superfamily of transcription factors that includes receptors for mineralocorticoids, progesterone, androgen, estrogen, thyroid hormones, vitamin D, and retinoic acid (Robinson-Rechavi et al. 2001). When glucocorticoid agonists are administered (by inhalation or systemically), they diffuse freely across the cell membrane and bind to these receptors, which then dissociate from chaperones and translocate to the nucleus of the cell where they can interact with various other molecular factors (see also Figure 1-3) to regulate inflammatory gene transcription (Bamberger et al. 1996).

Both gene activation and gene repression are involved in the anti-inflammatory action of corticosteroids. Figure 1-2 (Adcock and Ito 2005) shows the mechanisms of gene regulation by glucocorticoid receptor in inflammation. Inflammatory genes are regulated by the actions of pro-inflammatory transcription factors such as NF-κB and AP-1. Activated GR binds to these transcription factors, either directly or indirectly, and recruits corepressor proteins that blunt the ability of these transcription factors to switch on inflammatory genes, which is called transrepression (Ito et al. 2006a). As showed in Figure 1-2/process 1, the activated GR binds to the transcription factors AP-1 and NF-κB and prevents their ability to switch on inflammatory gene expression. Inhibition of cytokine and chemokine gene transcription implicated in inflammation may be the most important action of steroid drugs (Adcock 2003). Alternatively, the activated GR can induce the expression of key anti-inflammatory genes, like IL-10, following a direct association with DNA at GC response elements (GREs) in the promoter regions of these genes (process 3). This process is called trans-activation.

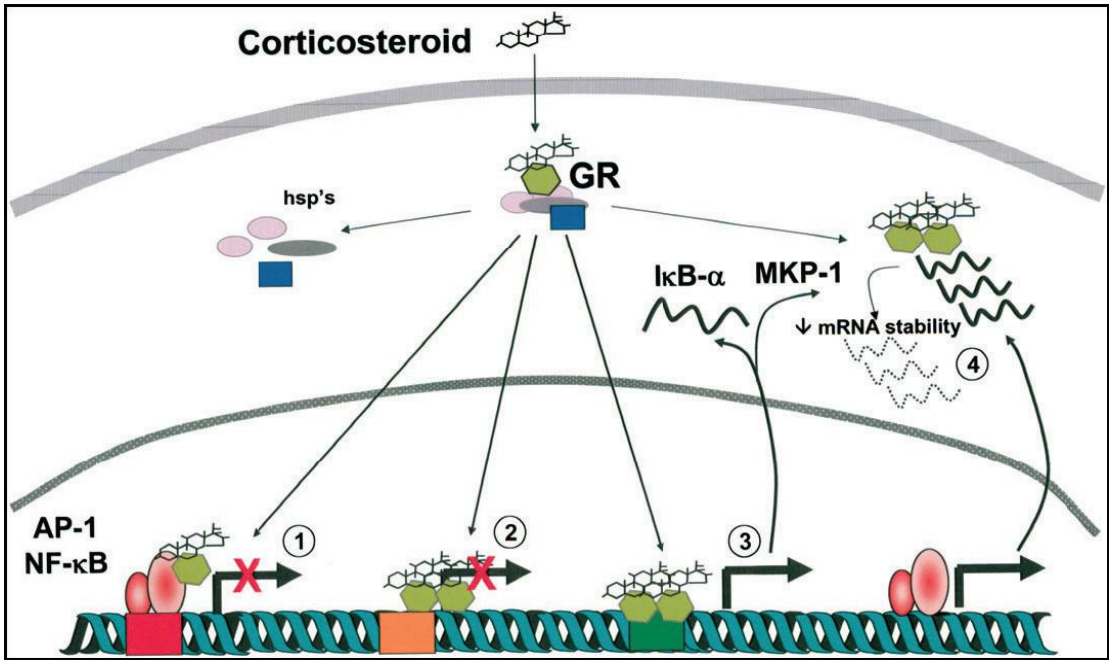

Figure 1-2 Mechanisms in regulation of gene expression in inflammation by the glucocorticoid receptor (GR) (Adcock and Ito 2005)

The corticosteroid can freely migrate across the plasma membrane, where it associates with the cytoplasmic GR. This results in activation of GR and dissociation from the heat shock protein (hsp90) chaperone complex. Activated GR translocates to the nucleus, where it can bind as a monomer either directly or indirectly with the transcription factors AP-1 and NF-κB, preventing their ability to switch on inflammatory gene expression (*1*). Second, the GR dimer can bind to a GRE that overlaps the DNA-binding site for a pro-inflammatory transcription factor or the start site of transcription to prevent inflammatory gene expression (*2*). Third, the GR dimer can induce the expression of the NF-κB inhibitor IκB-α or induce the dual specificity mitogen-activated protein kinase (MAPK) phosphatase-1 (MKP-1) that can regulate p38 MAPK-mediated mRNA stability (*3*). Fourth, corticosteroids can increase the levels of cell ribonucleases and mRNA-destabilizing proteins, thereby reducing the levels of mRNA (*4*).

In the GR action of suppressing inflammatory gene expression, HDAC activity and especially that of HDAC2, plays a crucial role. GR may repress NF-κB mediated gene activation through histone modifications and chromatin remodeling. GR acts both as a direct inhibitor of CBP (CREB binding protein)-associated histone acetyltransferase (HAT) activity and also by recruiting HDAC2 to the p65-CBP-HAT complex (Figure 1-3). GR-mediated deacetylation of histones results in increased tightening of DNA around histones, reduced access of transcription factors to their binding sites, and repression of inflammatory genes. The regulatory effect of HAT/HDAC in gene expression and inflammation will be discussed further in section 1.4. GR-mediated transrepression has shown to be blocked by inhibiting HDAC-2 (Kouzarides, 2000). However, how ligand-bound GR recruits HDAC-2 to the p65-CBP-HAT complex remains to be determined.

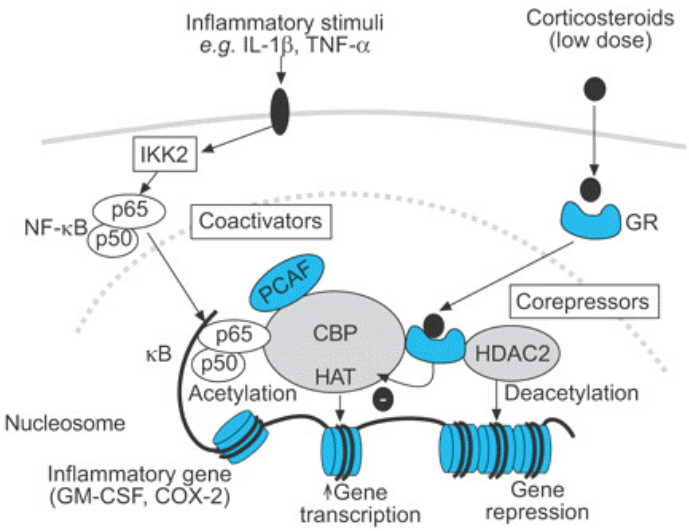

Figure 1-3 Inflammatory gene suppression by corticosteroids (Barnes 2008)

Inflammatory genes are activated by inflammatory stimuli, such as IL-1β or TNFα, resulting in activation of I-κB kinase (IKK) 2, which activates the transcription factor NF-κB. A heterodimer composed of p50 and p65 NF-κB proteins translocates to the nucleus and binds to specific κB recognition sites and also to coactivators, such as CREB-binding protein (CBP) or p300/CBP-activating factor (PCAF), which have intrinsic histone acetyltransferase (HAT) activity. This results in acetylation of lysines in core histone, resulting in increased expression of genes encoding inflammatory proteins, such as GM-CSF. After activation by corticosteroids, glucocorticoid receptors (GR) translocate to the nucleus and bind to coactivators to directly inhibit HAT activity, and histone deacetylases (HDAC) are recruited, thus resulting in histone acetylation reversal leading to the suppression of inflammatory genes like COX-2.

1.2.2 Putative factors involved in steroid insensitivity

There are a number of potential explanations for steroid insensitivity in the treatment of inflammatory lung diseases. As described in section 1.2.1, GCs act by binding to a cytosolic GC receptor, which is subsequently activated and is able to translocate to the nucleus. Once in the nucleus, the GR either binds to DNA and switches on the expression of anti-inflammatory genes or acts indirectly to repress the activity of a number of distinct signaling pathways such as NF-κB and AP-1. This latter step requires the recruitment of corepressor molecules. Based on this mechanism, a failure to respond may therefore result from reduced GC binding to GR, reduced GR expression, failure of GR translocation, enhanced activation of inflammatory pathways, or lack of corepressor activity (Leung et al. 1995). These events can be modulated by oxidative stress, T-helper type 2 cytokines, or high levels of inflammatory mediators, all of which may lead to a reduced steroid sensitivity (Adcock and Barnes 2008). Figure 1-4 (Adcock and Barnes 2008) shows the possible sites of regulation in GC insensitivity and the focus of this study was the role of oxiadative and nitrative stress in steroid insensitivity, which will be described in more details in the next section.

Understanding the molecular mechanisms of GR action, and inactivation, may lead to the development of new anti-inflammatory drugs or may reverse the relative steroid insensitivity in steroid insensitive inflammatory diseases.

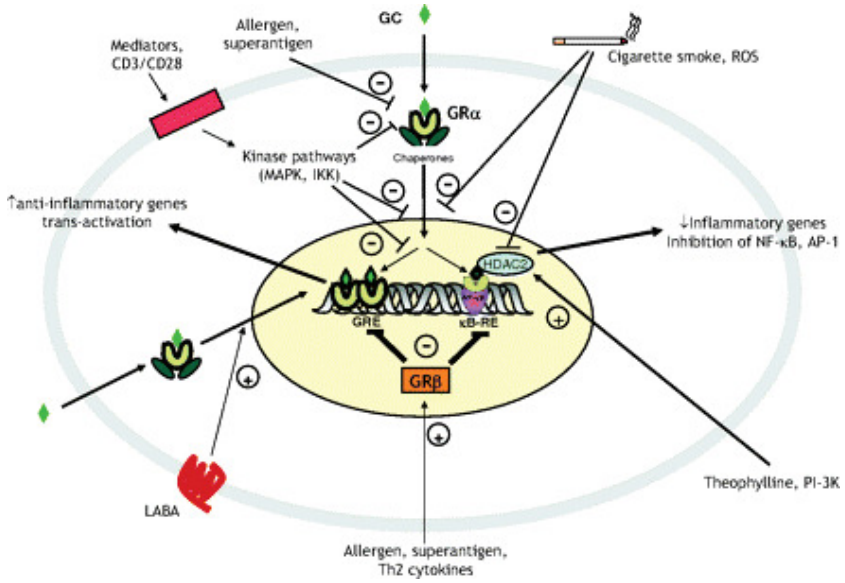

Figure 1-4 Mechanism of GC action by the GR and sites of regulation in GC insensitivity (Adcock and Barnes 2008)

GCs freely diffuse from the circulation across cell membranes where they interact with the GR. On ligand binding, the receptor is activated, released from a chaperone complex, and translocates to the nucleus where it can bind as a dimer to GRE and induce gene transcription. Alternatively, GCs may act by inhibiting the ability of other transcription factors such as NF-κB and AP-1 activated by cytokines to induce pro-inflammatory gene transcription. In this instance, GR acts as a monomer and recruits repressor proteins such as HDAC2. The activation of kinase pathways by inflammatory mediators or T-cell receptor coactivation (CD3/CD28) can attenuate GR function by reducing ligand binding and nuclear translocation, or by mutually suppressing/interacting with NF-κB or AP-1. Allergens and superantigens can also affect GR ligand binding but are also able, along with T helper type 2 cytokines, to induce GRβ. Cigarette smoke and reactive oxygen species (ROS) stress can prevent GR nuclear translocation or reduce the activity of HDAC2 reducing the ability of GR to switch off inflammatory genes. Drugs such as LABAs can enhance GR nuclear translocation, whereas theophylline can enhance HDAC2 activity. These different actions may account for their ability to improve GR function in disease. IKK = inhibitor of NF-κB kinase; RE = response element.

1.2.3 Hypothesis of the role of oxidative and nitrative stress in steroid insensitivity in COPD

Perhaps the most likely explanation for steroid insensitivity in COPD at present may involve the pivotal role of oxidative and nitrative stress. Peter Barnes has proposed that increased oxidative and nitrative stress in the lung of COPD patients leads to the reduction of HDAC2 activity, which is important in mediating the anti-inflammatory effects of steroids as discussed above, and hence, leading to steroid insensitivity (Barnes 2008).

As explained in section 1.1, COPD is associated with a chronic inflammation of the lung parenchyma and small airways and a high level of oxidative and nitrative stress. Corticosteroids, which are effective in treating inflammatory lung diseases such as asthma, have no anti-inflammatory or reduced effects in COPD. This may occur, as explained in section 1.2.1, because corticosteroids use HDAC2 to switch off activated inflammatory genes through deacetylation of their hyperacetylated histone residues. Various reports indicate that HDAC2 activity and expression are markedly reduced in COPD lungs, airways, and alveolar macrophages, which may account for the amplified inflammation and corticosteroid insensitivity seen in these patients (Ito et al. 2001; Ito et al. 2005). Moreover, this reduction in HDAC2 appears to be secondary to increased oxidative and nitrative stress, which can lead to tyrosine nitration, phosphorylation, and ubiquitination of HDAC2, resulting in loss of its activity and its degradation (Barnes 2008; Adenuga et al. 2009).

Based on Barnes' hypothesis, antioxidants and inhibitors of inducible nitric oxide synthase (iNOS) (see chapter 1.3) may therefore restore corticosteroid sensitivity in COPD. This may also be achieved by low concentrations of theophylline (Ito et al. 2002) and curcumin (Meja et al. 2008), which may act as HDAC activators by inhibiting PI3Kδ (Marwick et al. 2009). Although these compounds have been documented to restore corticosteroid function in different cell models, the mechanism of their action is largely unknown.

1.3 Inducible nitric oxide synthase (iNOS)

1.3.1 Nitric oxide (NO) and nitric oxide synthases (NOSs)

Nitric oxide (NO) is a ubiquitous reactive signaling molecule, synthesized by oxidative conversion of the amino acid L-arginine by NO synthases (NOSs). NO exerts a broad range of functions in many physiological and pathophysiological cell and tissue responses (Moncada et al. 1991). Under aqueous, aerobic conditions NO spontaneously oxidizes to its stable products nitrite and nitrate. The first described physiological effect of NO was activation of soluble guanylyl cyclase (sGC) (Ignarro et al. 1999). The rise in cGMP (3`,5`-cyclic guanosine monophosphate) level accounts for many of but not all cellular responses to NO. Although being a reactive radical NO may diffuse away from its point of origin, and therefore to carry out its function as a messenger molecule beyond cell borders (Wink and Mitchell 1998). NO has the

potential to interact directly or indirectly with metals, thiols (S-nitrosylation) and oxides, and therefore affects proteins, nucleic acids, lipids and sugars (Davis et al. 2001). Effects of NO depend on its concentration and the redox state of the cell.

Three NO synthase isoforms have been identified: endothelial NOS (eNOS, NOS-3), neuronal NOS (nNOS, NOS-1) and inducible NOS (iNOS, NOS-2). NOSs are active only as dimers. As shown in Figure 1-5, they contain tightly-bound cofactors (6R)-5,6,7,8-tetrahydro-L-biopterin (BH4), flavine-adenine dinucleotide (FAD), flavine mononucleotide (FMN) and iron protoporphyrin IX (haem) (Alderton et al. 2001). The activity of eNOS and nNOS is calcium-dependent, as Ca^{2+} stabilizes the calmodulin binding to its binding site in these two NOS isoforms, thereby initiating NO synthesis (Bredt and Snyder 1990). However calmodulin in iNOS is tightly bound and therefore its activity is calcium-independent (Vallance and Leiper 2002). eNOS and nNOS are regarded as constitutively expressed (together called cNOS), however it has been shown that expression of these enzymes is to some extent also regulated at the transcriptional level by local environmental conditions (Forstermann et al. 1998). After activation eNOS and nNOS produce nanomolar concentrations of NO, and are active for relatively short periods of time. Both isoforms are principally considered to participate in the regulation of physiological processes in the cardiovascular and nervous system, where they were first found (Marletta et al. 1998). However, their expression has been found later in other tissues and cell types.

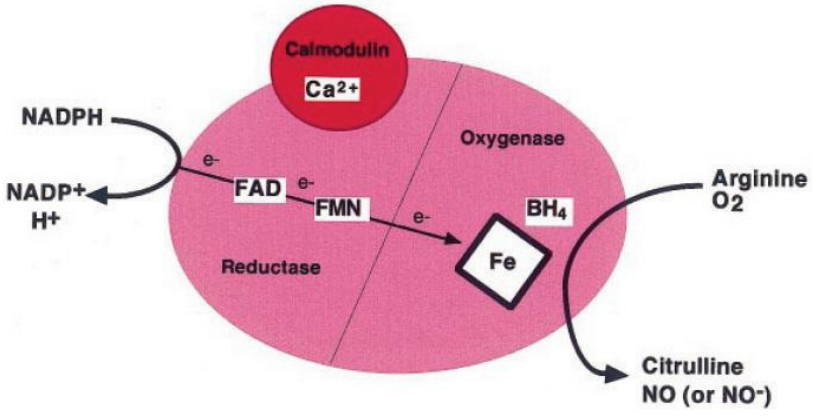

Figure 1-5 Overall reaction catalysed and cofactors of NOS (modified from (Alderton et al. 2001)

Electrons (e^-) are donated by NADPH to the reductase domain of the enzyme and proceed via FAD and FMN redox carriers to the oxygenase domain. There they interact with the haem iron and BH_4 at the active site to catalyse the reaction of oxygen with L-arginine, generating citrulline and NO as products. In some circumstances NO^- may be a product instead of NO. Electronflow through the reductase domain requires the presence of bound Ca^{2+}/CaM.

iNOS was first described in activated macrophages (Hibbs et al. 1988). This isoform is not usually expressed in healthy quiescent cells, but is rapidly transcriptionally induced in response to stimulation with bacterial endotoxins or pro-inflammatory cytokines (Vallance and Leiper 2002). Expression of iNOS has been found in many cell types like in human epithelium after induction (Guo et al. 1995). iNOS expression is regulated not only at the transcriptional level but also at the level of iNOS mRNA stability (Kleinert et al., 2000). Activation of transcription factor NF-κB seems to be an essential step for iNOS induction in most cells (Forstermann and Kleinert 1995). cAMP activated transcription factors like CREB and C/EBP seem also to be involved in the regulation of iNOS expression (Kleinert et al. 2004). Furthermore, regulation of iNOS expression involves also other transcription factors like AP1 or STAT1 (Xu et al. 2006). Additionally, glucocorticoids have been shown to interfere with iNOS expression in many cell types (Di Rosa et al. 1990). Inhibition of iNOS expression by glucocorticoids has been shown to result from inhibition of NF-κB activation (Mukaida et al. 1994; Kleinert et al. 1996), however, it is also proposed that iNOS expression in human lung epithelial cells, which is induced by pro-inflammatory cytokines, is not regulated directly by glucocorticosteroids (Donnelly and Barnes 2002).

Once induced, iNOS produces high amounts of NO (about 100x higher concentration as eNOS and nNOS) for a prolonged period of time (Nathan 1992). These high levels of NO are important for a host defence against infectious organisms (Nathan 1997). NO produced by iNOS regulates also the functional activity, growth and death of many immune and inflammatory cell types including macrophages, T lymphocytes, antigen-presenting cells, mast cells, neutrophils and natural killer cells (Coleman 2001).

iNOS is also induced in situations that are not involved in host defence and in these situations iNOS activity and NO signalling might be harmful and cause tissue damage. The production of high NO level in inflammation is considered to be responsible for many detrimental effects leading to tissue destruction. The increased induction of iNOS is implicated in a number of pathologies like septic shock (Titheradge 1999), ulcerative colitis, Crohn's disease (Cross and Wilson 2003), asthma and COPD (Barnes and Liew 1995). The pathophysiological functions of iNOS and iNOS-derived NO and peroxynitrite ($ONOO^-$) will be detailed in the following sections.

Table 1-1 Short characteristics of nitric oxide synthases.

	iNOS	eNOS	nNOS
expression	inducible	constitutive	constitutive
stimulated by	LPS, pro-inflammatory cytokines, dsRNA	-	-
calcium dependent	-	+	+
present in	epithelial cells, macrophages, lymphocytes, smooth muscle cells etc.	endothelial cells	neurons

1.3.2 Peroxynitrite ($ONOO^-$) and protein nitration

The NO radical reacts very rapidly with superoxide (O_2^-) to form peroxynitrite ($ONOO^-$). The rate constant of this reaction is near the diffusion-controlled limit ($k= 6{,}7 \times 10^9\ M^{-1} \bullet s^{-1}$) (Huie and Padmaja 1993). Superoxide anion can be generated in cells either enzymatically (NADPH oxidases) or by processes that produce reactive oxygen species (ROS) such as the electron transport chain in mitochondria. Although neither NO nor O_2^- is a strong oxidant, $ONOO^-$ is a potent and versatile oxidant that is thought to be a mediator of toxicity in inflammatory states, with strong oxidizing properties towards biological molecules, including thiol groups, ascorbate, lipid, methionine, tryptophan and DNA, and it can cause strand breaks in DNA (Briviba et al. 1996). Some of biologically important reactions of peroxynitrite are listed below.

Biological reactions of peroxynitrite:

- Nitration of tyrosine residues of proteins (Haddad et al. 1994; Reiter et al. 2000)
- Oxidation of thiol compounds (Radi et al. 1991a)
- Triggering of lipid peroxidation (Radi et al. 1991b)
- Inhibition of mitochondrial electron transport (Radi et al. 1994)
- DNA-strand breakage (Szabo 1996)
- Activation of poly(ADP-ribose) synthase (Jung et al. 2000)
- Activation of MMP's (Migita et al. 2005)
- Inactivation of TIMP (tissue inhibitor for MMP) and α1-proteinase inhibitor (Brown et al. 2004)
- Modulation of cyclooxygenase activity (Mollace et al. 2005)
- Apoptosis (Virag et al. 2003)

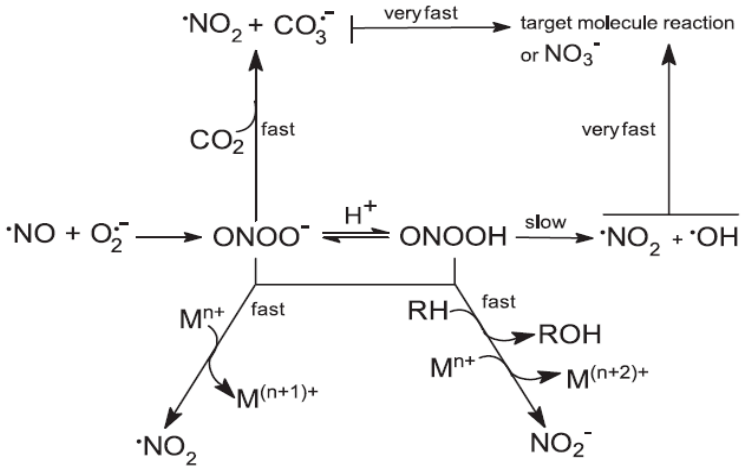

Figure 1-6 Overview of peroxynitrite reaction pathways (Alvarez and Radi 2003)

Peroxynitrite is formed from the diffusion-controlled reaction between nitric oxide and superoxide radicals. Peroxynitrite anion and peroxynitrous acid (pK_a=6.8) promote direct one- or two-electron oxidation reactions intransition metal centers and other biomolecules and yield nitrogen dioxide or nitrite respectively. Peroxynitrite anion can also react fast with carbon dioxide to secondarily yield nitrogen dioxide and carbonate radicals. Alternatively, peroxynitrous acid can undergo homolysis to hydroxyl and nitrogen dioxide radicals. The secondary peroxynitrite-derived radicals can initiate one-electron oxidations in target biomolecules or recombine to yield nitrate

Figure 1-6 (Alvarez and Radi 2003) demonstrates the various peroxynitrite reaction pathways. The peroxynitrite anion is stable; however, its conjugate acid, with a pKa of 6.8, and its CO_2 adduct, $ONOOCO_2$, are strong oxidants capable of rapidly oxidizing sulfhydryls and thioethers and nitrating aromatic compounds (Kong et al. 1996). Hence, peroxynitrite is a potent protein-nitrating agent. Especially aromatic tyrosine residues of proteins are susceptible to reaction with peroxynitrite, leading to the formation of 3-nitrotyrosine (Ischiropoulos et al. 1992)

Tyrosine nitration may alter the structure and function of proteins. On one hand, it may prevent tyrosine phosphorylation leading to alterations in signal transduction, which has been considered as pathological event, but on the other hand it might be also a part of cellular signaling mechanisms and emerging data implicate tyrosine nitration as a mediator of immune responses (Kong et al. 1996; Ischiropoulos 2009). Increased levels of 3-nitrotyrosine have been reported in many diseases, such as COPD, cancer, Parkinson`s disease and Alzheimers disease. Moreover, *in vitro* studies showed that peroxynitrite was able to reduce HDAC2 activity via tyrosine nitration and increase inflammatory gene expression (Ito et al. 2004).

In the present study, to investigate the effect of exogenous nitrative stress *in vitro*, 3-morpholinosyndnonimine (SIN-1) was applied. SIN-1 is the active metabolite of the vasodilator drug molsidomine and capable of releasing both NO and superoxide simultaneously, hence generating peroxynitrite (Hogg et al. 1992). Figure 1-7 shows the hydrolysis of SIN-1 to an open-ring form (SIN-1A) that undergoes an oxygen dependent release of NO with the concomitant production of superoxide (Feelisch et al. 1989). For this reason, SIN-1 has been used as an experimental model for the simultaneous generation of NO and superoxide, i.e., a peroxynitrite donor, in chemical and biological systems.

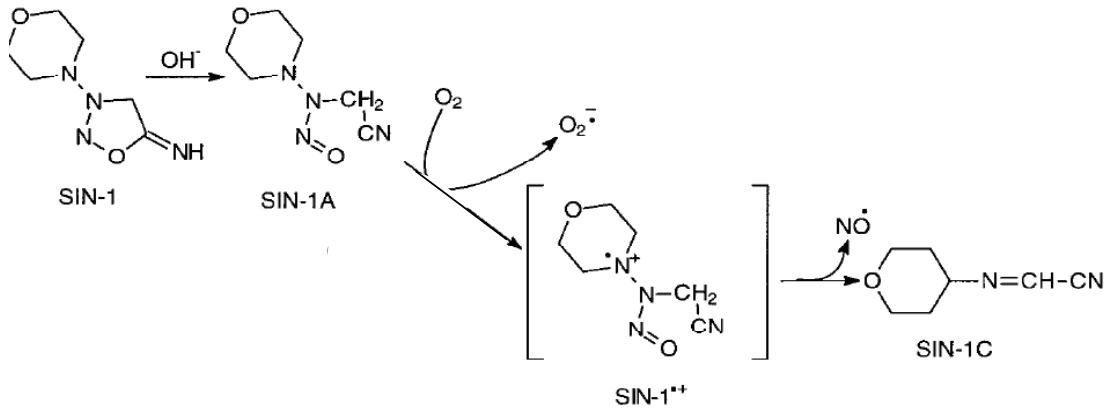

Figure 1-7 Oxidation of SIN-1 to SIN-1C by releasing superoxide and nitric oxide (Feelisch et al. 1989)

The mechanism of SIN-1 decomposition follows the following steps: (i) The sydnonimine ring opens, by a base-catalyzed mechanism, to give SIN-1A; (ii) SIN-1A reduces oxygen, in a one-electron transfer reaction, to give superoxide and SIN-1$^{\bullet+}$, a cation radical; and (iii) SIN-1$^{\bullet+}$, decomposes to form SIN-1C and NO$^{\bullet}$.

1.3.3 iNOS-derived NO and $ONOO^-$ in lung inflammation and steroid insensitivity

As explained in section 1.3.1 iNOS is an inducible protein and can be induced at sites of inflammation by mediators such as cytokines and LPS. Expression of iNOS has been shown in the epithelial cell layer, in inflammatory cells - mainly in neutrophils - and in skeletal muscle of COPD patients (Ichinose et al. 2000; Maestrelli et al. 2003; Agusti et al. 2004). Large amounts of NO and $ONOO^-$ can then be produced at sites of inflammation, which reflects the putative role of iNOS in lung diseases (Kroncke et al. 1998).

NO is an important mediator in the lung and has been shown to be associated with inflammatory lung diseases (Barnes and Liew 1995). Increased airway NO production in inflammatory respiratory tract diseases such as asthma may activate signaling

mechanisms to regulate inflammatory pathways, and epithelial barrier (dys-)function or repair (Bove and van der Vliet 2006). Additionally, nitrative stress from iNOS-derived NO may amplify the inflammatory response in the lung through peroxynitrite formation. Particularly, it has been demonstrated that peroxynitrite impairs HDAC2 activity through nitration of critical tyrosine residues. It has been proposed that in patients with COPD, HDAC2 function is impaired by oxidative and nitrative stress, leading to a pronounced reduction in responsiveness to corticosteroids. Therefore, iNOS may also be involved in the steroid insensitivity of COPD (Barnes et al. 2004).

On one hand, there is increasing evidence that iNOS-derived NO and $ONOO^-$ is involved in a wide variety of pathophysiological features in COPD, e.g in the development of local and systemic inflammation, hypoxic pulmonary hypertension, mucus hypersecretion and airway remodeling, and may be also implicated in exacerbations, emphysema and resistance to corticosteroids in COPD. Or, it may be an underlying causative factor for at least some of them.

On the other hand, it is largely unknown how iNOS-derived NO and $ONOO^-$ mediates its pro-inflammatory effects in detail, even though a wide variety of NO-dependent targets have been elucidated that may either be activated or inhibited by nitrosylation/denitrosylation or nitration/denitration. Especially regarding the role of NO which is derived from iNOS expressed in human epithelial cells during inflammation, there is only limited knowledge available (Pettersen and Adler 2002).

Based on these facts and Peter Barnes' hypothesis about the role of oxidative and nitrative stress through reduction of HDAC2 activity in steroid insensitivity, in the present study we intended to test the hypothesis, that iNOS by releasing NO and $ONOO^-$ formation may cause steroid insensitivity using different lung epithelial cells.

1.3.4 iNOS inhibitors and their functional effects on inflammation

In recent years a dogma was established that the constitutive forms of nitric oxide synthases, eNOS and nNOS, are critical to normal physiology and inhibition of these enzymes causes damage, whereas inducible NO synthase is considered as a pro-inflammatory enzyme and induction of the iNOS is harmful. The chronic production of large amounts of nitric oxide by induction of iNOS in response to cytokines and other stimuli may be deleterious and contribute to the inflammatory response in both airways and in lung parenchyma. Therefore, specific inhibition of this enzyme would be

beneficial and iNOS inhibitors might have therapeutic potential in inflammatory diseases. Also regarding the hypothesis about the correlation of iNOS and steroid insensitivity, specific iNOS inhibitors could be a helpful tool to study this molecular mechanism.

As L-arginine is a substrate for NOS several NOS inhibitors are analogues of arginine competing for the active site of the enzyme. L-NMMA (N^G-monomethyl-L-arginine) and L-NAME (N^G-nitro-L-arginine methyl ester) represent the group of NOS unspecific substrate analogues and their inhibitory action on NOS can be antagonized by high concentrations of L-arginine. L-NAME exhibits slightly higher potency towards constitutive enzymes. AMT (2-amino-5,6-dihydro-6-methyl-4*H*-1,3-thiazine) is a very potent (about 1000-fold more potent than arginine analogues presented here) (Nakane et al. 1995) and also a non-selective NOS inhibitor (Boer et al. 2000). Non-selective NOS inhibitors such as L-NMMA and L-NAME lead to hypertension by blocking eNOS in endothelial cells (Rees et al. 1989). To avoid side effects selective inhibitors of iNOS may be required. The first highly selective iNOS inhibitors were the bis-isothioureas reported by Garvey et al. (Garvey et al. 1994), which were approx. 200-fold more selective for iNOS than for eNOS, but only 5-fold in comparison to nNOS (Alderton et al. 2001). Improvement of iNOS selectivity was achieved with 1400W, an amidine-derived iNOS inhibitor. 1400W is not only highly selective as an iNOS inhibitor versus both eNOS and nNOS but also penetrates cells and tissues (Garvey et al. 1997). 1400W does exhibit an acute toxicity at high doses, which prevented its use in humans, but it can be used as a pharmacological tool in a variety of animal models (Alderton et al. 2001).

BYK191023 is an imidazopyridine derivative developed by Nycomed. Imidazopyridine compounds represent a novel class of NO-synthase inhibitors with high selectivity for the inducible isoform (Strub et al. 2006). BYK191023 is 200-fold more selective for human iNOS versus nNOS and 1000-fold in comparison to eNOS. BYK191023 did not show any toxicity in rodents and human cell lines up to high micromolar concentrations (Strub et al. 2006).

BYK402750 is another highly selective iNOS inhibitor from Nycomed and shows potent inhibition of human iNOS in the high nanomolar range and of iNOS-mediated NO production in various cell lines at low micromolar concentrations (Hesslinger et al.

2008). BYK402750 exhibited an acceptable pharmacokinetic profile both in rats and mice. In a clinically relevant model of cigarette smoke-induced pulmonary inflammation in C57Bl/6 mice, BYK402750 potently suppressed airway infiltration of various inflammatory cells, like neutrophils, macrophages and T lymphocytes. The reduction in cell numbers was associated with a significant attenuation of the smoke-induced increase in levels of the chemokines KC (IL-8 homologue) and MCP-1 in bronchoalveolar lavage fluid (BALF). Additional studies with the structurally unrelated iNOS inhibitor L-NIL confirmed the beneficial effect of iNOS inhibition on cell infiltration in this model, supporting the hypothesis that iNOS inhibition could represent a novel therapeutic approach to target inflammation in COPD (Hesslinger 2009).

Although iNOS inhibitors have been shown to exert beneficial anti-inflammatory effects in a wide variety of acute and chronic animal models of inflammation, iNOS-mediated *in vitro* effect still need to be characterized. In the present study, both BYK191023 and BYK402750 were used as valuable tools for the *in vitro* investigation of inflammation in lung epithelial cells which were induced to express iNOS.

Table 1-2 The selectivity of NOS inhibitors.

Inhibitor	Structure	Selectivity (fold)		
		iNOS/eNOS	iNOS/nNOS	nNOS/eNOS
L-NMMA	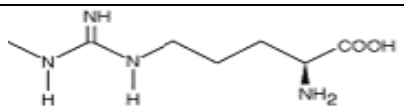	0,3	0,8	0,3
L-NAME	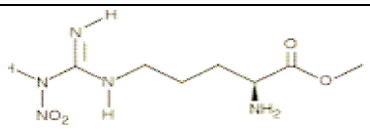	0,05	0,05	1
AMT	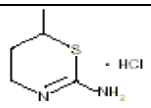	3	0,8	3
1400W	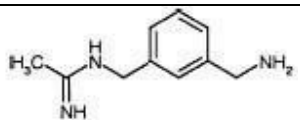	200	20	10
BYK191023	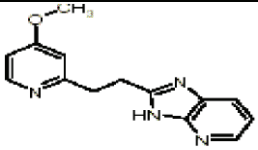	>1000	>200	-
BYK402750	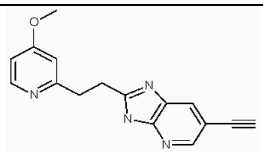	850	74	-

Source: L-NMMA, L-NAME, AMT and 1400W (Boer et al. 2000), BYK191023 (Strub et al. 2006), BYK402750 (Hesslinger et al. 2008)

There are also NOS inhibitors with distinct mechanisms of action than competing with L-arginine for the active site of these enzymes. For example BH_4 analogs, which act at BH_4 binding site, like 4-amino-H_4-biopterin (Werner et al. 2003) or inhibitors of NOS dimerization like imidazole derivatives (Ohtsuka et al. 2002).

Clinical trials with NOS inhibitors were started in septic shock patients, however they were not successful probably due to use of unspecific NOS inhibitors (L-NMMA) and had to be stopped because of increased mortality (Petros et al. 1994). Highly selective iNOS inhibitor GW274150 was tested in a Phase II study in human mild asthmatics. It could demonstrate potent inhibition of exhaled NO but failed to be effective on asthmatic responses to allergen, on methacholine-induced airway hyperreactivity and inflammatory cell influx into BALF (Singh et al. 2007).

1.4 Histone deacetylase (HDAC)

1.4.1 Histone de-/acetylation and regulation of transcription

In eukaryotic cells, genomic DNA is complexed with histone (H1, H2A, H2B, H3 and H4) and non-histone proteins to form chromatin. The basic repeating unit of chromatin is a nucleosome, which consists of 147 bp of super helical DNA wrapped around a histone octamer that itself comprises a central histone $(H3/H4)_2$ tetramer and two histone H2A/H2B dimers (Luger et al. 1997). H2A, H2B, H3 and H4 are called core histones.

In the resting cell, DNA is tightly compacted into nucleosomes, which act as a barrier to the initiation of transcription by preventing the access of transcription factors and RNA polymerase II, to their cognate recognition sequences (Workman and Buchman 1993). During activation of the cell this compact inaccessible DNA is made available to DNA binding proteins, thus allowing the induction of gene transcription (Beato 1996; Wolffe 1997). Core histone modifications play a critical role in transcriptional regulation. Core histones may be modified by acetylation, methylation, phosphorylation or ADP-ribosylation (Wu et al. 1986). Such post-translational modifications have long been thought to play an important role in chromatin structure and function (Wolffe and Hayes 1999). Figure 1-8 shows sites of post-translational modifications within the histone tail domain (Wolffe and Hayes 1999). The N-terminal tails of the core histones contain highly conserved lysines that are sites for posttranslational acetylation.

Of the histone modifications listed above, histone acetylation has been the most studied and appreciated, partially owning to the discovery of histone acetyltransferases (HATs) and histone deacetylase (HDACs), which are responsible for the steady-state balance of this modification (Strahl and Allis 2000). Furthermore, compelling evidence has recently been provided that acetylation of specific lysine residues in the amino termini of the core histones plays a fundamental role in transcriptional regulation (Kurdistani et al. 2004). The tails of histones H3 and H4 (Figure 1-8) are especially important for transcriptional regulation of numerous genes and it has been shown that mutations in these histone tails result in both derepression and reduced activation of the genes (Durrin et al. 1991; Mann and Grunstein 1992).

Histone acetylation is thought to be a dynamic process, which occurs on actively transcribed chromatin only (Perry and Chalkley 1982). In general, acetylation activity is correlated with transcriptional activation, whereas deacetylation activity is accompanied by transcriptional repression (Hildmann et al. 2007). However, the precise mechanism by which histone hyperacetylation facilitates transcriptional activation has remained elusive. According to the most simplistic model, acetylation of lysines in the histone tails neutralizes their positive charge, thereby weakening electrostatic interactions with DNA (Hong et al. 1993) and interactions between neighbouring nucleosomes (Luger et al. 1997). Accordingly, gene transcription only occurs when the chromatin structure is opened up, with unwinding of DNA so that RNA polymerase II and basal transcription complexes can now bind to the DNA to initiate transcription.

In addition to histones, a number of non-histone proteins, mainly transcription factors, are regulated also by de-/acetylation and are specifically targeted by HDACs (Spange et al. 2009). The focus in this study was to investigate the function of HDAC inhibition in inflammation, which will be detailed in section 1.4.3.

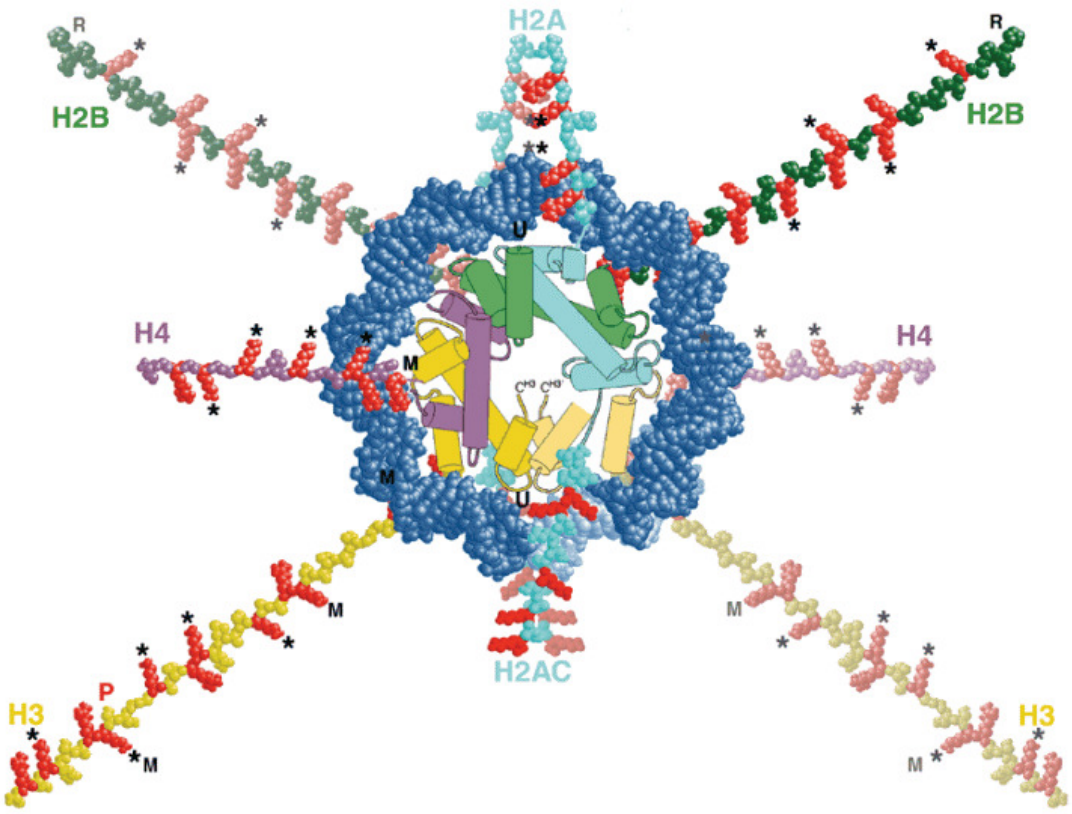

Figure 1-8 Sites of post-translational modifications within the histone tail domains (Wolffe and Hayes 1999)

Sites of post-translational modifications within the histone tail domains. The histone tail domains and the nucleosome core proper are viewed along the superhelical DNA axis. The tail domains are modeled as fully extended polypeptide chains to show the approximate length of these domains with respect to the largely [alpha]-helical histone fold domains (columns). Tail sequences are positioned according to the X-ray crystal structure of a nucleosome core (6). The top and bottom superhelical turns of core DNA are colored blue and light blue, respectively. H2A, H2B, H3 and H4 are colored cyan, green, yellow and magenta, respectively, while arginine and lysine residues in the tails are colored red. The H2A C-terminal tail is indicated as H2AC. Note that only the top four polypeptides are shown in their entirety; a portion of H3 from the bottom half of the nucleosome is shown (light yellow). Likewise, tails from histones in the bottom half of the nucleosome are shaded lighter than those from the top half. Well-characterized sites of acetylation on lysines are indicated by an asterisk (1). Sites of methylation (M), the site of phosphorylation (P) in the H3 tail (Ser10), and sites of ribosylation (R) and ubiquitination (U) in H2A and H2B are also indicated (1). Note that other sites of modifications such as phosphorylation of the N-terminal serines of H2A and H2B are not represented here.

1.4.2 Histone deacetylases

Eighteen HDAC isoenzymes have been identified and divided into four classes based on their homology to yeast deacetylase proteins (see Table 1-3). Different HDACs function in various subcellular compartments. Class I HDACs include the HDAC1, -2, -3, and -8 isoforms. These enzymes are ubiquitously expressed and have a predominant nuclear localization, except HDAC3. Class II HDACs, which include HDAC4, -5, -6, -7, -9, and –10, are further divided into two subclasses: IIa (HDAC4, -5,

-7, and -9) and IIb (HDAC6 and -10). These are cytosolic enzymes and have a more restricted tissue pattern of expression. Class IIa HDACs and HDAC10 are regulated by phosphorylation-dependent nucleocytoplasmic shuttling, whereas HDAC6 is mainly localized to the cytoplasm. Class III HDACs include sirtuins 1-7, whereas HDAC11 is the only member of class IV HDAC and shares properties of both class I and II HDACs (Hildmann et al. 2007). Classes I, II, and IV are closely related zinc-dependent enzymes and regarded as classical HDACs, whereas class III HDACs or sirtuins are structurally unrelated nicotinamide adenine dinucleotide (NAD)-dependent deacetylase enzymes (Grozinger and Schreiber 2002). Histone deacetylase (HDAC) modulate gene expression by increasing acetylation of histone proteins (Strahl and Allis 2000). Histone deacetylases can be recruited to specific promoters, whereupon they serve as transcriptional regulators (Struhl 1998; Kouzarides 1999). Further, as mentioned above, the HDACs have also many non-histone protein substrates, such as DNA binding transcription factors, steroid receptors and chaperone proteins (see Table 4), and they are also involved in regulation of gene expression, cell proliferation or cell death, thus, HDACs are more properly called “lysine deacetylases” or just deacetylases (Xu et al. 2007).

Table 1-3 Human histone deacetylases (Walkinshaw et al. 2008)

Class	Enzyme	Protein length (amino acids)	Catalytic domains	Mechanism	Subcellular localization
1	HDAC1	482	1	Zn^{2+}-dependent	Nuclear
	HDAC2	488	1	Zn^{2+}-dependent	Nuclear
	HDAC3	428	1	Zn^{2+}-dependent	Nuclear/cytopl.
	HDAC8	377	1	Zn^{2+}-dependent	Nuclear
2 a	HDAC4	1,084	1	Zn^{2+}-dependent	Nuclear/cytopl.
	HDAC5	1,122	1	Zn^{2+}-dependent	Nuclear/cytopl.
	HDAC7	855	1	Zn^{2+}-dependent	Nuclear/cytopl.
	HDAC9	1,011	1	Zn^{2+}-dependent	Nuclear
2 b	HDAC6	1,215	2	Zn^{2+}-dependent	Nuclear/cytopl.
	HDAC10	669	2	Zn^{2+}-dependent	Nuclear/cytopl.
3	SIRT1-7	310–747	1	NAD^{+}-dependent	Nuclear/cytopl.
4	HDAC11	347	1	Zn^{2+}-dependent	Nuclear

Table 1-4 Non-histone substrates of HDAC [partial list, adpted from (Xu et al. 2007)]

Function	Proteins
DNA binding Transcriptional factors	p53, c-Myc, BCL-6, E2F1, E2F2, E2F3, GATA-1, GATA-2, GATA-3, GATA-4, Ying Yang 1 (YY1), NF-κB (RalA/p65), TFIIF, CREB
Steroid receptors	glucocorticoid receptor, androgen receptor, estrogen receptor α
Transcription coregulators	Rb, DEK, MSL-3, HMGI(Y)/HMGA1, CtBP2
Signalling mediators	STAT3, Smad7, b-catenin, IRS-1
Inflammation mediator	HMGB1
DNA repair enzymes	Ku70, WRN, TDG, NEIL2, FEN1
Nuclear import	Rch1, importin-α7
Chaperone protein	HSP90
Structural protein	α-Tubulin

In recent years, understanding about the biological roles of HDACs is getting enhanced, however, a wealth of issues remain unexplored. HDAC has an important role in epigenetic control of gene expression, but surprisingly, significantly less than 10% of all genes seem to be regulated by HDACs, as has been revealed by various HDAC inhibitor-induced gene expression profiling studies (Della Ragione et al. 2001; Glaser et al. 2003). One reason could be that HDACs generally do not act autonomously but as components of large multiprotein complexes that mediate important transcription regulatory pathways (Hildmann et al. 2007). Another point is that the role of HDAC in the regulation of non-histone proteins is getting more and more interesting. For example, reversible acetylation of transcriptional regulators such as GR, p53, NF-κB, GATA1, and TFIIF may affect their DNA-binding properties (Minucci and Pelicci 2006) and hence their regulatory effects. In addition, acetylation of lysine residues in a target protein can prevent these from ubiquitination. Deacetylation, therefore, could promote ubiquitination and, thus, decreases the half-life of the protein (Gronroos et al. 2002). Furthermore, it is possible that acetylation is also a means of modulating the catalytic activity of an enzyme, directly or indirectly (Arendt and Hochstrasser 1999), as it is known for phosphorylation (Hurley et al. 1990). All of these

points need to be investigated in more details to elucidate the versatile biological roles of HDAC.

Taken together, HDAC signaling pathways connect to the broad nuclear signaling networks that regulate gene expression and other cellular processes, which can play a key role in numerous physiological and pathophysiological processes.

1.4.3 Role of HDAC in inflammation and steroid insensitivity in COPD

HDACs play a crucial role also in regulation of inflammatory gene expression. As explained in section 1.1.1, the chronic inflammation in COPD is associated with increased expression of multiple inflammatory proteins, including cytokines, chemokines, inflammatory enzymes and receptors. Increased expression of these inflammatory proteins is mainly regulated by pro-inflammatory transcription factors, such as NF-κB and AP-1 (Barnes 2006c). Precisely, when pro-inflammatory transcription factors are activated, they bind to specific recognition sequences in DNA and subsequently interact with large coactivator molecules, such as CREB-binding protein (CBP), p300 and p300/CBP-associated factor (PCAF), all of which have intrinsic histone acetyltransferase (HAT) activity (Barnes 2008). These coactivator molecules act as the molecular switches that control gene transcription. Conversely, inflammatory gene repression may be mediated via HDAC and other corepressors. These fundamental mechanisms of the inflammatory gene regulation as a reversible process are depicted in Figure 1-9 (Barnes 2008).

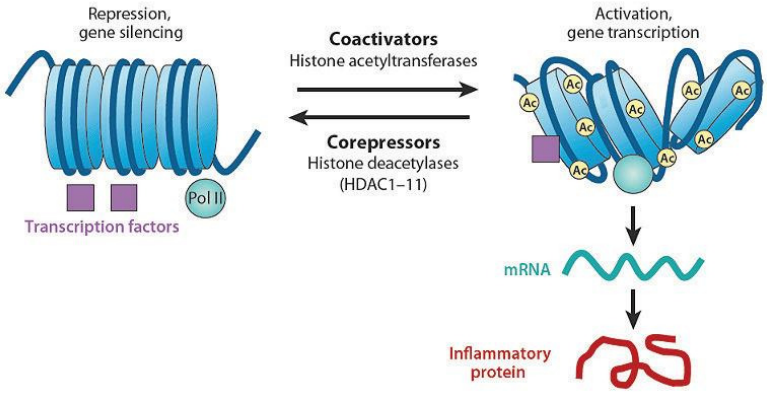

Figure 1-9 Chromatin remodeling and gene expression in inflammation (Barnes 2008)

Acetylation of core histones regulates gene activation and repression. Histone acetylation is mediated by coactivators that have intrinsic histone acetyltransferase activity, opening up the chromatin structure to allow the binding of RNA polymerase II (Pol II) and transcription factors. Gene repression is induced by histone deacetylases with corepressors, which reverse this acetylation.

Reduced HDAC2 activity may account for the increased lung inflammation in COPD. In COPD peripheral lung, airway biopsies, and alveolar macrophages, there is an increase in the acetylation of histones associated with the promoter region of inflammatory genes (Ito et al. 2005). This increase of histone acetylation is not correlated with increase of HAT activity but with a reduction in total HDAC and especially HDAC2 activity as well as a selective reduction in the expression of HDAC2, with lesser reductions in HDAC3 and HDAC5. The reduction in HDAC/HDAC2 activity in COPD may be secondary to oxidative and nitrative stress as a result of cigarette smoking and severe inflammation. However, the mechanisms whereby oxidative stress leads to impairment in activity of HDAC/HDAC2 are complex and remain to be determined. Oxidative and nitrative stress, which might lead to tyrosine nitration (Ito et al. 2004), phosphorylation (Adenuga et al. 2009), and ubiquitination (Osoata et al. 2009b) of HDAC2, may cause a loss of its activity and its degradation.

In the presence of excessive nitric oxide formation, oxidative stress might generate peroxynitrite, which nitrates tyrosine residues on HDAC2 and other proteins. This theory could be directly investigated by measurement of nitration of tyrosine residues on HDAC *in vitro*, and there is already some evidence for nitrotyrosine formation in alveolar macrophages in COPD (Ito et al. 2004). In the present work, it was intended to study the involvement of nitrative stress from iNOS-derived NO in epithelial cell model of steroid insensitivity.

The mechanisms that lead to a reduction of HDAC2 expression are still not clear. On one hand, in COPD lung in parallel with the reduced protein expression of HDAC2, there was also a reduction in its messenger RNA, suggesting that there may be a reduction in transcription of the HDAC2 gene or a reduced stability of its mRNA (Barnes 2008). On the other hand, Osoata et al have demonstrated recently in human lung epithelial cell line A549 that reduction in HDAC2 protein expression under nitrative stress was not due to greater instability of mRNA nor to reduced gene transcription but was due to increased proteasomal degradation following nitration of Y253 of HDAC2 (Osoata et al. 2009b).

It has been shown that for the regulation of inflammatory genes, HDAC2 is of critical importance (Ito et al. 2000; Ito et al. 2006b). In peripheral lung tissue of COPD patients it has been demonstrated that the reduction in HDAC2 expression and activity is

correlated with increased histone H4 acetylation at the κB binding site in the native IL-8 promoter and enhanced expression of IL-8 mRNA (Ito et al. 2005).

Reduction of HDAC/HDAC2 activity and expression in COPD was correlated not only with increased expression of inflammatory genes but also with corticosteroid insensitivity (Ito et al. 2006b). As depicted in Figure 1-3, corticosteroids switch off inflammatory genes through a combination of a direct inhibition of HAT activity and by the recruitment of HDAC2 to the activated NF-κB-stimulated inflammatory genes, such as IL-8 and GM-CSF. Restoration of HDAC2 expression to normal by transfection with a plasmid vector of HDAC2 reversed corticosteroid resistance in these cells, whereas transfection with an HDAC1 vector was without effect (Ito et al. 2006b). The reduction of HDAC2 by oxidative stress may therefore be reversed by antioxidants, peroxynitrite scavengers, theophylline and PI3K inhibitors. It has been shown that theophylline reversed corticosteroid resistance in cells from COPD patients and in smoking mice *in vivo* via inhibition of the PI3K pathway, which is activated by oxidative stress, to restore HDAC2 activity ((Cosio et al. 2004; Marwick et al. 2009). This also provides compelling evidence that the reduction in HDAC/HDAC2 activity and expression in COPD may account for the amplified inflammation and resistance to the actions of corticosteroids.

1.4.4 HDAC inhibitors

The wide range of HDAC inhibitors can be divided into five broad classes: Hydroxamic acid derivates, benzamides, carboxylates, cyclic peptides and electrophilic ketones (Miller et al. 2003). As listed in Table 3, all HDACs except class III HDAC (sirtuins) share a homologue, zink dependent catalytic domain. Since class III HDACs have a different catalytic mechanism to the “classical” HDACs and they are not targeted by the HDAC inhibitors used in this study and the discussion will focus on inhibitors of the “classical” HDACs. Most of these inhibitors contain a metal binding domain that chelates zink and thus, despite structural versatility of these inhibitors most of them work equally effective on all HDACs. Certain HDAC inhibitors may also selectively inhibit different HDACs, e.g. a few molecules can discriminate between class I or class II HDACs or even show an enzyme specific inhibition (Heltweg et al. 2004). The HDAC inhibitors used in this study are Suberoylanilide hydroxamic acid (SAHA), Trichostatin A (TSA) and MS-275 (Table 4). SAHA and TSA are both hydroxamic acid derivates and pan-inhibitors for class I and class II HDACs (Minucci and Pelicci 2006). SAHA is

chemically synthesized and TSA is originally a fermentation product of Streptomyces. MS-275 is a benzamide and class I-specific inhibitor (Blanchard and Chipoy 2005).

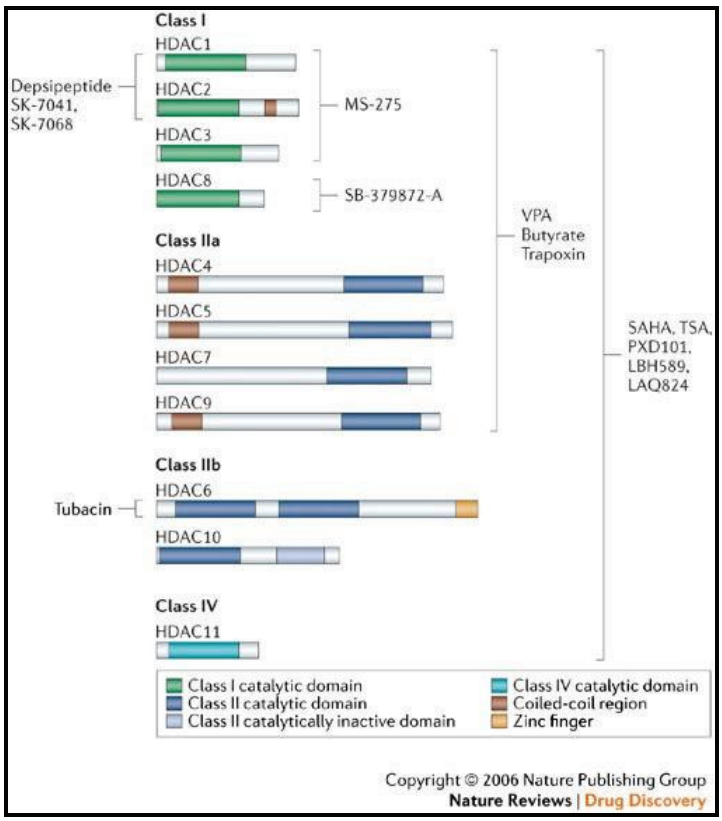

Figure 1-10 Histone deacetylases and inhibitors (Bolden et al. 2006) .

The figure shows the class I (HDAC1,2,3 and 8), class II (HDAC 4-7, 6 and 10) and class IV (HDAC 11) with their functional domains and inhibitors.

Inhibition of HDACs with HDAC inhibitors can have a far-reaching impact on cells because both histone and non-histone proteins involved in regulation of gene expression, cell proliferation and apoptosis can be affected and hence, their functions altered in different pathways. Histone de/-acetylation may directly change gene expression whereas de/-acetylation of non-histone substrates can alter gene expression indirectly via transcription factors. Thus, it is not surprising that inhibition of HDAC activity can result either in induction or repression of gene expression. It has been shown that the amount of up- and down-regulated genes is almost equal. HDAC inhibitors can therefore be regarded as partially epigenetic drugs and their effect can be cell-type and cell-stage specific and dependent on the normal or pathological state of the cell (Minucci et al, 2006).

Table 1-5 HDAC inhibitors used in this study

HDAC inhibitor	Structure	Target	Working concentration (in vitro)	Reference
SAHA	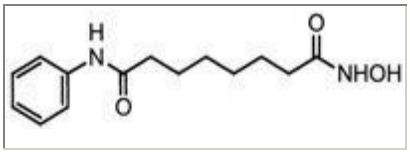	Class I and II HDAC	1-100 nM	(Minucci and Pelicci 2006)
TSA	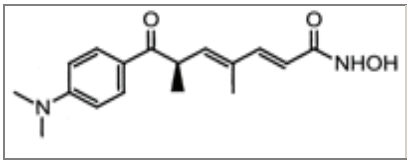	Class I and II HDAC	10-300 nM	(Minucci and Pelicci 2006)
MS-275	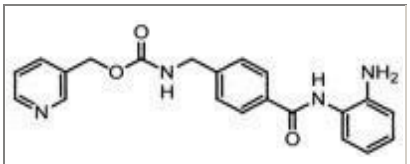	HDAC 1	IC50, 0,3 µM	(Blanchard and Chipoy 2005)
		HDAC 3	IC50, 8 µM	
		HDAC 8	IC50 >100 µM	

1.4.5 HDAC inhibitors as promising therapeutic agents for inflammatory diseases

HDACs have emerged as exciting drug targets for multiple pathological conditions, which can firstly be evidenced by the recent FDA approval of the HDAC inhibitor SAHA as an anti-cancer drug (trade name Zolinza) (Walkinshaw et al. 2008). Moreover, inhibition of HDACs by HDAC inhibitors has exhibited anti-inflammatory effects in various *in vivo* and *in vitro* models of relevant diseases and the analysis of the function of HDAC inhibitors in inflammation is of arising interest, which was also the focus of the present study.

Considering the elaborate discussion above about the correlation between reduced HDAC activity due to oxidative and nitrative stress and increased inflammation and steroid insensitivity, it might sound conflicting now to talk about the function of HDAC inhibitors in inflammatory diseases. But in the light of the substrates plurality and the function versatility in different cell processes of HDACs, it is not surprising that HDAC inhibitors have demonstrated pronounced anti-inflammatory effects besides their effects in the treatment of cancer. In fact, the effects of HDAC inhibitors have been described and discussed in various *in vivo* and *in vitro* models of inflammation. Leoni and colleagues showed that SAHA inhibited the secretion of TNFα, IL-1β, IL-6, and IFNγ in LPS-treated PBMC, and also inhibited their *in vivo* production as shown in an LPS-treated animal model (Leoni et al. 2002; Leoni et al. 2005). Klampfer et al. could even show that the HDAC inhibitors butyrate, SAHA and TSA inhibit the signaling by

IFN-γ and thus negatively regulated the expression of IFN-γ responsive genes (Klampfer et al. 2003; Klampfer et al. 2004). Another group (Carta et al. 2006) showed that SAHA inhibits IL-1β secretion in human monocytes. It has been recently revealed that HDAC inhibitors have anti-inflammatory activities via suppression of cytokines and nitric oxide (Blanchard and Chipoy 2005), TSA was shown to inhibit IL-8 expression in Caco-2 cells and IL-12 expression in SV-40-transformed lung epithelial cell line BEAS-2B (Hoshimoto et al. 2002; Iwata et al. 2002) and strongly decrease various NF-κB target gene expression induced by TNFα in A549 cells (Imre et al. 2006). Recently, TSA and butyrate have also been shown to suppress IL-1ß-induced iNOS and COX-2 expression (Chabane et al. 2008). Data from our research group in Nycomed have demonstrated that various HDAC inhibitors downregulated TLR4, 7, 8 and inhibited IL-6, TNF-α and IP10 production in PBMC, reduced GM-CSF release from human lung epithelial cells, TNFα from monocytes, IL-2 from T lymphocytes and inhibited also T lymphocyte proliferation (Imre et al. 2006; Boehm et al. 2007). Additionally, HDAC inhibitors have also demonstrated beneficial effects in *in vivo* model of inflammatory diseases such as multiple sclerosis (Gray and Dangond 2006) and lupus erythematosus (Mishra et al. 2003).

On the other hand, HDAC inhibitors can have opposing effects on the expression of inflammatory genes depending on the cell type and stimulus used (Dinarello 2006). Also inhibition of different HDAC isoforms shows positive or negative regulatory effects in the same inflammatory model. Using RNA interference Nuzinzon et al. showed that HDAC1, HDAC8, and HDAC6, influence IFNβ gene expression with opposing effects in response to viral infection. While HDAC1 and HDAC8 repress IFNβ expression, HDAC6 acts as a coactivator essential for enhancer activity (Nusinzon and Horvath 2006).

These controdictionary effects of HDACs and HDAC inhibitors in inflammation need further clarification. Trying to understand the essential mechanisms underlying the functional role of HDAC inhibitors in inflammation could help to find new therapeutic opportunities for the treatment of inflammatory diseases, especially COPD,

2 Aims of the study

COPD is characterized primarily by chronic local and systemic inflammation. There are no drug therapies available that have been shown to effectively prevent disease progression or reduce mortality. Moreover, insensitivity to inhaled corticosteroids has been shown for a majority of COPD patients. Thus, trying to understand lung inflammation and steroid insensitivity in COPD and to find new effective drugs to help the patients is a challenging task.

Oxidative and nitrative stress from cigarette smoke and cellular ROS/RNS appears to play a pivotal role in amplified inflammation in COPD by stimulating pro-inflammatory mediator release and tissue destruction. Furthermore, it appears to be an underlying cause of steroid insensitivity in COPD through tyrosine nitration of HDAC2 by peroxynitrite.

iNOS-derived NO has been recognized as an important trigger of inflammation and a source of nitrative stress through formation of peroxynitrite with superoxide. Highly selective and potent iNOS inhibitors have been developed by Nycomed. These inhibitors are capable of attenuating inflammation through inhibition of inflammatory cell recruitment and pro-inflammatory cytokine release in various *in vivo* rat and mouse models of inflammatory disease, including a steroid insensitive smoke mouse model of COPD. Whereas *in vivo* studies revealed the anti-inflammatory effect of specific iNOS inhibitors, their function in controlling inflammation in various *in vitro* cell models was largely unknown. Furthermore, human lung epithelial cells play an important role in lung inflammation as effector cells by producing various pro-inflammatory cytokines and chemokines. Therefore the first intention of the present study was to demonstrate that iNOS inhibitors exert anti-inflammatory functions in lung epithelial cells.

Second, we aimed to test the hypothesis that nitrative stress both from iNOS and from NO donors plays an important role in steroid insensitivity in human lung epithelial cells, possibly through formation of peroxynitrite and nitration of HDAC2, leading to a decline in the anti-inflammatory action of steroids in a human lung epithelial cell model of steroid insensitivity.

The anti-inflammatory role of steroids is mainly mediated through gene transcription regulation via glucocorticoid receptors (GR), where specific HDACs are of underlying

importance as co-repressors. Thus, we also aimed to analyze the link between steroid function and HDAC inhibition.

Moreover, in recent years, HDAC inhibitors have emerged as possible anti-inflammatory drugs. However, the mode of action of HDAC inhibitors is still controversial. Thus, by exploring the functional role of several HDAC inhibitors in human lung epithelial cell model of inflammation the effect of HDAC inhibition in inflammation should be studied.

The following stepwise approaches were proposed:

(I) To characterize human lung epithelial cell models to study lung inflammation *in vitro*.

(II) To evaluate iNOS mRNA expression and NO production in human lung epithelial cell line A549 and study the anti-inflammatory effects of iNOS inhibitors in human lung epithelial cell models of inflammation.

(III) To identify a lung epithelial cell model of steroid insensitivity and test the hypothesis of iNOS involvement in this cell model by modulating iNOS expression and NO level in the cells and analyzing their functional impact on steroid sensitivity.

(IV) To examine the putative interaction between the anti-inflammatory function of dexamethasone and HDAC inhibition using HDAC inhibitors

(V) To explore the functional effects of HDAC inhibitors in lung epithelial cell models of inflammation by assessing cytokine release and expression as well as histone acetylation at the IL-8 promotor during inflammation.

A better understanding of the role of iNOS and HDAC in lung epithelial cell model of inflammation and steroid insensitivity may help to explain inflammation and steroid insensitivity in COPD. Furthermore, detailed information about functional effects of iNOS and HDAC inhibitors in these cell models may help to define the rationale for the development of iNOS inhibitors and specific HDAC inhibitors that have an improved therapeutic profile.

3 Materials and methods

3.1 Materials

3.1.1 Chemicals

All chemicals not specifically mentioned were of analytical grade and were obtained from Sigma-Aldrich (Steinheim, Germany), Roth (Karlsruhe, Deutschland) or Merck (Darmstadt, Germany).

3.1.2 Reagents and kits

Table 3-1. Reagents and kits

Reagent / Kit	**Manufacturer**
Lumi Light^{Plus} Western Blot Substrate	Roche (Penzberg, Deutschland)
ELISA GM-CSF, MCP-1	R&D Systems (Minneapolis, USA)
ELISA IL-8, RANTES	Immunotech (Marseille, France)
Luminex 25-plex	Biosource (Nivelles, Belgium)
Non-Radioactive Cytotoxicity Assay	Promega (Madison, USA)
PCR Nucleotide Mix	Roche (Mannheim, Germany)
Precast Precise Protein Gels	Pierce (Rockford, USA)
QIAshredder Spin Columns	Qiagen (Hilden, Germany)
RC DC Protein Assay	Bio-Rad Laboratories (Muenchen, Germany)
RNeasy Mini Kit	Qiagen (Hilden, Germany)
SimpleChIP™ Enzymatic Chromatin IP (magnetic beads)	Cell Signaling Technology (Danvers, USA)
SuperFect Transfection Reagent	Qiagen (Hilden, Germany)
TaqMan Gene Expression Assays	Applied Biosystems (Darmstadt, Germany)

3.1.3 Buffers and solutions

Buffers and solutions were either provided by the manufacturer as content of various kits or were prepared as following.

Table 3-2. Buffers and solutions

% = w/v for solid substances and v/v for liquid substances. If not otherwise stated, buffers were prepared at room temperature.

Buffer / Solution	**Composition**
RNA lysis buffer	RLT buffer (Qiagen), 1% 2-mercaptoethanol

Lysis buffer (Western lysis buffer)	50mM Tris (TRIZMA® BASE) (pH 8,0), 150mM sodium chloride, 0,02% sodium azide, 1% NP-40, 0,5% Na-Desoxycholat, 0,2% SDS freshly added (10ml): 1mM Na-Vanadat (Tyrosin-Phosphatase inhibitor), 100µg / ml PMSF (Protease inhibitor), "Complete Mini" (Protease inhibitor cocktail tablets, Roche), 2µl/ml Benzonase (DNAse), 20mM Natrium fluorid (Serin/Threonin Phosphatase)
Laemmli running buffer	25 mM Tris-HCl pH 6.8, 192 mM glycin, 0.1% SDS
5 x SDS sample buffer	50 mM Tris-HCl pH 6.8, 12% glycerol, 4% SDS, 0.01% Coomassie Brilliant Blue G-250, 4% 2-mercaptoethanol
TBE	100 mM Tris-HCl pH 7.5, 100 mM boric acid, 2.5 mM EDTA
TBS	20 mM Tris-HCl pH 7.5, 100 mM sodium chloride
TBS-T	20 mM Tris-HCl pH 7.5, 100 mM sodium chloride, 0.05% Tween 20
10 x blotting buffer	250 mM Tris-HCl pH 8.3, 1.92 M glycin, 10% methanol, 0.01% SDS
Blocking buffer	5% non-fat dried milk in TBS-T buffer
Lysis buffer (HDAC assay)	50mM TRIS (TRIZMA® BASE), pH 8,0 (HCl), 137mM NaCl 2.7mM KCl, 1mM $MgCl_2$, 1% NP-40
Trypsin buffer (HDAC assay)	50mM TRIS (TRIZMA® BASE), pH 8,0 (HCl), 100mM NaCl
Developing buffer (HDAC assay)	0,5mg Trypsin / ml Trypsin buffer + 10µM TSA

3.1.4 Inhibitors

The iNOS inhibitors 1400W and AMT were purchased from Alexis Biochemicals, BYK191023 and BYK402750 were synthesized internally at the chemical facilities of Nycomed GmbH (Konstanz, Germany)

The HDAC inhibitor TSA was purchased from Calbiochem, SAHA and MS-275 were synthesized internally at the chemical facilities of Nycomed GmbH.

The inhibitors were generally dissolved as stock solution in DMSO, stored at –20°C and diluted to final concentrations in assay medium during the experiments. Generally

the final concentrationsd of DMSO did not exceeded 0,1%. To exclude any solvent influence on the experiment control cells were treated with vehicles. The cells were incubated with inhibitors 30 minutes prior to the stimulation with cytokines.

3.1.5 ROS and RNS generation

3 -Morpholinosydnonimine hydrochloride (SIN-1)

SIN-1 (Sigma) was used as $ONOO^-$ donor from 100 µM to 1 mM. Because of its short half life (30 min at 37 ℃) SIN-1 was freshly prepared as stock solution in PBS prior to cell stimulation and kept on ice before dissolved in assay medium.

Hydrogen peroxide (H_2O_2)

Hydrogen peroxide was used as resource for oxidative stress at a concentration from 10 µM to 100 µM. It was freshly prepared as stock solution in PBS before cell treatment and kept on ice before dissolved in assay medium.

Cigarette smoke extract (CSE)

CSE was prepared freshly before every experiment using an automatic rotary smoking machine from the toxicological research department of Nycomed GmbH. In the present study, the gas phase of the cigarette smoke was collected and applied for the CSE experiment. 30 cigarettes without filter (Kentucky research cigarette 2R4F) were puffed by the suction of a pump with 8 puffs/cigarette. The smoke was bubbled through 100 ml of DMEM medium and the resulting suspension was sterile filtered through a 0.45 µm pore filter to remove bacteria and large particles. Subsequently, the absorption over the entire spectrum from 230 nm to 550 nm was measured and the pattern of absorbance (spectrogram) observed at 260 nm, showed very little difference between different preparations of CSE: it had a typical peak at 260 nm with an OD value of around 0.7, which was set as 100% CSE. For each CSE preparation the OD value at 260 nm was detected and calculated proportionally according to the 100% CSE set at the first preparation. When the OD value at 260 nm of the solution was higher than 0.7, it was diluted with assay medium to 100%. This CSE preparation was applied to A549 cell cultures within 30 minutes of preparation. CSE concentrations in the current study ranged from 1%-10%. (CSE concentrations prepared in this manner of up to 30% after 48 hours exposure did not induce cytotoxicity according to the Alamarblue assay.)

3.1.6 Oligonucleotides

For Real-Time PCR

- 1x random Hexanucleotide Primer Mix as primers for the synthesis of cDNA was from Roche (Roche Pharma AG, Reinach, Switzerland).
- dNTPs PCR-3 Mix were purchased from Larova (Teltow, Germany).
- Forward/reverse primer and probe sets were purchased from Applied Biosystems (Darmstadt, Germany) and are shown below.

Table 3-3. Primer and probe sets designed.

Name, sequence (5'-3'), and final concentration in PCR reactions are indicated. Probes were either VIC- or FAM-labeled.

Gene Name	Primer and probe Sequence (5'-3')	Final conc. [nM]
18S rRNA	Forward: CGGCTACCACATCCAAGGAA	50
	Reverse: GCTGGAATTACCGCGGCT	50
	Probe: VIC-TGCTGGCACCAGACTTGCCCTC	50
iNOS	Forward: GGCTCGTGCAGGACTCACA	900
	Reverse: GAGCCTCATGGTGAACACGTT	900
	Probe: FAM-ACCTCAGCAAAGCCCTCAGCAGCAT	200
IL-8	Forward: GAGCACACAAGCTTCTAGGACAAGA	300
	Reverse: ACGGCCAGCTTGGAAGTCAT	600
	Probe: FAM-CTCACTGTGTGTAAAC	200

Table 3-4: Primers from Assay on demand.

Pre-designed Real-Time PCR assays from Applied Biosystems with 2 unlabeled PCR primers (900 nM each final concentration) and 1 FAM dye-labeled TaqMan® MGB probe (250 nM final concentration)

Name and order number	Reference sequence	Amplicon length (bp)
GM-CSF / Hs00929873_m1	NM_000758.2	85
IL-8 / Hs99999034_m1	NM_000584.2	81
TLR3 / Hs00152933_m1	NM_003265.2	94
TLR4 / Hs00370853_m1	NM_003266	68

For standard PCR

- PCR nucleotide mix from Roche (200 µM final concentration)
- Forward/reverse primers were designed according to the experiment (see below) and purchased from Sigma (10 µM final concentration)

Table 3-5. Primer and probe sets designed for standard PCR.

Gene Name	Primer and probe Sequence (5'-3')	Amplicon Length (bp)
IL-8 Pol II upstream	Forward: ATCATGGGTCCTCAGAGGTCAGAC Reverse: GGTGGGAGGGAGGTGTTATCTAAT	137
IL-8 Pol II Primer 1	Forward: TCAAAGAAAACTTTCGTCATACTC Reverse: TGGCTTTTTATATCATCACCCTAC	174
IL-8 Pol II Primer 2	Forward: AGGGGATGGGCCATCAGTTGCAAA Reverse: TGGTTCCTTCCGGTGGTTTCTTCC	192

3.1.7 DNA and RNA modifying enzymes

- DNAse I, used for on-column DNA digestion, was from Qiagen.
- Reverse transcriptase AMV, used for synthesis of cDNA, was purchased from Roche.
- 2 x TaqMan universal PCR master mix, containing AmpliTaq Gold DNA polymerase, was obtained from Applied Biosystems.
- Thermostable DNA polymerase blend for standard PCR was obtained from Roche (1U / 20 µl PCR reaction)

3.1.8 Antibodies

Table 3-6. Antibodies used for protein immunodetection on Western blots and ChIP assay

Antibody	Manufacturer	Dilution
Monoclonal Anti-Acetylated alpha-Tubulin (mouse)	Sigma-Aldrich (Steinheim, Deutschland)	1:500
Goat anti mouse IgG, peroxidase conjugated	Dianova, Hamburg, Deutschland	1:10000
Goat anti rabbit IgG, peroxidase conjugated	Dianova, Hamburg, Deutschland	1:1000
Monoclonal Anti-alpha-Tubulin (mouse)	Sigma-Aldrich (Steinheim, Deutschland)	1:500
Normal Rabbit IgG, ChIP formulated	Cell Signaling Technology (Danvers, USA)	1:500
Polyclonal Anti-Acetyl-Histone H3 (rabbit)	Cell Signaling Technology (Danvers, USA)	1:1000
Polyclonal Anti-Histone H3, (rabbit)	Cell Signaling Technology (Danvers, USA)	1:500
Polyclonal Anti-Histone H3, ChIP formulated (rabbit)	Cell Signaling Technology (Danvers, USA)	1:50
Polyclonal Anti-Pol II, ChIP formulated (rabbit)	Santa Cruz Biotechnology (Santa Cruz, USA)	1:500

3.1.9 Stimuli for the cell culture

For the stimulation of human lung epithelial cells IL-1β, TNFα and IFNγ were purchased from Tebu-Bio, dsRNA analog polyinosinic Acid polycytidylic Acid (polyIC) from Calbiochem (Darmstadt, Germany). Lipopolysaccharide (LPS) was from Sigma-Aldrich. Cytokines, dsRNA and LPS were dissolved as stock solution in PBS, stored at –20°C and diluted to final concentration in culture medium during the experiments.

Table 3-7. Cytokine, daRNA and LPS used for stimulation of the cells

Stimuli	Concentration
IL-1β	From 10 ng/ml to 100 ng/ml, generally used at 10 ng/ml
TNFα	From 10 ng/ml to 100 ng/ml, generally used at 10 ng/ml
IFNγ	From 10 ng/ml to 100 ng/ml, generally used at 100 ng/ml
Cytokine-mix(CM)	IL-1β 10 , 20 or 100 ng/ml TNFα 10, 20 or 100 ng/ml IFN γ 10, 20 or 100 ng/ml For Griess assay, generally used at cytokine combinations of 100 ng/ml
dsRNA	Generally100 ng/ml, also 200 and 400 ng/ml as indicated in the diagramms
LPS	1 and 10 μg/ml

3.1.10 Primary cells and cell lines

The alveolar type II epithelium-like cell line A549 is derived from human lung adenocarcinoma and was purchased from ATCC (Wesel, Germany).

The human bronchial epithelium cell line BEAS-2B is transfected with adenovirus-12 and SV40 hybrid virus and was purchased from ATCC (Wesel, Germany).

Both A549 and BEAS-2B cells are adherent cells and were grown on surfaces of special tissue culture flasks.

Primary cell MucilAir™ is a human airway epithelium reconstituted *in vitro* with cells isolated from human respiratory tracts and were obtained from Epithelix (Geneva, Switzerland). The differentiation of the airway epithelial cells was initiated by culturing the cells at an air-liquid interface and was evidenced by the formation of besting cilia. Each reconstituted epithelium contains about 400,000 cells

3.1.11 Cell culture media

For A549 cells

- A549 culture medium: DMEM (GIBCO, Invitrogen, Cat. No: 41965, 4500 mg/L D-glucose, Phenol Red) with 5% foetal calf serum (FCS), 100 µg/ml penicillin/streptomycin (P/S), 8mg/ml pyruvate
- A549 iNOS assay medium: DMEM (GIBCO, Invitrogen, Cat. No: 11880, 1000 mg/L D-glucose, w/o Phenol Red), 0,5% FCS, 100 µg/ml penicillin/streptomycin (P/S) and 2 mM L-glutamine.

For BEAS-2B cells

- BEAS-2B culture medium: BEBM (Cambrex, Cat. No. CC-3171) complemented with Supplement kit (Cambrex, Cat. No. CC-4175) containing BPE, Insulin, Hydro Cortison (HC), GA1000, Retinoic acid, Transferrin, Triiodothyronine and hEGF
- BEAS-2B assay medium: BEAS-2B culture medium without HC
- BEAS-2B plate coating medium: 98 ml BEBM (without supplement)
  + 1 ml 0.1% Fibronectin solution (Stock: 1.0 mg/ml, end conc. 0.01 mg/ml)
  + 1 ml 0.3% Vitrogen 100 (Stock: 3.0 mg/ml, end conc. 0.03 mg/ml)
  + 100 µl 1% BSA in DPBS (Stock: 1% BSA in DPBS, end conc. 0.01 mg/ml)
- Trypsin/EDTA for BEAS-2B cell detaching (100ml Cambrex, Art. CC-5012)
- TNS stop solution (100ml Cambrex, Art. CC-5002)

For Mucil Air cells

- MucilAir cell culture medium is ready-to-use and specifically designed for culturing MucilAir cells.

3.1.12 Devices and softwares

Table 3-8. Devices with type and manufacturer information

Devices	Type	Manufacturer
Biological Safety Cabinet	Hera Safe Biological Safety Cabinet	Thermo/Kendro, Hudson, USA
Cell counter	Z2 COULTER Counter	Beckman Coulter, Krefeld, Germany
Centrifugation	Megafuge 3.OR	Heraeus Instruments, Canada
Centrifuge	Centrifuge 5403	Eppendorf AG, Hamburg, Deutschland
Centrifuge	Centrifuge 5417R	Eppendorf AG, Hamburg, Deutschland
Cytokine assessment	Luminex 100	Luminex, Austin, USA
Electrophoresis system	Mini-PROTEAN II	Bio-Rad, Hercules, USA

Fluorescence microscope	Axioplan 2 Imaging	Zeiss, Oberkochen, Deutschland
Fluorescence microscope camera	AxioCam	Zeiss, Oberkochen, Deutschland
Homogenization of cells	Sonoplus HD 2070	Bandelin, Berlin, Deutschland
Incubator	Heraeus incubator	Heraeus Instruments, Canada
Light microscope	Microscope DM IRB	Leica, Wetzlar, Deutschland
Luminescence	luminescence image analyzer	Fujifilm, Duesseldorf, Germany
Luminex	Luminex 100 system	Biosource (Nivelles, Belgium)
Mixer	Thermomixer	Eppendorf AG, Hamburg, Deutschland
Multilabel counter	Victor 2 Plate reader	PerkinElmer/Wallac, Monza, Italy
pH Meter	pH Meter Seven Easy	Mettler Toledo
Pipette	2,5, 10, 20, 100, 200, 1000 [µl]	Eppendorf AG, Hamburg, Deutschland
Pipette, Multi Channel	12,5, 250, 1250 [µl]	Thermo Fisher Scientific, Hudson, USA
Precision balance	BP 61S	Sartorius, Göttingen, Deutschland
Pump station	Pump station Vacusafe	Integra Bioscience
SDS-Gelelektrophoresis	Power Pac Basic	Bio-Rad, Hercules, USA
SDS-Gelelektrophoresis	Trans Blot	Bio-Rad, Hercules, USA
Sequence detection system	ABI Prism 7900 HT	Applied Biosystems
Shaker	Thermostar	Biomedizintechnik Dr. Gurath GmbH, Offenburg, Deutschland
Spectrometer	SPECTRA Rainbow reader	Tecan, Mannedorf, Switzerland
Water bath	Water bath Thermostat	Julabo, Seelbach, Germany

Softwares

The SDS 2.1 software for TaqMan Real-Time PCR analysis (Applied Biosystems), the easyWIN fitting 6.0a software for an a SPECTRA Rainbow reader (Tecan, Mannedorf, Switzerland), an Aida image analyzer 3.22 software (Raytest, Straubenhardt, Germany) for Western blot analysis and the 2100 Expert software for the Agilent 2100 Bioanalyzer were used in the present study.

3.2 Cell culture

3.2.1 Thawing and Freezing of cell lines

Cell line A549 and BEAS-2B were thawed for culturing and frozen for storage as described below.

Frozen cells (stored in liquid nitrogen) were thawed in a water bath, quickly removed from the cryovial, and transferred to 10 ml complemented A549 medium (4°C). The cells were pelleted, resuspended in prewarmed medium (37°C), and cultivated in cell culture flasks, as described above. For long-term storage of A549 cells, 2.5 x 10^5 cells were pelleted and resuspended in 1 ml medium containing 40% DMEM, 40% FCS,

and 20% DMSO. Cells were frozen in cryovials with ~ -1 °C/min at -80 °C and were then transferred to the nitrogen storage unit.

3.2.2 A549 cells

Adherent A549 cells were cultivated in T-75 culture flasks in A549 medium in a humidified incubator at 37 °C, 5% CO_2. At about 90% confluence, the medium was removed and the cells were washed with 10 ml PBS. For detaching, cells were treated for 3 min with 5 ml pre-warmed trypsin (0.05% trypsin with EDTA, 1 x solution, Invitrogen). The trypsin incubation was stopped with fresh pre-warmed medium, and the cells were centrifuged for 5 min at 1200 rpm. The cells were then resuspended in growth medium (5 ml/fl) and one fourth of the cells were subject for further cultivation.

3.2.3 BEAS-2B cells

Adherent BEAS-2B cells were cultivated in T-75 culture flasks in a humidified incubator at 37 °C, 5% CO_2. Coating solution was required to ensure the adhesion of the cells on the growth surface. It was prepared as described and stored at 4 °C. This solution should not be warmed before coating, which can provokes a gel formation. Prior to splitting or seeding of the cells, the flasks or plates were treated with coating solution (for 75 cm^2 flasks: 5 ml/fl, for 24- well plates: 300µl/well) and the precoated dishes were put into a CO_2 incubator at 37 °C and incubated for at least 1 hour.

For subculturing growth medium was removed and cells were rinsed with PBS (10 ml/fl). 5 ml Trypsin/EDTA solution was added and the flask stayed about 5 minutes at 37 °C, until they began to detach. Through tapping the side of the flask all attached cells could be released. To stop detaching 10 ml trypsin inhibitor TNS was added. The cells in suspension were centrifuged for 5 min at 1500 rpm and then resuspended in growth medium (5 ml/fl). The cell number was quantified with cell camber and the cells were splitted according to their density or seeded according to the experimental settings.

3.2.4 MucilAir cells

Primary lung epithelial cells MucilAir (from Epithelix, Geneva) were grown in air-liquid interface culture in a transwell of 6.5 mm of diameter, with a pore size of 0.4 µm, in a humidified incubator at 37 °C, 5% CO_2. Each well contained about 400,000 cells.

The differentiation of the airway epithelial cells was initiated by culturing the cells at air-liquid interface, and was evidenced by the formation of beating cilia. (Once differentiated, the epithelium will remain at a homeostasis state for several months, accordingly to the information of the manufacturer). The maintenance of MucilAir requires a specific culture medium, which was delivered with the cells. The medium was changed every 2-3 days. To do this, in a new 24-wells plate 0.5 ml culture medium, pre-warmed up to 37°C, was filled in the wells and the inserts with the cells were transferred to the new plate with a forceps.

In order to clean up the secretion from the surface of the cells, a wash procedure was conducted at least every two weeks. The apical and basal surface of the inserts was washed 3 times with culture medium: For washing the basal surface of the insert, the inserts were incubated for 5 min in a well filled with 0.5 ml of culture medium at 37°C and this procedure was repeated 3 times; For washing the apical surface of MucilAir cells, the inserts were incubated for 5 min with 200 µl culture medium at 37°C. The apical solution was carefully removed from the cell surface with a pipette without disturbing the epithelium. This procedure was also repeated for 3 times.

3.3 Cell treatment with stimuli and substances

3.3.1 Stimulation and substance treatment of A549 and BEAS-2B cells

Generally, for stimulation and substance treatment A549 and BEAS-2B cells were treated using the same protocol. The numbers of the cells seeded for the experiments were cell-type dependent. For A549 cells 4 x 10^5 cells were seeded per well in 24-well plates in 500 µL culture medium or 2x10^4 cells in 96-well plates in 200 µL culture medium. For BEAS-2B cells 3 x 10^5 cells were seeded per well in 24-well plates in 500 µL culture medium or 3x10^4 cells in 96-well plates in 200 µL culture medium.

For ELISA and Griess assay

Cells were cultured as described above (section 3.2). After reaching confluence, cells were seeded in 24-well plate or 96-well plate and incubated for 24 hours at 37°C, 5% CO_2. Afterwards the cells were stimulated at least as duplicates with different stimuli in assay medium. Alternatively, the cells were pre-treated with iNOS or HDAC inhibitors and/or dexamethasone at different concentrations for 30 min before stimulation. After another 20 to 24 hours incubation the supernatant was collected for

cytokine/chemokine assessment with ELISA or Luminex multianalyte profiling (MAP) technology and for nitrite and nitrate measurement with Griess assay.

For gene expression with Real-Time PCR

1 x 10^6 cells were seeded per well in 6-well plates in 2 ml culture medium and stimulated after 24 hours incubation at least as duplicates with different stimuli in assay medium. Alternatively, the cells were pre-treated with iNOS- or HDAC-inhibitors and/or dexamethasone at different concentrations for 30 min before cytokine stimulation. According to the experiment the cells were stimulated for 3, 6 12 or 24 hours and afterwards, the cells were washed with PBS and lysed with 350 µl RLT buffer (Qiagen) complemented with 1% 2-mercaptoethanol, and stored at -80°C until RNA isolation for gene expression assessment with TaqMan Real-Time PCR.

Generally, for the study of concentration-dependent effect of dexamethasone on cytokine release, the cells were treated with dexamethasone at end concentrations from 0,1 nM to 10 µM, To achieve the final substance concentrations in the assays at a DMSO concentration of ~0.1% (v/v), stock solutions of dexamethasone (1000x, from 100nM to 10 mM in DMSO) were diluted first 1:50 (v/v) in assay medium and then 25 µl of the substance dilutions were applied in 24-well plate with 475 µl assay medium (dilution 1:20) and 10 µl in 96-well plate with 190 µl assay medium (dilution 1:20). Optionally, the iNOS inhibitor 1400W or AMT were included at a final concentration of ~10 µM and/or ~30 µM, respectively and HDAC inhibitor TSA, SAHA and MS-275 at a final concentration of 10 nM, 1 µM and 1 µM, respectively. Again, to achieve the final substance concentrations at a DMSO concentration of ~0.1% (v/v), for the combination of both, dexamethasone (100nM to 10 mM in DMSO) and 1400W/AMT (10 or 30 mM in DMSO) or dexamethasone and TSA/SAHA/MS-275 (10 µM, 1 mM and 1 mM in DMSO), equal volumes were mixed (dilution 1:2) and subsequently diluted 1:25 (v/v) in medium. 25 µl of the substance dilutions were applied in 24-well plates with 475 µl assay medium (dilution 1:20) and 10 µl in 96-well plates with 190 µl assay medium (dilution 1:20). After incubation of the cells at 37°C, 5% CO_2 for 30 min, the stimuli were added and the cells were further incubated for 24 hours.

3.3.2 Treatment of A549 cells with cigarette smoke extract

In the initial experiments, 5 x 10^3 A549 cells were seeded per well in 96-well plates in 0.2 ml culture medium and after 24 hours incubated at least as duplicates with CSE at

a concentrations of 1, 3, 10, 20 or 30 % for 24 h or 48 h. CSE concentrations prepared in this manner of up to 10% and with a incubation of 48 h did not affect cell viability according to Alarmarblue assay. Therefore, CSE concentrations used in the current study ranged from 1% to 10%.

CSE was prepared as explained above and diluted to 1% and 10% in assay medium according to the experiments. For Real-Time PCR detection of IL-8 mRNA-expression, 1 x 10^6 A549 cells were seeded per well in 6-well plates in 2 ml culture medium and stimulated after 24 hours incubation at least as duplicates with CSE (1 and 10%) in presence or absence of cytokine-mix (10 ng/ml IFNγ, 10 ng/ml IL-1β, 10 ng/ml TNFα) for 3, 6 or 24 h. The cells were then washed with PBS and lysed with 350 µl RLT buffer (Qiagen) complemented with 1% 2-mercaptoethanol, and stored at -80°C until RNA isolation for TaqMan Real-Time PCR.

3.3.3 Stimulation of MucilAir cells

The cells (4 x 10^5 cell/well) were grown on air-liquid surfaces of an insert transwell with apical and basal site with 500 µl culture medium in basal side. One day before stimulation, the medium was changed (500 µl) and the apical side was treated with 200 µl culture medium for 1 h at 37°C, 5% CO_2. Afterwards the apical medium was removed from the cell surface carefully without disturbing the epithelium. The inserts were stored in an incubator at 37°C, 5% CO_2 for 24 h. On the day of treatment, 500 µl of medium with substances were prepared in a new 24-well plate and the inserts were transferred into the new plate which was then incubated in an incubator at 37°C, 5% CO_2 for another 24 h. The remaining medium in the old plate was stored at –20°C for measurement of cytokine levels (background values). 24 h after the treatment, the inserts were transferred to another new plate with culture medium and the remaining medium was collected for the measurement of cytokine release together with the background medium. It could also be stored at –20°C for later measurements.

According to our experiences, one week after removing the stimulators from MucilAir cells, cytokine release would return to the basal level. Another round of stimulation on the same inserts could then be performed.

3.4 Molecular biology methods

3.4.1 RNA isolation and quantification

For expression studies 1 x 10^6 A549 or BEAS-2B cells in 2ml per each well were seeded in 6-well plates and treated as described above. The treated cells were washed in PBS, lysed with 350 µl RLT buffer (Qiagen) supplemented with 1% 2-mercaptoethanol, collected and immediately stored at -80°C. Shortly before RNA isolation, the lysate was thawn and homogenized with QIAshredder spin columns (Qiagen). Subsequently, total RNA was isolated using RNeasy mini columns with silica-gel membranes, according to the instructions of the manufacturer (Qiagen). Briefly, the homogenized lysate was diluted with 1 volume of ice cold 70% ethanol, mixed, and transferred to RNeasy columns. All subsequent steps were performed at RT. After centrifugation and a washing step with 350 µl RW1 buffer, 5 µl of RNase-free Dnase-I in 35 µl RDD buffer (Qiagen) was applied for one on-column digestion of DNA (20 min). The columns were washed once with 350 µl RW1 buffer and twice with 500 µl RPE buffer. RNA was eluted by pipetting 20 µl of nuclease-free water (Eppendorf, Hamburg, Germany) onto the dried membrane, followed by an incubation period of 1 minute and subsequent centrifugation for 1 min at 14000 rpm in a benchtop centrifuge. This elution step was repeated with 20 µl of nuclease-free water. Finally, RNA concentration was determined by OD_{260} measurement using a full-spectrum (220-750nm) spectrophotometer NanoDrop® ND-1000 (Wilmington, USA) according to manufacturer's instruction.

3.4.2 cDNA synthesis and quantitative PCR

In this study, gene expression quantification was carried out using two-step reverse transcription-polymerase chain reactions in which the PCR step was coupled with a 5' fluorogenic nuclease assay (Heid et al. 1996). For reverse transcription of RNA, 1 µg RNA in a volume of 10 µl nuclease-free water (Eppendorf) was incubated for 60 min at 42°C with 1 µl dNTPs (final 0.5 mM each; Larova), 1.5 µl hexanucleotide mix (final 0.75x, Roche), 1 µl AMV reverse transcriptase (final 20 units, Roche), and 4 µl incubation buffer (Roche). Thus, the total volume of the reaction was 20 µl. The cDNA was diluted by the addition of 230 µl of nuclease-free water (Eppendorf) to a concentration of 4 ng cDNA/µl. Total RNA and cDNA obtained were stored at -80°C.

Quantitative Real-Time PCR reactions were performed on an ABI Prism 7900 HT sequence detection system (Applied Biosystems) with primer and probe sets detecting 18S rRNA as internal standard and IL-8, GM-CSF, iNOS, TLR3, TLR4 as target genes (see section 3.1.6). All experiments were carried out as triplicates.

The Real-Time PCR reactions were performed in a total volume of 25 µl in triplicates, each containing 2.5 µl cDNA (10 ng), 1.25 µl per primer and probe detecting *18S rRNA* (0.125 µl in the case of using assay on demand), 1.25 µl per primer and probe detecting the target gene (1.25 µl primer and probe set in the case of using assay on demand), 12.5 µl of 2x TaqMan universal PCR master mix (Applied Biosystems) and 3.75 µl nuclease-free water (8.375 µl nuclease-free water in the case of using assay on demand). The thermal cycler protocol was standardized and consisted of a 2 min period at 50°C (uracil removal for PCR carryover protection), a 10 min period at 95°C (denaturation of native DNA), and of 40 cycles of 15 sec at 95°C (denaturation of PCR product) followed by 1 min at 60°C (annealing/extension). Additionally, water was used as 'template' to test whether the primer and probe sets were DNA-free.

First denaturation and activation of the HotStar Taq DNA polymerase was obtained at 95°C for 10 min after 2 min at 50°C, followed by 40 cycles of amplification (15 s at 95°C and 60 s at 60°C).

3.4.3 Relative expression calculated by the $\Delta\Delta C_t$ method

Quantification of PCR experiments was conducted by using the comparative $\Delta\Delta C_t$ method. The measured fluorescent signal intensities of both the probe detecting *18S rRNA* and the probe detecting the target gene were semilogarithmically plotted against the number of PCR cycles, generating C_t values (cycle at threshold). To normalize for input amounts of RNA within one sample, the C_t of *18S rRNA* was subtracted from the corresponding target C_t, generating the normalized ΔC_t. Untreated cells were then defined as calibrator, and the normalized ΔC_t value of the calibrator was subtracted from all other normalized ΔC_t values of the other samples, generating $\Delta\Delta C_t$ values. As final output, the expression of each sample relative to the calibrator was obtained by calculating $2^{-\Delta\Delta Ct}$.

3.4.4 Standard PCR Method

To detect the enrichment of DNA sequences in ChIP assay standard PCR was conducted. The samples to be analyzed included the 2% input sample, the positive control Histone H3 sample, the negative control Normal Rabbit IgG sample, water control for DNA contamination and the samples of unstimulated, IL-1β-stimulated and stimulated and treated with SAHA (1µM) or TSA (10 nM).

0.5 µl of the appropriate DNA sample was first diluted with 4.5 µl nuclease-free water and then added to the 0.2 ml PCR tube with 1 µl of forward primer, 1 µl of reverse primer (Table 3-5), 9.6 µl nuclease-free H_2O, 2.0 µl 10X PCR buffer (Roche), 1.0 µl 4 mM dNTP mix (Roche), Taq DNA Polymerase 0.4 µl (1U). Additionally, water was used as 'template' to test whether the primer and probe sets were DNA-free.

The thermal cycler (Eppendorf) protocol was standardized and consisted of a 5 min period at 95°C (initial denaturation), of 40 cycles of 30 sec at 95°C (denaturation of PCR products) followed by 30 sec at 60°C (annealing) and 30 sec at 68°C (extension), and of a final 5 min period at 68°C (final extension).

1 µl of each PCR product was removed for analysis by Agilent Bioanalyzer 2100 with a 1000 bp DNA marker. This analysis could show both the concentration and the size of the DNA products precisely. The value of each IP sample was subtracted by the value of the control Normal Rabbit IgG and normalized by the value of histone H3. Afterwards, the amount of immunoprecipitated DNA in each sample was calculated as signal relative to the total amount of input chromatin.

3.5 Biochemical methods

3.5.1 Cell extract and Protein determination

1 x 10^5 A549 cells / well in a 6-well plate were seeded and treated with SAHA or TSA (dissolved in DMSO) at different concentrations following IL-1β stimulation. DMSO-treated samples were used as negative controls. After 24h the cells were washed with cold PBS and then a lysis buffer (300 µl) for Western blot sample was added (Table 3-2) and the cells were incubated for 2 min. The cells were then collected with a cell scraper and then incubated for 30 min on ice by shaking. Then the solution was centrifuged for 20 min at 14.000 rpm, 4°C and the supernatants were stored at –20°C.

Protein determination was performed using DC protein assay kit according to the instructions of the manufacturer (Bio-Rad). 5 µl of lysate was used for the measurement and 1 - 6 µg of BSA stock solution (1 µg/µl, Bio-Rad) in a 1:160 dilution of the lysis buffer were included as standards. Samples were vortexed with the reagent vigorously, incubated for 15 min at RT, and analyzed in a 96-well microplate reader at 750 nm (Rainbow reader, Tecan, Mannedorf, Switzerland).

3.5.2 SDS-Polyacrylamide gel electrophoresis (SDS-PAGE)

For immunoblotting experiments with lysates from A549 cells, SDS-PAGE was performed using 8-16 % precast polyacrylamide gradient gels (Pierce). Gels were prepared according to the instructions of the manufacturer (Pierce) and run in a Mini-PROTEAN II electrophoresis system (Bio-Rad). 12 µg of protein in 23 µl lysis buffer were mixed with 7 µl 5 x SDS sample buffer and incubated at 95°C for 5 min. Samples were loaded onto the gels and were separated with 120 V for 1 h in Laemmli running buffer. Full range prestained Precision Plus Protein Standards (Bio-Rad, 10 - 250 kDa, Dual Color) was used as protein standard. Additionally, for the direct visualizationo of protein standard bands after Westen blot MagicMark XP Western protein standard (20-200 kDa) was also used.

3.5.3 Western blotting and protein detection

Proteins subjected to SDS-PAGE were electroblotted onto a PVDF membrane (Amersham) using a semi-dry blotting system (Multiphor II) with blotting buffer at 100 V for 1h. Nonspecific binding sites were blocked with 5% non-fat dried milk freshly made in TBS-T buffer rocked on the orbital shaker for 1h.

Afterwards blots were rinsed 3 times in TBS-T buffer and incubated with the primary antibody (Table 3-6), diluted in the TBS + 1% BSA, overnight at 4°C on the rotating shaker. On the next day membranes were washed 3 times with TBS-T for 15 min and incubated with horseradish peroxidase-conjugated secondary antibody, diluted in TBS-T for 1h at RT. After the membranes were washed four times in a washing buffer, the immunopositive spots were visualized by using LumiLight-Plus (Roche) as directed by the manufacturer. Image capturing was performed using a LAS-1000 Luminescence Image analyser (Fuji Film). Obtained images were analyzed using the Aida Image Analyzer software.

3.5.4 HDAC activity assay

All HDAC activity measurements were based on a procedure described by Wegener et al. (Wegener et al. 2003). In this study, both cellular and biochemical HDAC activity assays were performed. Cells were either treated with HDAC inhibitors or with SIN-1 and H_2O_2.

HDAC cellular activity assay

A549 cells and BEAS-2B cells were seeded in 96-well plates in the respective assay medium. A549: 10^4 cells/well in 200µl assay medium. BEAS-2B: $5x10^3$ cells/well in 200µl assay medium; the plate was coated with coating solution for at least 1h before cells were seeded. After 24h 1µl of a HDAC inhibitor dilution series (200x) was added (n=4). The dilution series was made in DMSO (dilution factor 1:3,16, final concentration of DMSO: 0,5%). To determine the range of potential inhibition only DMSO (100% activity) and 2 mM TSA in DMSO (0% activity) were also measured. After 4h the medium was removed and 100µl substrate medium with 200 µM Boc-K(Ac)-AMC (Bachem) per well was added. The plates were incubated for another 3h before the wells were washed with 200µl PBS and incubated for 5min with 100µl developing buffer. Another 100µl lysis buffer was added per well and fluorescence was measured after 20min at extinction λ = 355nm and emission of λ = 460nm for 0,1 s. All incubation times were carried out at 37°C and in the dark. The peptide substrate Boc-K(Ac)-AMC added in this assay is first deacetylated through HDACs and can then be cleaved by trypsin. One of the resulting products is a fluorescent molecule and thus, the intensity of the signal is proportional to uninhibited HDACs.

In case of SIN-1 and H_2O_2 treatment the cells were preincubated at RT for 2, 4, 6, 16 or 24h before adding the substrate peptide. Optionally, the treatment with SIN-1 and H_2O_2 was repeated 30 min after the first treatment. After the treatment the medium was removed and 100µl substrate solution was added and the plates were then incubated for 3h at 30°C. Then 100µl developing buffer was added and the plates were incubated for 40min at RT in darkness. Another 100 µl lysis buffer was then added per well and the fluorescence was measured at extinction λ = 355 nm and emission of λ = 460 nm for 0,1 s.

HDAC biochemical activity assay

Biochemical HDAC-assays were carried out with the recombinant enzymes rHDAC-1. Assays were performed in 96-well plates. Recombinant enzyme and substrate peptides were diluted in enzyme buffer. Dilution series (100x) of HDAC inhibitors in DMSO (dilution factor 1:3,16) were made prior to addition. Assays were carried out with HDAC inhibitors SAHA and MS275 (n=4). To determine the range of potential inhibition DMSO (100% activity) and a high concentration of TSA that completely inhibits HDAC activity (0% activity) was also measured. The assay was performed in 96-well plates.

In case of SIN-1 and H_2O_2 investigation the plates with rHDAC1 were preincubated at RT for 2 or 4h before adding the 30 µl substrate peptide. The plates were then incubated for 3h at 30°C. Then 25 µl stop solution was added and the plates were incubated for 40 min at RT in darkness. The fluorescence was measured at extinction λ = 355 nm and emission of λ = 460 nm for 0,1 s.

3.5.5 Cellular viability assay / Alamarblue assay

To detect the cell viability, Alamarblue assay was used. The active ingredient of Alamarblue reagent resazurin is an indicator that uses the natural reducing power of living cells to convert resazurin to the fluorescent molecule, resorufin. Resazurin is blue in color and upon entering cells, resazurin is reduced to resorufin, which produces very bright red fluorescence. Viable cells continuously convert resazurin to resorufin, thereby generating a quantitative measure of viability - and cytotoxicity. Alamarblue reagent was purchased from Invitrogen and the assay was conducted according to manufacturer's instruction in 96-well plate. Briefly, 20 µl Alamarblue reagent was added directly to the cells in medium which was treated according to experimental settings and incubated for 4 h, and absorbance was measured at 590 nm.

3.5.6 Cytotoxicity assay / LDH assay

To directly detect the cytotoxic effects of HDAC inhibitors or oxidative stress, CytoTox 96 Non-Radioactive Cytotoxicity Assay (Promega) was used to determine the LDH activity. 50 µl of cell culture medium from the treated cells was used as sample, the assay was performed according to the manufacturer's instructions in 96-well plate. As

positive control cells were incubated with 1% triton X-100 and the result was calculated as 100% of LDH release.

3.5.7 Griess Assay

The production of nitrite (NO_2^-) and nitrate (NO_3^-), both stable metabolites of NO, was determined by the Griess assay. For determination of total nitrate and nitrite content, nitrate from 150 µl cell culture supernatant in 96-well microtiter plates was reduced to nitrite by adding 10 µl of reduction buffer (1 U/ml nitrate reductase, 530 µM FAD and 1 mM NADPH). After 15 min of incubation at 37°C interfering NADPH was depleted by adding 10 µl of buffer containing lactate dehydrogenise (200 U/µl) and sodium pyruvate (33 mM). After 5 min of incubation at 37°C the supernatant was incubated at 4°C for 10 min. After addition of 10 µl of 1% sulphanilamide in 0.1 N HCl and 10 µl of 0.1% N-(1-naphtyl)-ethylendiamine and 10 min of incubation at room temperature absorbance at 544 nm in reference to 690 nm was read in a micro plate reader (Perkin-Elmer Wallac). Measurements were carried out as duplicates.

3.6 Transient transfection of A549 cells with SuperFect™

For the transfection of A549 cells for the purpose of iNOS overexpression, the transfection reagent SuperFect™ (Qiagen) was used. In general, significantly higher transfection efficiencies were shown in various cell lines than for widely used liposomal reagents. It is a new class of specifically designed activated-dendrimer transfection reagent, which possesses a defined spherical architecture, with branches radiating from a central core and terminating at charged amino groups. SuperFect–DNA complexes possess a net positive charge, which allows them to bind to negatively charged receptors, such as sialylated glycoproteins on the surface of eukaryotic cells. Once inside the cell, SuperFect Reagent buffers the lysosome after it has fused with the endosome, leading to pH inhibition of lysosomal nucleases. This ensures the stability of SuperFect–DNA complexes and the transport of intact DNA to the nucleus. SuperFect is suitable for both adherent and suspension cells. (Qiagen 2002)

The plasmid pENOS2-N1 (from research department of Nycomed, see Supplement) containing iNOS (NM_000625) coding sequence (cds) was used for the transient transfection of A549 cells. The plasmid pEGFP-N1 (see Supplement) expressing

EGFP was used as a fluorescence control of the transfection efficiency. Plasmid pENOS2-N1 was originally modified from pEGFP-N1 through exchange of EGFP-cds with iNOS-cds. The transfection in the adherent cell line A549 for iNOS overexpression was generally carried out according to manufacturer's instructions. But to achieve optimal transfection efficiency with plasmid pENOS2-N1 in A549 cells, a number of parameters were optimized and these were: the amount of SuperFect reagent and plasmid DNA pENOS2-N1, the ratio of SuperFect to DNA, the cell number/confluency prior to transfection, the length of exposure of cells to SuperFect–DNA complexes. Briefly, the optimization was started with parameters recommended in the instruction and for every optimization two parameter were chosen. While keeping one of the parameter constants, the other was varied in different ranges. The parameters yielding maximum transfection efficiency for the overexpression of iNOS in A549 were determined by concomitant transfection of pEGFP-N1 and subsequent fluorescence microscopy. The optimized parameters of transfection were kept constant in every following experiment (see next paragraph). Measurement of the transfection efficiency and overexpression of iNOS in A549 cells were done by Griess assay and quantitative PCR.

One day before transfection, 2×10^5 A549 cells in a volume of 500 µl complemented medium per well were plated in 24-well tissue culture plates (Corning) for cytokine stimulation experiment. For iNOS expression assay after transfection, 1×10^6 A549 cells in a volume of 2 ml complemented medium per well were plated in 6-well plate also one day before transfection. The cells were incubated under their normal growth conditions (37°C and 5% CO_2). On the day of transfection, for the transfection in 24-well plates 3 µg DNA was diluted with cell growth medium containing no serum, proteins, or antibiotics to a total volume of 30 µl. For the transfection in 6-well plates 10 µg DNA was diluted with 100 µl cell growth medium. The solution was mixed and centrifuged down for a few seconds to remove drops from the top of the tube. In all experiments, the ratio of DNA to reagent was 1:10: for experiments in a 24-well plate 30 µl reagent was added to 3.0 µg plasmid DNA and in a 6-well plate 100 µl reagent was added to 10 µg plasmid. The reagent and DNA solution was mixed by pipetting up and down 5 times and incubated at RT for 10 min to allow transfection-complex formation. During complex formation taking place, the cells were washed once with PBS and fresh growth medium was added. Afterwards, the transfection-complex was

diluted with growth medium containing serum and then added to the A549 cells. After 5 h incubation at 37℃ the transfection medium was carefully removed and fresh growth medium was added. And the cells were incubated over night for downstream experiments. As control, only DMEM (= untreated control) or DMEM containing 30/100 µl SuperFect (= reagent control) were applied.

3.7 Cytokine level assessment with ELISA and Luminex assay

Cytokine levels in the culture medium were measured using specific enzyme-linked immunosorbent assays and Luminex multianalyte profiling technology.

Human IL-8, GM-CSF MCP-1and RANTES were measured using ELISA assay kits as listed in Table 3-1 according to manufacturer's instruction.

For Luminex assay human cytokine 25-plex antibody bead kit was purchased from Biosource (Nivelles, Belgium). This kit comprises cytokine specific components for the measurement of human IL-1β, IL-1Ra, IL-2, IL-2R, IL-4, IL-5, IL-6, IL-7, IL-8, IL-10, IL-12p40/p70, IL-13, IL-15, IL-17, TNF-α, IFN-α, IFN-γ, GM-CSF, MIP-1α, MIP-1β, IP-10, MIG, Eotaxin, RANTES, and MCP-1. The assay was conducted as indicated in the manufacturer's instructions and to give a brief overview of this method: 5.6 µm polystyrene beads which are internally dyed with red and infrared fluorophores of different intensities (bead regions) and conjugated to protein-specific capture antibodies were added along with samples (including standards of known protein concentration, control samples, and test samples) into the wells of a filter-bottom microplate. After 2-hour incubation protein-specific biotinylated detector antibodies were added and incubated with the beads for another 1 hour. (During this incubation, the protein-specific biotinylated detector antibodies bind to the appropriate immobilized proteins.) After removal of excess biotinylated detector antibodies, streptavidin conjugated to the fluorescent protein, R-Phycoerythrin (Streptavidin-RPE), was added and allowed to incubate for 30 minutes. (The Streptavidin-RPE binds to the biotinylated detector antibodies associated with the immune complexes on the beads, forming a four-member solid phase sandwich.) After washing to remove unbound Streptavidin-RPE, the beads are analyzed with the 100™ dual laser detection system manufactured by Luminex Corporation. By concomitantly monitoring the spectral properties of the

beads and the amount of associated R-Phycoerythrin (RPE) fluorescence, the concentrations of the specific cytokine were determined.

3.8 Chromatin immunprecipitation / ChIP assay

In order to study the relationship of the promotor histone-modification and HDAC inhibition, chromatin immunoprecipitation assay was used to measure the relative amount of histone H3 hyperacetylation and RNA polymerase II binding to the IL-8 promotor during IL-1β stimulation and HDAC inhibitor treatment of A549 cells. ChIP assay was conducted with SimpleChIP™ Enzymatic Chromatin IP Kit. Several accommodations and adaptations were made to the manufacturer's instructions to validate them in the A549 cell model in this study, including formaldehyd crosslinking, chromatin digestion, chromatin immunoprecipitation using specific antibodies and PCR procedures. All buffers and reagents were contents of the kit or prepared according to the instructions.

Prior to crosslinking cells were stimulated and or treated with the HDAC inhibitor SAHA or TSA as described in section 3.3.1.

3.8.1 Formaldehyde Crosslinking

A549 cells of 90% confluency were used for crosslinking. For this, one day before crosslinking $9X10^6$ A549 cells in a volume of 20 ml growth medium were plated in 15 cm culture dishes. For one experiment 5 dishes were seeded and these cells could generate one chromatin preparation, which could be used for up to 10 immunoprecipitaions. To crosslink proteins to DNA, 540 µl of 37% fresh formaldehyde (Sigma), which is a reversible protein-DNA crosslinking agent, was added to each culture dish containing 20 ml medium (final formaldehyde concentration: 1%). The mixture was swirled briefly and incubated for 10 minutes at room temperature. Then, 2 ml of ice-cold 10X glycine was added to each dish, mixed, and incubate for 5 minutes at room temperature (glycine stops the crosslinking by reacting with formaldehyde). The medium was removed and cells were washed two times with 20 ml ice-cold 1X PBS. 5 ml ice-cold 1X PBS + PMSF (1 mM) were then added to the 15 cm dishes. Cells were scraped into cold buffer with a rubber policeman. Cells from all 5 plates were combined into one 50 ml Falcon conical tube and centrifuged at 1,500 rpm in a

bench top centrifuge (Megafuge 3.0R, Heraeus) for 5 min at 4°C. Supernatant was removed and cell pellets were used for subsequent nuclei preparation.

3.8.2 Nuclei Preparation

To lyse the cells and release the nuclei, cell pellets were resuspended in 10 ml ice-cold Buffer A + DTT (0.5 mM) + PMSF (1 mM) + Protease Inhibitor Cocktail (PIC, 1x) and incubated on ice for 10 min (mix by inverting tube every 3 min). The nuclei were pelleted by centrifugation at 3,000 rpm in a bench top centrifuge (Megafuge 3.0R, Heraeus) for 5 min at 4°C. Supernatant was removed and the pellet was resuspended in 10 ml ice-cold Buffer B + DTT (0.5 mM). Centrifugation was repeated, the supernatant was removed and the pellet was resuspended in 1.0 ml Buffer B + DTT. This chromatin sample was transfered to a 1.5 ml microcentrifuge tube (Eppendorf) and used for the subsequent chromatin digestion.

3.8.3 Digestion of Chromatin

For immunoprcipitaiton the best size of chromatin fragment is 1 to 5 nucleosomes / approximately 150-900 bp, which ensures specific epitop recognition through antibodies. Fragmentation of chromatin can be done either by sonication or by enzymatic digestion. To get the optimal conditions for digestion of cross-linked DNA in A549 cells in this study, both the power of sonication and the concentration of Micrococcal Nuclease were optimized through variation separately or combined. Chromatin digestion was assessed after DNA purification with either agarose gel or the gel-free DNA quantification system Agilent 2100 Bioanalyzer (Agilent).

The amount of Micrococcal Nuclease required to digest DNA to the optimal length was determined empirically for A549 cells described in the manufacturer's instruction. Briefly, 200 µl of the nuclei preparation was transferred into individual microcentrifuge tubes (on ice) and Micrococcal Nuclease (1:5 dilution in 1X Buffer B + DTT) was added to the tubes in the range: 0 µl, 2.5 µl, 5 µl, 7.5 µl or 10 µl. The tubes were inverted several times to mix and incubated for 20 min at 37°C with frequent mixing. Digest was stopped by adding 20 µl of 0.5 M EDTA and placing the tubes on ice. Nuclei pellet was collected by centrifugation and resuspended in 200 µl of 1X ChIP buffer + PIC +PMSF and kept on ice for 10 min.

Subsequently, lysates were sonicated with Sonoplus HD2070 (Bandelin, Germany) with defined parameters, including the duration of pulse, the percentage of power and the repeats of treatment. The samples were kept 30 sec on wet ice between pulses. After sonication a specimen with lysate was prepared for every variation and observed under light microscope. Fine fragments proved the complete lysis of nuclei. Lysates were clarified by centrifugation at 10,000 rpm in a microcentrifuge for 10 min at 4℃.

Optimization protocol was repeated through adjusting the amount of Micrococcal Nuclease and parameters of sonication in each digest accordingly until DNA was in the desired size range of 150-900 bp.

The best result of chromatin digestion for A549 in this study was gained by using 2.5 µl of Micrococcal Nuclease to digest DNA to length of approximately 150-900 bp and A549 nuclei were completely lysed after 3 sets of 10-second pulses using the sonicator Sonoplus HD2070 at setting 30% power.

The sonicated lysates were clarified by centrifugation at 10,000 rpm in a microcentrifuge for 10 min at 4℃ and the supernatant was transfered to a new 1.5 ml tube. These cross-linked chromatin preparations were stored at -80℃ until further use. 50 µl of the chromatin preparation was removed for analysis of DNA digestion as described in manufacturer's instruction.

DNA concentration was determined with Nanodrop by measurement of the OD260. The prepared DNA concentrations were between 100 and 200 µg/ml, which were suggested for optimal immunoprecipitation results.

3.8.4 Chromatin immunprecipitation using specific antibodies

Any DNA sequences that are associated with the protein or histone modification of interest will co-precipitate as part of the cross-linked chromatin complex and the relative amount of that DNA sequence will be enriched by the immunoselection process.

For each precipitation 400 µl of 1X ChIP Buffer (40 µl of 10X ChIP Buffer + 360 µl water) and 2 µl Protease Inhibitor Cocktail were prepared and put on ice. To the prepared ChIP buffer, the equivalent of 100 µl (10 to 20 µg of chromatin DNA) of the crosslinked chromatin preparation for each immunoprecipitation was added. The

desired number of immunoprecipitation included the positive control Histone H3, negative control Normal Rabbit IgG, RNA polymerase II antibody and acetylated histone H3 antibody samples. 10 µl sample of the diluted chromatin as 2% Input Sample was transferred to a microfuge tube and stored at -20°C until further use. The immunoprecipitating antibody was added to the diluted chromatin sample. The amount of antibody used for IP was listed in section 3.1.8. IP samples were incubated overnight at 4°C with rotation. On the second day, 30 µl of ChIP Grade Protein G magnetic beads was added to the samples and incubated for 2 h at 4°C with rotation.

Subsequently, the beads were washed and the DNA-chromatin complexes were eluted from the antibody/protein G beads according to the manufacturer's instructions. The crosslinked samples of the DNA-chromatin complex (including input samples) were reversed by incubated 2 h at 65°C with 5 M NaCl and 2 µl Proteinase K. For the subsequent PCR assay DNA was purified using spin columns according to the manufacturer's instructions.

3.8.5 DNA quantification

The particular DNA sequences amplified by standard PCR and analyzed subsequently by the DNA quantification system Agilent 2100 Bioanalyzer (see section 3.4.4)

The primers for the amplification of IL-8 promotor specific sequences from IP enrichment were shown in section 3.1.6 by using control primers included in the kit specific for the human or mouse RPL30 gene. Primer 1 (IL-8 Pol II 1) and primer for the upstream of IL-8 promotor were chosen from literature (Hoffmann et al. 2005) and primer 2 (IL-8 Pol II 2) was designed with following criteria: primer length: 24 nucleotides; optimum temperature: 60°C; optimum GC: 50%; amplicon size: 150 to 200 bp.

3.9 Bioinformatics

Averages are presented as mean ± SD. For statistical analysis, statistical tools of Excel and GraphPad Prism 5.0 (GraphPad Software, San Diego, USA), were used.

4 Results

The aim of this study was to evaluate the anti-inflammatory effects of iNOS inhibitors and HDAC inhibitors in human lung epithelial cells, to test the hypothesis that iNOS-mediated NO production plays a role in steroid insensitivity correlating with increased HDAC nitration and decreased HDAC activity and to clarify the putative link between steroid sensitivity and HDAC inhibition in human epithelial cells. For these purposes, first of all, the production of pro-inflammatory cytokines and chemokines in lung epithelial cell models of inflammation was elucidated.

4.1 Characterization of lung epithelial cell models for inflammation studies *in vitro*

In the present study, two human lung epithelial cell lines, A549 and BEAS-2B and primary human bronchial epithelial cells MucilAir, were chosen to study lung inflammation and steroid insensitivity *in vitro*. A549 and BEAS-2B are both immortalized cell lines, which are relatively easy to handle and were used for most of the experiments in this study. MucilAir is a human primary cell culture, which is maintained under special air-liquid conditions. It was only used in certain experiments to validate the results derived from the cell lines.

To stimulate the lung epithelial cells for inflammation study, various specific pro-inflammatory cytokines IL-1β, TNFα and IL-1β, either alone or in combination, were used in order to mimic the physiological conditions (Cohn and Adler 1992). Similarly, bacterial lipopolysaccharide (LPS), as well as the synthetic dsRNA analog poly-riboinosinic-ribocytidylic acid [poly(I:C)] as a molecular mimetic of virus infection, which are both known to be potent triggers of lung epithelial cells to release inflammatory mediators, were also used as physiological stimuli for this study (Khair et al. 1996; Alexopoulou et al. 2001; Diks et al. 2004).

In this study, cytokine release and cytokine mRNA expression was used as readout of inflammation. To assess the induction of cells treated with various stimuli, the release of specific cytokines and chemokines, such as IL-8 and GM-CSF, in the cell-free supernatants was measured by specific enzyme- linked immunosorbent assay (ELISA) and their mRNA expression was evaluated by Real-Time PCR.

4.1.1 Induction of IL-8 release in human lung epithelial cell line A549

A549 were cultivated and stimulated as described in the section of Materials and Methods. In the initial experiments, various conditions were tested for the stimulation, including composition of culture medium, cell number, concentration range of stimuli and duration of treatment (data not shown). The optimal conditions for the stimulation were determined according to the results of IL-8 release.

IL-8 ELISA analysis of supernatants of $4x10^6$ cells per well in 24-well plate showed that A549 cells exhibited basal secretion of IL-8 (15 ng/ml in 24 h) (Figure 4-1). Whereas after stimulation with IFNγ or dsRNA alone there was no or only a slight increasing effect detectable, IL-8 secretion upon stimulation with IL-1β or TNFα or IL-1β with IFNγ or cytokine-mix (CM) of IL-1β, TNFα and IFNγ was increased (IL-1β: 187 ng/ml, CM/dsRNA: 148 ng/ml in 24 h). dsRNA in combination with other cytokines stimulated IL-8 release synergistically (CM: 72 ng/ml, CM/dsRNA: 148 ng/ml). Interestingly, IL-1β alone at the used concentration stimulated a higher secretion of IL-8 from A549 than in combination with other cytokines. Taken together, A549 cells treated with IL-1β, TNFα or combined with IFNγ produced IL-8 and dsRNA enhanced the IL-8 production in A549 cells further to these cytokine stimulations.

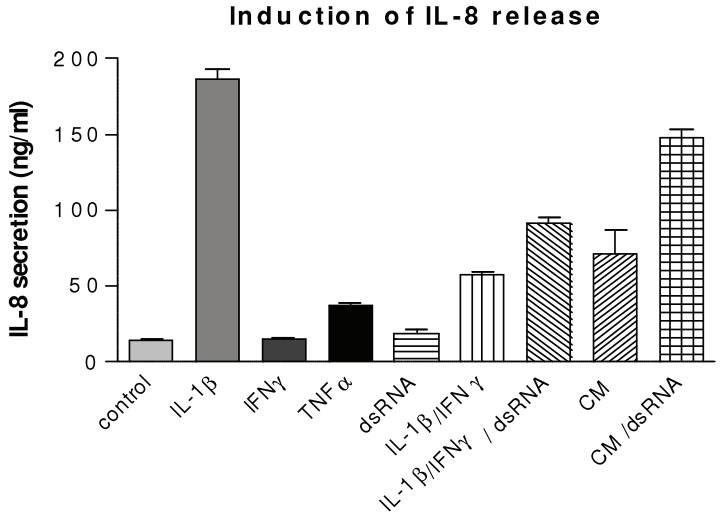

Figure 4-1: Induction of IL-8 release with various stimuli in A549 cells.

About $4x10^5$ cells were seeded per each well. After 24 h culture, the cells were incubated with the indicated stimuli for 20 h. IL-8 concentration in the cell culture medium was determined by ELISA analysis. Whereas IFNγ and dsRNA alone did not increase IL-8 levels, IL-1β alone dramatically enhanced the rate of secreted IL-8, compared to the control. Different combinations of cytokines and dsRNA also lead to amplified IL-8 levels in the cell culture supernatant. IL-1β: 10 ng/ml, IFNγ: 100 ng/ml, TNFα: 10 ng/ml, dsRNA: 100 µg/ml, CM: 10 ng/ml IL-1β, 10 ng/ml TNFα, 100 ng/ml IFNγ. n=3

4.1.2 Induction of IL-8 mRNA expression in A549 cells

Based on the results of IL-8 ELISA and to gain an insight of the regulation of IL-8 expression upon stimulation in A549 cells, IL-8 mRNA expression was evaluated by Real-Time PCR. A549 cells were stimulated and collected as described in detail in Materials and Methods. Briefly, total RNA of the A549 cell lysate was isolated using an RNA isolation kit from Qiagen. After quantification of the RNA concentration, the total RNA was reverse transcribed to cDNA using random hexamer primers and used as template for Real-Time PCR. At standard concentrations of 200 nM of the FAM-labelled probe, IL-8 mRNA detection was optimal with forward and reverse primer concentrations of 900 nM. The Real-Time PCR detection was performed as described in Materials and Methods.

For all quantitative Real-Time PCR experiments in this study, ribosomal *18S rRNA* was used as internal standard. Earlier experiments in the laboratory of the Department of Biochemistry (Nycomed, Konstanz) showed that it is not differentially expressed upon cell stimulation and thus *18S rRNA* detection is useful for normalization in quantitative PCR experiments. Using the $2^{-\Delta\Delta Ct}$ Method of duplex reactions (i.e., the combined detection of *18S rRNA* and a target gene within one PCR reaction) the relative expression o f IL-8 mRNA was calculated (Figure 4-2).

Whereas A549 cells stimulated with dsRNA alone did not show IL-8 mRNA expression, addition of TNFα or IL-1β alone was sufficient to induce IL-8 mRNA expression. Similar to ELISA experiments, IL-1β alone induced IL-8 mRNA expression as high as a combination of IFNγ, IL-1β, TNFα and dsRNA did (IL-1β: 75-fold, CM/dsRNA: 75-fold). Addition of IFNγ and TNFα to IL-1β did not change the IL-8 mRNA expression significantly. dsRNA enhanced the effect of the different cytokine cocktails, although in case of CM (IFNγ, IL-1β, TNFα) this effect is only slight. In this experiment, the combination of IL-1β/IFNγ/dsRNA induced the maximal IL-8 mRNA expression (111-fold) and dsRNA demonstrated a synergistic effect on IL-8 mRNA expression induced by IL-1β/IFNγ (70-fold). Although not all results from RNA preparations were similar to those from IL-8 ELISA, these results indicate that the induction of pro-inflammatory cytokine IL-8 in A549 cells is regulated at expression level and dependent on different stimuli.

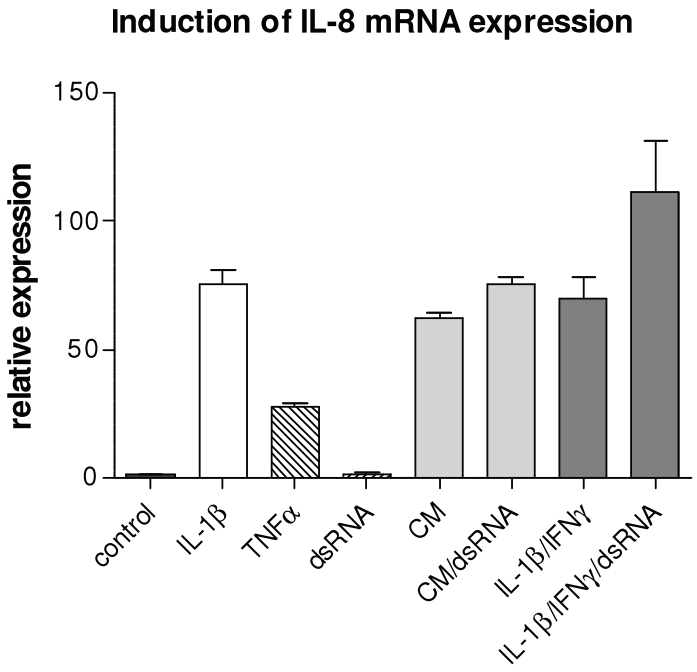

Figure 4-2: Induction of IL-8 mRNA expression with various stimuli in A549 cells.

About $1x10^6$ cells were seeded per each well. After 24 h of culture, the cells were stimulated as indicated in the figure. After 6 h of incubation, total RNA was isolated and transcribed into cDNA. Real-Time PCR was performed with IL-8 mRNA specific primers. Whereas dsRNA alone was not sufficient to induce IL-8 mRNA expression, TNFα and IL-1β alone increased IL-8 mRNA levels by 25-fold and 80-fold, respectively, compared to the control. Combinations of cytokines, or cytokines and dsRNA, did also augment IL-8 expression significantly. IL-1β: 10 ng/ml, TNFα: 10 ng/ml, IFNγ: 100 ng/ml, dsRNA: 100 µg/ml. CM: 10 ng/ml IL-1β, 10 ng/ml TNFα, 100 ng/ml IFNγ. n=2

4.1.3 Characterization of TLR3 and TLR4 mRNA expression in A549

Different Toll-like receptors (TLRs) react with specific bacterial or viral components, such as TLR3 with double stranded (viral) RNA (dsRNA) and TLR4 with lipopolysaccharide (LPS), and lead to increased expression of specific cytokines. In order to optimize the selection of stimuli combinations for the cytokine induction and also later for induction of iNOS, the expression of TLR3 and TLR4 mRNA expression in A549 cells was determined by Real-Time PCR. The detection was conducted as described in Materials and Methods and both the Ct values and calculation of $2^{-\Delta\Delta Ct}$ were used to evaluate the TLR3 and TLR4 mRNA expression in control or stimulated samples (Figure 4-3). The Ct values of the control samples for TLR3 (Ct ≈ 28) and TLR4 (Ct ≈ 31) show that TLR3 mRNA compared to TLR4 mRNA is expressed 8-fold higher in A549 cells (Figure 4-3a). Whereas dsRNA alone was not sufficient to increase TLR3 or TLR4 mRNA amounts strongly, a combination of cytokines leads to a 5-fold increase in TLR3 mRNA level and 2-fold in TLR4 mRNA level (Figure 4-3b). The

addition of dsRNA to the cytokine cocktail slightly enhanced this increase. Comparatively, expression of TLR3 mRNA was 3-fold more increased than that of TLR4 mRNA after incubation with CM (IFNγ, IL-1β and TNFα) with or without addition of dsRNA. Considering the high levels of both the basal and the CM-induced TLR3 mRNA expression, dsRNA was used as additional stimulus to cytokines in the study of inflammation and iNOS expression.

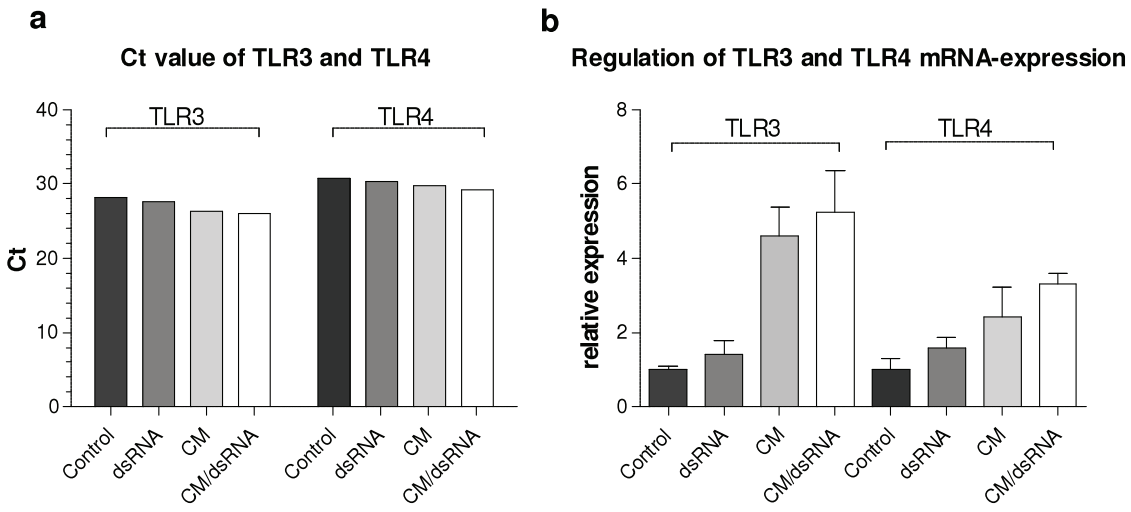

Figure 4-3: Expression of TLR3 and TLR4 mRNA in response to cytokine/dsRNA stimulation in A549 cells.

About $1x10^6$ A549 cells were seeded per each well. After 24 h cells were stimulated with the indicated stimuli for 6 h. Isolated RNA was reverse transcribed into cDNA, and Real-Time PCR analysis was performed with TLR3 and TLR4 specific primers. a) Ct values of TLR3 and TLR4 Real-Time PCR. The lower Ct values for TLR3 indicate a higher cellular amount of TLR3 mRNA compared to TLR4. b) Relative expression of TLR3 and TLR4 mRNA by A549 cells in response to cytokine/dsRNA stimuli. The magnitude change of TLR3 mRNA is expressed as $2^{-\Delta\Delta Ct}$. CM: 100 ng/ml IFNγ, 10 ng/ml IL-1β, 10 ng/ml TNFα. dsRNA: 100 µg/ml.

4.1.4 Induction of GM-CSF release in BEAS-2B and MucilAir cells

To further elucidate the effects of cytokines on epithelial cell stimulation, the response of the SV-40 immortalized human bronchial epithelial cell line BEAS-2B and human primary lung epithelial cells MucilAir, to different cytokine stimuli was investigated. Besides IL-8, GM-CSF is another well-known pro-inflammatory cytokine, which can be secreted by epithelial cells during inflammation. Here, GM-CSF release was used to characterize the stimulation of BEAS-2B and MucilAir cells. Similar to the IL-8 release in A549 cells, BEAS-2B and MucilAir cells responded to the cytokine stimuli in a

concentration-dependent manner and secreted different ranges of GM-CSF when using different stimuli. GM-CSF release in BEAS-2B and MucilAir cells was increased moderately upon treatment of IL-1β or TNFα and it was strongly increased after treatment with combination of cytokines (IL-1β/TNFα in BEAS-2B cells and CM in MucilAir cells). In our experiments, BEAS-2B cells were refractory to LPS in culture to produce GM-CSF and in MucilAir cells LPS could just slightly increase GM-CSF release.

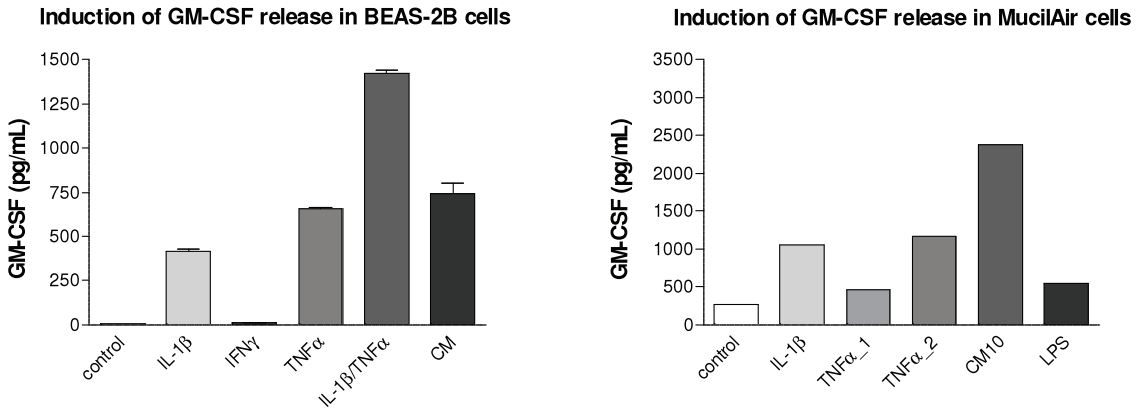

Figure 4-4: Induction of GM-CSF release in BEAS-2B and MucilAir cells after treatment with different stimuli.

About $4x10^5$ of MucilAir cells were cultured per each well in a 24-well plate at an air-liquid surface and $3x10^4$ of BEAS-2B cells were seeded in a 96-well plate at normal culture condition. After 24 h, the cells were incubated with the indicated stimuli for 20 h. GM-CSF concentration in the cell culture medium was determined by ELISA analysis. (a) Whereas IFNγ did not increase GM-CSF levels, IL-1β or TNFα alone or CM enhanced the rate of secreted GM-CSF, and the combination of IL-1β and TNFα increased the secretion of GM-CSF dramatically, compared to the control. (b) IL-1β and TNFα at 100 ng/ml (TNFα_2) increased the secretion of GM-CSF and TNFα at 10 ng/ml (TNFα_1) and LPS at 10 µg/ml slightly increased the GM-CSF level and CM10 lead to strongly amplified GM-CSF level in the cell culture supernatant. IL-1β: 10 ng/ml, TNFα and TNFα_1: 10 ng/ml, TNFα_2: 100 ng/ml, IFNγ: 100 ng/ml. CM: 10 ng/ml IL-1β, 10 ng/ml, 100 ng/ml IFNγ, CM10: 10 ng/ml IL-1β, 10 ng/ml TNFα, 10 ng/ml IFNγ, LPS: 10 µg/ml

4.1.5 Induction of multiple cytokine release in A549, BEAS-2B and MucilAir cells (Luminex assay)

To further elucidate the pro-inflammatory cytokine release in epithelial cells, the response of the human lung epithelial cell lines A549 and BEAS-2B, as well as primary lung epithelial cell MucilAir to different cytokine stimuli (IL-1β, TNFα or CM) was investigated by multi analytes profiling (MAP) using Luminex technique. This technique facilitates the simultaneous evaluation of multiple immune mediators with the

advantage of higher throughput (in this study 25-Plex) and smaller sample volume in comparison to ELISA.

The cells were seeded and stimulated as described in Materials and Methods. Similar to an ELISA assay, analysis of cytokine release was performed 20 hours post final cytokine challenge with IL-1β, TNFα or CM. For the measurements, a 25-plex kit including standards was applied according to the manufacturer's instructions, which was briefly described in Materials and Methods. By using this 25-plex kit the simultaneous measurement of human IL-1β, IL-1ra, IL-2, IL-2R, IL-4, IL-5, IL-6, IL-7, IL-8, IL-10, IL-12 (p40), IL-13, IL-15, IL-17, TNFα, IFNα, IFNγ, GM-CSF, MIP-1α, MIP-1β, IP-10, MIG, Eotaxin, RANTES, and MCP-1 was conducted. Since the profiles of cytokine release under stimulation with TNFα or CM were very similar to that of IL-1β stimulation and data differed only at the absolute concentrations of the analytes, the data from TNFα or CM stimulation were not shown. All of the three cell models responded to cytokine (IL-1β or TNFα) or cytokine-mix treatment by secreting a number of different pro-inflammatory cytokines. They differed in details at the magnitudes of specific cytokine release, which reflected different effects of IL-1β, TNFα or CM on epithelial cell stimulation.

Figure 4-5 shows the levels of all analytes from A549 (a), BEAS-2B (b) and MucilAir (c) control and after stimulation with IL-1β. Interestingly, although three different cell models were used, all of them (A549, BEAS-2B and MucilAir cells) exhibited basal secretion of IL-6, IL-7, IL-8, RANTES und MCP-1 and their secretion was significantly increased after stimulation with IL-1β. The results of IL-8 release in A549 cells is consistent with previous results from IL-8 ELISA. GM-SCF is also typical cytokine released by epithelial cells upon cytokine stimulation, which could be observed also here, although in comparison to IL-8 or MCP-1, it is in a low concentration range. Compared with A549 cells, more analytes, such as IL-10, TNFα, MIP-1β and IP-10, were present and detected in BEAS-2B and MucilAir cells, although some of them were in a low concentration range. Moreover, the activated T-cell chemoattractant IP-10 were strongly increased after IL-1β stimulation in BEAS-2B cells, which is in consistent with the results from Sauty et al (Sauty et al. 1999).

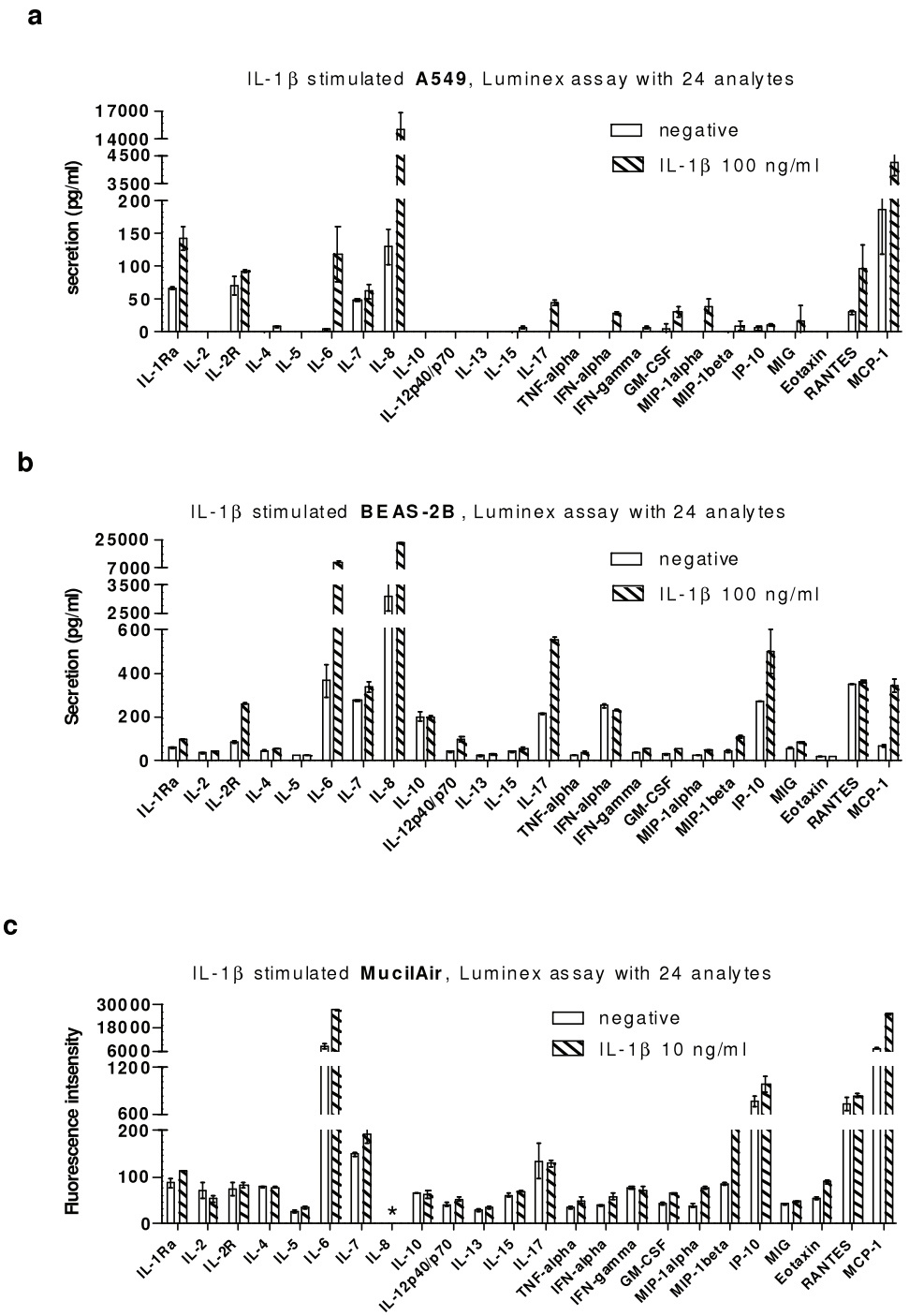

Figure 4-5: Induction of cytokine release by A549, BEAS-2B and MucilAir cells (Luminex assay).

About 4x10^5 cells of A549 and MucilAir in 24-well plate and 3x!0^4 of BEAS-2B in 96-well plate were seeded. After 24 h of cultivation, the cells were incubated with IL-1β at 100 ng/ml for A549 and BEAS-2B cells and at 10 ng/ml for MucilAir cells for 24 h. Concentrations of analytes in the cell culture supernatant were determined with 25-Plex Luminex kit. IL-1β dramatically enhanced the rate of secreted IL-6, IL-7, IL-8, RANTES and MCP-1 compared to the control. (* The data of IL-8 secretion in MucilAir cells was out of range and it could be assessed using ELISA assay.)

In contrast to the strongly induction of cytokines like IL-6, IL-8 and MCP-1, there was no or only a slight change in response to cytokines in the other analytes included in the multiplex, like IL-2, IL4, IL-5, IL-10, IL-13, MIG and Eotaxin. Some of the cytokine concentrations were out of expected range and could not be quantified here, which could be selected and assessed using ELISA in combination with other cytokine stimulation experiments (see also Figure 4-16).

Based on Luminex data, firstly, the profiles of pro-inflammatory cytokine release upon cytokine stimulation in A549, BEAS-2B and MucilAir cells could be roughly characterized. Secondly, these *in vitro* results indicate that activated bronchial epithelium is an important source of pro-inflammatory cytokines and chemokines, which may play versatile role in lung inflammation, e.g. through activation of protease and ROS/RNS release and recruitment of inflammatory cells, like neutrophils and activated T cells.

4.1.6 Induction of IL-8 mRNA expression in A549 cells using cigarette smoke extract

The oxidative stress from cigarette smoke has been shown to contribute and amplify the inflammation in the lung (Mio et al. 1997; Hellermann et al. 2002). Exposure to cigarette smoke activates an inflammatory cascade in the airway epithelium resulting in the production of a number of potent cytokines and chemokines, damage to the lung epithelium, increase of permeability, and recruitment of macrophages and neutrophils to the airway. In this study the effect of cigarette smoke extract (CSE) on IL-8 mRNA expression in lung epithelial cells was studied. CSE was prepared as described in Material and Methods using an automatic rotary smoking machine. Briefly, cigarettes without filter were puffed by the suction of a pump and the smoke was bubbled through assay medium. The resulting suspension was then sterile filtered und added to the cells to mimic the conditions of cigarette smoking in human. Cells were incubated with cigarette smoke extract at concentrations of 1% or 10% in presence or absence of cytokines. To better observe the effect of CSE on IL-8 mRNA-expression, the cells were treated for 3, 6 or 24 hours with CSE and/or CM before RNA collection. The IL-8 mRNA expression was analyzed using Real-Time PCR.

As shown in Figure 4-6, cytokine-mix (CM) stimulation of A549 upregulated IL-8 mRNA expression in a time dependent manner: at 6 hours it reached the maximum and at 24

h the expression reduced to the level at 3h. But CSE, either at 1% or at 10%, did not show any effect on IL-8 mRNA expression under our experimental conditions. Also the combination of CM and CSE did not affect IL-8 mRNA expression significantly. Laan et al showed that in BEAS-2B cells pretreatment with cigarette smoke extract concentration dependently inhibited the LPS-induced IL-8 mRNA expression and protein release (Laan et al. 2004). In contrast, Mio et al demonstrated that CSE augmented IL-8 release from bronchial epithelial cells in a concentration- and time-dependent manner (Mio et al. 1997) and Hellermann et al could show that normal human bronchial epithelial cells (NHBEs) exposed to cigarette smoke condensate - the particulate fraction of tobacco smoke - showed increased mRNA expression of IL-8 and GM-CSF (Hellermann et al. 2002). Our data and these controversial results indicate that the effects of cigarette smoke on cytokine and chemokine release and expression *in vitro* are possibly dependent on the different experimental settings, such as time and way of treatment, cell culture and stimulation conditions and readouts.

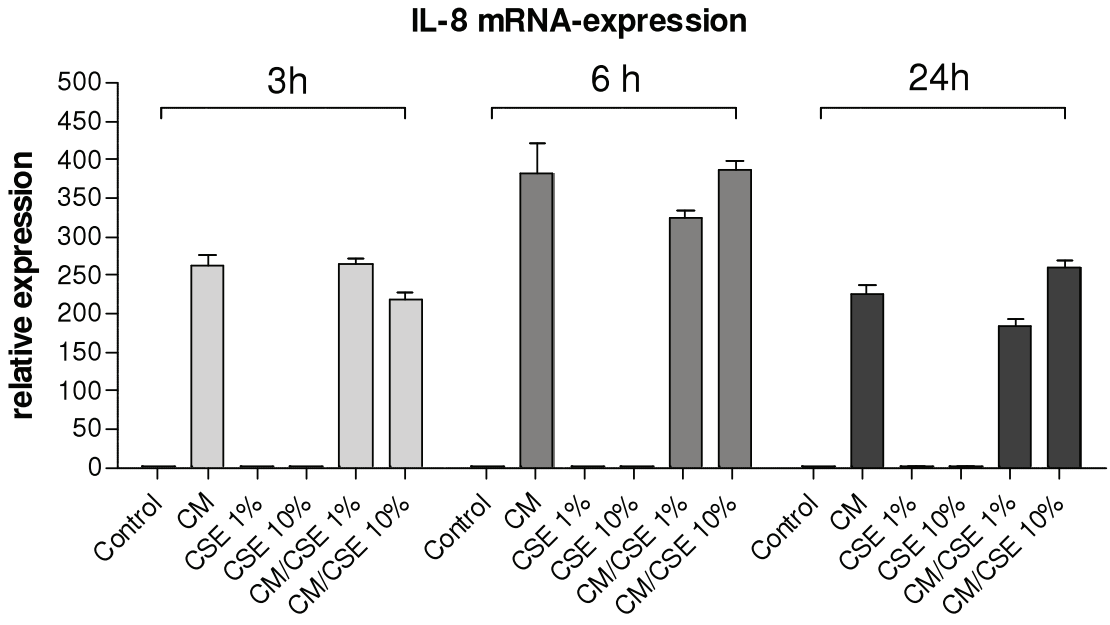

Figure 4-6: No induction of IL-8 mRNA expression in A549 cells after treatment with cigarette smoke extract (CSE).

About 1x10^6 A549 cells were seeded per each well. After 24 h cells were incubated with culture medium with 1or 10% CSE in presence or absence of cytokine mix (10 ng/ml IFNγ, 10 ng/ml IL-1β, 10 ng/ml TNFα) for 3, 6 or 24 h as indicated. Isolated RNA was transcribed into cDNA. IL-8 mRNA expression was evaluated with Real-Time PCR. CM stimulation of A549 cells upregulated IL-8 mRNA expression in a time dependent manner: at 6 hours it reached the maximum and at 24 h the expression reduced to the level at 3h. But CSE, either at 1% or at 10%, did not show any effect on IL-8 mRNA expression under our experimental conditions. Also the combination of CM and CSE did not affect IL-8 mRNA expression significantly.

4.2 Functional effects of iNOS inhibitors in cell models of lung inflammation

iNOS-derived NO has been recognized as an important trigger of inflammation and a source of nitrative stress through formation of peroxynitrite with superoxide. Highly selective and potent iNOS inhibitors have been developed by Nycomed. These inhibitors are capable of attenuating inflammation through inhibition of inflammatory cell recruitment and pro-inflammatory cytokine release in various *in vivo* rat and mouse models of inflammatory diseases, including a steroid insensitive smoke mouse model of COPD (Hesslinger et al. 2008). Whereas *in vivo* studies revealed the anti-inflammatory effect of specific iNOS inhibitors, their function in controlling inflammation in cell models was largely unknown. To establish a stable cell culture system for future research into disease related iNOS activity, its induction and the production of NO-metabolites nitrite and nitrate in A549 cell culture supernatants depending on different pro-inflammatory stimuli of cytokines and dsRNA was assessed firstly.

4.2.1 Induction of iNOS mRNA expression in A549 cells by various stimuli

It has been demonstrated in various studies that the combination of IL-1β, TNFα and IFNγ (CM) can induce iNOS in A549 cells (Kamosinska et al. 1997; Donnelly and Barnes 2002; Vallance and Leiper 2002). In order to determine the cytokine stimulus that causes the highest iNOS induction in the cell systems used, we examined different combinations of cytokines, varied their concentrations and incubation time, and added dsRNA or LPS to cytokines. Since there is evidence that iNOS expression is serum-dependent (Uetani et al. 2001), A549 cells were also subjected to different serum concentrations. On the one hand, A549 cells were first cultured in medium with 5% FCS for 24h, then the medium was replaced with medium containing 0.5% FCS. 24h later, stimulation with cytokine mix was performed in medium with 5% FCS. On the other hand, cells were seeded and cultured in medium containing 5% FCS after 24 hours they were directly incubated with cytokine-mix in medium with 0.5% FCS without additional pre-incubation with medium containing 0.5% FCS. The first variation of treatment did not enhance NO_x (nitrite and nitrate) production effectively (data not shown), so the cells were incubated and stimulated with the second variation of treatment. To assess the regulation of iNOS mRNA expression in the cells, Real-Time PCR was applied subsequently with the total cell lysate of A549 cells.

In a first subset of Real-Time PCR experiments the expression of eNOS and iNOS in A549 cells was determined. Coincident with findings of Pechkovsky et al. and Wei et al (Pechkovsky et al. 2002; Wei et al. 2005), no eNOS mRNA expression was identified according to the high Ct values in either unstimulated or stimulated cells (Ct ≅ 35). Real-Time PCR analysis showed that iNOS was expressed in cytokine-mix stimulated cells (Ct ≅ 20), but not in unstimulated cells (Ct ≅ 33) (Ct data not shown, see also Figure 4-7 for relative expression of iNOS in A549 cells after stimulation).

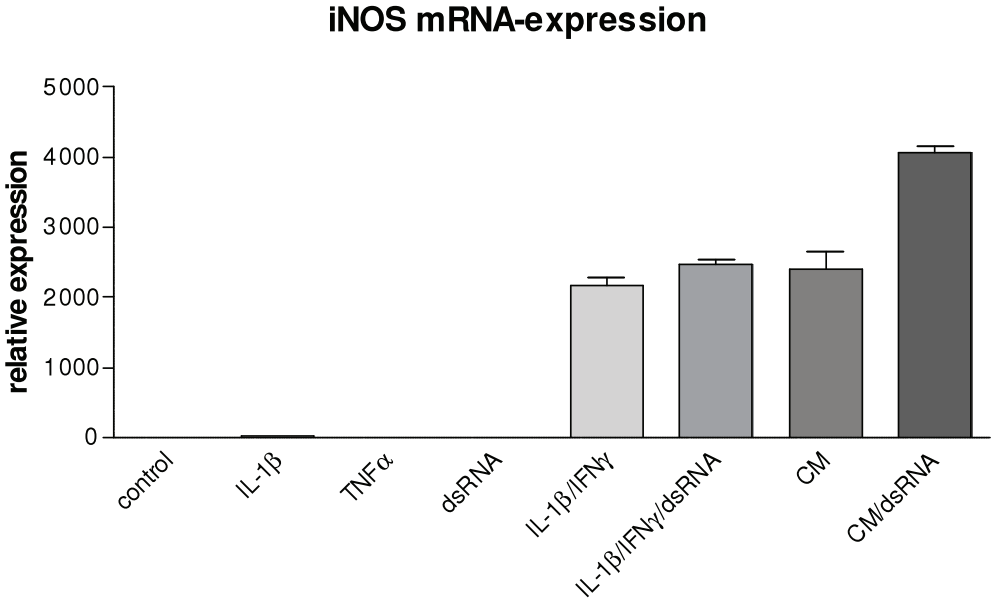

Figure 4-7: Induction of iNOS mRNA expression in response to cytokine and dsRNA stimuli in A549 cells.

About 1x10^6 A549 cells were seeded per each well. After 24 hours cells were stimulated with the indicated stimuli for 6 h. Isolated RNA was reverse transcribed into cDNA, and Real-Time PCR was performed with iNOS specific primers with *18sRNA* as internal control. The magnitude change of the iNOS mRNA is expressed as $2^{-\Delta\Delta Ct}$. Whereas IL-1β, TNFα and dsRNA alone were not sufficient to increase iNOS mRNA amounts, a combination of IFNγ and IL-1β already lead to about 2100-fold increase in iNOS mRNA levels compared to the control. The addition of dsRNA to IL-1β and IFNγ enhanced this increase to about 2500-fold. A mix of IFNγ, IL-1ß and TNFα led to about 2400-fold increase in iNOS mRNA levels compared to the control. Here, the addition of dsRNA to CM significantly augmented the iNOS mRNA rate to about 4000-fold. IL-1β: 10 ng/ml, TNFα: 10 ng/ml, IFN γ: 100 ng/ml, dsRNA: 100 µg/ml, CM: 100 ng/ml IFNγ, 10 ng/ml IL-1β, 10 ng/ml TNFα.

Stimulation of A549 cells with various cytokine combinations demonstrated that IL-1β, TNFα, IFNγ, and dsRNA were all required for maximum induction of iNOS mRNA expression (Figure 4-7). Stimulation with combination of IL-1β and IFNγ was sufficient to induce iNOS mRNA expression (2100-fold), and additional of TNFα and dsRNA acted synergistically to enhance the iNOS induction (4000-fold). Only using CM without

addition of dsRNA reduced the iNOS induction by about 33%. To note, the values of iNOS relative expression in stimulated A549 cells are at a very high range from about 2000-fold to 4000-fold, which is caused by the very low value of iNOS relative expression in unstimulated A549 cells.

Subsequently, the additional effect of dsRNA and the effect of CM on iNOS mRNA expression were studied at different concentrations. The concentrations of dsRNA in range of 100 µg/ml to 400 µg/ml were of no importance for enhancing the cytokine-mediated iNOS mRNA expression (Figure 4-8a), nor was the increase of CM concentrations used able to augment the iNOS mRNA expression (Figure 4-8b).

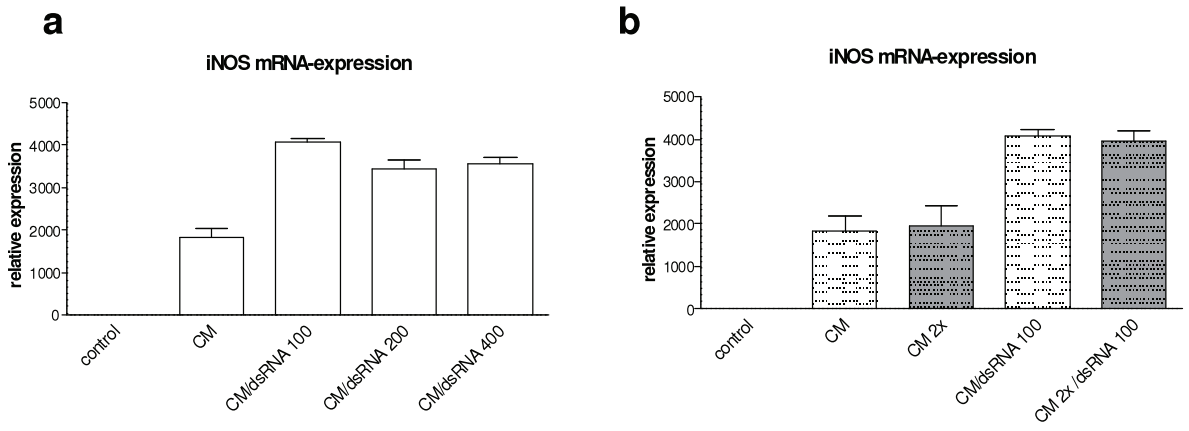

Figure 4-8: Concentration-independent induction of iNOS mRNA expression by CM and dsRNA in A549 cells.

About 1x10^6 A549 cells were seeded per each well. After 24 hours cells were stimulated with the indicated CM and dsRNA at different concentrations for 6 h. Isolated RNA was transcribed into cDNA, and Real-Time PCR was performed with iNOS specific primers with *18sRNA* as internal control. The magnitude change of the iNOS mRNA is expressed as $2^{-\Delta\Delta Ct}$ and this analysis revealed that: (a) compared to samples treated with 100 µg/ml dsRNA, higher concentrations of dsRNA (200 µg/ml and 400 µg/ml) did not lead to further enhanced iNOS mRNA expression; (b) duplication of CM concentration did not lead to the increase of iNOS mRNA expression, also not in the combination of dsRNA at 100 µg/ml. dsRNA: 100 µg/ml, 200 µg/ml 400 µg/ml as indicated in the diagrams, CM: 100 ng/ml IFNγ, 10 ng/ml IL-1β, 10 ng/ml TNFα.

4.2.2 Regulation of iNOS-derived NO production in A549 by various stimuli

To further evaluate the ability of different cytokines to induce iNOS and iNOS-mediated NO_x production in human lung epithelial cells, A549 cells were treated with single cytokine or different cytokine combinations and the levels of nitrite (NO_2^-) and nitrate (NO_3^-), stable end products of NO, in cell culture supernatants were quantified by the

Griess assay. Figure 4-9 shows that the highest NO_x levels were measured for 100 ng/ml IFNγ and 10 ng/ml IL-1β in combination with 10 ng/ml TNF (CM). Cells treated with IL-1β, IFNγ or TNFα alone barely showed an increase in NO_x production and a combination of IFNγ and IL-1β increased NO_x production modestly.

In order to find conditions, which could further increase NO_x production, dsRNA or LPS was added to cytokines to stimulate the cells. Figure 4-10 shows that dsRNA or LPS alone was not enough to increase NO_x production in A549 cells. The addition of dsRNA but not LPS to IL-1β and TNFα could augment the NO_x production. This was identical when using CM stimulation: addition of LPS could not increase the NO_x production but CM in combination with 100 μg/ml of dsRNA led to a maximum of NO_x production in A549 cells, consistent with the analysis of iNOS mRNA expression in CM/dsRNA-stimulated A549 cells (Figure 4-7). Since only little amounts of TLR4 mRNA were expressed by human A549 cells and also the treatment with CM could not upregulate TLR4 mRNA expression significantly as showed in Figure 4-3, we had expected just a slight induction of NO_x-production in response to LPS treatment. In fact, the addition of LPS to cells incubated with cytokines did not induce a further increase in NO_x-production. Compared to LPS, the supplement with dsRNA increases the production of NO_x. In all experiments it became obvious that the addition of dsRNA to a mix of cytokines led to a further, significant increase in NO_x levels, thereby enhancing IFNγ/IL-1β-induced NO_x production about the 1.4-fold and CM-induced NO_x production about the 1.8 fold (Figure 4-10). This effect was highly reproducible. Additionally, increasing concentrations of dsRNA in the range from 100 μg/ml to 300 μg/ml had no further effect on NO_x levels (data not shown).

Interestingly, the induction of NO_x production by cytokines was closely dependent on the number of cell culture passages after thawing of A549 cells. With an increase of the numbers of passages, A549 cells appeared to become less responsive to cytokine stimulation. For this reason, the maximum passage number used in the experiments was about 20.

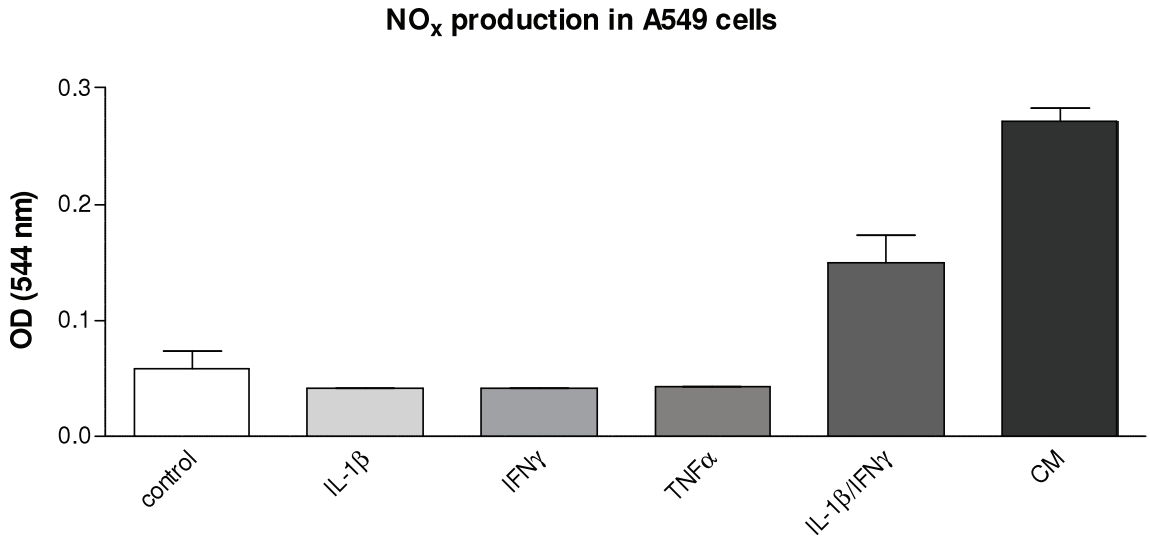

Figure 4-9: Induction of NO_x production by A549 cells stimulated with different cytokines

About $4x10^5$ A549 cells were seeded per each well. After 24 h the cells were stimulated with the indicated cytokines in medium containing 0.5% FCS for 20 h. NO_x levels in the medium were determined by Griess assay. In comparison to negative control, IL-1β, IFNγ or TNFα alone was not able to induce iNOS to produce NO and combination of 10 ng/ml IL-1β and 100 ng/ml IFNγ was able to increase iNOS activity to produce NO. Addition of TNFα (CM) was able to further augment NO_x concentrations and the highest amounts were obtained. IL-1β: 10 ng/ml, IFNγ: 100 ng/ml, TNFα: 10 ng/ml. CM: 100 ng/ml IFNγ, 10 ng/ml IL-1β, 10 ng/ml TNFα. Value of NO_x control $NaNO_3$ (30 µM) = 0.79. n= 3

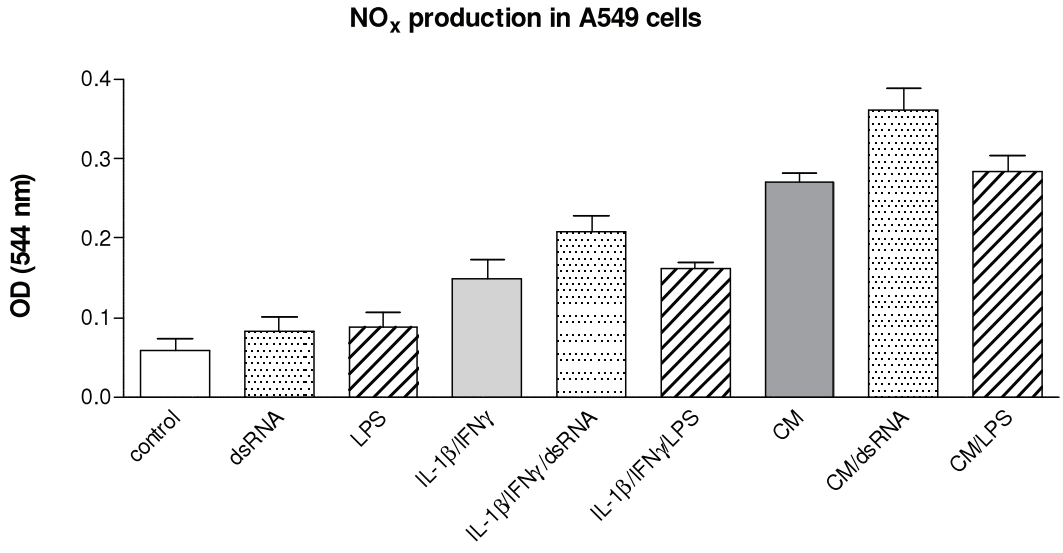

Figure 4-10: Induction of NOx production by A549 cells stimulated with combinations of cytokines and dsRNA or LPS.

About $4x10^5$ A549 cells were seeded per each well in DMEM containing 5% FCS. After 24 h cells were treated with different cytokines and dsRNA or LPS as indicated for 20 h in DMEM containing 0.5% FCS. Production of NO_x was then determined by Griess assay. Addition of dsRNA but not LPS led to a further increase in NO_x production. dsRNA: 100 µg/ml. LPS 1 µg/ml, IL-1β: 10 ng/ml. IFNγ: 100 ng/ml.. CM: 100 ng/ml IFNγ, 10 ng/ml IL-1ß, 10 ng/ml TNFα. Value of NO_x control $NaNO_3$ ((30 µM) = 0.79. n= 2

4.2.3 Inhibition of iNOS-derived NO production by iNOS inhibitor BYK191023

One of the aims of this study was to evaluate the anti-inflammatory effects of iNOS inhibitors in lung epithelial cells. BYK191023 is an imidazopyridine derivative and a highly selective iNOS inhibitor (Strub et al. 2006). Firstly, the potency of iNOS inhibition by BYK191023 was tested in A549 cells. Expression of iNOS was induced by the addition of IL-1β, TNFα, IFNγ (CM) and dsRNA, which was assessed by Griess assay and Real-Time PCR. NO_x (nitrite and nitrate) production measured by Griess assay was shown to be inhibited by BYK191023 with an IC_{50} value of 10 µM (pIC_{50} = 5.0) as determined by the dose-response relationship of BYK191023 in A549 cells (Figure 4-11). This result is comparable with the IC_{50}-values of 13 µM in human HEK293/iNOS cells, 33 µM in the rat mesangial cell line RMC and 3.1 µM in murine macrophage cell line RAW (Strub et al. 2006).

Additionally, cell viability determination using MTT assay showed that BYK191023, even at high micromolar concentration of 100 µM, did not exhibit any toxic effect in HEK293, RMC and RAW cell models (data not shown) .

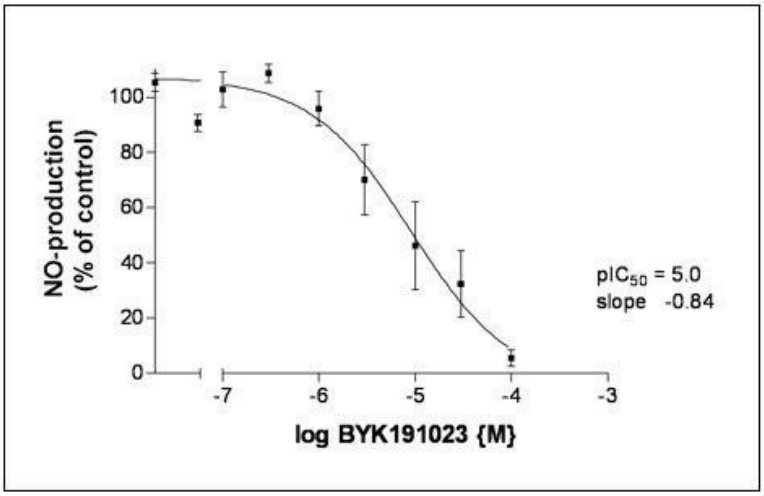

Figure 4-11: BYK191023-mediated inhibition of iNOS-derived NO_x production in CM-stimulated A549 cells.

$4x10^5$ cells were seeded per each well in 24-well plates and cultured in DMEM (5% FCS) for 24h. iNOS induction was then stimulated by the addition of CM and dsRNA for 24h in the presence of iNOS inhibitor BYK191023. Griess assay for detection of nitrite and nitrate was performed as described in Materials and Methods. pIC_{50} value of 5.0 for BYK191023 in A549 cells was obtained. CM: 100ng/ml IFNγ, 10ng/ml IL-1β, 10ng/ml TNFα, dsRNA: 100µg/ml. Each data point represents the mean of n = 4 determinations.

4.2.4 Effects of iNOS inhibitor BYK191023 on IL-8 mRNA expression and secretion in A549 cells

The focus of this part of the work was to investigate functional effects of BYK191023 in the cytokine-induced inflammation in lung epithelial cells. Since there is evidence that NO augmented several cytokine and chemokine expression, including IL-8, upon stimulation with cytokines (Wetzler et al. 2000), cytokine-mediated IL-8 mRNA expression and secretion was chosen to determine the influence of BYK191023 on lung epithelial cell inflammation. In presence of BYK191023 at 100 μM, A549 cells were stimulated with combinations of cytokines (IL-1β and IFNγ or CM) with or without dsRNA, which had been characterized before to induce both IL-8 and iNOS expression. To determine a possible influence of iNOS-derived NO on IL-8 secretion, IL-8 ELISA was performed and for its influence on IL-8 mRNA expression, IL-8 mRNA levels in A549 after stimulation was measured using Real-Time PCR. Dexamethasone (Dex) at 1 μM was used as control to inhibit IL-8 induction.

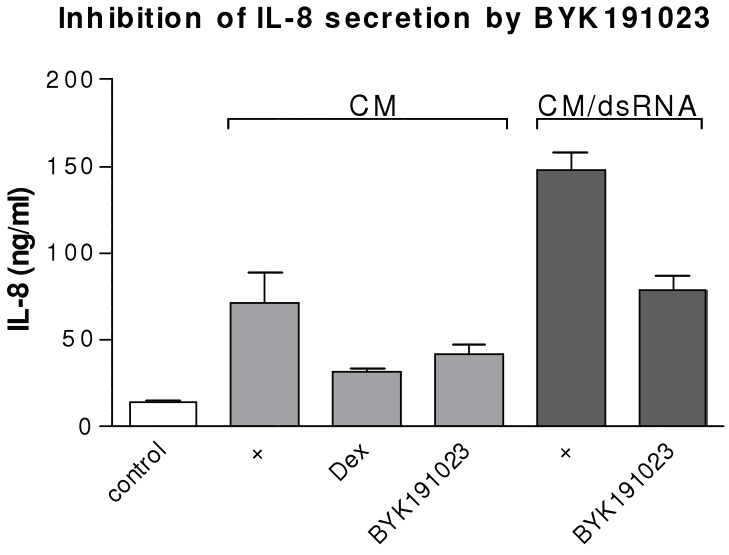

Figure 4-12: BYK101023- and dexamethasone-mediated inhibition of IL-8 secretion in CM- or CM/dsRNA-induced A549 cells.

About $4x10^5$ cells were seeded per each well. After 24 h culture, the cells were exposed to the indicated substances for 30 min and then stimulated with CM or CM/dsRNA for 20 h. IL-8 concentrations in the cell culture medium were determined by ELISA assay. Whereas CM increased IL-8 level compared to negative control, addition of dsRNA dramatically enhanced the rate of secreted IL-8. In case of CM stimulation, control dexamethasone reduced the increase IL-8 secretion to approximately 40% of the CM control (+). BYK191023 lowered the IL-8 secretion upon stimulation to 60% of the CM control and, in case of CM stimulation with additional dsRNA, even down to 50% of CM/dsRNA control. n=2. CM: 100 ng/ml IFNγ, 10 ng/ml IL-1β, 10 ng/ml TNFα. dsRNA: 100 μg/ml. BYK191023: 100 μM. Dexamethasone: 1 μM.

As shown in Figure 4-12, in case of CM stimulation, control dexamethasone reduced the increase IL-8 secretion to approximately 40% of the CM control (+). BYK191023 lowered the IL-8 secretion upon stimulation to 60% of the CM control and, in case of CM stimulation with additional dsRNA, even down to 50% of CM/dsRNA control

Subsequently, BYK191023-mediated regulation of IL-8 mRNA expression in cytokine/dsRNA-stimulated A549 cells was evaluated by Real-Time PCR (Figure 4-13). Dexamethasone as control to inhibit IL-8 induction diminished IL-8 mRNA expression by 40% in the case of CM/dsRNA stimulation and accordingly 70% in the case of IL-1β/IFNγ stimulation. Treatment with BYK191023 decreased CM/dsRNA- or IL-1β/IFNγ-induced expression of IL-8 mRNA by 20% and 30%, respectively (Figure 4-13). Although not all results of IL-8 mRNA expression were similar to a sample in IL-8 ELISA, these results indicate that the inhibition of IL-8 secretion by BYK191023 and dexamethasone is at least partially transcriptionally regulated in cytokine/dsRNA-stimulated A549 cells.

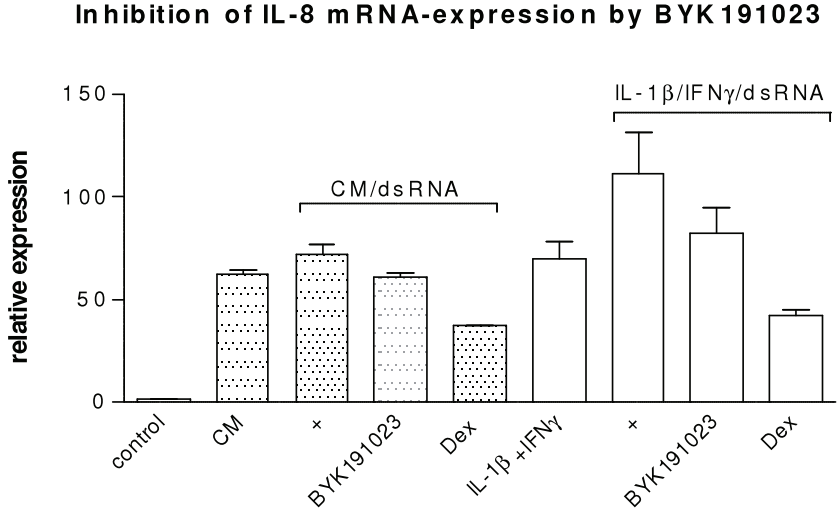

Figure 4-13: BYK191023- and dexamethasone-mediated inhibition of IL-8 mRNA expression in cytokine/dsRNA-stimulated A549 cells

About $1x10^6$ cells were seeded per each well. After 24 h of culture, the cells were exposed to the indicated substances for 30 min and then stimulated with cytokine combinations with or without dsRNA. After 6 h of incubation, total RNA was isolated and transcribed into cDNA. Real-Time PCR was performed with IL-8 mRNA specific primers. Both CM and IL-1β/IFNγ could increase IL-8 mRNA expression and addition of dsRNA further increased this effect, especially in the case of IL-1β/IFNγ (70-fold to 111-fold). BYK191023 and dexamethasone both reduced the cytokine-mediated IL-8 expression significantly. Whereas BYK191023 decreased IL-8 mRNA levels by up to 30%, dexamethasone reduced them by up to 70% in the case of IL-1β/IFNγ/dsRNA stimulation. CM: 100 ng/ml IFNγ, 10 ng/ml IL-1β, 10 ng/ml TNFα. IFNγ: 100 ng/ml, IL-1β : 10 ng/ml. dsRNA: 100 µg/ml. BYK191023: 100 µM. Dex: 1 µM.

To note, against our expectation dexamethasone at 1µM as control to inhibit IL-8 did not totally inhibit IL-8 secretion or mRNA-expression induced by cytokine mix, although its IC50 is normally between 1 nM and 10 nM (see Chapter 4.3.1.1 for more details).

4.2.5 Functional effects of the iNOS inhibitor BYK402750 in BEAS-2B and MucilAir cells

BYK402750 is another highly selective iNOS inhibitor, which showed potent anti-inflammatory effects in a cigarette smoke mouse model mimicking certain aspects of human COPD by suppressing inflammatory cell influx (neutrophils, alveolar macrophages and T cells) and production of pro-inflammatory cytokine and chemokines (MIP-1α, MCP-1 and KC) in BALF (Hesslinger et al. 2008). In this study it was intended to elucidate the anti-inflammatory role of BYK402750 in human lung epithelial cell line BEAS-2B and primary lung epithelial cell culture MucilAir by assessing multiple cytokine and chemokines release using the Luminex technique and ELISA.

The cells were seeded and cultured as described in Materials and Methods. BEAS-2B cells were stimulated with CM and MucilAir cells with TNFα or CM after exposure to different concentrations of BYK402750. The induction of iNOS mRNA expression in BEAS-2B cells was proved by Real-Time PCR (data not shown, see also results from similar experiments in Figure 4-30). Due to the relatively low level of NO_x production in BEAS-2B cell, Griess assay was not able to detect the production of NO_x. Due to the special medium composition of MucilAir cells, which produced a high background, the NO_x production was not be assessed by Griess assay.

For the Luminex assay with the samples treated by BYK402750, a 25-plex kit including standards was applied according to the manufacturer's instructions (see also Materials and Methods or Chapter 4.1.5). By using this 25-plex kit the simultaneous measurement of human IL-1β, IL-1ra, IL-2, IL-2R, IL-4, IL-5, IL-6, IL-7, IL-8, IL-10, IL-12 (p40), IL-13, IL-15, IL-17, TNFα, IFNα, IFNγ, GM-CSF, MIP-1α, MIP-1β, IP-10, MIG, Eotaxin, RANTES, and MCP-1 was conducted.

Coincident with the results of cytokine stimulation study from ELISA (Figure 4-4) and Luminex assay (Figure 4-5), both cell models responded to cytokine or cytokine-mix treatment by secreting a number of different cytokines and chemokines detected here

(Luminex data of all analytes not shown, see also Figure 4-14, Figure 4-15Figure 4-16 for induction of certain cytokines and chemokines).

Table 4-1 demonstrates an overview of the effects of BYK402750 on cytokine and chemokine release measured in Luminex assay in BEAS-2B and MucilAir cells. Red fields present inhibitory effects of BYK402750 and in yellow fields the cytokine and chemokine levels were not changed through BYK402750 treatment. In the gray fields the levels of cytokines and chemokines were out of range, which could be selected and assessed by ELISA (examples see Figure 4-16). The release of some of the cytokines and chemokines in both cell models could be inhibited by BYK402750 in a concentration-dependent manner (3μM and 30 μM). Generally, as a control, dexamethasone at 1 μM could inhibit most of the cytokine release and Dex at 1 nM showed less effect on cytokine and chemokines release. But in some cases, against our expectation, Dex even at the high concentration of 1 μM could not inhibited cytokine and chemokines release totally (see also Figure 4-16 and Figure 4-32 for details). This putative steroid insensitivity of certain pro-inflammatory cytokine and chemokine release in CM- or TNFα-stimulated MucilAir cells was also identical to the results in Figure 4-13, which showed a insensitive IL-8 mRNA expression in CM-stimulated A549 cells (see Chapter 4.3.1.1 for more details).

In BEAS-2B cells, the release of GM-CSF, MCP-1 and RANTES was inhibited by BYK402750 at 3μM and 30 μM concentration-dependently to different extents (Figure 4-14). IL-8 release was not and only slightly inhibited by BYK402750 at 3 μM and 30 μM, respectively (data not shown in diagram). In contrast, IL-8 release in CM- and CM/dsRNA-stimulated A549 cells were reduced by BYK191023 (100 μM) to 60% and 50% of the positive controls, respectively (Figure 4-12). The less or no effect of BYK402750 on the release of IL-8 and some other cytokines and chemokines in BEAS-2B cells demonstrated in Table 4-1 was possibly caused by relatively low inhibitor concentrations used here. By increasing inhibitor concentration, more effects may be detected.

Further, in MucilAir cells IL-8 release induced by TNFα was significantly reduced by BYK402750 at 30 μM to 40% of the control (Figure 4-16a). In contrast, CM-induced IL-8 release in MucilAir cells was just slightly decreased by BYK402750 (Figure 4-16b). Moreover, Table 4-1 showed that BYK402750 could reduce release of most cytokines

and chemokines determined by Luminex assay in TNFα-stimulated MucilAir cells to different extents, but only IL-6, IL-2 and IL-2R release was clearly decreased in CM-stimulated MucilAir cells. Especially IL-6 release in TNFα-stimulated MucilAir was almost totally inhibited by BYK402750 both at 3 µM and 30 µM (Figure 4-15). These results indicate a stimulus- and hence readout-dependent effect of BYK402750 in the lung epithelial cell model of inflammation.

Table 4-1: Inhibitory effect of BYK402750 on cytokine and chemokines release in BEAS-2B and MucilAir cells

	BEAS-2B				MucilAir							
	CM(100ng/ml)				TNFalpha 100 (ng/mL)				CM(10ng/ml)			
	Byk402750		Dex		Byk402750		Dex		Byk402750		Dex	
Analytes	3µM	30µM	1nM	1µM	3µM	30µM	1nM	1µM	3µM	30µM	1nM	1µM
IL-1Ra												
IL-6												
IL-8												
GM-CSF												
IL-1β												
TNFα												
IL-7												
IL-12												
IL-15												
IL-17												
IL-13												
IFN-α												
RANTES												
MIP-1α												
MIP-1β												
IP-10												
MIG												
MCP-1												
Eotaxin												
IFN-γ												
IL-2												
IL-2R												
IL-4												
IL-5												
IL-10												

inhibition | no change | out of range

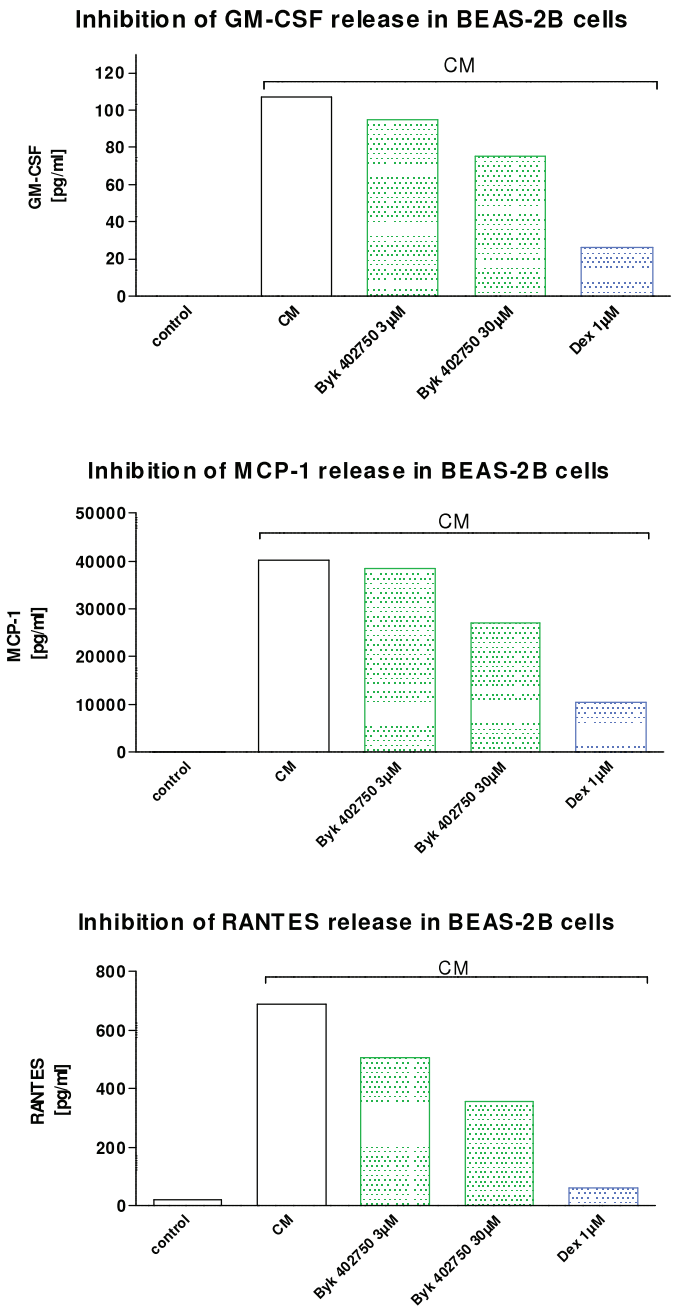

Figure 4-14: Inhibition of GM-CSF, MCP-1 and RANTES release by BYK402750 in CM-stimulated BEAS-2B cells (Luminex assay).

About $3x10^4$ cells were seeded per each well in 96-well plate. After 24 h culture, the cells were pretreated with the indicated substances for 30 min and subsequently stimulated with CM. Concentration of GM-CSF, MCP-1 and RANTES in the cell culture medium was determined by Luminex assay as described in Materials and Methods. Whereas CM strongly increased GM-CSF, MCP-1 and RNATES levels compared to negative control, treatment with BYK402750 decreased the levels of secreted cytokines and chemokines concentration-dependently to different extends. Dexamethasone at 1 µM was used as control and it significantly reduced cytokine secretion compared to the positive control. CM: 100 ng/ml IFNγ, 100 ng/ml IL-1β, 100 ng/ml TNFα. BYK402750: 3 µM and 30 µM. Dex: 1 µM.

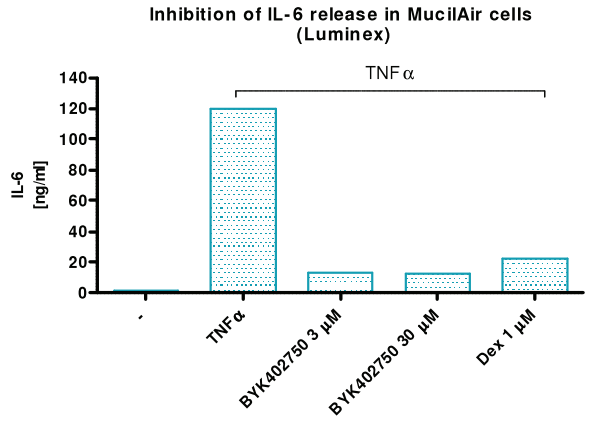

Figure 4-15: Inhibition of IL-6 release by BYK402750 in TNFα stimulated MucilAir cells (Luminex assay).

MucilAir cells were cultured as described in Materials and Methods. The cells were pretreated with the indicated substances for 30 min and then stimulated with TNFα. IL-6 concentration in the cell culture medium was determined by Luminex assay. Treatment with BYK402750 at 3 µM and 30 µM decreased the concentrations of IL-6 significantly. Dexamethasone at 1 µM as a control could also strongly reduce IL-6 secretion compared to the positive control. TNFα: 100 ng/ml, BYK402750: 3 µM and 30 µM. Dex: 1 µM.

Since the concentrations of some cytokines and chemokines were out of the expected range (the gray fields in also identical to the results in Figure 4-13, which showed a insensitive IL-8 mRNA expression in CM-stimulated A549 cells (see Chapter 4.3.1.1 for more details).

In BEAS-2B cells, the release of GM-CSF, MCP-1 and RANTES was inhibited by BYK402750 at 3µM and 30 µM concentration-dependently to different extents (Figure 4-14). IL-8 release was not and only slightly inhibited by BYK402750 at 3 µM and 30 µM, respectively (data not shown in diagram). In contrast, IL-8 release in CM- and CM/dsRNA-stimulated A549 cells were reduced by BYK191023 (100 µM) to 60% and 50% of the positive controls, respectively (Figure 4-12). The less or no effect of BYK402750 on the release of IL-8 and some other cytokines and chemokines in BEAS-2B cells demonstrated in Table 4-1 was possibly caused by relatively low inhibitor concentrations used here. By increasing inhibitor concentration, more effects may be detected.

Further, in MucilAir cells IL-8 release induced by TNFα was significantly reduced by BYK402750 at 30 µM to 40% of the control (Figure 4-16a). In contrast, CM-induced IL-8 release in MucilAir cells was just slightly decreased by BYK402750 (Figure 4-16b). Moreover, Table 4-1 showed that BYK402750 could reduce release of most cytokines

and chemokines determined by Luminex assay in TNFα-stimulated MucilAir cells to different extents, but only IL-6, IL-2 and IL-2R release was clearly decreased in CM-stimulated MucilAir cells. Especially IL-6 release in TNFα-stimulated MucilAir was almost totally inhibited by BYK402750 both at 3 μM and 30 μM (Figure 4-15). These results indicate a stimulus- and hence readout-dependent effect of BYK402750 in the lung epithelial cell model of inflammation.

Table 4-1Additionally, some of the results from Luminex assay could be validated by ELISA assay. Figure 4-16 demonstrate the effects of BYK402750 on IL-8 and GM-CSF release in TNFα- or CM-stimulated MucilAir cells using ELISA. Consistent with the results from Luminex assay, BYK402750 inhibited TNFα-induced IL-8 release in MucilAir cells in a concentration-dependent manner as described above (Figure 4-16a). In comparison to TNFα-stimulated cells, BYK402750 had only slightly effect on IL-8 release in CM-stimulated cells, which was out of range in Luminex assay and assessed here in ELISA assay (Figure 4-16b). GM-CSF release was reduced by BYK402750 (30 μM) about 30% in CM-stimulated MucilAir cells (Figure 4-16c).

Taken together, in this part of the work, the anti-inflammatory effects of iNOS inhibitor BYK191023 in CM-stimulated lung epithelial cells A549 were verified by BYK402750, another selective iNOS inhibitor, by reducing release of various cytokines and chemokines in BEAS-2B and MucilAir cells through Luminex assay. The reduced effect of dexamethasone to inhibit certain cytokine and chemokine release in A549 and MucilAir cells indicate a possible steroid insensitive situation in the cytokine-stimulated lung epithelial cells.

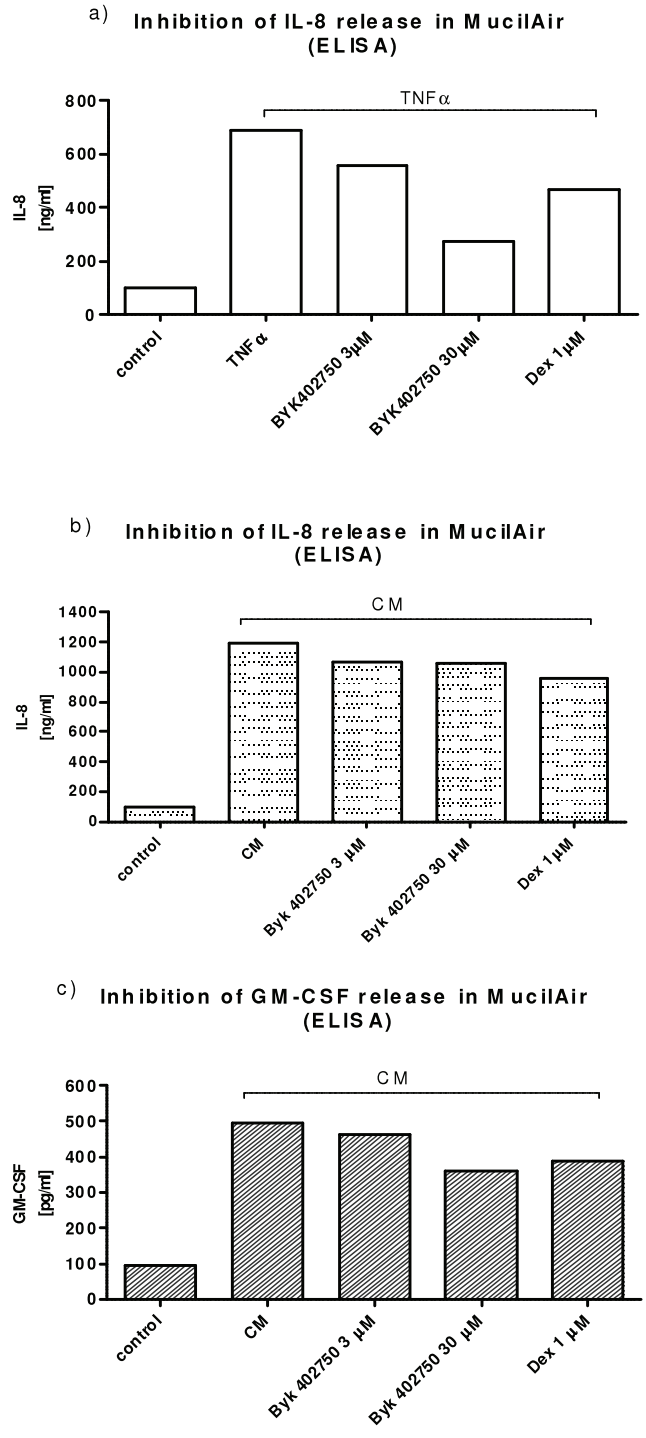

Figure 4-16: Inhibition of IL-8 and GM-CSF release by BYK402750 in TNFα- or CM-stimulated MucilAir cells (ELISA).

MucilAir cells were cultured as described in Materials and Methods. The cells were pretreated with the indicated substances for 30 min and subsequently stimulated with TNFα or CM. IL-8 and GM-CSF concentrations in the cell culture medium were determined by ELISA. Treatment with BYK402750 at 30 µM decreased the concentrations of TNFα-induced IL-8 significantly. BYK402750 decreased the concentrations of CM-induced IL-8 or GM-CSF slightly. Dexamethasone at 1 µM could just very slightly reduce IL-8 and GM-CSF secretion compared to the positive control TNFα: 100 ng/ml, BYK402750: 3 µM and 30 µM. Dex: 1 µM.

4.3 Potential role of iNOS in steroid insensitivity

Various studies have reported steroid insensitivity in induced sputum cells, airway biopsy specimens or alveolar macrophages from patients with COPD who smoke (Barnes et al. 2004; Barnes and Adcock 2009). Barnes has hypothesized that this insensitivity depends on increased oxidative and nitrative stress, either from exogenous sources or from iNOS-derived NO and $ONOO^-$, and reduced HDAC2 activity due to its nitration (Barnes 2006a). Less is known about the role of iNOS in steroid insensitivity in lung epithelial cells. The aim of this part of the work was to characterize the role of iNOS in steroid insensitivity, using a human lung epithelial cell model and different modes of iNOS/NO modulation, like iNOS inhibitors, iNOS overexpression and NO/$ONOO^-$ donors.

4.3.1 Identification and characterization of A549 epithelial cell model of steroid insensitivity

To establish a cell model of steroid insensitivity, first of all, a dose-dependent anti-inflammatory effect of dexamethasone in A549 cells was elucidated at different stimulation conditions.

4.3.1.1 Effects of dexamethasone on cytokine –mediated induction of IL-8 mRNA expression

To study the responsiveness towards steroids in cytokine-stimulated lung epithelial cells, the effect of dexamethasone on cytokine-induced IL-8 mRNA expression in A549 cells was examined by Real-Time PCR. According to the results from the last chapter, that stimulation of A549 cells with a cytokine-mix (CM) induced the expression of iNOS and iNOS-mediated NO production, A549 cells were stimulated with either IL-1β alone or CM (IL-1β, IFNγ, TNFα) and dsRNA with concomitant treatment of different concentrations of dexamethasone. As depicted in Figure 4-17, in cells stimulated with IL-1β alone, thus expressing no iNOS, dexamethasone at concentrations from 10 nM till 1 μM was able to reduce cytokine-mediated IL-8 mRNA expression by about 90%. Lower concentrations had no (Dex 0.1 nM) or only slight (Dex 1 nM) effects on IL-8 mRNA levels, suggesting an IC_{50} of approximately 1 nM to10 nM. Interestingly, in cells that were treated with CM and dsRNA, and hence expressed iNOS, dexamethasone treatment even at high μM concentrations did not lead to a decrease of IL-8 mRNA expression to less then 40% of the positive control. We had expected, that

dexamethasone would totally inhibit both IL-1β and CM/dsRNA stimulated IL-8 mRNA-expression, but in fact, IL-8 mRNA expression in CM/dsRNA–stimulated A549 was only marginally affected by dexamethasone and showed a partial steroid insensitivity.

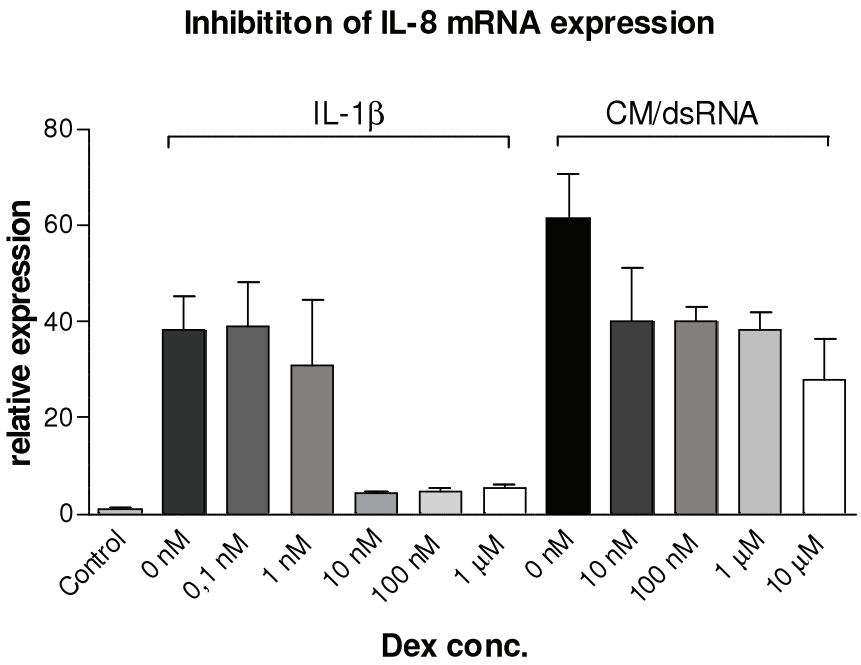

Figure 4-17: Dexamethasone-mediated inhibition of IL-1β- or CM/dsRNA-induced IL-8 mRNA expression in A549 cells.

About $1x10^6$ cells were seeded per each well. After 24 h of culture, the cells were treated with either 100 ng/ml IL-1β alone or a combination of cytokines (CM: 100 ng/ml IFNγ, 10 ng/ml IL-1β and 10 ng/ml TNFα) and 100 µg/ml dsRNA. After 6 h of incubation, total RNA was isolated and transcribed into cDNA. Real-Time PCR analysis revealed, that in cells treated with IL-1β alone, dexamethasone was able to inhibit cytokine-stimulated IL-8 expression by up to 90% in a dose-dependent fashion. Interestingly, in cells treated with CM/dsRNA, dexamethasone only reduced IL-8 mRNA levels by up to 60%. These cells thus showed a partial insensitivity to dexamethasone.

4.3.1.2 Effects of dexamethasone on cytokine- mediated release of IL-8

Various studies of the anti-inflammatory effects of dexamethasone have reported that it provides IC_{50} values between 1 and 10 nM (Cronstein et al. 1992; Lasa et al. 2001), and according to the results of IL-8 Real-Time PCR, this prediction applied to our results for cells stimulated with IL-1β, but not to those of cells treated with cytokine-mix. Under the given conditions, A549 cells treated with cytokine-mix and dsRNA, which expressed iNOS, were found to be less sensitive towards corticosteroid treatment than cells treated with IL-1β alone, which did not express iNOS. To test whether this effect could be also shown for IL-8 secretion, the dose-response

relationship of dexamethasone against IL-8 secretion was ascertained in A549 cells. Figure 4-18 demonstrated that regarding IL-8 secretion, dose-response curves of dexamethasone in CM/dsRNA stimulated A549 cells is shifted upwards and to the right, compared to that in IL- 1β stimulated cells and the IC_{50} value was increased 10-fold. Thus, CM-treated cells did not fully respond even to high concentrations of Dex, suggesting a – at least partial- steroid insensitivity.

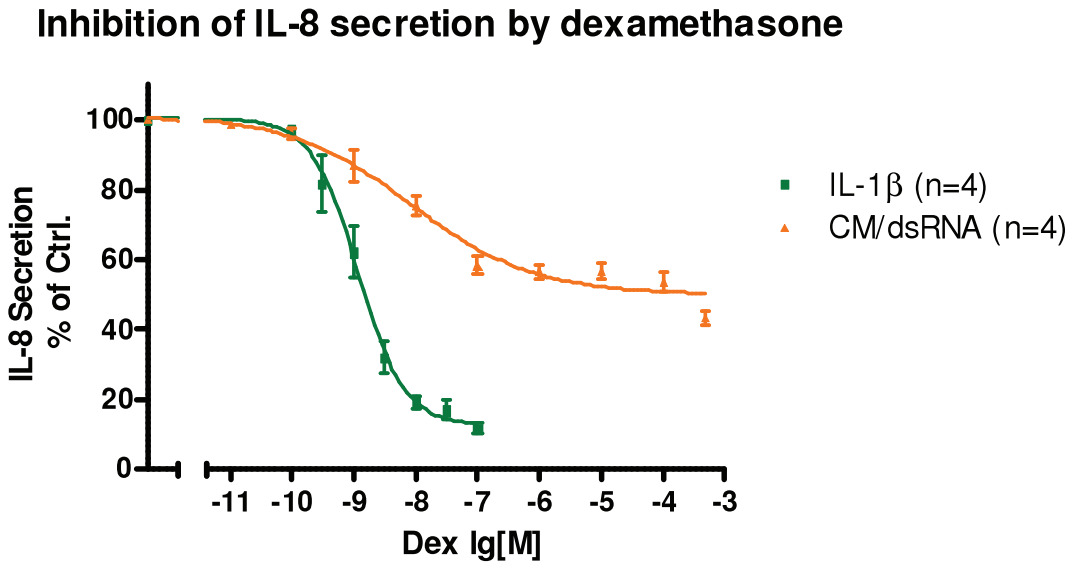

	IL-1β (n=4)	CM/dsRNA (n=4)
LogEC50	-8.939	-8.077

Figure 4-18: Concentration-dependent effects of dexamethasone on IL-1β- or CM/dsRNA-induced IL-8 release in A549 cells.

About $4x10^5$ A549 cells were seeded per each well. After 24 h culture, the cells were stimulated with IL-1β or Cytokine-Mix with dsRNA and concomitantly treated with increasing concentration of dexamethasone for 20 h to detect concentration of IL-8 in the cell culture supernatants by ELISA analysis. Whereas IL-1β stimulated IL-8 release in A549 was dexamethasone sensitive and reduced the release down to 10% of postive control,Cytokine-Mix/dsRNA stimulated IL-8 release in A549 was dexamethasone insensitive and reduced the release only to about 50% even at high concentrations. IL-1β: 100 ng/ml, CM: 100 ng/ml IFNγ, 100 ng/ml IL-1β, 100 ng/ml TNFα. dsRNA: 100 µg/ml. Dexamethasone: 0.1 nM to 100 µM.

In order to characterize the dose response of dexamethasone in cytokine-stimulated A549 cells, the cells were also stimulated with CM (without dsRNA) or with a combination of IL-1β and TNFα. Compared with cells stimulated only by IL-1β, IL-8 secretion in cells stimulated with CM or IL-1β and TNFα showed also insensitivity to dexamethasone treatment like the cells treated with CM/dsRNA (Figure 4-19). Both of the dose-response curves of dexamethasone regarding IL-8 secretion in A549 cells

were shifted upwards and to the right to different degrees, compared to that in IL-1β stimulated cells, again suggesting a steroid insensitivity.

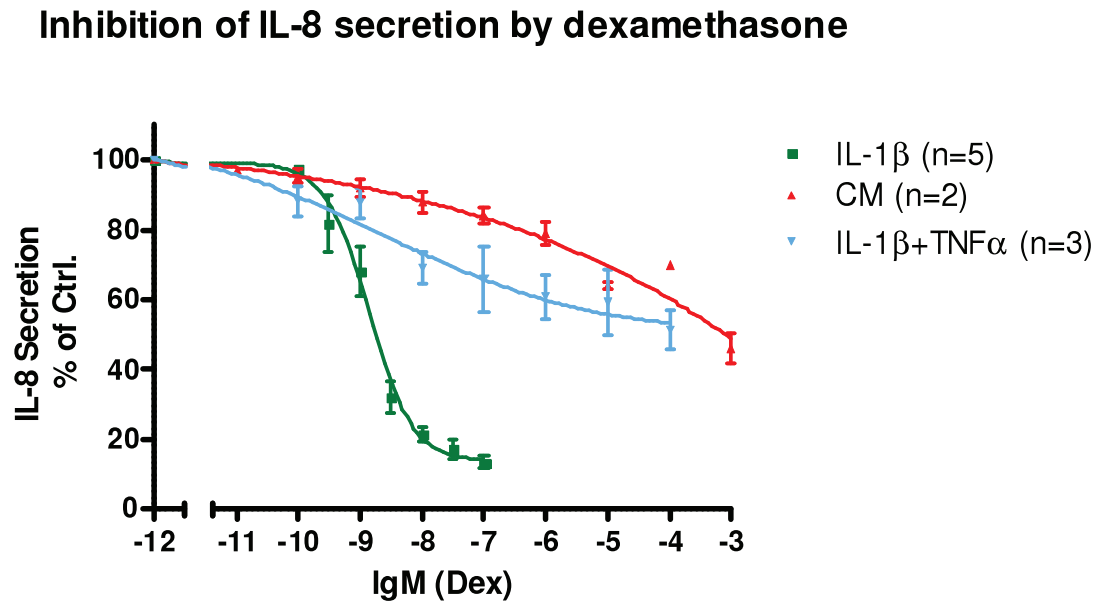

	IL-1β/Dex (n=5)	CM/Dex (n=2)	IL-1β+TNFα/Dex (n=3)
LogEC50	-8.867	~ 2.690	-8.599

Figure 4-19 Concentration-dependent effects of dexamethasone on IL-1β-, IL-1β+TNFα- or CM-induced IL-8 release in A549 cells.

About 4x10^5 A549 cells were seeded per each well. After 24 h culture, the cells were stimulated with IL-1β or cytokine-mix or IL-1β and TNFα and concomitantly treated with increasing concentration of dexamethasone for 20 h to detect concentration of IL-8 in the cell culture supernatants by ELISA analysis. Whereas IL-1β stimulated IL-8 release in A549 was dexamethasone sensitive and reduced the release down to 10% of positive control, CM or IL-1β and TNFα stimulated IL-8 release in A549 was dexamethasone insensitive and reduced the release only to about 55% and 50% at a high concentration, respectively. IL-1β: 100 ng/ml, TNFα: 100 µg/ml CM: 100 ng/ml IFNγ, 100 ng/ml IL-1β, 100 ng/ml TNFα. Dexamethasone: 0.1 nM to 100 µM.

4.3.1.3 Steroid responsiveness of cytokine release through Luminex assay

To analyze whether the steroid insensitivity only limits to IL-8 secretion, the Luminex technology was applied to test 25 cytokines and chemokines in parallel. Table 4-2 shows an overview of the steroid responsiveness of all measured cytokines and chemokines. Of the 25 cytokines measured, 11 cytokines were induced by IL-1β and CM. IL-1Ra, RANTES, IL-8 showed a partially steroid insensitivity and GM-CSF and IL-2R showed strongly reduced responsiveness towards dexamethasone treatment (Figure 4-20).

Table 4-2: Evaluation of steroid responsiveness in cytokine-induced A549 cells using Luminex technology

Cytokine measured	IL-1ß, IL-1Ra, IL-2, IL-2R, IL-4, IL-5, IL-6, IL-7, IL-8, IL-10, IL-12, IL-13, IL-15, IL-17, IFN-α, IFN-γ, GM-CSF, MIP-1α, MIP-1β, IP-10, MCP-1, RANTES, Eotaxin, MIG
Inducible by IL-1β and CM	IL-1Ra, IL-2R, IL-6, IL-7, IL-8, IFN-α, GM-CSF, MIP-1α, IP-10, MCP-1, RANTES,
Partially steroid insensitive	IL-1Ra, RANTES, IL-8
Steroid insensitive	GM-CSF and IL-2R

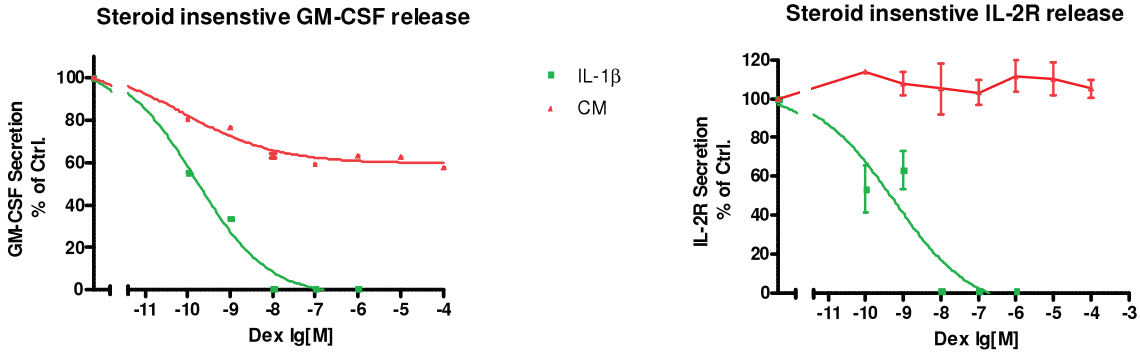

Figure 4-20: Steroid-insensitive GM-CSF and IL-2R release in CM-stimulated A549 cells.

About $4x10^5$ A549 cells were seeded per each well. After 24 h culture, the cells were stimulated with IL-1β or cytokine-mix and concomitantly treated with increasing concentration of dexamethasone for 20 h to detect concentration of GM-CSF and IL-2R in the cell culture supernatants by Luminex assay. Whereas IL-1β stimulated GM-CSF and IL-2R release in A549 cells was dexamethasone sensitive and was inhibited by Dex totally, CM-stimulated GM-CSF and IL-2R release in A549 was dexamethasone insensitive. IL-1β: 100 ng/ml, TNFα: 100 µg/ml CM: 100 ng/ml IFNγ, 100 ng/ml IL-1β, 100 ng/ml TNFα. Dex: 0.1 nM to 100 µM.

4.3.1.4 Assessment of NO_x production in the steroid insensitive A549 cells

As demonstrated in section 4.2, stimulation of A549 cells with CM and dsRNA activated iNOS expression and NO production. To confirm these results in the steroid insensitive system, the NO_x (nitrite and nitrate) production was assessed by Griess assay parallel to ELISA assay. As illustrated in Fig. 1-18: the steroid insensitive system produced high amount of NO and concomitant treatment of dexamethasone at concentrations from 0.01 nM to 10 µM had only modest effect on NO_x production. Only at the highest concentration of 100 µM dexamethasone, NO_x production was reduced

by about 30%. Therefore, the steroid insensitivity exists in this cell system in parallel with iNOS activity.

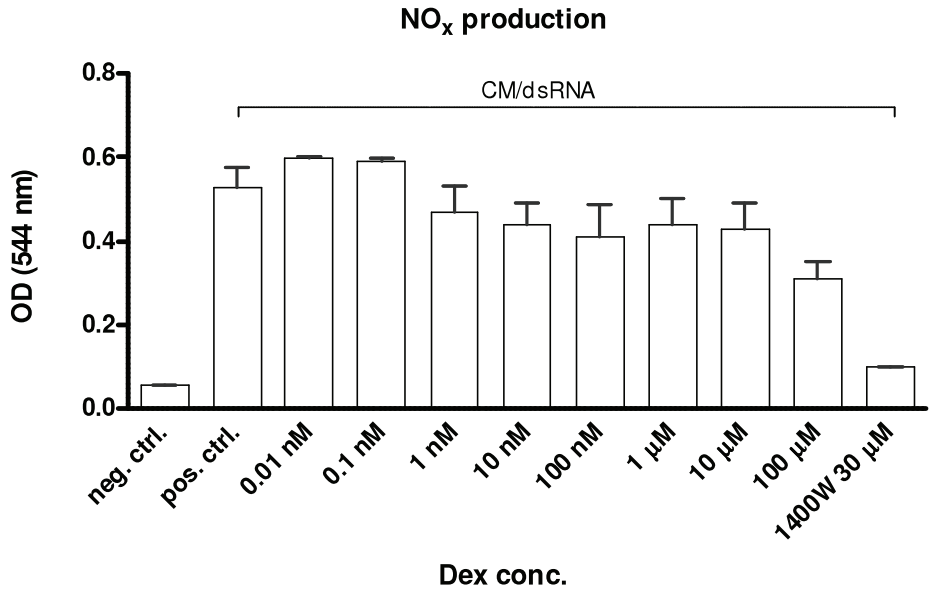

Figure 4-21: Steroid-insensitive NO_x production in CM/dsRNA-stimulated and dexamethasone-treated A549 cells.

$4x10^5$ cells were seeded per each well in 24-well plates and cultured in DMEM (5% FCS) for 24h. NO_x production was then stimulated by the addition of CM/dsRNA for 24h in the presence of dexamethasone at different concentrations from 0,01nM to 100 µM. iNOS inhibitor 1400W (30 µM) was used as control of iNOS inhibition. The Griess assay for detection of nitrite and nitrate was performed as described in Materials and Methods. Stimulation of A549 cells with CM/dsRNA increased NO production and concomitant treatment of dexamethasone has less effect on NO_x production. Only at the highest concentration of 100 µM dexamethasone NO_x production was reduced about 30% of control. n=4. CM: 100 ng/ml IFNγ, 100 ng/ml IL-1β, 100 ng/ml TNFα, dsRNA: 100 µg/ml. NO_x control (30 µM $NaNO_3$) = 0.85

4.3.2 Suggested Responsiveness of HDAC activity upon exogenous oxidative and nitrative stress in A549 cells

Steroid insensitivity in COPD is suggested to be dependent on increased oxidative and nitrative stress. According to the hypothesis of the involvement of iNOS in steroid insensitivity, iNOS-derived NO may increase the nitrative stress through formation of peroxynitrite, which may lead to the nitration of HDAC and hence reduction of HDAC activity (Barnes 2006a; Barnes 2008). To determine the responsiveness of HDAC activity in lung epithelial cells A549 upon oxidative and nitrative stress, in this part of the work, the effects of hydrogen peroxide (H_2O_2) and SIN-1, a superoxide and nitric oxide donor, which can form peroxynitrite, on HDAC activity in A549 cells were studied.

To analyze the effects of SIN-1 and H_2O_2 on HDAC activity, A549 cells were treated with SIN-1 (50, 100 or 500µM) and H_2O_2 (10, 50 or 100 µM) alone or in combination at different concentrations as indicated in the diagrams (Figure 4-22 and Figure 4-23). The effect of oxidative and nitrative stress on recombinant (Figure 4-24) and cellular (Figure 4-22 and Figure 4-23) HDAC activity was detected with a HDAC colorimetric assay as described in Materials and Methods.

In the first experiments A549 cells were treated with H_2O_2 at a concentration range from 1 µM to 100 mM for 2, 4 and 6 hours and H_2O_2 between 10 mM and 100 mM apparently resulted in cell death due to massive oxidative stress already after 2 hours of treatment. Therefore, H_2O_2 was generally used at a maximum concentration of 1mM.

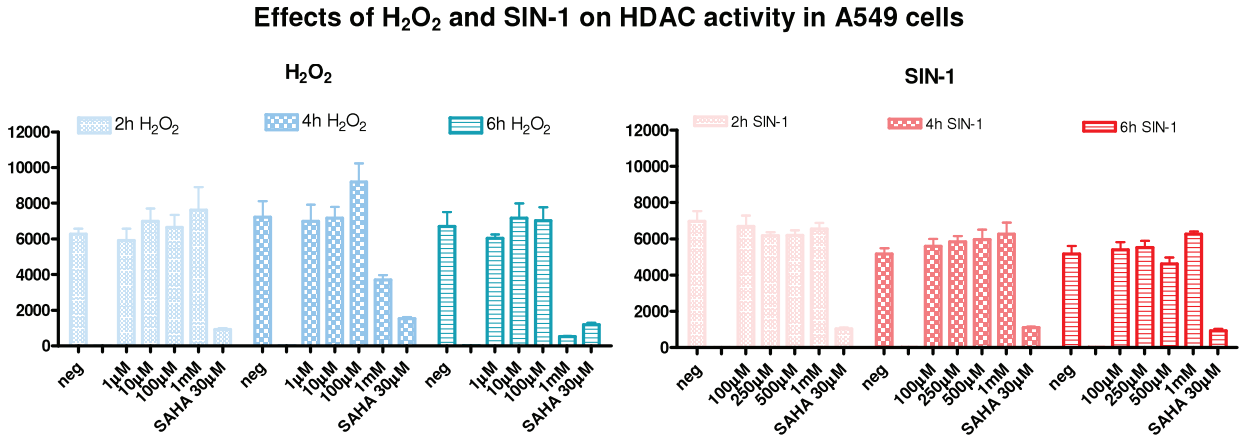

Figure 4-22: Effect of H_2O_2 (left side) and SIN-1 (right side) at different concentrations and time points on HDAC activity in A549 cells.

A549 cells were seeded and cultured as described in Materials and Methods. After 24 h cells were exposed to H_2O_2 or SIN-1 at the concentrations as indicated for 2, 4, and 6h. Afterwards the HDAC cellular activity was detected with a HDAC colorimetric assay as described in Materials and Methods. Compared to negative (without substance treatment) and HDAC inhibitor (SAHA) controls, SIN-1 treatment (100 to 500 µM) apparently did not affect HDAC activity. Treatment with H_2O_2 did not affect HDAC activity after 2 h treatment, but after 4 h treatment and at 100µM, H_2O_2 increased HDAC activity slightly. HDAC activity was schown to be reduced after 4 h and 6 h treatment with 1 mM H_2O_2, which was due to the cytotoxic effect of H_2O_2 according to LDH assay (data not shown). n=2, SAHA: 30µM

Figure 4-22 demonstrates the effects of H_2O_2 and SIN-1 on HDAC activity in A549 cells at different concentrations and time points of treatment. SIN-1 treatment (100 to 500 µM) apparently did not affect HDAC activity. Additionally, treatment with H_2O_2 did not affect HDAC activity after 2 h treatment, but after 4 h treatment and at 100µM, H_2O_2 increased HDAC activity slightly. HDAC activity was schown to be reduced after 4 h and 6 h treatment with 1 mM H_2O_2, which was due to the cytotoxic effect of H_2O_2

according to LDH assay (data not shown). In contrast to Ito et. al, who reported a reduction of HDAC activity in A549 cells treated with sub-leveled cytotoxic H_2O_2 concentrations, we could not show any significant effect on HDAC activity under the conditions used.

As H_2O_2 or SIN-1 alone did not affect HDAC activity in A549 cells, in the subsequent experiments combinations of H_2O_2 and SIN-1 were explored. Furthermore, considering the relatively slow degradation of HDAC via the proteasome we examined the HDAC activity after 16 hours and 24 hours of treatment (Figure 4-23). Compared to control there was a slight increase in HDAC activity in the cells treated with combinations of SIN-1 with 10 µM H_2O_2. Combinations of various SIN-1 concentrations with 50 µM H_2O_2 reduced HDAC activity slightly and combinations with 100µM H_2O_2 significantly reduced HDAC activity in A549 cells. However, treatment with 100 µM H_2O_2 for 24 hours resulted in slight cytotoxicity using LDH assay (data not shown).

Taken together, HDAC activity in A549 cells was sensitive towards the oxidative and nitrative treatment with a combination of SIN-1 and H_2O_2 treatment under the conditions used in this study.

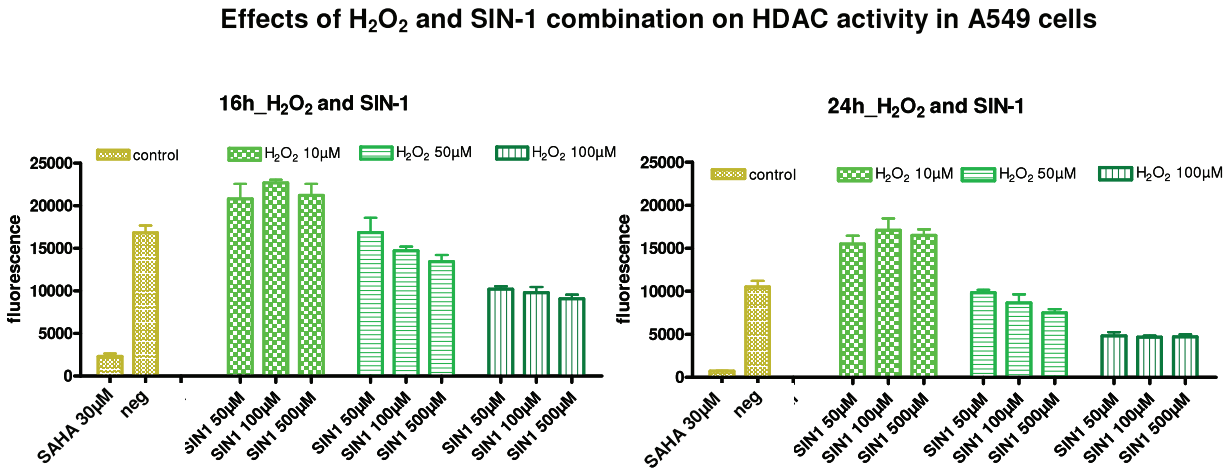

Figure 4-23: Effects of H_2O_2 and SIN-1 as combinations at different concentrations and time points (16 h left, 24 h right) on HDAC activity in A549 cells.

A549 cells were incubated with H_2O_2/SIN-1 combinations as indicated for 16h and 24h and the HDAC activity were measured afterwards (n=4). Compared to negative (without substance treatment) and HDAC inhibitor (SAHA) controls, there was a slight increase in HDAC activity in the cells treated with combinations of SIN-1 with 10 µM H_2O_2. Combinations of various SIN-1 concentrations with 50 µM H_2O_2 reduced HDAC activity slightly and combinations with 100µM H_2O_2 significantly reduced HDAC activity in A549 cells. However, treatment with 100 µM H_2O_2 for 24 hours resulted in slight cytotoxicity using LDH assay (data not shown). n=2. SAHA: 30µM

To further elucidate the effects of oxidative and nitrative stress on HDAC activity, subsequently, the effect of H_2O_2 and SIN-1 on the activity under cell-free conditions of recombinant HDAC1 was measured after treatment for 2 or 4 hours (Figure 4-24, data of 2 hours treatment not shown). Within a concentration range between 10 nM and 100 µM, H_2O_2 did no affect HDAC activity neither after 2 hours nor 4 hours treatment. In comparison to H_2O_2, SIN-1 reduced rHDAC1 activity in a concentration-dependent manner. At very high SIN-1 concentrations of 316 µM and 1 mM the rHDAC1 activity was significantly decreased to about 40% and less than 10%, respectively. At lower concentrations, SIN-1 did not affect HDAC activity reduction significantly.

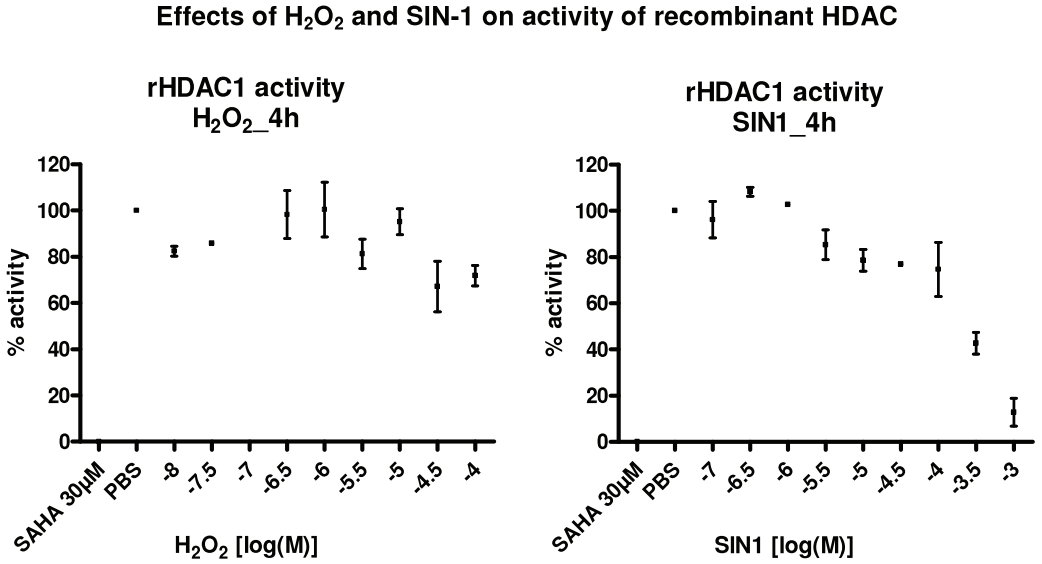

Figure 4-24: Effects of H_2O_2 and SIN-1 on rHDAC1 activity under cell-free conditions.

rHDAC1 enzyme was treated with H_2O_2 and SIN-1 as described in Materials and Methods at the indicated concentration. The rHDAC1 activity assay was conducted as described in Materials and Methods. The values from treatment with SAHA (30 µM) were set as 0%, and from PBS control as 100% (n=2). H_2O_2 treatment had no effect on rHDAC1 activity and SIN-1 reduced rHDAC1 activity in a concentration-dependent manner.

To briefly summarize this part of the results, A549 cells stimulated with CM showed concomitant steroid insensitivity regarding the release of several but not all analytes and iNOS activity. While dexamethasone inhibited effectively IL-1β- induced expression and secretion of these cytokines in a concentration-dependent manner, the sensitivity towards dexamethasone was markedly reduced when A549 cells were stimulated with the cytokine-mix that elevated iNOS activity. Even at very high concentrations, dexamethasone only marginally affected the expression and release of IL-8. Moreover, HDAC activity in this cell system was sensitive to the exogenous

oxidative and nitrative stress of combined H_2O_2 and SIN-1 treatment. These data suggest that this lung epithelial cell model could be used for the study of the potential involvement of iNOS in steroid insensitivity *in vitro*.

4.3.3 Effects of modulation iNOS expression and NO levels on steroid sensitivity in A549 cells

To study the potential role of iNOS and iNOS-derived NO in steroid insensitive A549 cell model, several strategies of modulating iNOS/NO like using iNOS inhibitors, iNOS overexpression and applying NO/$ONOO^-$ donors in the cells were used. First of all, the effect of iNOS inhibition by selective iNOS inhibitors on the Dex-insensitive cytokine release was studied.

4.3.3.1 Effects of iNOS inhibitors on Dex insensitivity

To analyze the effect of iNOS inhibition, CM/dsRNA-stimulated A549 cells were pre-treated with iNOS inhibitor 1400W at 10 μM and 30 μM and concomitantly increasing concentrations of dexamethasone (0.1 nM to 10 μM). 1400W is a highly selective iNOS production and inhibits NO production in various cell lines at low micromolar concentrations, e.g. IC_{50} = 0.23 μM in RAW cell line (Strub et al. 2006) and IC_{50} = 2.5 μM in A549 cell line (data not shown). Figure 4-25 shows that 1400W neither at 10 μM nor at 30 μM could increase steroid responsiveness in this cell model.

To confirm and also to verify the results of iNOS inhibitor effects, cytokine-mix stimulated and dex-treated A549 cells were pre-exposed to 1400W at a concentration of 100 μM and to another non-selective potent NOS inhibitor AMT at 30 μM. As illustrated in Figure 4-26, iNOS inhibitor 1400W (100 μM) or AMT (30 μM) had no effect on steroid insensitivity of CM-stimulated A549 cells, even through fully inhibiting iNOS activity at these concentrations (Boer et al. 2000).

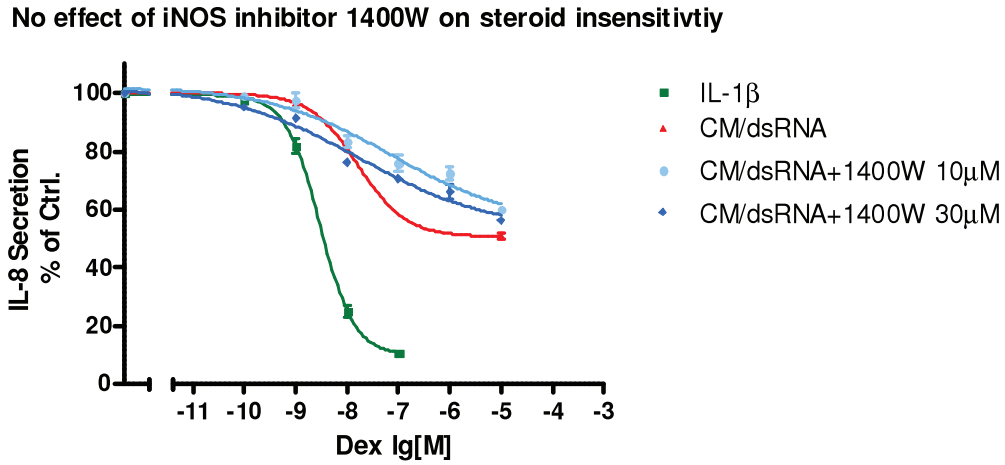

	IL-1β	CM/dsRNA	CM/dsRNA+1400W 10 μM	CM/dsRNA+1400W 30 μM
LogEC50	-8.531	-7.794	-7.141	-7.757

Figure 4-25: Effects of the selective iNOS inhibitor 1400W on the Dex responsiveness in cytokine/dsRNA-stimulated A549 cells.

A549 cells were exposed to vehicle or iNOS inhibitor 1400W (10 μM and 30 μM) for 30 minutes, then dexamethasone at different concentrations and CM/dsRNA stimulus were added in the presence of vehicle or iNOS inhibitors for another 20 hours. In parallel control, the cells were stimulated with IL-1β and treated with Dex. IL-8 secretion in A549 cell supernatants was assessed using ELISA (n=4 for each data point). 1400W neither at 10 μM nor at 30 μM could increase steroid responsiveness in this cell model of steroid insensitivity. IL-1β: 100 ng/ml, CM: 100 ng/ml IFNγ, 100 ng/ml IL-1β, 100 ng/ml TNFα, dsRNA: 100 μg/ml.

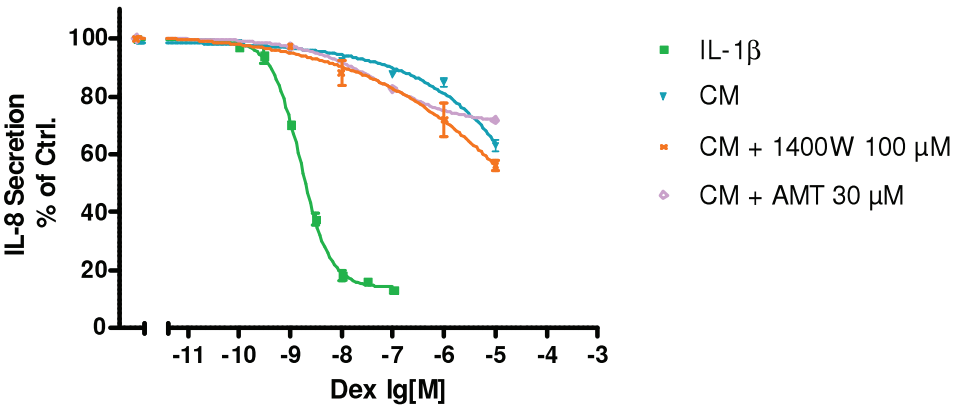

	IL-1β	CM	CM + AMT 30 μM	CM + 1400W 100 μM
LogEC50	-8.803	~ 2.258	-7.275	-3.788

Figure 4-26: Effect of the selective iNOS (1400W, 100 μM) and the non-selective NOS (AMT 30 μM) inhibitors on the steroid responsiveness in CM-stimulated A549 cells.

A549 cells were exposed to vehicle or iNOS inhibitor 1400W (100 μM) and non-selective NOS inhibitor AMT (30 μM) for 30 minutes, then dexamethasone at different concentrations and CM stimulus were added in the presence of vehicle or iNOS inhibitors for another 20 hours. In parallel as control, the cells were stimulated with IL-1β and treated with dex. IL-8 secretion in A549 cell supernatants was ascertained using ELISA (n=4 for each data point). 1400W (100 μM) and AMT (30 μM) had no effect on steroid insensitivity of CM-stimulated A549 cells. IL-1β: 100 ng/ml, CM: 100 ng/ml IFNγ, 100 ng/ml IL-1β, 100 ng/ml TNFα.

4.3.3.2 Effects of iNOS overexpression on Dex sensitivity

As a next step to modulate iNOS, iNOS overexpression in A549 cells was applied. A549 cells were transiently transfected with a iNOS-expressing plasmid pENOS2-N1 [modified from plasmid pEGFP-N1 with iNOS(NOS2)-coding sequence (NM_000625)] or with a control EGFP-expressing plasmid pEGFP-N1 (see Materials and Methods). The efficiency of the transfection was controlled by fluorescence microscopy and then NO production in A549 cells was assessed by Griess assay, which showed an 8-fold increase of NO production compared to non-transfected cells (data not shown in diagram). Finally, the iNOS mRNA expression was quantified by Real-Time PCR. represents the iNOS mRNA expression in A549 cells transfected with pENOS2-N1 plasmid and subsequently stimulated with IL-1β and treated with different concentrations of dexamethasone. iNOS mRNA was expressed in all of samples and IL-1β-stimulation or Dex-treatment had no effect on the iNOS mRNA expression.

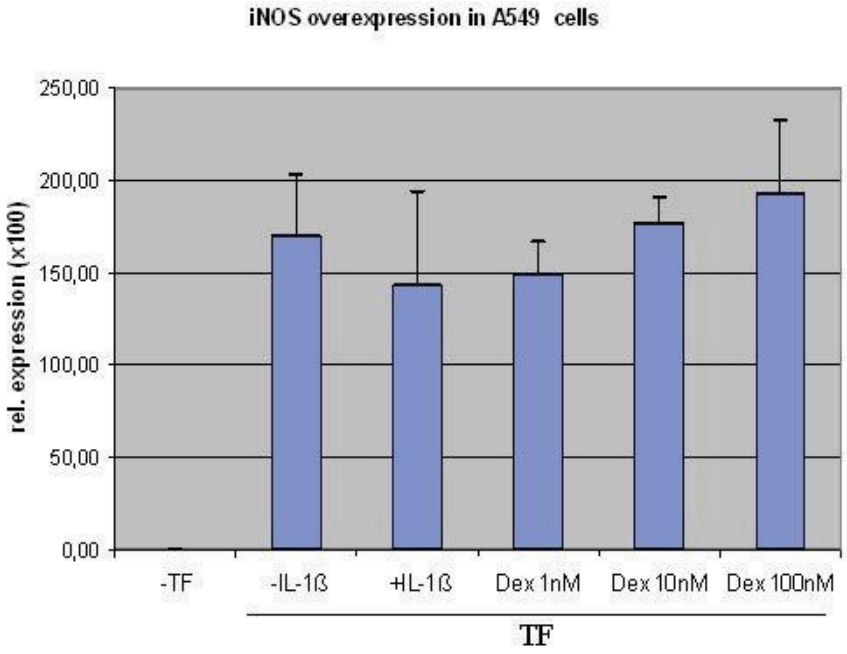

Figure 4-27: iNOS mRNA expression in A549 cells after transient transfection with iNOS-expressing pENOS2-N1.

Transient-transfection (TF) of A549 cells with iNOS-expressing plasmid pENOS2-N1 was performed using Superfect from Qiagen as detailed in Materials and Methods. After transfection, the cells were cultured overnight and then stimulated with IL-1β with concomitant treatment of dexamethasone. After 6 hours, cells were collected for RNA isolation. Total RNA was then reverse transcribed into cDNA and Real-Time PCR was performed with iNOS specific primers with *18sRNA* as internal control. The magnitude change of the iNOS mRNA is expressed as $2^{-\Delta\Delta Ct}$ (n=3). iNOS mRNA was expressed in all of the samples and IL-1β-stimulation or Dex-treatment had no effect on iNOS mRNA-expression. IL-1β: 100 ng/ml.

To define the effect of iNOS overexpression on steroid responsiveness, IL-8 release after IL-1β-stimulation in iNOS-transfected A549 cells were determined using ELISA assay. iNOS overexpression had no effect on steroid sensitivity in iNOS-overexpressing and IL-1ß-stimulated A549 cells (Figure 4-28).

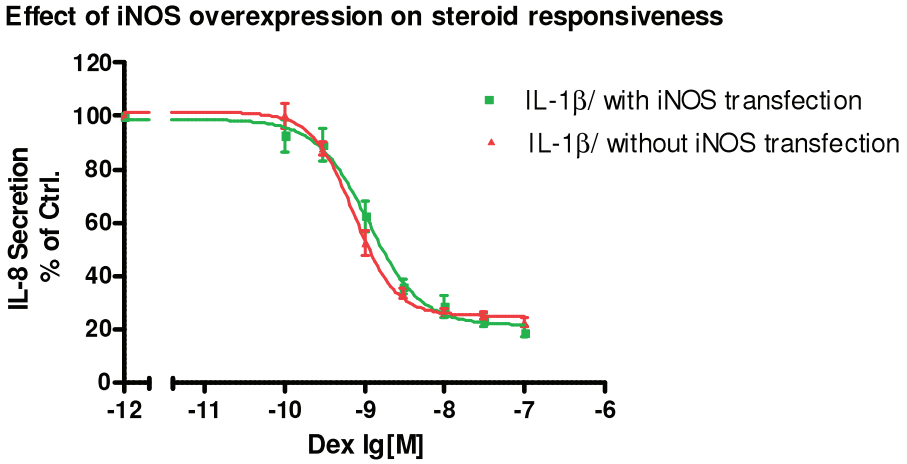

Figure 4-28: No effect of iNOS overexpression on steroid responsiveness in IL-1β-stimulated A549 cells.

A549 cells were transiently transfected with iNOS-expressing plasmid pENOS2-N1 using Superfect from Qiagen as detailed in Materials and Methods. After transfection, the cells were cultured overnight and then stimulated with IL-1β with concomitant treatment of dexamethasone at different concentrations (0.1 nM to 100 nM). After 20 hours, ELISA of IL-8 concentration in the cell supernatants were performed and the IL-8 secretion was calculated as percent of positive control without Dex-treatment (n=3). iNOS overexpression had no effect on steroid sensitivity in IL-1ß-stimulated A549 cells. IL-1β: 100 ng/ml.

4.3.3.3 Effects of exogenous nitrative and oxidative stress on steroid sensitivity using SIN-1 and H_2O_2

As presented above, the endogenous modulation of NO level through iNOS inhibition and iNOS overexpression did not show effect on steroid responsiveness in A549 cells. To further analyze effects of exogenous nitrative and oxidative stress on steroid responsiveness, IL-1β-stimulated A549 cells were treated with the NO/$ONOO^-$ donor SIN-1 (500 µM, once or twice) alone or with addition of H_2O_2 (100 µ, twice) in presence of dexamethasone. The effect of SIN-1 and H_2O_2 on steroid efficacy IL-8 secretion was analysed. As illustrated in Figure 4-29, neither SIN-1 nor a combination of SIN-1 and H_2O_2 affected steroid responsiveness in IL-1β-stimulated A549 cells, although these SIN-1 and H_2O_2 concentrations were shown to reduce HDAC activity in both the HDAC cellular assay and HDAC enzyme assay under cell free conditions before (see Figure 4-23 and Figure 4-24).

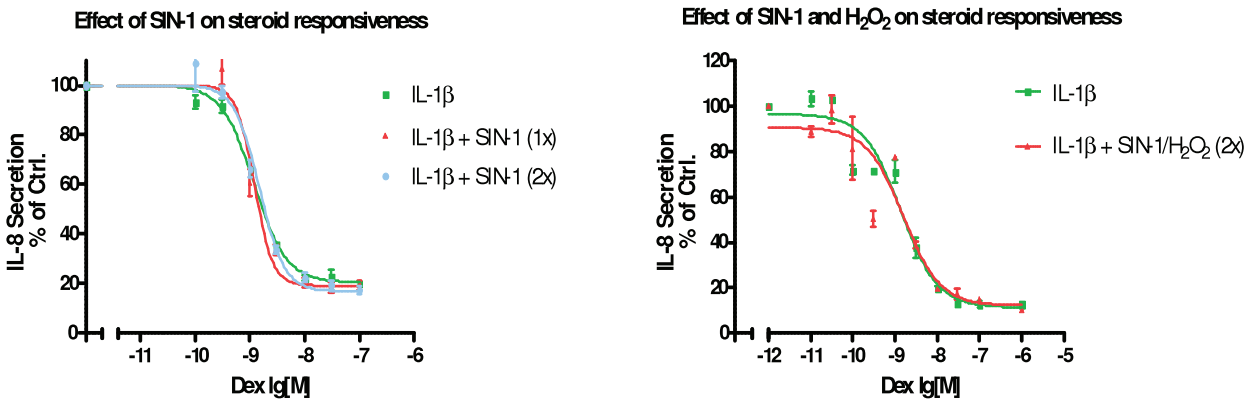

Figure 4-29: No effect of SIN-1 or SIN-1/H_2O_2 treatment on steroid responsiveness in IL-1β-stimulated A549 cells.

$2x10^5$ A549 cells/well in 24-well plates were exposed to vehicle or to SIN-1 500 µM or the combination of SIN-1 (500 µM) and H_2O_2 (100 µM) for 30 min before the cells were stimulated with IL-1β and exposed to dexamethasone at different concentrations. In the case of a second treatment, SIN-1 500 µM or the combination of SIN-1 (500 µM) and H_2O_2 (100 µM) were added after 30 min of stimulation. After 20 hours, IL-8 concentration in the cell supernatants was determined (n=4 for SIN-1 treatment, n=2 for SIN-1/H_2O_2 treatment). Neither SIN-1 nor SIN-1 and H_2O_2 affected steroid responsiveness in IL-1β-stimulated A549 cells. IL-1β: 100 ng/ml.

To briefly summarize this part of the work, the results indicate that inhibition of iNOS using the iNOS-selective inhibitor 1400W or non-selective NOS inhibitor AMT following cytokine stimulation with cytokine-mixture did not alter steroid insensitivity in A549 cells. Even at high concentration, which totally inhibited iNOS activity, neither of them improved steroid sensitivity. Overexpression of iNOS in A549 cells, confirmed by RT-PCR and Griess Assay, did not influence the efficacy of Dex on IL-8 secretion in IL-1β-stimulated A549 cells. Finally, treatment with the exogenous NO/$ONOO^-$ donor SIN-1 or the combination of SIN-1 and H_2O_2 following IL-1β-stimulation did not show any effect on steroid sensitivity. Taken together, these results suggest that, at least in the A549 cell model used, iNOS does not influence steroid sensitivity.

4.3.4 Characterization of the steroid sensitivity in other lung epithelial cell models

The CM-stimulated A549 cells have provided a valuable cell system to study steroid insensitivity on cytokine release in lung epithelial cells. To test whether these conditions in A549 cells could be transferred to other cell models, the identical conditions were applied in lung epithelial cell line BEAS-2B and primary lung epithelial cells MucilAir and the effects were studied using ELISA and Luminex assay.

4.3.4.1 Effects of dexamethasone on cytokine release in BEAS-2B cells

In BEAS-2B cells, like in A549 cells, cytokine-mix and dsRNA was again used to stimulate iNOS expression and NO production. In this case Griess assay could not detect iNOS-derived NO production, but as represented by Figure 4-30, CM was able to induce iNOS mRNA expression in BEAS-2B cells and the induction was augmented by addition of dsRNA. CM10 led to about 80-fold increase in iNOS mRNA levels compared to the control. The addition of dsRNA to CM enhanced this increase to about 150-fold. CM20 led to about 100-fold increase in iNOS mRNA levels compared to the control. Here, the addition of dsRNA to CM significantly augmented the iNOS mRNA rate to about 250-fold, although still over 20-fold less than in A549 cells (see Figure 4-7).

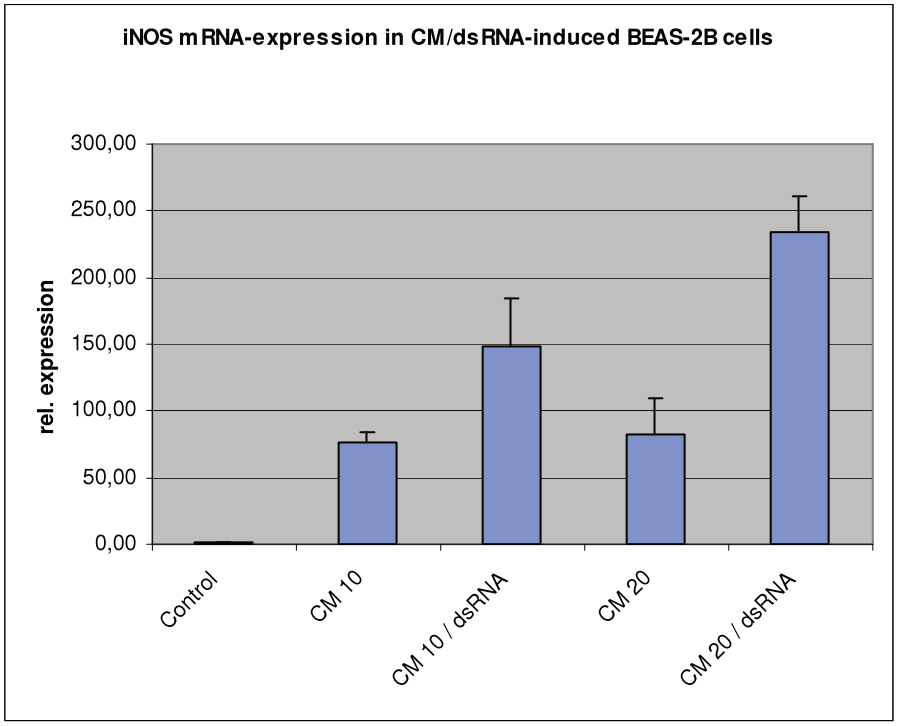

Figure 4-30: iNOS mRNA expression in CM- or CM/dsRNA-stimulated BEAS-2B cells

About $1x10^6$ BEAS-2B cells were seeded per each well. After 24 hours cells were stimulated with the indicated stimuli for 6 h. Isolated RNA was reverse transcribed into cDNA, and Real-Time PCR was performed with iNOS specific primers with *18sRNA* as internal control. The magnitude change of the iNOS mRNA is expressed as $2^{-\Delta\Delta Ct}$. CM10 led to about 80-fold increase in iNOS mRNA levels compared to the control. The addition of dsRNA to CM enhanced this increase to about 150-fold. CM20 led to about 100-fold increase in iNOS mRNA levels compared to the control. Here, the addition of dsRNA to CM significantly augmented the iNOS mRNA rate to about 250-fold. CM10: 10 ng/ml IFNγ, 10 ng/ml IL-1β, 10 ng/ml TNFα, CM20: 20 ng/ml IFNγ, 20 ng/ml IL-1β, 20 ng/ml TNFα, dsRNA: 100 µg/ml. (n=3)

GM-CSF is also an important mediator in inflammation and its secretion was strongly increased in BEAS-2B cells upon cytokine stimulation, as depicted in Figure 4-4. GM-CSF release in CM-stimulated A549 cells showed also insensitivity towards Dex treatment. To study the steroid sensitivity in CM-stimulated BEAS-2B cells, GM-CSF concentrations were determined. Under the given conditions, BEAS-2B cells treated with cytokine-mix and dsRNA, which expressed iNOS, were similarly sensitive towards dexamethasone treatment as cells treated with IL-1β alone, which did not express iNOS. Both IL-1β- and CM/dsRNA-induced GM-CSF release in BEAS-2B cells was dexamethasone sensitive and reduced the release down to 20% of positive control (Figure 4-31). The dose-response relationship curve of dexamethasone on GM-CSF secretion shows the almost equal IC_{50} values at about 10 nM (Log IC_{50} of IL-1β stimulation at –8.3 and Log IC_{50} of CM/dsRNA stimulation at about 8.1). Thus, suggesting that CM treatment of BEAS-2B cells, in contrast to A549 cells, did not result in a steroid insensitivity.

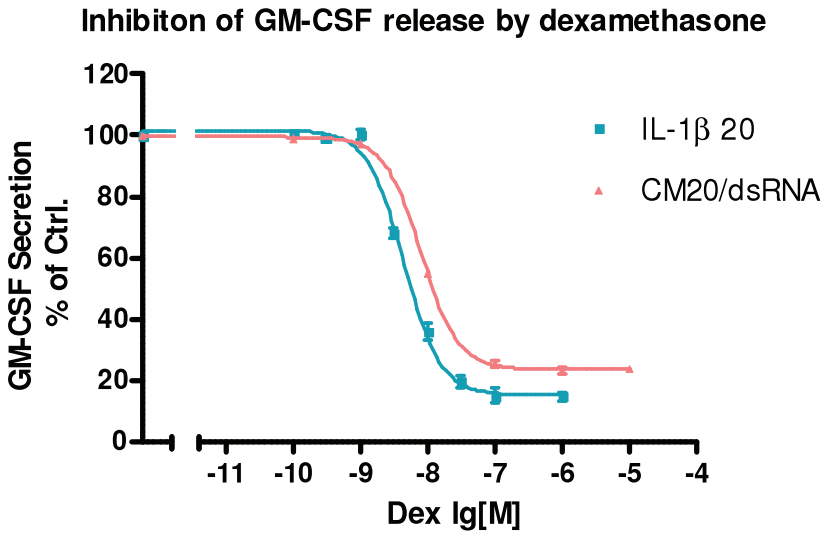

	IL-1β 20	CM 20 / dsRNA
LogEC50	-8.348	-8.092

Figure 4-31: Concentration-dependent effects of dexamethasone on IL-1β- or CM/dsRNA-induced GM-CSF release in BEAS-2B cells

About $3x10^5$ BEAS-2B cells were seeded per each well. After 24 h culture, the cells were stimulated with IL-1β or Cytokine-Mix with dsRNA and concomitantly treated with increasing concentration of dexamethasone for 20 h to detect concentration of GM-CSF in the cell culture supernatants by ELISA analysis. Both IL-1β- and CM/dsRNA-stimulated GM-CSF release in BEAS-2B cells was dexamethasone sensitive and reduced the release down to 20% of positive control. IL-1β: 20 ng/ml, CM20: 20 ng/ml IFNγ, 20 ng/ml IL-1β, 20 ng/ml TNFα. dsRNA: 100 µg/ml. Dexamethasone: 0.1 nM to 100 µM.

4.3.4.2 Effects of dexamethasone on cytokine release in MucilAir cells

To get more insight on steroid responsiveness in lung epithelial cells in inflammation, human primary airway epithelial cells MucilAir® (from Epithelix, Geneva), which were grown in air-liquid culture, were stimulated with different cytokines and exposed to dexamethasone. TNFα and CM were used at concentrations of 1 nM and 1µM. Using 25-Plex Luminex technology the profile of cytokine release in MucilAir cells were explored and selected cytokine were validated using ELISA.

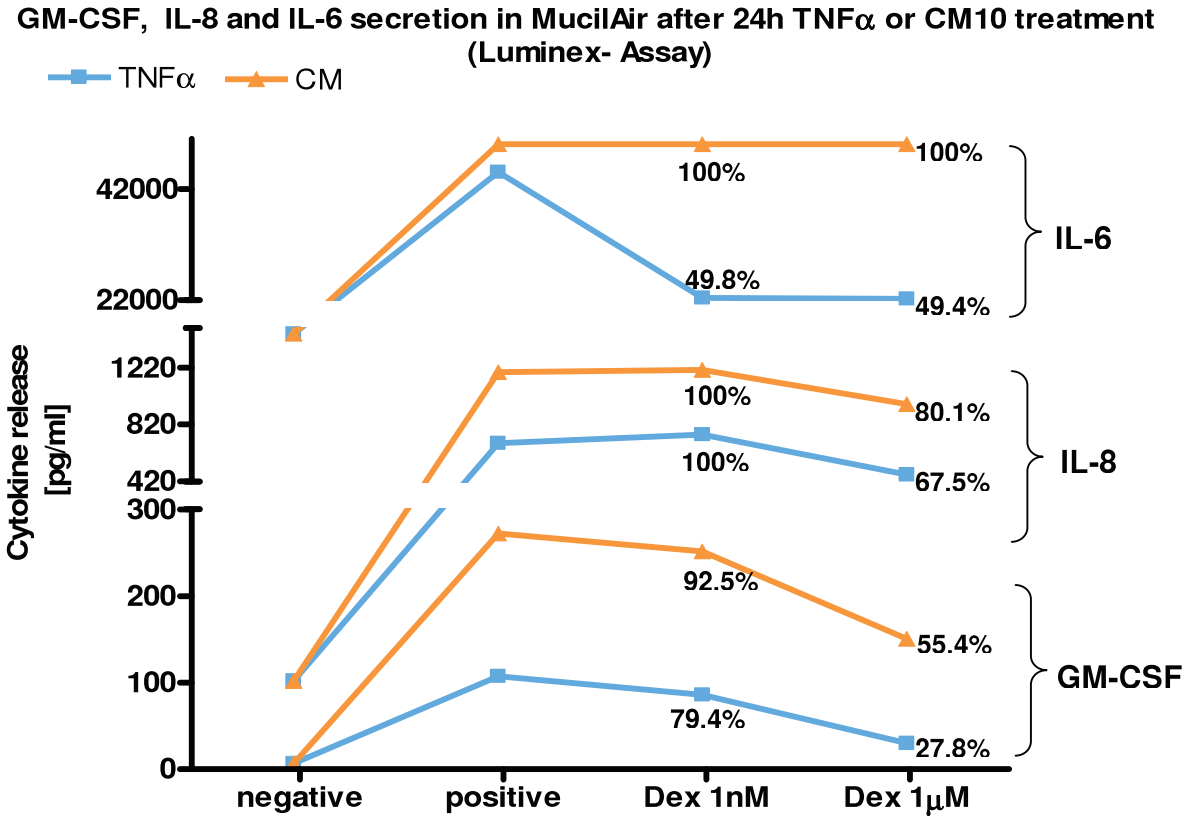

Figure 4-32: Steroid insensitivity of IL-6, IL-8 and GM-CSF release in CM-stimulated MucilAir cells.

MucilAir cells were cultured as detailed in Materials and Methods. TNFα and CM were used to stimulate the cells with concomitant treatment of dexamethasone at 1 nM and 1µM. After 24 h 25-Plex Luminex was conducted to explore the profile of cytokine release (n=1). The inhibition of IL-6, IL-8 and GM-CSF release was presented in percent of positive control and the values demonstrated a putative steroid insensitivity in CM-stimulated and dex-treated MucilAir cells TNFα-stimulated IL-6, IL-8 and GM-CSF release was steroid sensitive. TNFα: 100 ng/ml, CM10: 10 ng/ml IFNγ, 10 ng/ml IL-1β, 10 ng/ml TNFα.

Interestingly, preliminary Luminex data of IL-6, IL-8 and GM-CSF release demonstrated a possible steroid insensitivity in CM-stimulated and Dex-treated MucilAir cells (Figure 4-32). Comparatively, TNFα-stimulated IL-6, IL-8 and GM-CSF

release was steroid sensitive. The cytokine release in percent to positive control was illustrated in Figure 4-32 and the data of IL-8 and GM-CSF were confirmed with ELISA (see also Figure 4-16).

In conclusion, on one hand, in contrast to A549 cells, BEAS-2B cells were steroid sensitive regarding CM/dsRNA-induced GM-CSF release, although a low level of iNOS was expressed after CM/dsRNA stimulation. On the other hand, preliminary data using primary lung epithelial cells MucilAir demonstrated steroid insensitivity regarding IL-6, IL-8 and GM-CSF release after stimulation with CM, in contrast to steroid sensitivity when stimulating with TNFα.

4.4 Steroid function and HDAC inhibition in lung epithelial cell model of inflammation

It was hypothesized that iNOS-derived NO may play an important role in steroid insensitivity in lung inflammation in COPD due to the fact that the nitrative and oxidative stress reduces HDAC activity, which is of great importance in the anti-inflammatory function of steroids (see Introduction). As this hypothesis could not be confirmed in the human lung epithelial cell system we used in this study, it became even more interesting to ask the question about the involvement of HDAC activity in the steroid function of controlling inflammation in lung epithelial cells.

Therefore, the intension of this part of the work was to evaluate the steroid responsiveness during HDAC inhibition.

4.4.1 Effects of HDAC inhibitors on HDAC activity in lung epithelial cells

For the inhibition of cellular HDAC activity, SAHA, MS275 and TSA were used. SAHA and TSA are HDAC pan-inhibitors and MS-275 is an HDAC class I inhibitor.

In a first step, the potency of SAHA and MS-275 were quantified in A549 cells. As shown in Figure 4-33, the inhibitory effect of SAHA and MS-275 on HDAC activity in A549 cells is concentration dependent and Log IC_{50} of SAHA is -4.9 (IC_{50} = 10μM) and that of MS-275 is –5.5 (IC_{50} = 3.3 μM). Based on these data and various literature reports (Minucci and Pelicci 2006), the concentrations for the in vitro assays in this study were chosen: SAHA 100 nM, MS-275 1 μM and TSA 10 nM.

It is well known that HDAC inhibitors have cytotoxic effect on tumor cells and can induce cell cycle arrest and cell death. Therefore the cytotoxic effect of these inhibitors were determined using Alamarblue assay (see Materials and Methods) in A549 cells treated with HDAC inhibitors for 48h. The IC_{50} of SAHA, TSA and MS-275 in these cells were 3.6μM, 0.28 μM and 4.0 μM, respectively. Considering the short-term (within 24 h) treatment of the cells and the low concentrations used, there was no or just very slightly cytotoxic effect in the experiments.

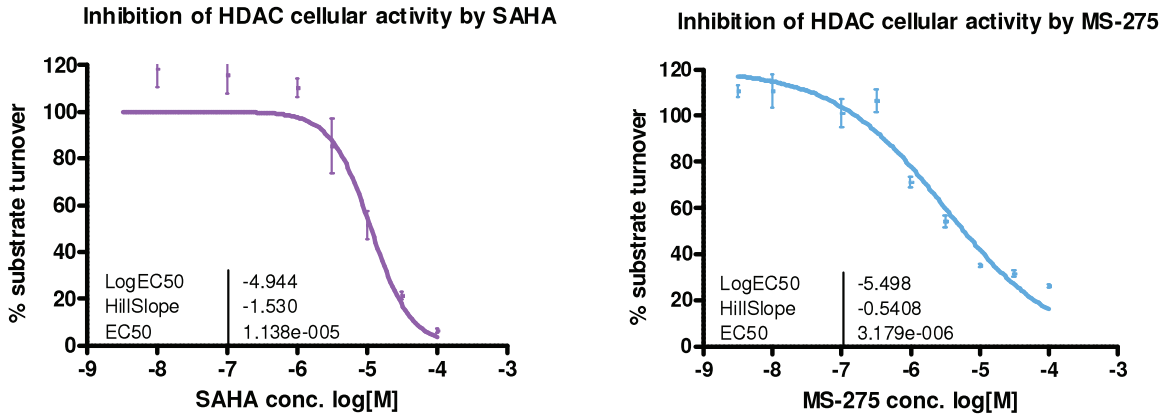

Figure 4-33: Concentration-dependant inhibition of cellular HDAC activity by HDAC inhibitor SAHA and MS-275.

$1x10^4$ A549 cells/well were seeded and incubated in 96-well plate for 24 hours. The cellular HDAC activity assay was conducted as described in Materials and Methods (n=4). Log IC_{50} was calculated for each HDAC inhibitor: SAHA: Log IC_{50} =-4.9 and MS-275: Log IC_{50} = -5.5.

4.4.2 Effects of HDAC inhibition on steroid sensitivity in BEAS-2B cells

To evaluate the steroid responsiveness during HDAC inhibition, BEAS-2B cells were exposed to HDAC inhibitors and subsequently stimulated with IL-1β and treated with dexamethasone at increasing concentrations. Cytokine release in the stimulated cells was subsequently quantified by ELISA.

4.4.2.1 Effects of HDAC inhibitors on steroid sensitivity of IL-8 secretion

In the first subset of these experiments, IL-8 concentrations in the cell supernatants were measured (Figure 4-34a) and used for the calculation of the IC_{50} values of dexamethasone to show effects of HDAC inhibitors on dexamethasone-mediated inhibition of IL-8 release (Figure 4-34b). Both graphs in Figure 4-34 show that the inhibition of IL-8 release by dexamethasone during HDAC inhibition in BEAS-2B cells is concentration-dependent. Interestingly, MS-275 (1μM) increased the level of IL-8 release significantly by 75% in the IL-1β-stimulated A549 cells and further, this increasing effect of HDAC inhibition by MS-275 on IL-8 release was also during the concomitant dexamethasone treatment (Figure 4-34a). TSA (10 nM) and SAHA (100 nM) had no significant effect on IL-8 levels in the IL-1β-stimulated and dexamethasone-treated cells. LogIC_{50} values revealed from the dose-response curves showed that TSA at 10 nM, MS-275 at 1μM and SAHA at 100 nM had no effect on the

dexamethasone-mediated inhibition of IL-8 release in IL-1β-stimulated BEAS-2B cells (Figure 4-34b), which indicates a HDAC-independent dexamethasone inhibition on IL-8 release.

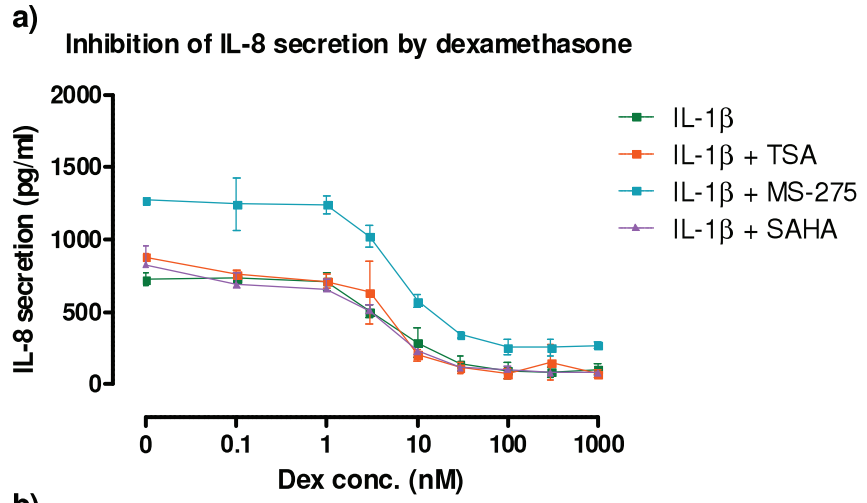

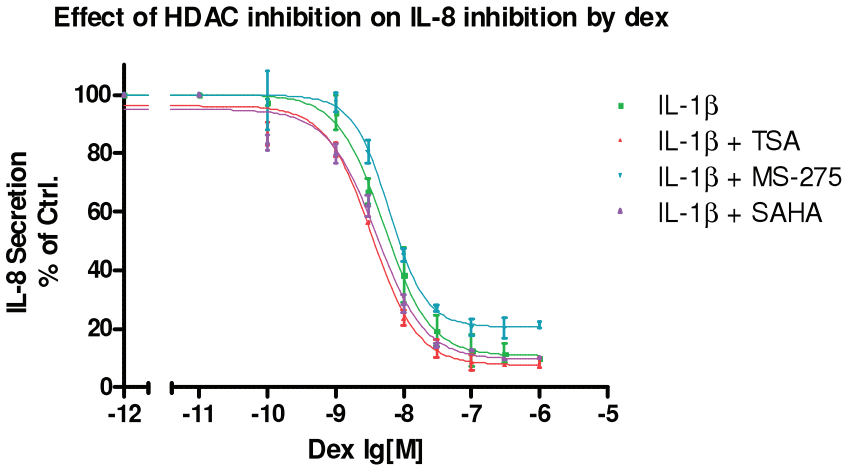

	IL-1β	IL-1β + TSA	IL-1β + MS-275	IL-1β + SAHA
LogEC50	-8.292	-8.469	-8.210	-8.405

Figure 4-34: Effect of HDAC inhibition on IL-8 inhibition by dexamethasone in IL-1β-stimulated BEAS-2B cells.

BEAS-2B cells were exposed to vehicle or HDAC inhibitor TSA, MS-275 and SAHA for 30 minutes, then dexamethasone at different concentrations as indicated and IL-1β stimulus were added in the presence of vehicle or HDAC inhibitors for another 20 hours. IL-8 secretion in cell supernatants was determined using ELISA (n=4). Both graphs show that the inhibition of IL-8 release by dexamethasone during HDAC inhibition in BEAS-2B cells is concentration dependent. a) MS-275 (1μM) increased the level of IL-8 release significantly (about 75%), TSA (10 nM) and SAHA (100 nM) had no significant effect on IL-8 levels in the stimulated cells. b) LogIC_{50} values revealed from the dose-response curves showed that TSA (10 nM), MS-275 (1μM) and SAHA (100 nM) had no effect on dexamethasone-mediated inhibition of IL-8 release in IL-1β-stimulated BEAS-2B cells. Dex: 0.1 nM to 1 μM. TSA: 10 nM, MS-275: 1μM, SAHA: 100 nM IL-1β: 10 ng/ml.

4.4.2.2 Effects of HDAC inhibitors on steroid sensitivity of GM-CSF secretion

In the second subset of these experiments, GM-CSF concentrations in the cell supernatants were measured (Figure 4-35a) and used for the calculation of the IC_{50} values of dexamethasone to show effects of HDAC inhibitors on dexamethasone-mediated inhibition of GM-CSF release (Figure 4-35b).

The inhibition of GM-CSF release by dexamethasone in BEAS-2B cells like that of IL-8 release is concentration dependent (Figure 4-35). Interestingly, in contrast to the increasing effect of MS-275 on IL-8 release, HDAC inhibition by MS-275 at 1µM decreased the levels of GM-CSF release significantly by 55% in the IL-1ß-stimulated cells (Figure 4-35a). In contrast to the slight effects on IL-8 levels, TSA (10 nM) increased the levels of GM-CSF by 38% in the IL-1ß-stimulated cells. SAHA (100 nM) had no effect on GM-CSF levels in the cell supernatants. Similar to the results presented in Figure 4-34b, $LogIC_{50}$ values revealed from the dose-response curves showed that TSA at 10 nM, MS-275 at 1µM and SAHA at 100 nM had no effect on the dexamethasone-mediated inhibition of GM-CSF release in IL-1β-stimulated BEAS-2B cells (Figure 4-35b).

Taken together, according to the IC_{50} values HDAC inhibition using the HDAC inhibitor TSA, SAHA and MS-275 had no effect on dexamethasone-mediated inhibition of IL-8 and GM-CSF release in cytokine-stimulated BEAS-2B cells. Interestingly, the HDAC inhibitors used in this study showed to a different degree effects on cytokine release, in general, some increasing the release of certain cytokines while others decreasing cytokine release depending on the cytokine studied. Therefore in the following, we aimed to characterize the functional role of HDAC inhibitors in the lung epithelial cell model of inflammation.

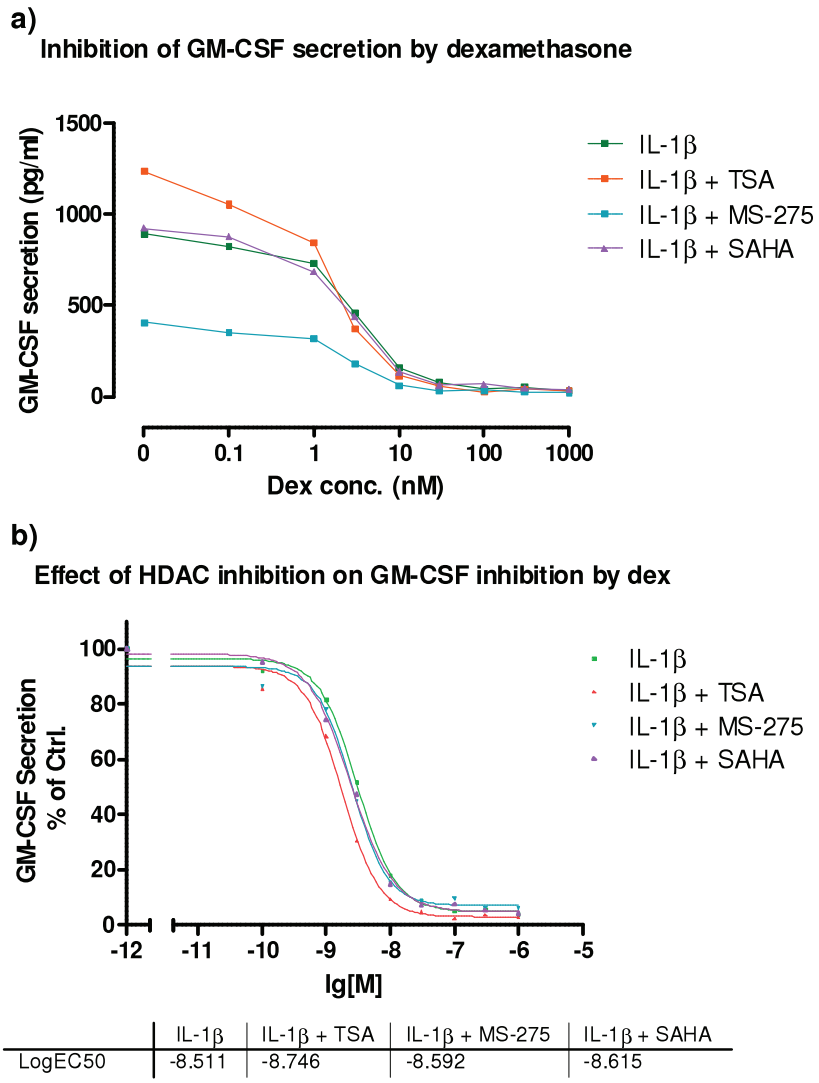

	IL-1β	IL-1β + TSA	IL-1β + MS-275	IL-1β + SAHA
LogEC50	-8.511	-8.746	-8.592	-8.615

Figure 4-35: Effect of HDAC inhibition on GM-CSF inhibition by dexamethasone in IL-1β-stimulated BEAS-2B cells.

BEAS-2B cells were exposed to vehicle or HDAC inhibitor TSA, MS-275 and SAHA for 30 minutes, then dexamethasone at different concentrations and IL-1β stimulus were added in the presence of vehicle or HDAC inhibitors for another 20 hours. GM-CSF secretion in cell supernatants was determined using ELISA (n=4). Both graphs show that the inhibition of GM-CSF release by dex in BEAS-2B cells is concentration dependent. a) MS-275 (1μM) decreased the levels of GM-CSF release significantly (55%), TSA (10 nM) increased the levels of GM-CSF release (38%) and SAHA (100 nM) had no effect on GM-CSF levels in the IL-1β-stimulated cells. b) LogIC_{50} values revealed from the dose-response curves showed that TSA (10 nM), MS-275 (1μM) and SAHA (100 nM) had no effect on dexamethasone-mediated inhibition of GM-CSF release in IL-1β-stimulated BEAS-2B cells. Dex: 0.1 nM to 1 μM. TSA: 10 nM, MS-275: 1μM, SAHA: 100 nM IL-1β: 10 ng/ml.

4.5 Functional effects of HDAC inhibitors in lung epithelial cell models of inflammation

To identify the potential role of HDAC inhibitors in inflammation, GM-CSF and IL-8 release both in A549 and BEAS-2B cells after treatment with different cytokine stimuli were assessed and effects of different HDAC inhibitors with different selectivity and mode of action were analyzed. In the present study, SAHA and TSA as pan HDAC inhibitors and MS-275 as an HDAC class I inhibitor were used.

4.5.1 Effects of HDAC inhibitors on cytokine release in lung epithelial cells after cytokine stimulation

4.5.1.1 Effect of HDAC inhibitors on GM-CSF release in A549 cells

Firstly, the GM-CSF secretion after stimulation with different cytokine stimuli was determined. As illustrated in Figure 4-36, SAHA showed strong anti-inflammatory effects in cytokine –stimulated A549 cells and inhibited GM-CSF release induced with IL-1β, TNFα and CM by more than 50%. Due to the low level of GM-CSF in IFNγ-stimulated cells, the effect of SAHA could not be analyzed.

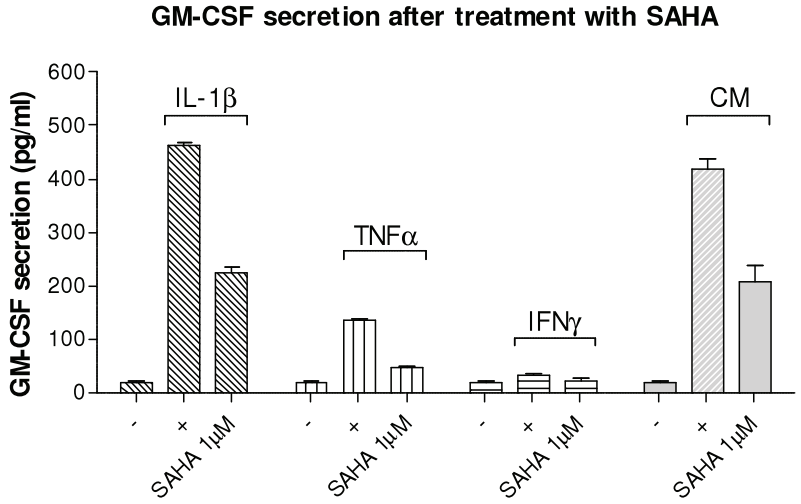

Figure 4-36: Effect of SAHA on GM-CSF secretion in cytokine-stimulated A549 cells

A549 cells were seeded in 24-well plates. After 24h the cells were expose to vehicle or SAHA for 30 min and then the different cytokine stimuli as indicated were added. After 20h GM-CSF release was measured in the cell supernatants. Each data point represents the average of four times determination. SAHA showed strong anti-inflammatory effects in cytokine –stimulated A549 cells and inhibited GM-CSF release induced with IL-1β, TNFα and CM by more than 50%. Due to the low level of GM-CSF in IFNγ-stimulated cells, the effect of SAHA could not be analyzed. IL-1β:10 ng/ml, TNFα: 10 ng/ml, IFNγ: 10 ng/ml, CM: 10 ng/ml TNFα, 10 ng/ml IL-1β, 10 ng/ml IFNγ. SAHA: 1µM

In the following experiments, the concentration-dependent effects of HDAC inhibitors SAHA and MS-275 on GM-CSF release in A549 cells was determined. As represented in Figure 4-37, GM-CSF release induced with IL-1β was inhibited by both SAHA and MS-275 in a concentration dependent manner. Log IC_{50} values of -6,3 for SAHA and -5,5 for MS-275 was obtained, suggesting a strong anti-inflammatory effect of both pan HDAC inhibitors and class I selective inhibitors.

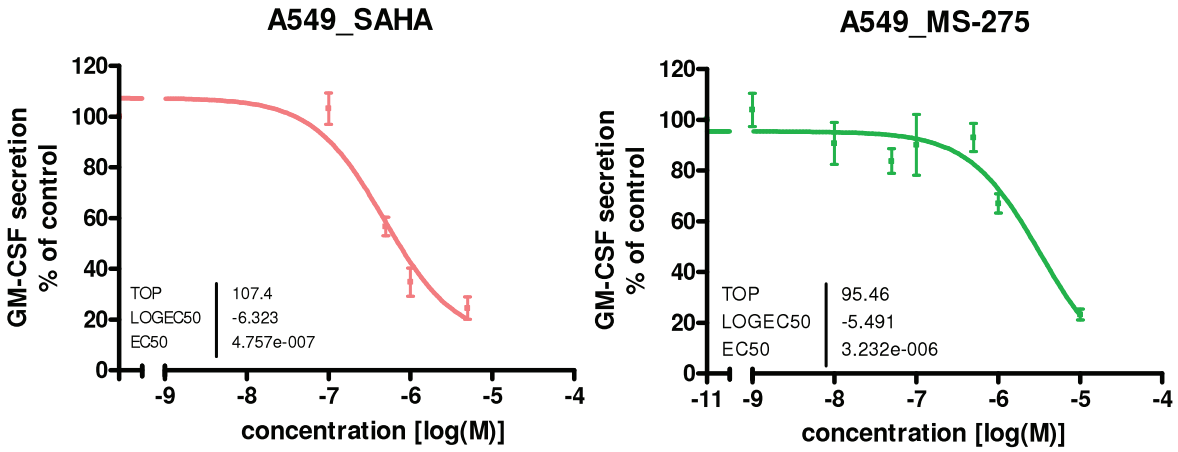

Figure 4-37: Concentration-dependent effect of SAHA (left) and MS-275 (right) on GM-CSF secretion in IL-1β-stimulated A549 cells.

A549 cells were seeded in 24-well plates. After 24h the cells were expose to vehicle or SAHA and MS-275 at increasing concentrations for 30 min and then the different IL-1β was added to stimulate the cells. After 20h GM-CSF release was measured in the cell supernatants. Each data point represents the average of four times determination. GM-CSF release inducted with IL-1β was inhibited by both SAHA and MS-275 in a concentration dependent manner. Log IC_{50} value of -6,3 for SAHA and -5,5 for MS-275 was obtained. IL-1β: 10 ng/ml. SAHA and MS-275: 1 nM to 10 µM

4.5.1.2 Effect of HDAC inhibitors on GM-CSF and IL-8 release in BEAS-2B cells

Regarding the cell cycle arrest effect of HDAC inhibitors on tumor cells and also to verify the effects of different HDAC inhibitors in inflammation in another non-tumor lung epithelial cell model, BEAS-2B cells were exposed to different HDAC inhibitors (TSA, MS-275 and SAHA) before stimulated with cytokines. Here, we used different cytokines alone (IL-1β or TNFα) or cytokine combinations (IL-1β+TNFα or CM) as stimuli and cytokine release of GM-CSF and IL-8 in BEAS-2B cells were subsequently determined. The regulation profiles in respect to different stimuli were quite similar and Figure 4-38 represents GM-CSF (left) and IL-8 (right) secretion after stimulation with IL-1β. SAHA at 1 µM showed strong inhibitory effects on both GM-CSF (about 70%) and IL-8 (about 50%) secretion. SAHA at 100 nM showed no effect on release of both

cytokines. Quite astonishingly but very interestingly, MS-275 at 1 µM affected GM-CSF and IL-8 release just in the opposite direction: whereas GM-CSF release was reduced by about 50%, IL-8 release was increased by about 50%. In addition, TSA at 10 nM augmented GM-CSF release by about 30% of control and had no effect on IL-8 release.

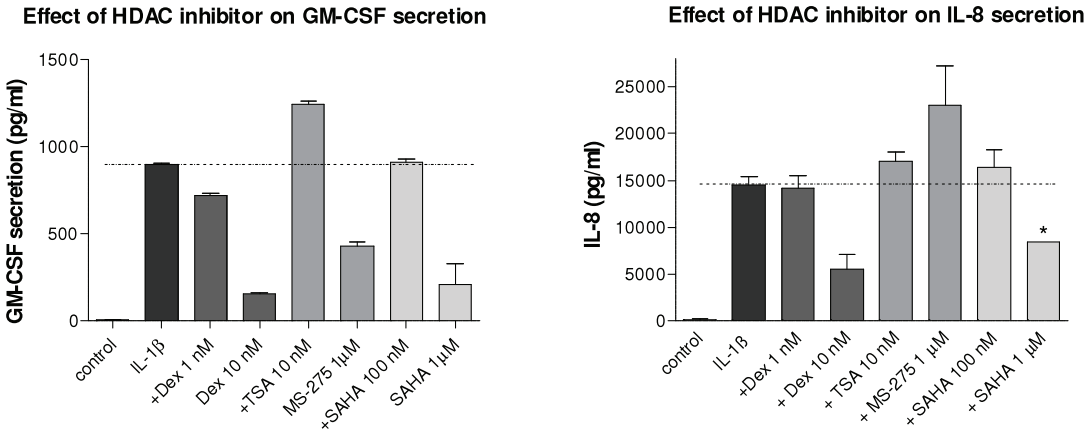

Figure 4-38: Effect of TSA, MS-275 and SAHA on GM-CSF (left) and IL-8 (right) secretion in IL-1β-stimulated BEAS-2B cells

BEAS-2B cells were seeded in 96-well plates. After 24h the cells were expose to vehicle, dexamethsone (1 nM and 10 nM) as control or HDAC inhibitors, TSA, MS-275 and SAHA, for 30 min and then IL-1β were added. After 20h GM-CSF and IL-8 release in the cell supernatants was measured. Each data point represents the average of four times determination. SAHA at 1 µM showed strong inhibitory effects on both GM-CSF (about 70%) and IL-8 (about 50%) secretion. SAHA at 100 nM showed no effect on release of both cytokines. Quite astonishingly but very interestingly, MS-275 at 1 µM affected GM-CSF and IL-8 release just in the opposite direction: whereas GM-CSF release was reduced by about 50%, IL-8 release was increased by about 50%. TSA at 10 nM augmented GM-CSF release by about 30% of control and had no effect on IL-8 release. IL-1β: 10 ng/ml. TSA: 10 nM, MS-275: 1µM and SAHA: 100 nM and 1µM

In the following, the concentration-dependent effects of HDAC inhibitors on GM-CSF release in BEAS-2B cells were determined. As represented in Figure 4-39, GM-CSF release induced with IL-1β was inhibited by both SAHA and MS-275 in a concentration dependent manner. LogIC_{50} value of –5.1 for SAHA and –6.8 for MS-275 was obtained, similar to the results in the A549 cells (Figure 4-37), suggesting a strong anti-inflammatory effect of both pan HDAC inhibitors and class I selective inhibitors.

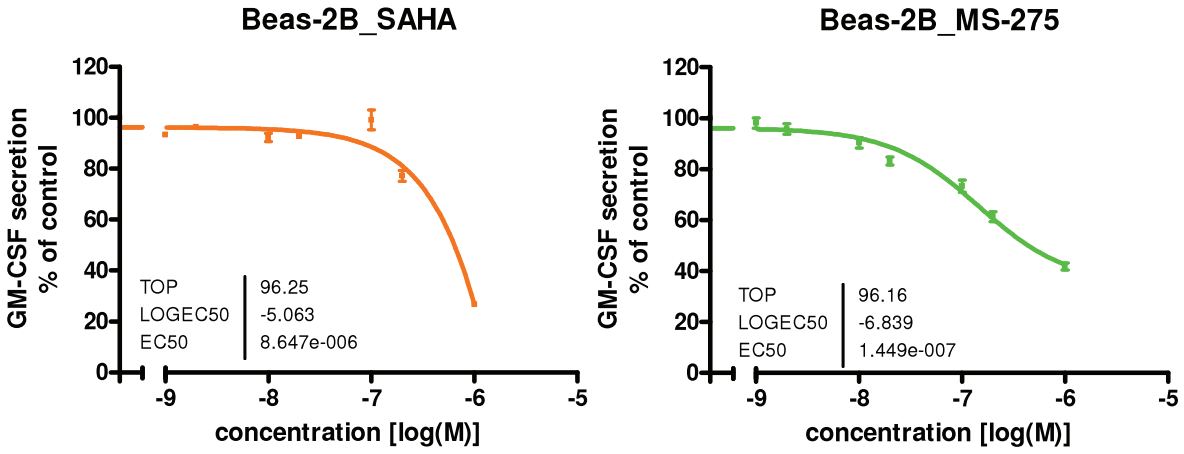

Figure 4-39: Concentration-dependent effect of SAHA (left) and MS-275 (right) on GM-CSF secretion in BEAS-2B cells stimulated by IL-1β.

BEAS-2B cells were seeded in 96-well plates. After 24h the cells were expose to vehicle or SAHA and MS-275 at different concentrations for 30 min and then the different IL-1β was added to stimulate the cells. After 20h GM-CSF release was measured in the cell supernatants. Each data point represents the average of four times determination. GM-CSF release inducted with IL-1β was inhibited by both SAHA and MS-275 in a concentration dependent manner. Log IC_{50} values of –5.1 for SAHA and –6.8 for MS-275 were obtained. IL-1β: 10 ng/ml. SAHA and MS-275: 1 nM to 10 µM

To give a comprehensive overview of the experimental results, the concentration dependent effects (Log IC_{50}) of SAHA and MS-275 on IL-8 and GM-CSF release in A549 and BEAS-2B cells were summarized in Table 4-3. To note, for MS-275 at 1 µM an increasing effect at 1.5-fold on IL-8 release was detected in IL-1β-stimulated BEAS-2B cells and for SAHA at 1 µM an decreasing effect of 50% of control on IL-8 release was detected in IL-1β-stimulated A549 cells.

Table 4-3 Summary of effects of HDAC inhibitors on cytokine release in IL-1β-stimulated A549 and BEAS-2B cells (Log IC_{50}).

HDAC inhibitor	IL-8		GM-CSF	
	A549	BEAS-2B	A549	BEAS-2B
SAHA	-50% at 1 µM	-6.6	-6.3	-5.1
MS-275	ND	+ 1.5-fold at 1 µM	-5.5	-6.8

ND: not determined

4.5.2 Effects of HDAC inhibitors on cytokine mRNA expression in A549 cells after stimulation

HDAC activity plays an important role in regulating gene expression and therefore the functional effects of HDAC inhibitors on cytokine release may result from the regulation of cytokine mRNA expression or on the other hand, from modifying signaling pathways (see also Introduction for non-histone substrates of HDAC). In this part of the work, we first examined the transcriptional profiles of different pro-inflammatory genes after treatment with HDAC inhibitors in cytokine-stimulated A549 cells.

4.5.2.1 Effects of HDAC inhibitors on IL-8 mRNA expression

We first studied the effect of pan-HDAC inhibitors SAHA and TSA on IL-8 mRNA expression in IL-1β-stimulated A549 cells. As demonstrated in Figure 4-40, IL-8 mRNA expression in IL-1β-stimulated A549 cells was regulated in a time-dependent fashion and the samples measured at 16 h reached the maximum level of expression. However, SAHA and TSA did not show effect on IL-8 mRNA expression, irrespective of the type or concentration of the compound and the time range of treatment. (Value of TSA treatment at 100 nM for 6 hours was not determined and hence the according effects could not be analyzed.)

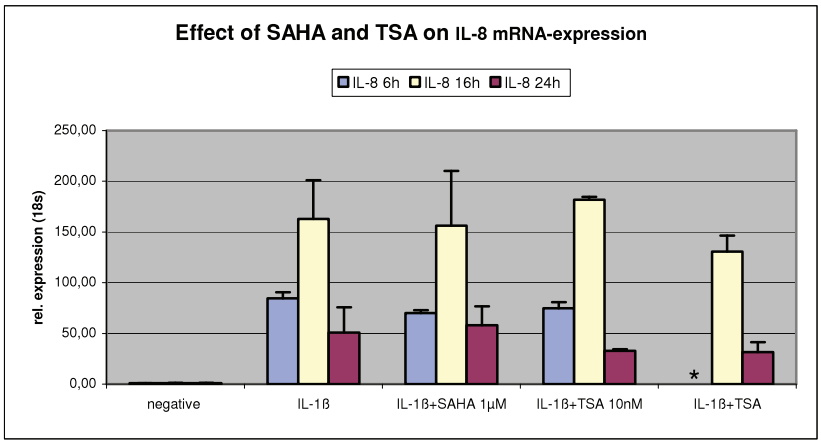

Figure 4-40: No effect of SAHA and TSA on IL-1β-induced IL-8 mRNA expression in A549 cells.

About $1x10^6$ cells were seeded per each well. After 24h the cells were expose to vehicle or SAHA (1µM) and TSA (10 nM and 100 nM) for 30 min and then IL-1β was added to stimulate the cells. After 6 h, 16 h and 24 h of incubation as indicated, total RNA was isolated respectively and transcribed into cDNA. Real-Time PCR analysis revealed, that IL-8 mRNA expression in IL-1β-stimulated A549 cells was increased in a time-dependent fashion and the samples measured at 16 h reached the maximum level of expression. But SAHA and TSA did not show effect on IL-8 mRNA expression, irrespectively of the type or concentration of the compound and the time range of treatment. IL-1β: 10 ng/ml. (* Value of TSA treatment at 100 nM for 6 hours was not determined.)

In a parallel experiment, the IL-8 release was assessed in IL-1β-stimulated A549 cells 16 hours or 24 hours after HDAC inhibitor treatment (Figure 4-41). Treatment with SAHA at 1μM and TSA at 10 and 100 nM for 16 h inhibited IL-8 release strongly by more than 50%, 40% and 60%, respectively. However, in this single experiment SAHA treatment for 24 h showed just very slight effect on IL-8 release, whereas in Figure 4-38 SAHA reduced IL-8 release by about 50% of control after 20 h of treatment. Regarding the results at 16 h from this experiment and at 20 h from Figure 4-38, SAHA (1μM) should inhibit IL-8 release in IL-1β-stimulated A549 cells within the time range used. TSA at 10 nM and 100 nM after 24 h treatment did not affect IL-8 release significantly.

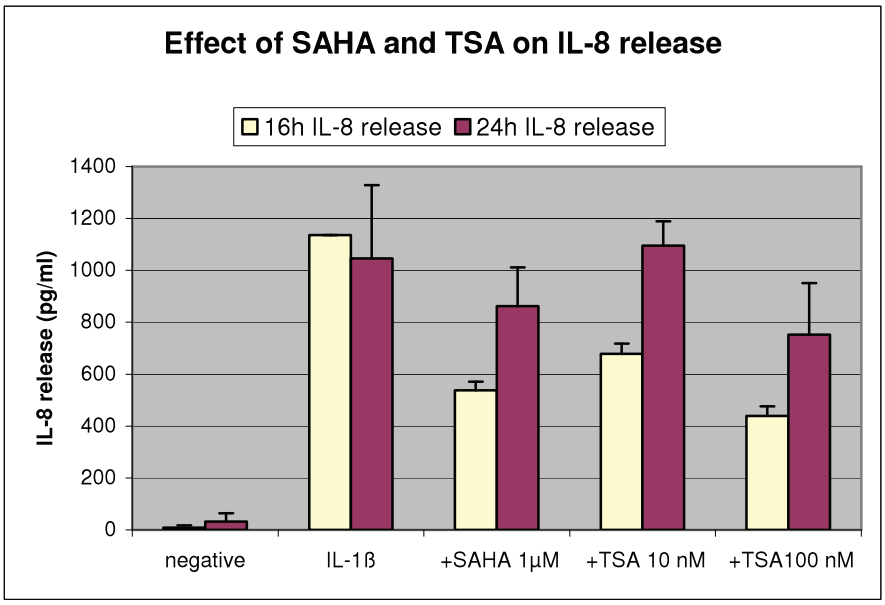

Figure 4-41: Effect of SAHA and TSA on IL-1β-induced IL-8 release in A549 cells.

About $4x10^5$ cells were seeded per each well in 24-well plate. After 24h the cells were expose to vehicle or SAHA (1μM) and TSA (1 nM and 100 nM) for 30 min and then IL-1β was added to stimulate the cells. After 16 h and 24 h of incubation as indicated, IL-8 release was determined using ELISA assay. Treatment with SAHA at 1μM and TSA at 10 and 100 nM for 16 h inhibited IL-8 release strongly by more than 50%, 40% and 60%, respectively. SAHA treatment for 24 h showed just very slight effect on IL-8 release in this experiment (see also discussion above). TSA at 10 nM and 100 nM after 24 h treatment did not affect IL-8 release significantly. IL-1β: 10 ng/ml.

4.5.2.2 Effects of HDAC inhibitors on GM-CSF mRNA expression

Subsequently, effects of SAHA and TSA on GM-CSF mRNA expression in IL-1β-stimulated A549 cells were elucidated. In contrast to IL-8 mRNA expression (Figure 4-40), GM-CSF mRNA expression in IL-1β-stimulated A549 cells was only detectable at 6 h (Figure 4-42). However, the level of GM-CSF mRNA expression was about 10-

fold higher than that of IL-8 at 16 h stimulation, which may indicate that within the time range used induction of IL-8 by IL-1β had a long-term effect and induction of GM-CSF is rather short-term but much stronger. SAHA (1μM) reduced GM-CSF mRNA expression almost 70% and TSA showed less effect on GM-CSF mRNA expression at 6 hours (Value of TSA treatment at 100 nM for 6 hours was not determined and could not be analyzed) (Figure 4-42).

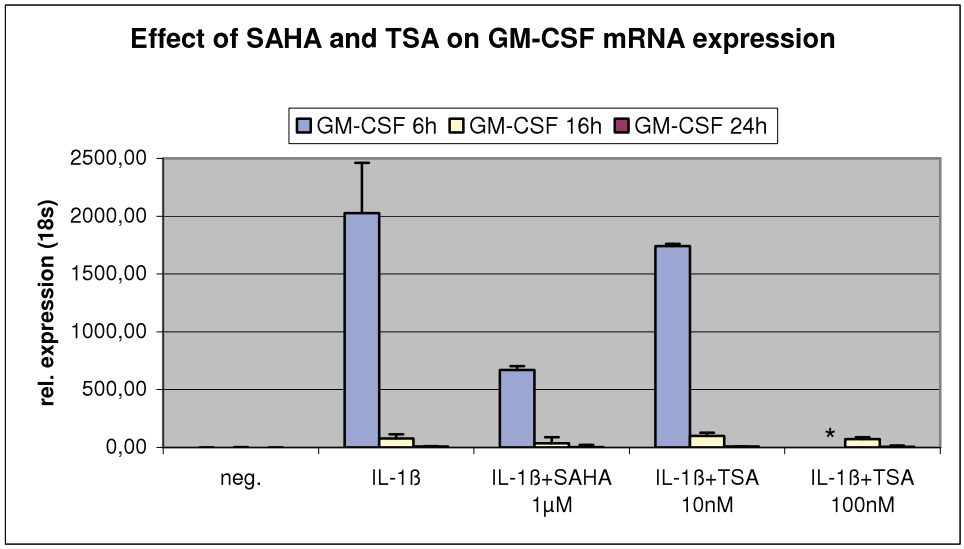

Figure 4-42: Effect of SAHA and TSA on IL-1β-induced GM-CSF mRNA expression in A549 cells.

About 1x10^6 cells were seeded per each well. After 24h the cells were expose to vehicle or SAHA (1μM) and TSA (10 nM and 100 nM) for 30 min and then IL-1β was added to stimulate the cells. After 6 h, 16 h and 24 h of incubation as indicated, total RNA was isolated respectively and transcribed into cDNA. Real-Time PCR analysis revealed, that IL-8 mRNA expression in IL-1β-stimulated A549 cells was increased in a time-dependent fashion and the samples measured at 16 h reached the maximum level of expression. But SAHA and TSA showed no effect on IL-8 mRNA-expression, irrespectively of type or concentration of compound and time of treatment. IL-1β: 10 ng/ml. (* Value of TSA treatment at 100 nM for 6 hours was not determined.)

Figure 4-43 represents the parallel measurement of GM-CSF release 16 h or 24 h after SAHA (1μM) or TSA (10 nM and 100 nM) treatment in IL-1β-stimulated A549 cells. The effect of these two HDAC inhibitors on GM-CSF release at the two time points measured was not time-dependent. SAHA treatment inhibited GM-CSF release by about 57% in IL-1β-induced A549 cells and the inhibitory effect of TSA at 100 nM was by about 37% while TSA at 10 nM did not affect GM-CSF release in this experiment.

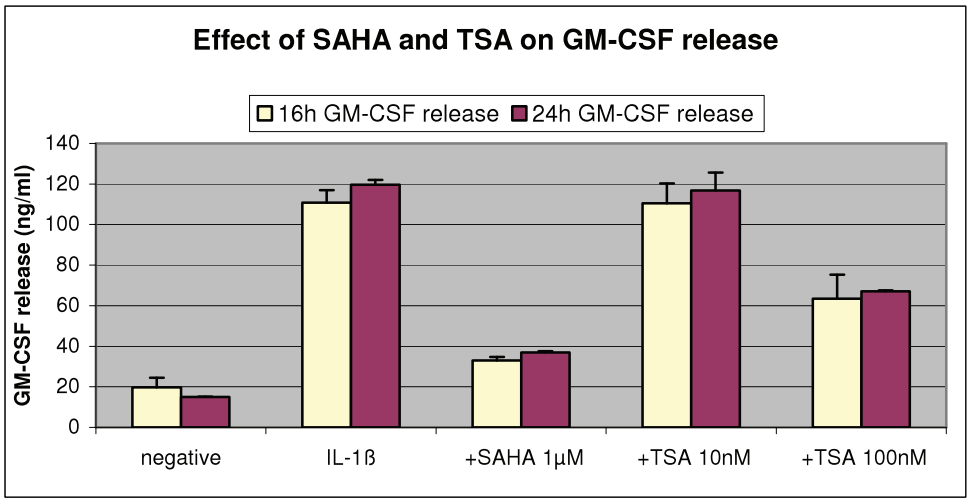

Figure 4-43: Effect of SAHA and TSA on IL-1β-induced GM-CSF release in A549 cells.

$2x10^5$ BEAS-2B cells were seeded in 24-well plates. After 24h the cells were expose to vehicle or HDAC inhibitor SAHA (1µM) and TSA (1 nM and 100 nM) for 30 min and then IL-1β was added to stimulate the cells. After 16 h and 24 h of incubation as indicated, GM-CSF release was determined using ELISA. The effect of these two HDAC inhibitors on GM-CSF release at the two time points measured was not time-dependent. SAHA treatment inhibited GM-CSF release by about 57% in IL-1β-induced A549 cells and the inhibitory effect of TSA at 100 nM was by about 37% while TSA at 10 nM did not affect GM-CSF release in this experiment. IL-1β: 10 ng/ml.

To briefly conclude this part of the study: dependent on the compound type used and the cytokine measured HDAC inhibitors could either increase or decreased cytokine release in IL-1β-stimulated lung epithelial cells. SAHA and MS-275 reduced GM-CSF release in A549 and BEAS-2B cells concentration-dependently. SAHA at 1µM decrease also IL-8 release in A549 cells. Interestingly, in contrast to these inhibitory effects of HDAC inhibitors, MS-275 at 1 µM increased IL-8 release and TSA at 10 nM increased GM-CSF release in BEAS-2B cells. Moreover, at the level of mRNA expression, HDAC inhibitors SAHA and TSA had no effect on the levels of IL-8 mRNA expression, whereas they decreased the mRNA expression of GM-CSF. These complex effects of HDAC inhibition on cellular function led us to further investigate the mode of action of HDAC inhibitors at the level of histone modification.

4.5.3 Induction of histone hyperacetylation by HDAC inhibitors in A549 cells

De-/acetylation of specific lysine residues in the amino termini of the core histones by HDACs and HATs plays a fundamental role in transcriptional regulation (Kurdistani et al. 2004). To further investigate the mode of action of HDAC inhibitors in inflammation, firstly, the HDAC inhibitor-mediated genome-wide histone hyperacetylation was evaluated in this section. For this purpose Western blot analysis of histone H3 and

hyperacetylated histone H3 (Ac-H3) in A549 cells exposed to SAHA and TSA was performed. αTubulin is known as a non-histone cellular substrate of HDACs (see Introduction) and was used as a control of hyperacetylation to evaluate the hyperacetylating effect of HDAC inhibitors on non-histone substrates, Western blot analysis (see Materials and Methods) was also applied with antibodies for αTubulin and hyperacetylated Ac-αTubulin in A549 cells.

In the first experiments, A549 cells were treated with SAHA at 10 µM and TSA at 10 nM for 24 hours. Figure 4-44 demonstrates a strong induction of histone H3 and α-Tubulin hyperacetylation in A549 cells treated with SAHA and TSA, in comparison to vehicle control.

Induction of H3 hyperacetylation by SAHA and TSA

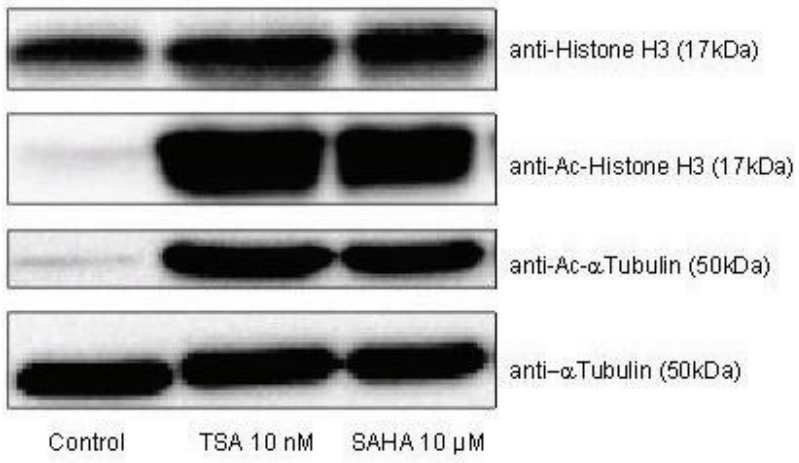

Figure 4-44: Induction of histone H3 and αTubulin hyperacetylation in A549 cells treated with SAHA and TSA (Western blot analysis)

1 x 10^5 A549 cells / well was seeded in 6-well plate. After 24 hours the cells were treated with DMSO (0.1%) control or HDAC inhibitor SAHA (10 µM) and TSA (10 nM) at a final DMSO concentration of 0.1% and incubated for another 24 hours. Cells were then collected for the detection of histone H3 and αTubulin hyperacetylation using Western blot, which was performed as described in Materials and Methods. A strong induction of histone H3 and αTubulin hyperacetylation in A549 cells treated with SAHA and TSA was detected, in contrast to vehicle control with DMSO (0.1%).

The concentration-dependent effects of SAHA on cytokine release in A549 cells (see Figure 4-37 and Figure 4-39) led us to determine the possible concentration-dependent hyperacetylation mediated by SAHA in A549 cells. Figure 4-45 illustrates the clear concentration dependence of histone H3 and αTubulin hyperacetylation in A549 cells treated with SAHA from 10 nM to 100 µM. Increasing amounts of Ac-H3 and Ac-α-Tubulin were detected, whereas amounts of H3 and αTubulin remained

constant. Additionally, the Western blot analysis showed that an obvious hyperacetylaiton of histone H3 and α-Tubulin was induced by SAHA at a minimum concentration of 1 µM, which may explain the faint effects of SAHA at 100 nM on cytokine release in cytokine-stimulated A549 cells (Figure 4-34a and Figure 4-35a).

Taken together, inhibition of HDAC activity using pan-HDAC inhibitor SAHA and TSA in A549 cells induced genome-wide histone H3 hyperacetylation as well as hyperacetylation of non-histone substrate αTubulin. Moreover, the induction of hyperacetylation with SAHA in A549 cells was concentration dependent and a clear hyperacetylating effect could be observed at a minimum SAHA concentration of 1 µM.

Concentration-dependent H3 hyperacetylation by SAHA

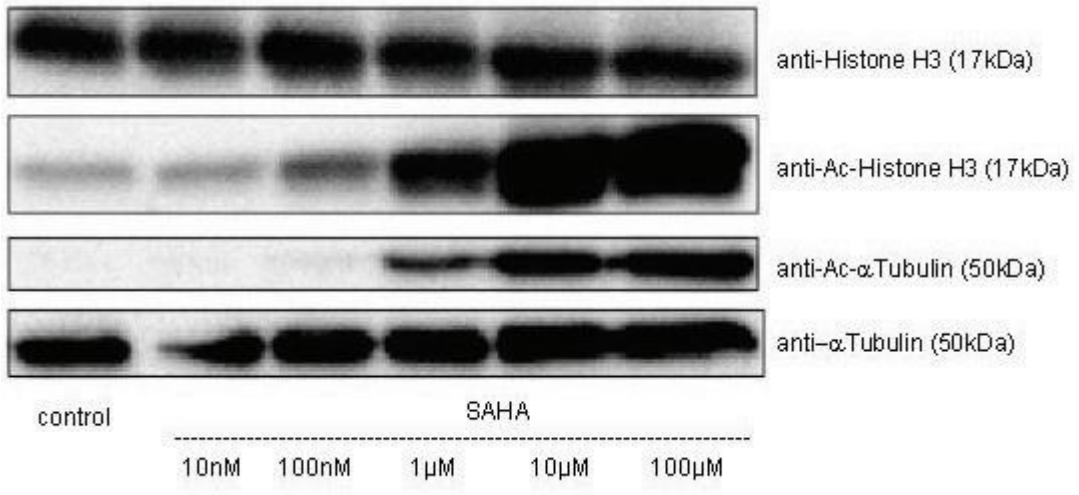

Figure 4-45: Concentration-dependent induction of histone H3 and α-Tubulin hyperacetylation in A549 cells treated with SAHA. (Western blot analysis)

The experiment was performed as described in Figure 1-44 (see also Materials and Methods) and the concentration-dependent histone H3 and αTubulin hyperacetylation in A549 cells treated for 24h with SAHA at increasing concentration as indicated was analysed by Western blot. SAHA concentration-dependently induced histone H3 and αTubulin hyperacetylation in A549. An obvious hyperacetylaiton of histone H3 and α-Tubulin was induced at a minimum SAHA concentration of 1 µM. Vehicle control: cells treated with DMSO at 0.1%

4.5.4 Effects of HDAC inhibitors on IL-8 promotor hyperacetylation in IL-1β-stimulated A549 cells

Results from the last section highlighted the effects of SAHA and TSA on core histone H3 hyperacetylation, which may be correlated with transcriptional regulation of pro-inflammatory genes, like IL-8 (see Introduction). To investigate histone

hyperacetylation at the promoter region of IL-8 gene in IL-1β-stimulated A549 cells after HDAC inhibitor treatment, the chromatin immuno-precipitation (ChIP) assay was performed.

Since the ChIP assay kit used (Cell signalling) provided a general protocol, to specify the assay for the study of IL-8 promotor hyperacetylation in A549 cells, several procedures needed to be adjusted and the established protocol was described in Materials and Methods. One of the most critical steps was to digest DNA to a length of approximately 150-900 bp (1-5 nucleosomes), which ensures an optimal immuno-precipitation using ChIP-formualted antibodies (Table 3-6). The amount of Micrococcal Nuclease required to digest DNA to the optimal length was determined empirically. After digestion and purification DNA segments were detected and quantified using gel-free Agilent 2100 Bioanalyzer DNA 1000 kit. Figure 4-46 demonstrates that the optimal digestion of DNA from nuclei of $4x10^7$ A549 cells to the optimal length was obtained by using the amount of 2.5 µl (5000 unit) nuclease.

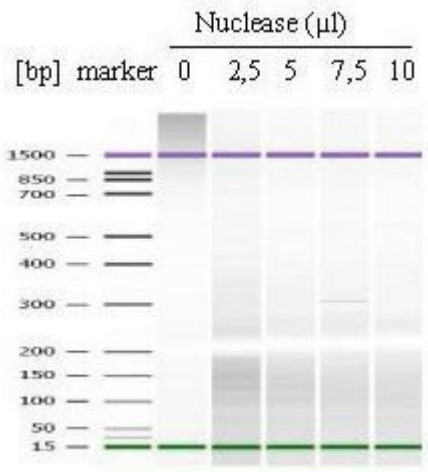

Figure 4-46: DNA digestion using Micrococcal Nuclease.

DNA digestion using Micrococcal Nuclease was performed as described in Materials and Methods. The amount of Micrococcal Nuclease (2000 unit/µl) required to digest DNA from Nuclei of $4x10^7$ A549 cells to the optimal length was determined empirically at 2.5, 5, 7.5 and 10 µl. Purified DNA was detected and quantified using gel-free Agilent 2100 Bioanalyzer DNA 1000 kit, The optimal digestion of DNA from nuclei of $4x10^7$ A549 cells to the optimal length was obtained by using the amount of 2.5 µl/5000 unit nuclease.

After optimization of the protocol histone H3 hyperacetylation at the IL-8 gene promoter region in A549 cells was analyzed by ChIP assay. Briefly, A549 cells were pretreated with vehicle or HDAC inhibitor SAHA or TSA for 30 min and then stimulated with IL-1β for 4 hours. ChIP assay for Ac-H3 was conducted using ChIP-formulated antibodies Table 3-6 as described in Materials and Methods. As important controls of a

successful ChIP experiment a positive control histone H3 antibody and a negative control normal rabbit IgG antibody were used (data not shown). To control the induction of the promoter of IL-8 gene, immuno-precipitation of RNA polymerse II (Pol II) DNA binding using ChIP-validated Pol II antibody was also conducted. Two sets of specific primers for two different sequences of IL-8 promotor gene (S1 and S2) were chosen to detect the enriched and purified DNA sequences using standard PCR. To ensure the specificity of the results, a primer set covering a region upstream of the transcription start site of IL-8 was also used in the PCR amplification. PCR products were run with a gel-free Agilent 2100 Bioanalyzer DNA 1000 kit (see Materials and Methods) to facilitate quantification, and the level of enrichment of the DNA sequence was determined relative to the total amount of specific sequences in the input samples.

The PCR detection using samples from immuno-precipitation with positive control H3 antibody showed a high level amplification of all three sequences (upstream, S1 and S2) and sample from IgG antibody a slightly background amplification of the three sequences (data not shown).

As indicated in Figure 4-47, IL-1β stimulation of A549 cells led to an increased level of RNA polymerase II DNA binding to the IL-8 promotor region S1 and S2, but not to the control upstream region of IL-8 promotor, which indicates a possible transcriptional activation of IL-8 promotor. At the same time, importantly, IL-1β-stimulation caused an increase of histone H3 hyperacetylation at the IL-8 promotor, which may directly open up the chromatin structure and may contribute to transcription activation. Treatment of cells with the HDAC inhibitor SAHA caused a strong increase of histone acetylation at the S1 region of the IL-8 promotor and treatment with TSA caused a slight increase at the S2 region of the IL-8 promotor. However, the RNA polymerase II binding to promoter regions of both sequences S1 and S2 was decreased to a various extend, which could possibly explain the decrease of IL-8 production in the cytokine-stimulated cells treated with SAHA or TSA in comparison to non-treated A549 cells (Figure 4-38 and Figure 4-41). Considering the increased histone H3 hyperacetylation at the IL-8 promoter region, the reduced binding of Pol II could be an upstream effect. On the other side, the level of IL-8 mRNA expression in SAHA- or TSA-treated and IL-1β-stimulated A549 cells was not clearly changed in comparison to non-treated cells (Figure 4-40), which is contradictionary to the decrease of Pol II binding to the IL-8 promotor.

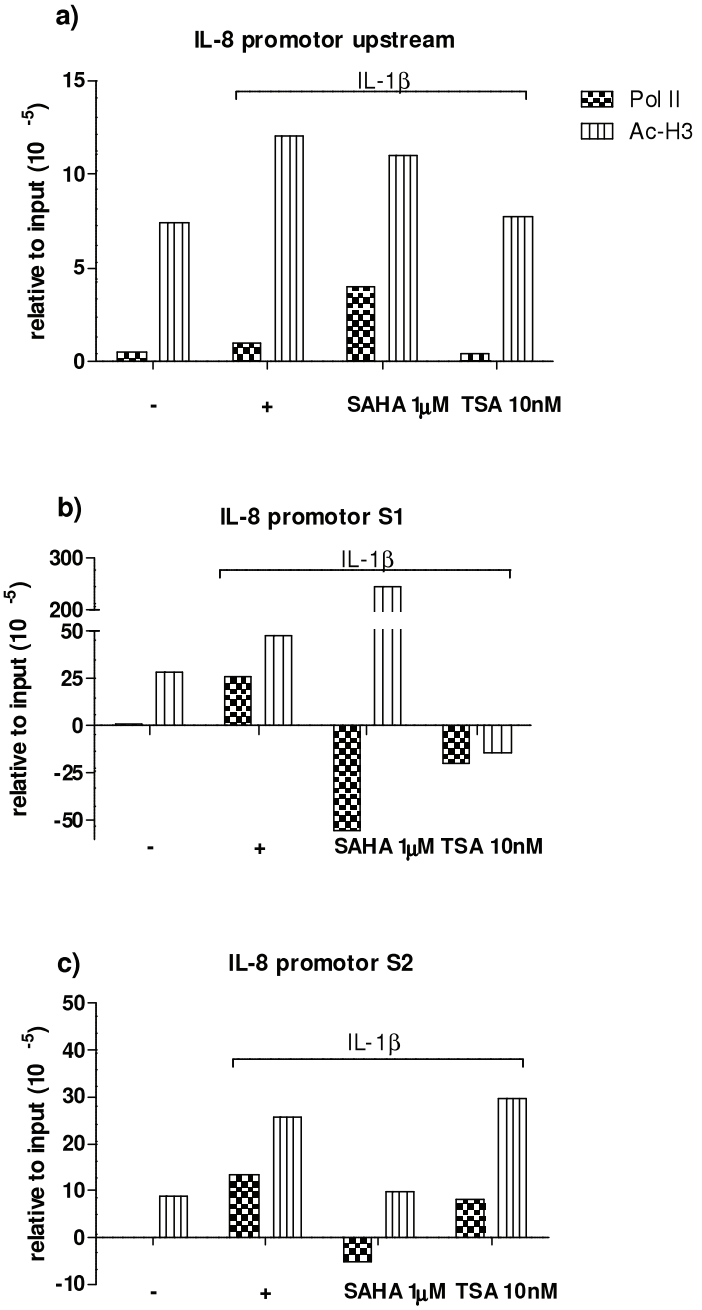

Figure 4-47: Polymerase II binding and histone H3 hyperacetylation at IL-8 promotor in HDAC inhibitor-treated and IL-1β-stimulated A549 cell (ChIP assay and PCR quantification).

A549 cells were pretreated with vehicle or HDAC inhibitor SAHA (1 μM) or TSA (10 nM) for 30 min and then stimulated with IL-1β (10 ng/ml) for 4 hours. ("-": non-stimulated and non-treated cells; "+": IL-1β-stimulated, non-treated cells). Chromatin immunoprecipitations were performed using nuclease digested chromatin and the indicated ChIP-validated antibodies (Pol II and Ac-H3). Purified DNA was amplified by standard PCR , using primers specific for the IL-8 promotor region (S1 and S2, diagram b and c) and upstream of promotor (upstream, control primer set, diagram a). The amount of immunoprecipitated DNA in each sample is represented as signal relative to the total amount of input chromatin. IL-1β: 10 ng/ml)

5 Discussion

The initial aim of the present study was to investigate new anti-inflammatory strategies in lung inflammation and steroid insensitivity in COPD using human lung epithelial cells. iNOS and HDAC, due to their important role in inflammation and potential involvement in steroid insensitivity as well as the successful development of specific inhibitors for both, were the focus of this study. The following points were of special interest and studied in detail: firstly, we aimed to characterize several human lung epithelial cell models including A549, BEAS-2B and MucilAir cells with various stimuli for the *in vitro* study of lung inflammation; next, we intended to evaluate iNOS mRNA expression and NO production in the human lung epithelial cell line A549 and to study the anti-inflammatory effects of specific iNOS inhibitors in lung epithelial cell models of inflammation; subsequently, it was intended to identify a lung epithelial cell model of steroid insensitivity concomitantly expressing iNOS and to test the hypothesis of the iNOS involvement in this cell model; the next aim was to clarify the correlation between steroid sensitivity of cytokine release and HDAC inhibition using HDAC inhibitors; the final goal was to explore the functional effects of HDAC inhibitors in lung epithelial cell models of inflammation by assessing release and gene expression of the pro-inflammatory cytokines and elucidating histone hyperacetylation at the promoter region of the IL-8 gene.

5.1 *In vitro* study of lung inflammation in COPD using human lung epithelial cells

Initially only taken as structural cells of the lung, there is upcoming evidence on the similarly important role of human lung epithelial cells in lung inflammation, compared to that of human immune cells, such as macrophages and T lymphocytes. But in fact, the lung epithelium is not only a target for factors released by infiltrating inflammatory cells, but also a major effector of inflammation (Martin et al. 1997) and plays a crucial role in the lung inflammation in COPD (Takizawa 1998; Pettersen and Adler 2002). In the present study, we characterized three cell models including A549: human alveolar epithelial carcinoma cell line, BEAS-2B: SV40-transformed human bronchial epithelial cell line and MucilAir: human primary airway epithelial cells maintained in air-liquid culture for the *in vitro* study of lung inflammation induced with various stimuli, including

pro-inflammatory cytokines and dsRNA. All three cell types produced upon stimulation a wide variety of pro-inflammatory mediators like cytokines and chemokines, which under physiological conditions may amplify the inflammation and cause injury of the lung.

In fact, *in vivo*, respiratory epithelial cells can upregulate and secrete various pro-inflammatory mediators in response to bacterial stimuli or endogenous inflammatory mediators. In the present study, to closely mimic the physiological conditions relevant to human, pro-inflammatory cytokines, including IL-1β, TNFα and IFNγ, either alone or in combination, were used in the experiments. Similarly, bacterial LPS, as well as the synthetic dsRNA analog poly(I:C) as a molecular mimetic of virus infection, which are both known to be potent triggers of lung epithelial cells to release inflammatory mediators, were also tested as physiological stimuli in this study (Khair et al. 1996; Alexopoulou et al. 2001; Diks et al. 2004). The induction of inflammatory cytokines through various stimuli in epithelial cells is predominantly due to activation of transcription factors nuclear NF-κB and AP-1.

Toll Like Receptors (TLRs) are key mediators of innate immunity, sensing invading microorganisms and activating subsequent immune responses. Recently, researchers have identified a new role for lung epithelial cells in the innate immune response in mice, as they could show that TLRs on epithelial cells but not those on immune cells are involved in the initial antigen sensing and inflammatory responses (Hammad et al. 2009). TLRs recognize disease-associated molecular patterns, termed as PAMPs (pathogen associated molecular patterns). The different TLRs bind to specific PAMPs, such as LPS to TLR4 and double stranded (viral) RNA to TLR3, leading to increased expression of pro-inflammatory cytokines and enzymes. TLR3 mRNA expression in CM- or dsRNA-stimulated A549 cells was strongly enhanced, correlating with increased pro-inflammatory cytokine and chemokine release. This finding is in agreement with a study of Rudd et al. (Rudd et al. 2005) who reported that TLR3 is upregulated and mediates inflammatory mediator production in virus-infected human lung fibroblast cells and A549 lung epithelial cells. Previous studies have demonstrated controversial results about TLR4 expression in A549 cells. While Monick (Monick et al. 2003) and MacRedmond (MacRedmond et al. 2005) presented increased levels of TLR4 mRNA and protein, and increased TLR4 membrane localization, Zhang et al. (Zhang et al. 2005) reported that TLR4 may not be involved in the innate immune

response in A549 cells. In contrast to the expression of TLR3, RT-PCR analysis of TLR4 expression revealed a low level of TLR4 mRNA transcription both under control and stimulation conditions and in addition, LPS was not able to increase pro-inflammatory cytokine release. Therefore, the expression of TLR4 and its involvement in inflammatory responses in A549 cells may be dependent on the source of the cells, the culture conditions or the stimuli used and thus, in our study LPS was not used to stimulate the cells due to the limited TLR4 expression.

In contrast, cytokine stimuli were very efficient to induce pro-inflammatory cytokine release in lung epithelial cells. IL-1β and TNFα, cytokines generated during the initial immune responses by macrophages, are among the most potent stimuli for the epithelial cell cytokine production and the stimulation of epithelial cells by IL-1β and TNFα contributes strongly to enhancement and progression of chronic lung inflammation (Standiford et al. 1990). IL-1β and TNFα, alone or in combination, could significantly augment the release of diverse pro-inflammatory mediators in all three cell models, as demonstrated in 25-plex Luminex assay. Especially, IL-8 release and mRNA transcription was significantly enhanced. It is well known that neutrophils are strongly implicated in the pathogenesis of COPD and IL-8 stimulates the accumulation of neutrophils in the lung. Standiford and coworkers have elaborately studied IL-8 expression in A549 cells induced by IL-1β and TNFα. Their Northern blot analysis demonstrated that induction of IL-8 mRNA transcription, in either IL-1β or TNFα treated A549 cells, occurred in both a dose- and time-dependent fashion. Similarly, significant increase of IL-8 release assessed by specific ELISA was detected from IL-1β- or TNFα-stimulated A549 cells in a time-dependent fashion with maximal IL-8 level at 24 h post stimulation. These results are in accordance with our data. Additionally, they could show on one hand that in this system the levels of IL-8 mRNA or protein in the LPS-treated A549 cells was not different from the unstimulated cells. On the other hand, the culture media from LPS-treated alveolar macrophages induced the IL-8 mRNA expression in the A549 cells significantly, while preincubation of LPS-treated alveolar macrophage culture media with anti-human IL-1β- or TNFα- neutralizing antibodies resulted in a significant decrease of IL-8 gene expression in A549 cells. Our data confirmed a part of the data above and provided more information with a wide variety of cytokines and chemokines induced in the human lung epithelial cell models using Luminex assay. These findings demonstrate I) IL-1β- and TNFα play an

important role in epithelial cell induction to produce pro-inflammatory mediators, including the neutrophil chemoattractant IL-8, and may potentiate lung inflammation; II) IL-1β- and/or TNFα-stimulated human epithelial cells provide a useful *in vitro* system to study lung inflammation.

To note, in addition to the induction of pro-inflammatory cytokines such as IL-8, GM-CSF, RANTES and MCP-1, stimulation of lung epithelial cells resulted also in the increase of anti-inflammatory cytokines, such as IL-1Ra, as demonstrated in the Luminex assay. IL-1Ra is a physiological receptor antagonist of IL-1β and can bind to IL-1β and block the action of IL-1β. IL-10 is another important anti-inflammatory cytokine, which could not be detected in A549 cells in the Luminex assay. The production of anti-inflammatory cytokines indicates that the immune response in lung epithelial cells is a dynamic process, which is regulated to reach a balance, at least at a normal situation.

Cigarette smoking is the underlying cause of COPD and the high level of oxidative stress from cigarette smoke has been shown to be strongly involved in airway inflammation in COPD. Moreover, cigarette smoke causes inflammation by inducing inflammatory mediator release in the lung epithelial cells and alveolar macrophages and by recruiting of neutrophils and T lymphocytes in the lung (Mio et al. 1997; Hellermann et al. 2002; Kent et al. 2008). Considering these facts, cigarette smoke could also be interesting as inducer or co-activator of cytokine release for the study of lung inflammation *in vitro*. Therefore, in the present study, the cells were also treated with cigarette smoke extract (CSE) in presence or absence of cytokine stimuli to mimic the conditions of cigarette smoking in human. But CSE, neither at 1% nor at 10% showed any effect on IL-8 mRNA expression under the experimental conditions used. Also, the addition of CSE to cytokine-mix did not show an additional effect on IL-8 mRNA transcription. Previous studies using cigarette smoke as stimuli have reported opposing data. While Walters et al. presented that cigarette smoke activates IL-8 release in human monocytes and macrophages and further, this effect is synergistically increased by concomitant treatment with IL-1β and TNFα (Walters et al. 2005), Kent reported that cigarette smoke caused a reduction of cytokine release from BAL macrophages of COPD patients (Kent et al. 2008). On one hand, the functionality and effect of cigarette smoke on lung epithelium of smokers depends on a lot of (patho-) physiological factors, which can not be easily imitated *in vitro*. On the other

hand, the concentration of active ROS/RNS in prepared cigarette smoke extract was possibly too low to activate a detectable cytokine expression. Moreover, the cells have also the capacity to neutralize RNS/RNS using their endogenous antioxidants, as reported by Lannan et al. that both intra- and extracellular GSH have important roles in protecting A549 cells from the injurious effects of the oxidants in cigarette smoke (Lannan et al. 1994). To optimize the experiments of cigarette smoke stimulation, the level of ROS/RNS should be quantified and inhibitors of enzymes depleting oxidants or antagonists of endogenous antioxidants may be applied prior to and during the CSE treatment.

5.2 Anti-inflammatory effects of iNOS inhibitors

Elevated levels of iNOS expression have been shown in the epithelial cell layer, in inflammatory cells - mainly in alveolar macrophages, neutrophils, eosinophils - and in skeletal muscle cells of COPD patients, compared to healthy individuals (Ichinose et al. 2000; Maestrelli et al. 2003; Agusti et al. 2004; Ricciardolo et al. 2005). This increase correlates well with augmented levels of NO in exhaled air and peroxynitrite in exhaled condensate, with enhanced expression of 3-nitrotyrosine in the lung and with disease severity (Maestrelli et al. 2003). These facts suggest that enhanced transcription and activation of iNOS, and thus production of iNOS-derived NO and peroxynitrite play a substantial role in the development and perpetuation of lung inflammation in COPD.

However, it has been reported that iNOS expression in airway epithelial cells is lost within 24 h of removal from the airway and unstimulated lung epithelial cell cultures express no iNOS (Guo et al. 1995). Many studies demonstrated that iNOS is rapidly induced in response to stimulation with bacterial endotoxins in rodents or pro-inflammatory cytokines (Kamosinska et al. 1997; Donnelly and Barnes 2002; Vallance and Leiper 2002). For our study on the role of iNOS in lung inflammation *in vitro* using human lung epithelial cells, various stimuli like cytokines or cytokine combinations of IL-1β, TNFα and IFNγ as well as dsRNA were used to induce iNOS expression. Under the given conditions A549 cells expressed iNOS mRNA in response to stimulation with a combination of IFNγ and IL-1β. Additional stimulation with TNFα and/or dsRNA resulted in a significant increase in iNOS mRNA levels. But in contrast to the mouse macrophage cell line RAW 264.7, which expresses iNOS under LPS stimulation

(Lorsbach et al. 1993), the human lung epithelial cell line did not show iNOS mRNA transcription after LPS stimulation. Also stimulation alone with dsRNA did not induce iNOS expression, although the basic level of TLR3 expression was 8-fold higher than that of TLR4. But in combination with cytokine-mix stimulation, dsRNA synergistically increased iNOS expression and activity, which is in accordance with the significant enhancement of TLR3 mRNA expression after CM stimulation in A549 cells. This result is in agreement with that of Uetani and co-authors, who showed that dsRNA in combination with IFNγ strongly induced iNOS expression and activity in BEAS-2B cells through activation of NF-κB and IRF-1 (IFN regulatory factor 1) in BEAS-2B cells (Uetani et al. 2001). IFNγ may be an important cytokine for the induction of iNOS in human airway epithelial cells. Guo et al. reported that IFNγ could induce iNOS in primary human airway epithelial cells (Guo et al. 1997). Further studies are required to explain the role of IFNγ signaling in iNOS induction. Although the mechanism underlying iNOS induction in human lung epithelial cells is only partially understood, activation of nuclear factor NF-κB and IRF-1 suggests to play a pivotal role (see introduction).

Coincident with the RT-PCR analysis of iNOS mRNA transcription, we found that A549 cells produced elevated amounts of iNOS-derived NO-metabolites nitrite and nitrate after stimulation with cytokines and dsRNA. Similar to RT-PCR analysis, the combination of IFNγ and IL-1β were sufficient to induce NO-production, and addition of TNFα and/or dsRNA led to significantly increased levels of NO-metabolites. These results are partially in accordance with those of Donnelly and Barnes, who showed a generally higher NO-level in the cytokine-mix stimulated A549 cells (Donnelly and Barnes 2002). In agreement to our data, Kamosinska et al. demonstrated that iNOS upregulated by inflammatory factors, in contrast to constitutive eNOS and nNOS, which produce picomolar concentration of NO, could produce NO in nanomolar concentration range and showed a long–term activity in A549 cells (Kamosinska et al. 1997).

Moreover, they could demonstrate that cells treated with cytokine-mix showed increased levels of peroxynitrite ($ONOO^-$), compared with the control, or cells that were treated with the cytokine-mix and 1400W or SOD (superoxide dismutase)/catalase. The strongly increased nitrative and oxidative stress from iNOS-derived NO/$ONOO^-$

could further affect the activity of a lot of enzymes by oxidizing functional groups crucial for this enzyme function and hence their cellular function and cause pathophysiological changes, which was discussed in details in introduction (see Chapter 1.3.2 and 1.3.3).

The CM-mediated production of NO_x in A549 cells was shown to be effectively inhibited by the iNOS inhibitor BYK191023 (pIC_{50} = 5.0). For this reason we assumed that iNOS was the main source for elevated NO levels. Additionally, RT-PCR with eNOS specific primers detected only very low levels of eNOS mRNA expression in CM-stimulated A549 cells, which was similar to the data of Kamosinska et al., showing in their Western blot analysis unchanged levels of eNOS in samples of both control and stimulated cells, but a significantly increased expression of iNOS (Kamosinska et al. 1997). Taken together, with conditions for iNOS expression and activity characterized, a convenient and valuable *in vitro* system using A549 human lung epithelial cell line was provided to investigate the anti-inflammatory effect of iNOS inhibition using iNOS-specific inhibitors and to test the hypothesis of the iNOS involvement in steroid insensitivity in human respiratory epithelial cells.

iNOS overexpression in COPD and excessive NO produced by iNOS has been recognized as an important trigger of inflammation and considered to be responsible at least in part for tissue destruction. Numerous studies, both *in vivo* and *in vitro,* demonstrated that inflammatory responses correlate well with increase of iNOS expression and NO production and even better with the formation of peroxynitrite (Barnes and Liew 1995; Ricciardolo et al. 2005). Moreover, the iNOS/NO-mediated effects in inflammation studies *in vitro* showed that NO upregulated chemokine expression and augmented IL-1β-induced IL-8 mRNA expression in a human keratinocyte cell line (Wetzler et al. 2000). It has also been shown that NO is an important modulator of leukocyte recruitment (Kuo et al. 1997). Thus, this is evidence that NO alters leukocyte recruitment through modulating IL-8 secretion. We demonstrated that I) IL-8 mRNA transcription and secretion by A549 cells, similar to iNOS mRNA and NO production, is induced by CM and dsRNA; II) iNOS specific inhibitor BYK191023 inhibited the cytokine (CM/dsRNA- or IL-1β/IFNγ) mediated increase IL-8 at both transcriptional and protein levels. These results indicate that iNOS derived NO may play a positive role in activation of IL-8 during inflammation. This is in contrast to the findings of Kuo et al., who proposed that the production of NO

in airway inflammatory diseases may play a negative feedback role in inflammatory responses (Kuo et al. 1997).

As mentioned, besides the detrimental effects which may directly be mediated by iNOS-derived NO, the more potent and harmful oxidant peroxynitrite formed by NO and superoxide seems to play a major role in inflammatory responses of the lung cells. Recently, Osoata et al. showed significantly elevated peroxynitrite levels in the exhaled breath condensate of COPD patients when compared with healthy volunteers and smokers, correlating well with disease severity (Osoata et al. 2009a; Osoata et al. 2009b). Especially, the formation of 3-nitrotyosine by peroxynitrite correlates well with increased iNOS expression and disease severity in COPD (Maestrelli et al. 2003).

Hence, the development of highly selective iNOS inhibitors seems to be a promising approach for the treatment of lung inflammation in COPD, which has been reviewed recently (Hesslinger 2009). A pathological role of iNOS-derived excessive NO production was shown in a variety of animal models of inflammation using iNOS inhibitors. Our previous study demonstrated that administration of both a semi-selective NOS inhibitor (L-NIL) and highly selective iNOS inhibitors (GW274150 and BYK402750) potently diminished influx of inflammatory cells and cytokine levels in BALF in an 11-day smoke mouse model mimicking certain aspects of human COPD (Hesslinger et al. 2008). In contrast, iNOS inhibition was ineffective in a 3-day smoke mouse model (unpublished work), suggesting that iNOS inhibitors preferentially affect subacute and chronic smoke-induced inflammation but are ineffective under acute inflammatory conditions. The question whether the anti-inflammatory activity of iNOS inhibition eventually results in a reduction of emphysema induction and airway remodelling has to be tested in long-term smoke models. Selective inhibition of the inducible form of NOSs resulted in potent anti-inflammatory and tissue protective effects in almost all animal models tested (Hesslinger 2009). But due to the different regulation of iNOS expression in humans and animals which may affect the efficacy of iNOS inhibitors, the transfer of *in vivo* data from animal to human may be difficult. In fact, initial clinical trials with iNOS inhibitors in asthmatic lung inflammation were disappointing. *In vitro* data from this study using human lung epithelial lines A549 and BEAS-2B and primary lung epithelial cells MucilAir demonstrated that the iNOS inhibitors BYK191023 and BYK402750 reduced specifically the pro-inflammatory cytokine release induced by CM in a concentration-dependent manner. These data

may, at least in a very basic way, help to characterize the anti-inflammatory effects of iNOS inhibitors in the humans. Using iNOS inhibitors for the treatment of lung inflammation may require a deeper understanding of its functional effects in various models.

5.3 Role of iNOS in a human epithelial cell model of steroid insensitivity

Besides the role of iNOS and iNOS-derived NO/$ONOO^-$ in lung inflammation, their involvement in steroid insensitivity has been proposed by Peter Barnes in many peer-reviewed articles (Barnes et al. 2004; Barnes 2006a; Barnes 2008). Peter Barnes hypothesized that increased oxidative and nitrative stress in the lung of COPD patients may lead to reduction of HDAC2 activity by HDAC tyrosine-nitration, which is important in mediating the anti-inflammatory effects of steroids, and hence, steroid insensitivity.

Various studies have reported steroid insensitivity in induced sputum, airway biopsy specimens or alveolar macrophages from patients with COPD who smoke. Increased nitrative stress in a COPD lung may result both from cigarette smoke and iNOS-derived NO and peroxynitrite. To test the hypothesis in respect of involvement of iNOS as well as iNOS-derived NO and peroxynitrite in steroid insensitivity *in vitro*, we firstly established a human lung epithelial cell system stimulated by cytokine-mix, which concomitantly express iNOS and IL-8. While dexamethasone inhibited effectively IL-1β-induced expression and secretion of IL-8 in a dose-dependent manner, the sensitivity towards dexamethasone was markedly reduced when A549 cells were stimulated with the cytokine-mix. Even at very high concentrations, dexamethasone only marginally affected the release of IL-8. This steroid insensitivity of cytokine release could be validated using the Luminex technology for some more inflammatory cytokines and chemokines, including GM-CSF and IL-2R. This steroid insensitivity is at least partially in accordance with data from Ito et al. and Marwick et al., who could also show steroid insensitivity of IL-8 release in their cell system exposed to oxidative stress caused by H_2O_2 (Ito et al. 2004; Marwick et al. 2004).

Since Barnes' hypothesis is based on the decrease of HDAC activity, we tested HDAC activity in this cell system after exposure to the exogenous nitrative and oxidative stress and could show that HDAC activity was responsive to the oxidative and nitrative stress, as exposure to SIN-1 (peroxynitrite donor) and H_2O_2 caused a reduction of

HDAC activity. These results are in agreement with a report from Osoata et al. who showed that nitrative and oxidative stress from SIN-1, H_2O_2 and peroxynitrite reduced HDAC, especially HDAC2, protein expression and enzymatic activity in A549 cells (Osoata et al. 2009b). The reduction of HDAC activity was also partially confirmed by the *in vitro* study in A549 cells of Ito et al. using H_2O_2 and Marwick et al. using both cigarette smoke extract and H_2O_2 (Ito et al. 2004; Marwick et al. 2004).

Additionally, dexamethasone in a relevant concentration range did not show any effect on iNOS activity in this cell model, which ensures a situation of steroid insensitivity with concomitant iNOS expression. This result is also in agreement of that from Donnelly et al. who showed that dexamethasone failed to inhibit the expression of iNOS mRNA and protein and NO_x-production induced by cytokine-mix in human lung epithelial cells (Donnelly and Barnes 2002). As discussed in the introduction, expression of the iNOS gene in human intestinal epithelial cell lines may require activation of the transcription factor STAT-1, whereas activation of STAT-1 has been demonstrated to be steroid insensitive (Kleinert et al. 1998). A similar mechanism in A549 human lung epithelial cells would explain the steroid-insensitive iNOS expression following cytokine-mix stimulation in lung epithelial cells.

To test the hypothesis that iNOS is involved in steroid insensitivity in the lung epithelial cell model used, iNOS inhibitors were used to modulate iNOS activity. In contrast, the results indicate that inhibition of iNOS using the iNOS-selective inhibitor 1400W or non-selective NOS inhibitor AMT following the cytokine-mix stimulation did not alter steroid insensitivity. In addition, a second strategy of iNOS modulation through iNOS overexpression did not influence IL-1β–induced steroid sensitivity of IL-8 release in A549 cells. Also the modulation of nitrative and oxidative stress using SIN-1 and a combination of SIN-1 and H_2O_2 following IL-1β stimulation did not affect steroid sensitivity of IL-8 release in A549 cells. In contrast to Peter Barnes' hypothesis, these results suggest that, at least in the A549 lung epithelial cell model used, iNOS activity or expression and nitrative and oxidative stress through SIN-1 and H_2O_2 does not influence steroid responsiveness.

On the other hand, Marwick et al. showed that in their steroid-insensitive cell model under conditions of oxidative stress, theophylline restored steroid sensitivity of pro-inflammatory release. Other groups have shown to restore steroid sensitivity which is

related to excessive oxidative and nitrative stress by using antioxidants. It has also been shown that through the ability to restore HDAC activity curcumin (Meja et al. 2008) and resveratrol (Yang et al. 2006) could reverse steroid insensitivity, which may highlight the importance of HDAC in steroid insensitivity in COPD.

In fact, many studies have shown that ROS/RNS can inactivate HDAC and this is achieved through increased nitration or carbonylation (Marwick et al. 2004). Coupled with ROS/RNS-induced histone acetylation through activation of NF-κB and AP-1 transcription factors, this has the net effect of promoting pro-inflammatory gene expression (Rahman and Adcock 2006). Yang et al. have demonstrated that cigarette smoke extract (CSE) reduced histone deacetylase (HDAC) activity and expression and increased IL-8 release in a human macrophage cell line. But pre-treatment of cells with the antioxidant GSH monoethyl ester could reverse cigarette smoke-induced reduction in HDAC levels and significantly inhibited IL-8 release (Yang et al. 2006). Although we could not demonstrate IL-8 induction by CSE and H_2O_2, at least under the conditions used, we could show that oxidative and nitrative stress from a combination of SIN-1 and H_2O_2 reduced HDAC activity in our cell system.

Moreover, the impact of ROS and RNS on histone deacetylase 2 (HDAC2) is particularly important as it has also been shown to be required for corticosteroid-mediated inhibition of the inflammatory responses and reduced HDAC2 activity has been hypothesized to result in corticosteroid insensitivity in COPD (Rahman and Adcock 2006). Various reports indicate that HDAC2 activity and expression are markedly reduced in COPD lungs and alveolar macrophages (Ito et al. 2001; Ito et al. 2005). Ito et al. have shown in alveolar macrophage that oxidative stress reduced HDAC2 expression and lead to steroid insensitivity and that HDAC2 knock-down by using siRNA induced steroid insensitivity of cytokine release (Ito et al. 2001; Ito et al. 2006b). Reduction in HDAC2 appears to be caused by tyrosine-nitration, phosphorylation, and ubiquitination, resulting in loss of its activity and increased degradation secondary to increased oxidative and nitrative stress (Adenuga et al. 2009; Osoata et al. 2009b).

Besides focusing on the involvement of iNOS and NO, we did try to investigate other mechanisms, which could result in steroid insensitivity in our A549 cell model. Steroids act by binding to their cytosolic receptor (GR), which is subsequently activated and is able to translocate to the nucleus. Once in the nucleus, the GR either binds to DNA

and switches on the expression of anti-inflammatory genes or acts indirectly to repress the activity of a number of distinct signaling pathways such as NF-κB and AP-1. Based on this mechanism, a failure to respond may therefore result from reduced steroid binding to GR, reduced GR expression or failure of GR translocation (Leung et al. 1995). We intended to study the GR translocation by applying confocal microscopy. To achieve this, we tried to overexpress GR in A549 cells, which was not successful due to a possible cytotoxic effect of the overexpression

5.4 HDAC activity and steroid function

The hypothesis from P. Barnes on steroid insensitivity is based on the predominant mechanism of steroid function, that steroid receptors use histone deacetylase as corepressor to inhibit expression of pro-inflammatory mediators (Barnes et al. 2004). Activated glucocorticoid receptors interact with co-repressor molecules, specifically HDAC2, to attenuate NF-κB-associated coactivator activity, which is responsible for the transcription of inflammatory mediators, thus reducing histone acetylation, causing chromatin remodelling and inhibiting RNA polymerase II action, and by that the transcription of inflammatory genes.

Since we could not prove the hypothesis of iNOS being involved in our steroid-insensitive cell model, it was interesting to ask the question, whether the action of the steroids in our cell model is dependent on the HDAC activity and thus, we aimed to explain the relevance of steroid responsiveness and HDAC inhibition in lung epithelial cells. The HDAC activity assay showed that cytokine (IL-1β or CM) stimulation did not affect total HDAC activity. Although other studies have shown that expression of specific HDACs could be regulated upon various stimuli (Schmeck et al. 2008), the activity of most if not all HDACs is regulated by protein-protein interactions (Sengupta and Seto 2004). Upon treatment with the different HDAC inhibitors (pan-HDAC inhibitors SAHA and TSA; Class I HDAC inhibitor: MS-275, see also introduction) at appropriate concentrations without cytotoxic effects in the time range of treatment, HDAC activity in A549 cells was inhibited at different degrees. Dexamethasone inhibited GM-CSF and IL-8 release in IL-1β-stimulated BEAS-2B human lung epithelial cells efficiently without pre-treatment with HDAC inhibitors. Although pre-treatment of the cells with HDAC inhibitors showed both increasing or decreasing effects on the

overall levels of GM-CSF or IL-8 release in dexamethasone treated and IL-1β-stimulated BEAS-2B cells, the efficiency of dexamethasone was not changed. This may indicate that steroid function in this lung epithelial cell system is HDAC independent, which is again in contrast to P. Barnes hypothesis.

Besides recruitment of HDAC, there are a number of other potential explanations for steroid anti-inflammatory function in the used cell systems as described in section 1.2.1. Steroid receptors may also activate anti-inflammatory factors in the cells, which facilitate the downregulation of inflammatory cytokines or they can bind to a GRE that overlaps the DNA-binding site for a pro-inflammatory transcription factor or the start site of transcription to prevent inflammatory gene expression. Both of these processes are not dependent on the co-repressor function of HDAC (Ito et al. 2006a) and may explain the steroid function in our system, although the actual cause remains to be determined.

5.5 Histone acetylation and HDAC inhibitors in inflammation

HDAC inhibition using the pan HDAC inhibitors TSA and SAHA as well as the HDAC class I inhibitor MS-275 had no effect on dexamethasone-mediated inhibition of IL-8 and GM-CSF release in cytokine-stimulated BEAS-2B cells. Interestingly, the HDAC inhibitors alone showed different effects on cytokine and chemokine release in human epithelial cells induced by various cytokine stimuli, either an increasing or a decreasing effect depending on the type of HDAC inhibitors used (SAHA, TSA, MS-275), cytokines and chemokines analyzed (IL-8, GM-CSF, partially RANTES) and cell types used (A549 and BEAS-2B cells).

HDACs have emerged as exciting drug targets for multiple pathological conditions. Recently, HDAC inhibitor SAHA has been approved by the US FDA as an anti-cancer drug (trade name Zolinza) (Walkinshaw et al. 2008). In inflammatory processes histone acetylation is normally correlated with transcriptional activation of pro-inflammatory genes and histone deacetylation with gene repression (see Introduction). Additionally, a plenty of studies, as mentioned above, showed reduced HDAC activity due to oxidative and nitrative stress correlated with increased inflammation and steroid insensitivity in COPD. And due to the substrates plurality (not only histones, but also non-histone substrates, see Table 1-4) and consequently the function versatility in

different cell processes of HDACs, it is not surprising that HDAC inhibitors have demonstrated pronounced anti-inflammatory effects besides their efficiency in the treatment of cancer.

Leoni and colleagues showed that SAHA inhibited the secretion of TNFα, IL-1β, IL-6, and IFNγ in LPS-induced PBMC cells, and also a SAHA-mediated inhibition of their *in vivo* production in an LPS-induced animal model (Leoni et al. 2002; Leoni et al. 2005). In agreement to their data, we showed that SAHA inhibited GM-CSF and IL-8 release in human lung epithelial cells significantly. Klampfer et al. could show that the pan-HDAC inhibitors butyrate, SAHA and TSA inhibit the signaling by IFNγ and thus negatively regulates the expression of IFNγ responsive genes (Klampfer et al. 2003; Klampfer et al. 2004). Another group (Carta et al. 2006) showed that SAHA inhibited IL-1β secretion in human monocytes. Moreover, it has been shown recently that HDAC inhibitors have anti-inflammatory activities via suppression of cytokines and nitric oxide (Blanchard and Chipoy 2005). TSA was shown on the one hand to inhibit IL-8 expression in Caco-2 cells and IL-12 expression in BEAS-2B cells and to decrease various NF-κB target gene expression induced by TNFα in A549 cells (Imre et al. 2006), but on the other hand to induce IL-8 production in BEAS-2B cells (Hoshimoto et al. 2002; Iwata et al. 2002). The latter is consistent with our data, which showed TSA increased IL-8 secretion in cytokine-stimulated BEAS-2B cells. Recently, TSA and butyrate have also been shown to suppress IL-1ß-induced iNOS and COX-2 expression (Chabane et al. 2008). Very interestingly, data from our research group in Nycomed have demonstrated that various HDAC inhibitors downregulated TLR4, 7, 8 and inhibited IL-6, TNFα and IP10 production in PBMCs, reduced GM-CSF release from human lung epithelial cells, TNFα from monocytes, IL-2 from T lymphocytes and inhibited also T lymphocyte proliferation (Imre et al. 2006; Boehm et al. 2007). Additionally, HDAC inhibitors have demonstrated beneficial effects in *in vivo* models of inflammatory diseases, such as multiple sclerosis (Gray and Dangond 2006) and lupus erythematosus (Mishra et al. 2003).

On the other hand, the cells and mediators involved and thus, the gene expression profiles, differ between inflammatory models and as consequence it is also not surprising that HDAC inhibitors can have opposing effects on the expression of inflammatory genes depending on the cell types and stimuli used (Dinarello 2006). In addition, different HDAC inhibitors show positive or negative regulatory effects in the

same inflammatory model (Nusinzon and Horvath 2006), which may be reflected by our own data. MS-275 (1 µM) enhanced induction of GM-CSF in cytokine-stimulated BEAS-2B cells and decreased that of IL-8, whereas TSA (10 nM) enhanced both induction of GM-CSF (strongly) and IL-8 (slightly) in cytokine-stimulated BEAS-2B cells.

The mode of action of HADC inhibitors has been investigated by many groups and the results are still controversial. Therefore, the major mechanisms underlying the functional roles of HDAC inhibitors in inflammation still need to be determined. Except for their effects at the regulation of the TLR-receptor expression and at different cytokine signaling pathways like the IFNγ signalling pathway mentioned above, the effect of HDAC inhibitors on DNA binding activity of the transcription factor NF-κB was demonstrated (Hoshimoto et al. 2002; Imre et al. 2006; Suuronen et al. 2006; Chabane et al. 2008). The cellular effects of various HDAC inhibitors have been demonstrated to be both histone-dependent and histone-independent. However, the data postulated were mainly from pan HDAC inhibitors and varied with cell types and types of HDAC inhibitors. Future experiments with specific HDAC inhibitors could provide more information. In addition, the presence of HDAC isoforms is tissue/cell type-specific. Using HDAC-siRNA may help to define the relevance of different HDACs in *in vitro* inflammation models. ChIP-on-chip studies of every HDAC in different cell types will help to find relevant target genes pointing to new functions of specific HDAC isoenzymes. Additionally, the processes regulated by sirtuins could also be interesting (Walkinshaw et al. 2008).

To gain an insight into the mode of action of HDACs in our cells, the effect of HDAC inhibitors on specific cytokine mRNA expression using Real-Time PCR and the promoter histone H3 hyperacetylation of IL-8 gene during induction and HDAC inhibitor treatment was conducted using ChIP assay. In contrast to their effects on IL-8 release, SAHA and TSA showed no effect on IL-8 mRNA expression, irrespectively of type or concentration of the compound and time of treatment, whereas they decreased the mRNA expression of GM-CSF. Inhibition of HDAC activity using the pan-HDAC inhibitors SAHA and TSA in A549 cells induced a concentration-dependent genome-wide hyperacetylation of histone H3 and αTubulin, a non-histone substrate. These results postulated that HDAC inhibitors show a gene-specific regulatory effect at the level of mRNA transcription. Although core histones of the genes can be

hyperacetylated, the regulation of the expression of different genes may happen at different levels. The regulatory effects of factors upstream or downstream of the transcriptional level may be more important. And these can also be modified by de-/acetylation, like αTubulin, and consequently their function would be altered.

In the ChIP assay, we could show that IL-1β-stimulation of A549 cells led to an increased level of RNA polymerase II DNA binding to the IL-8 promotor region but not to the control upstream region of the IL-8 promotor, which indicates a possible activation of the gene. At the same time, IL-1β-stimulation caused an increase of histone H3 hyperacetylation at the IL-8 promotor, which can directly open the chromatin structure and may contribute to transcription activation. Surprisingly, treatment of cells with the HDAC inhibitors SAHA or TSA increased H3 hyperacetylation, but decreased the RNA polymerase II binding to the promoter region of IL-8 gene. Sakamoto and co-worker showed that treatment of cells with the HDAC inhibitor TSA inhibited selected IFNβ-stimulated immediate early genes by reducing recruitment of RNA Pol II to promoter, i.e. HDAC activity was required for Pol II recruitment (Sakamoto et al. 2004), which may also explain our findings. On the other hand, the level of IL-8 mRNA expression in SAHA- or TSA-treated and IL-1β-stimulated A549 cells was not altered in comparison to non-treated cells (Figure 4-40). This is contradictionary to the decrease of Pol II binding to IL-8 promotor, although the produciton of IL-8 was also reduced upon treatment with HDAC inhibitor SAHA at 1 µM. The anti-inflammatory effects of HDAC inhibitors leading to reduced cytokine release may due to a up- or down-stream mode of action. To give a certain answer and to explain the unchanged mRNA level, more experiments are needed, especially in respect of histone lysine-specific hyperacetylation through HDAC inhibitors, which could be deciding for the change of chromatin structure.

5.6 Putative impact on COPD therapy

One part of a putative new therapy for COPD is to overcome the steroid insensitivity. Although iNOS involvement in steroid insensitivity in our lung epithelial cell model was devalidated, the strategy of reducing anti-oxidative stress to reverse steroid insensitivity in the disease is prominent. Anti-oxidants and also HDAC2 activators, like theophylline (Ito et al. 2002; Barnes 2006b) and curcumin (Meja et al. 2008) could be

helpful; also further investigations of iNOS inhibitors could bring new findings (Barnes and Adcock 2009).

In looking for alternatives of steroids for the treatment of lung inflammation in COPD, both iNOS and HDAC inhibitors could be interesting due to their effects in various animal and cell models. The current development for iNOS inhibitors in lung-related diseases including COPD have been recently reviewed (Hesslinger 2009). The researching on HDAC inhibitors, besides in the field of anti-cancer and expanding lifespan mentioned above, is expanding, especially regarding a number of non-histone substrates and specific HDAC inhibitors. With the increasing knowledge about HDAC function, the possibility of finding new therapies for COPD is promising.

6 Summary

One of the hallmarks of chronic obstructive pulmonary disease (COPD) is chronic systemic and local inflammation of the lung. A majority of COPD patients show insensitivity to inhaled corticosteroids, which are usually very effective drugs for the treatment of chronic lung inflammation. Expression of inducible NO synthase (iNOS) has been shown in the lung epithelial, inflammatory and skeletal muscle cells of COPD patients and correlates well with increased NO and peroxynitrite ($ONOO^-$) production, leading to increased nitrative stress and amplified inflammation in COPD. iNOS inhibitors have been shown to potently block inflammation in a tobacco smoke-induced steroid-insensitive mouse model of COPD. Furthermore, iNOS and iNOS-derived NO and $ONOO^-$ has been hypothesized to be involved in steroid insensitivity through tyrosine nitration of histone deacetylase 2 (HDAC2), as the anti-inflammatory action of corticosteroids works, at least partially, via HDAC-mediated histone deacetylation and reduction of the inflammatory gene transcription. In contrast, HDAC inhibition by HDAC inhibitors revealed potent anti-inflammatory effects in a wide variety of animal and cell models, which suggests an even more complex situation.

The objectives of the present study were i) to characterize several human lung epithelial cell models including A549, BEAS-2B and MucilAir cells for their applicability to study lung inflammation *in vitro*; ii) to evaluate iNOS mRNA expression and NO production in the human lung epithelial cell line A549 and to study the anti-inflammatory effects of specific iNOS inhibitors in these cell models; iii) to identify an iNOS expressing lung epithelial cell model of steroid insensitivity and to test the hypothesis that iNOS is involved in steroid insensitivity by modulating iNOS activity and expression as well as NO/$ONOO^-$ level; iv) to analyze a putative connection between steroid sensitivity of cytokine release and HDAC inhibition; v) to explore the functional effects of HDAC inhibitors in lung epithelial cell models of inflammation by assessing release and gene expression of pro-inflammatory cytokines and chemokines, and elucidating histone hyperacetylation at IL-8 promoter region.

Initially, stimulation of human lung epithelial cells using various cytokine stimuli such as IL-1β and TNFα induced the production and mRNA expression of amounts of pro-inflammatory cytokines and chemokines substantially, suggesting the critical role of

lung epithelial cells in lung injury and also in regulating the inflammatory responses together with immune cells in the lung.

Previously, potent inhibitory effects of several iNOS inhibitors on inflammatory cell influx (neutrophils, alveolar macrophages and T lymphocytes) into the lung and accumulation of various cytokines and chemokines [MIP-1α, MCP-1 and KC (IL-8 homologue)] in BALF (bronchoalveolar lavage fluid) were shown using a clinically relevant tobacco smoke mouse model of COPD. With the intention to elucidate these anti-inflammatory effects of selective iNOS inhibitors in lung epithelial cells, iNOS expression and NO production by A549 cells in response to different cytokine stimuli were characterized. The combination of IL-1β, TNFα and IFNγ as cytokine-mix (CM) upregulated iNOS mRNA expression and iNOS-derived NO production in A549 cells substantially and dsRNA further enhanced this induction. We could show that highly selective and potent iNOS inhibitor BYK191023 inhibited IL-8 release and gene expression in CM-stimulated A549 cells. This effect was verified by BYK402750, another selective iNOS inhibitor, by reducing release of various cytokines and chemokines in CM-stimulated lung epithelial cell line BEAS-2B and primary lung epithelial cells MucilAir.

Subsequently, a cellular model of steroid insensitivity of IL-8 release using cytokine mix (CM) stimulated A549 cells was established and characterized. CM-stimulated A549 cells showed steroid insensitivity and concomitantly expressed iNOS. They also demonstrated reduction of HDAC activity upon exposure to exogenous nitrative and oxidative stress caused by SIN-1 and H_2O_2. Using multiple analyte profiling (Luminex) steroid insensitivity of cytokine release was shown for a wide variety of cytokines and chemokines, including GM-CSF and IL-2R. However, modulating iNOS or the level of $NO/ONOO^-$ did not affect steroid responsiveness of cytokine release, neither by using selective iNOS inhibitors or iNOS overexpression nor by usage of the $NO/ONOO^-$ donor SIN-1 in presence or absence of H_2O_2. Additionally, steroid sensitivity in BEAS-2B cells and in MucilAir cells was analyzed using identical conditions and preliminary data suggested steroid-insensitive responses of IL-6, IL-8 and GM-CSF release in primary lung epithelial cells but not in BEAS-2B cells. Thus, iNOS does not seem to play a role in steroid insensitivity, at least in the CM-stimulated A549 cell model used.

Furthermore, the dexamethasone-mediated anti-inflammatory effects on cytokine release were not changed by HDAC inhibition in lung epithelial cells by addition of

various HDAC inhibitors, again suggesting an HDAC independent mode of action of steroid under the conditions used.

Studying functional effects of HDAC inhibitors on pro-inflammatory mediator release and mRNA expression in cytokine-stimulated human lung epithelial cells indicated that HDAC inhibitors can act both anti- and pro-inflammatory depending on the HDAC inhibitor used, on the cell type (primary cells vs. cancer cell line) and on the target gene, which may suggest different target gene/promoter-specific mode of action of HDAC inhibitors. For some of the cytokines and chemokines studied, this effect was partially regulated at the level of mRNA expression, which may involve the induction of histone H3 hyperacetylation at the IL-8 promoter.

In conclusion, the present study demonstrated that iNOS inhibitors show anti-inflammatory effects on the release of specific cytokines and chemokines in human lung epithelial cells, which may help to define the rationale for the development of potent iNOS inhibitors for the treatment of lung inflammation. Nevertheless, our results suggest that iNOS does not influence steroid sensitivity, at least in the cell model used, and that steroid sensitivity of cytokine release in cell model used may be independent of HDAC activity. Moreover, HDAC inhibition revealed both pro- or anti-inflammatory effects, depending on the HDAC inhibitors studied and gene targeted. The induction of histone H3 hyperacetylation at the promoter of IL-8 gene may help to explain the mode of action of SAHA in its functional effects in inflammation.

7 Zusammenfassung

Zu den wichtigsten Kennzeichen der chronisch obstruktiven Lungenerkrankung (COPD) zählt neben einer systemischen Inflammation auch eine lokale Entzündung des Lungengewebes. Darüber hinaus zeigt eine Mehrheit der COPD-Patienten eine Insensitivität gegenüber einer Behandlung mit Corticosteroiden, welche üblicherweise eine sehr wirksame medikamentöse Therapie zur Behandlung von entzündlichen Erkrankungen wie z. B. Asthma darstellen. Die molekularen und zellbiologischen Grundlagen dieser Steroidinsensitivität werden momentan weltweit untersucht. Erste Ergebnisse verschiedener Gruppen zeigen dabei eine wichtige Rolle von oxidativen und nitrativen Stress, sowie der Histondeacetylierung. Eine gesteigerten Produktion von Stickstoffmonoxid (NO) und Peroxynitrit ($ONOO^-$), welche zu erhöhtem nitrativen Stress und verstärkter Inflammation in der COPD führen kann, wurde zusammen mit einer verstärkten Expression der induzierbaren NO Synthase (iNOS) bereits in Lungenepithelzellen, inflammatorischen Zellen und Skelettmuskelzellen von COPD-Patienten nachgewiesen. Darüber hinaus konnte bereits eine gute Wirksamkeit von iNOS-Inhibitoren in einem Zigarettenrauch-induzierten steroid-insensitiven Maus-Modell der COPD gezeigt werden. In diesem Zusammenhang wurde die Hypothese aufgestellt, dass iNOS und durch iNOS produziertes NO und $ONOO^-$ die Steroid-Insensitivität durch Tyrosinnitrierung der Histone Deacetylase 2 (HDAC2) vermitteln kann, wobei die anti-inflammatorische Wirkung von Steroiden auf eine Interaktion mit Histondeacetylasen (HDAC), welche die Transkription inflammatorischer Gene durch Histondeacetylierung hemmt, zurückzuführen ist. Im Gegensatz dazu konnte gezeigt werden, dass HDAC-Inhibitoren in vielen *in vivo* und *in vitro* Modellen anti-inflammatorische Wirkung besitzen.

Die Ziele der vorliegenden Arbeit waren: I) Charakterisierung der Lungenepithelzelllinien A549 und BEAS-2B und der primären bronchialen Lungenepithelzellen MucilAir bezüglich ihrer pro-inflammatorischen Funktionalität *in vitro*; II) Ermittlung der iNOS-Expression und NO-Produktion in A549 Zellen und Untersuchung der anti-inflammatorischen Wirkung von iNOS-Inhibitoren in humanen Lungenepithelzellen; III) Identifizierung eines iNOS-exprimierenden und steroid-insensitiven Lungenepithelzell-Modells und Überprüfung der Hypothese zur iNOS-Beteiligung an der Steroidinsensitivität in diesem Zellmodell durch Modulation der

iNOS-Aktivität und der NO-Produktion in diesen Zellen; IV) Untersuchung des Zusammenhangs zwischen der Steroidsensitivität der Zytokinfreisetzung und der HDAC-Inhibition mit Hilfe unterschiedlich selektiver HDAC-Inhibitoren; V) Erforschung der funktionellen Effekte von HDAC-Inhibitoren in Lungenepithelzell-Modellen auf die Freisetzung sowie die mRNA-Expression inflammatorischen Zytokine und durch Bestimmung der Histon-Hyperacetylierung im IL-8 Promotorenbereich.

Erste Experimente zeigten, dass die Stimulation der Lungenepithelzellen mittels verschiedener Zytokine wie IL-1β und TNFα die mRNA-Expression und Freisetzung von vielen pro-inflammatorischen Zytokinen und Chemokinen induzierte, was eine wichtige Funktion der Lungenepithelzellen im Zusammenhang mit inflammatorischen Reaktionen der Lunge bestätigte.

In unseren früheren Studien in einem klinisch relevanten Zigarettenrauch-induziertem Maus-Modell der COPD, konnten wir zeigen, dass hochselektive iNOS-Inhibitoren sowohl die Rekrutierung inflammatorischen Zellen (Neutrophile, Makrophagen und T-Lymphozyten) als auch die Produktion pro-inflammatorischer Zytokine und Chemokine [MIP-1α, MCP-1 und KC (einem IL-8 Analog)] in der Lunge hemmen. Um nun die anti-inflammatorische Wirkung der iNOS-Inhibitoren *in vitro* näher zu bestimmen, wurde zunächst die iNOS mRNA-Expression und die NO-Produktion in zytokin-stimulierten A549 Zellen charakterisiert. Eine Kombination von IL-1β, TNFα und IFNγ (als Zytokin-Mix CM bezeichnet) konnte die iNOS mRNA-Expression und die NO-Produktion stark hochregulieren, wobei der Zusatz von dsRNA zu diesem Zytokin-Mix die iNOS-Induktion wesentlich verstärkte.

Im Folgenden wurden diese CM-stimulierten und iNOS-exprimierenden A549 Zellen als Zellmodell für die weitere Untersuchung der iNOS-Funktion in Inflammation und Steroid-Insensitivität benutzt. Dabei konnte gezeigt werden, dass die Freisetzung und mRNA-Expression von IL-8 durch den hochselektiven iNOS-Inhibitor BYK191023 gehemmt wurde. Dieser Effekt von iNOS-Inhibitoren auf die Freisetzung weiterer pro-inflammatorischen Zytokinen und Chemokinen konnte in der zytokin-stimulierten Zelllinie BEAS-2B und den primären Lungenepithelzellen MucilAir mittels Luminex Assay weiter bestätigt werden.

Im Anschluß wurde ein steroid-insensitives Zellmodel von CM-stimulierten A549 Zellen anhand der Freisetzung und mRNA-Expression von IL-8 etabliert und charakterisiert.

Mittels Luminex Assay wurde die Steroid-Insensitivität der Zytokin-Freisetzung in A549 Zellen bezüglich verschiedener Zytokine und Chemokine überprüft, wobei die Freisetzung von GM-CSF und IL-2R als steroid-insensitiv dargestellt werden konnte. Da dieses Zellmodell darüber hinaus sowohl eine iNOS-Expression als auch eine Reduktion der HDAC-Aktivität gegenüber oxidativen und nitrativen Stress zeigte, erfüllte es die Bedingungen für die Überprüfung der Hypothese der iNOS-Beteiligung an der durch HDAC-Aktivitätsreduktion verursachten Steroid-Insensitivität. Entgegen der Hypothese hatte jedoch die iNOS-Modulation durch iNOS-Inhibitoren keinen Einfluss auf die Steroid-Insensitivität. Außerdem beeinflusste weder eine iNOS-Überexpression noch der Zusatz des NO/$ONOO^-$ -Donors SIN-1 (mit/ohne H_2O_2) in IL-1β-stimulierten A549 Zellen die Steroid-Sensitivität der IL-8-Freisetzung. Daraufhin wurde die Steroid-Sensitivität von BEAS-2B und MucilAir Zellen unter ähnlichen Bedingungen wie in A549 Zellen analysiert. Dabei konnte eine Steroid-Insensitivität der IL-6, IL-8 und GM-CSF-Freisetzung in MucilAir Zellen, nicht aber in BEAS-2B Zellen gezeigt werden.

Schliesslich wurde der Zusammenhang zwischen einem steroid-vermittelten, anti-inflammatorischen Effekt auf die Zytokin-Freisetzung und der HDAC-Aktivität in zytokin-stimulierten Lungenepithelzellen untersucht. Wir konnten zeigen, dass die Steroid-Sensitivität der Zytokin-Freisetzung durch die Behandlung der Zellen mit verschiedenen HDAC-Inhibitoren nicht beeinflusst wurde. Dies deutet auf eine HDAC-unabhängige Wirkungsweise von Steroiden unter den verwendeten experimentellen Bedingungen hin.

Im Anschluss wurden funktionelle Effekte von HDAC-Inhibitoren auf zytokin-stimulierte Lungenepithelzellen untersucht. Hier konnten sowohl induzierende als auch inhibierende Wirkungsweisen auf die Freisetzung und mRNA-Expression verschiedener pro-inflammatorischer Zytokine und Chemokine gezeigt werden, wobei die Effekte abhängig vom verwendeten Zelltypus waren (primäre Zellen vs Zelllinien), sowie von den verwendeten HDAC-Inhibitoren und untersuchten Zielgenen. Letzteres würde ein promotor-spezifischer Wirkmechanismus erklären.

Andererseits konnten die inhibitorischen Effekte der HDAC-Inhibitoren SAHA und TSA auf die IL-1β-induzierte IL-8- und GM-CSF-Freisetzung nicht in jedem Fall mit einer Inhibition der jeweiligen mRNA-Expression korreliert werden, was auf differenzielle Wirkmechanismen für unterschiedliche Zytokine hindeutet.

Schlussfolgernd legt die vorliegende Arbeit dar, dass selektive iNOS-Inhibitoren anti-inflammatorische Effekte auf die Freisetzung von spezifischen Zytokinen und Chemokinen in humanen Lungenepithelzellen zeigen. Dies könnte zur Entwicklung von wirksamen iNOS-Inhibitoren zur Therapie von COPD beitragen. Andererseits konnte keine Beeinflussung der Steroid-Sensitivität der Freisetzung von pro-inflammatorischen Zytokinen durch iNOS und durch iNOS produziertes NO gezeigt werden, welche darüber hinaus auch unabhängig von einer HDAC-Inhibierung war. Im Gegensatz dazu führte eine HDAC-Inhibition sowohl zu anti- als auch zu pro-inflammatorischen Effekten auf die Freisetzung und mRNA-Expression von Zytokinen und Chemokinen, abhängig vom Zelltypus, HDAC-Inhibitor und untersuchtem Zielgen, was eine komplexe, nicht ausschliesslich transkriptionelle Regulation inflammatorischer Vorgänge durch Histondeacetylasen vermuten lässt.

8 List of tables and figures

8.1 List of Tables

8.2 List of Figures

9 References

Abdelaziz, M. M., J. L. Devalia, et al. (1995). "The effect of conditioned medium from cultured human bronchial epithelial cells on eosinophil and neutrophil chemotaxis and adherence in vitro." Am J Respir Cell Mol Biol 13(6): 728-37.

Adcock, I. M. (2003). "Glucocorticoids: new mechanisms and future agents." Curr Allergy Asthma Rep 3(3): 249-57.

Adcock, I. M. and P. J. Barnes (2008). "Molecular mechanisms of corticosteroid resistance." Chest 134(2): 394-401.

Adcock, I. M. and K. Ito (2005). "Glucocorticoid pathways in chronic obstructive pulmonary disease therapy." Proc Am Thorac Soc 2(4): 313-9; discussion 340-1.

Adenuga, D., H. Yao, et al. (2009). "Histone deacetylase 2 is phosphorylated, ubiquitinated, and degraded by cigarette smoke." Am J Respir Cell Mol Biol 40(4): 464-73.

Adler, K. B., N. J. Akley, et al. (1992). "Platelet-activating factor provokes release of mucin-like glycoproteins from guinea pig respiratory epithelial cells via a lipoxygenase-dependent mechanism." Am J Respir Cell Mol Biol 6(5): 550-6.

Agusti, A., M. Morla, et al. (2004). "NF-kappaB activation and iNOS upregulation in skeletal muscle of patients with COPD and low body weight." Thorax 59(6): 483-7.

Alderton, W. K., C. E. Cooper, et al. (2001). "Nitric oxide synthases: structure, function and inhibition." Biochem J 357(Pt 3): 593-615.

Alexopoulou, L., A. C. Holt, et al. (2001). "Recognition of double-stranded RNA and activation of NF-kappaB by Toll-like receptor 3." Nature 413(6857): 732-8.

Alvarez, B. and R. Radi (2003). "Peroxynitrite reactivity with amino acids and proteins." Amino Acids 25(3-4): 295-311.

Arendt, C. S. and M. Hochstrasser (1999). "Eukaryotic 20S proteasome catalytic subunit propeptides prevent active site inactivation by N-terminal acetylation and promote particle assembly." Embo J 18(13): 3575-85.

Baldwin, A. S., Jr. (1996). "The NF-kappa B and I kappa B proteins: new discoveries and insights." Annu Rev Immunol 14: 649-83.

Bamberger, C. M., H. M. Schulte, et al. (1996). "Molecular determinants of glucocorticoid receptor function and tissue sensitivity to glucocorticoids." Endocr Rev 17(3): 245-61.

Barnes, P. J. (1994). "Cytokines as mediators of chronic asthma." Am J Respir Crit Care Med 150(5 Pt 2): S42-9.

Barnes, P. J. (2006a). "How corticosteroids control inflammation: Quintiles Prize Lecture 2005." Br J Pharmacol 148(3): 245-54.

Barnes, P. J. (2006b). "Reduced histone deacetylase in COPD: clinical implications." Chest 129(1): 151-5.

Barnes, P. J. (2006c). "Transcription factors in airway diseases." Lab Invest 86(9): 867-72.

Barnes, P. J. (2007). "Chronic obstructive pulmonary disease: a growing but neglected global epidemic." PLoS Med 4(5): e112.

Barnes, P. J. (2008). "Role of HDAC2 in the Pathophysiology of COPD." Annu Rev Physiol.

Barnes, P. J. and I. M. Adcock (2009). "Glucocorticoid resistance in inflammatory diseases." Lancet 373(9678): 1905-17.

Barnes, P. J., K. Ito, et al. (2004). "Corticosteroid resistance in chronic obstructive pulmonary disease: inactivation of histone deacetylase." Lancet 363(9410): 731-3.

Barnes, P. J. and F. Y. Liew (1995). "Nitric oxide and asthmatic inflammation." Immunol Today 16(3): 128-30.

Beato, M. (1996). "Chromatin structure and the regulation of gene expression: remodeling at the MMTV promoter." J Mol Med 74(12): 711-24.

Becker, S., H. S. Koren, et al. (1993). "Interleukin-8 expression in normal nasal epithelium and its modulation by infection with respiratory syncytial virus and cytokines tumor necrosis factor, interleukin-1, and interleukin-6." Am J Respir Cell Mol Biol 8(1): 20-7.

Blanchard, F. and C. Chipoy (2005). "Histone deacetylase inhibitors: new drugs for the treatment of inflammatory diseases?" Drug Discov Today 10(3): 197-204.

Boehm, M., H. Hofmann, et al. (2007). "Suppression of TLR agonist mediated immune responses by HDAC inhibitors." AACR annual meeting.

Boer, R., W. R. Ulrich, et al. (2000). "The inhibitory potency and selectivity of arginine substrate site nitric-oxide synthase inhibitors is solely determined by their affinity toward the different isoenzymes." Mol Pharmacol 58(5): 1026-34.

Bolden, J. E., M. J. Peart, et al. (2006). "Anticancer activities of histone deacetylase inhibitors." Nat Rev Drug Discov 5(9): 769-84.

Bove, P. F. and A. van der Vliet (2006). "Nitric oxide and reactive nitrogen species in airway epithelial signaling and inflammation." Free Radic Biol Med 41(4): 515-27.

Bredt, D. S. and S. H. Snyder (1990). "Isolation of nitric oxide synthetase, a calmodulin-requiring enzyme." Proc Natl Acad Sci U S A 87(2): 682-5.

Briviba, K., I. Roussyn, et al. (1996). "Attenuation of oxidation and nitration reactions of peroxynitrite by selenomethionine, selenocystine and ebselen." Biochem J 319 (Pt 1): 13-5.

Brown, D. J., B. Lin, et al. (2004). "Elements of the nitric oxide pathway can degrade TIMP-1 and increase gelatinase activity." Mol Vis 10: 281-8.

Carta, S., S. Tassi, et al. (2006). "Histone deacetylase inhibitors prevent exocytosis of interleukin-1beta-containing secretory lysosomes: role of microtubules." Blood 108(5): 1618-26.

Chabane, N., N. Zayed, et al. (2008). "Histone deacetylase inhibitors suppress interleukin-1beta-induced nitric oxide and prostaglandin E2 production in human chondrocytes." Osteoarthritis Cartilage 16(10): 1267-74.

Chan-Yeung, M., R. Abboud, et al. (1988). "Peripheral leucocyte count and longitudinal decline in lung function." Thorax 43(6): 462-6.

Chaudhuri, R., E. Livingston, et al. (2006). "Effects of smoking cessation on lung function and airway inflammation in smokers with asthma." Am J Respir Crit Care Med 174(2): 127-33.

Church, D. F. and W. A. Pryor (1985). "Free-radical chemistry of cigarette smoke and its toxicological implications." Environ Health Perspect 64: 111-26.

Cohn, L. A. and K. B. Adler (1992). "Interactions between airway epithelium and mediators of inflammation." Exp Lung Res 18(3): 299-322.

Coleman, J. W. (2001). "Nitric oxide in immunity and inflammation." Int Immunopharmacol 1(8): 1397-406.

Cosio, B. G., L. Tsaprouni, et al. (2004). "Theophylline restores histone deacetylase activity and steroid responses in COPD macrophages." J Exp Med 200(5): 689-95.

Cronstein, B. N., S. C. Kimmel, et al. (1992). "A mechanism for the antiinflammatory effects of corticosteroids: the glucocorticoid receptor regulates leukocyte adhesion to endothelial cells and expression of endothelial-leukocyte adhesion molecule 1 and intercellular adhesion molecule 1." Proc Natl Acad Sci U S A 89(21): 9991-5.

Cross, R. K. and K. T. Wilson (2003). "Nitric oxide in inflammatory bowel disease." Inflamm Bowel Dis 9(3): 179-89.

Davis, K. L., E. Martin, et al. (2001). "Novel effects of nitric oxide." Annu Rev Pharmacol Toxicol 41: 203-36.

Della Ragione, F., V. Criniti, et al. (2001). "Genes modulated by histone acetylation as new effectors of butyrate activity." FEBS Lett 499(3): 199-204.

Di Rosa, M., M. Radomski, et al. (1990). "Glucocorticoids inhibit the induction of nitric oxide synthase in macrophages." Biochem Biophys Res Commun 172(3): 1246-52.

Diks, S. H., D. J. Richel, et al. (2004). "LPS signal transduction: the picture is becoming more complex." Curr Top Med Chem 4(11): 1115-26.

Dinarello, C. A. (2006). "Inhibitors of histone deacetylases as anti-inflammatory drugs." Ernst Schering Res Found Workshop(56): 45-60.

Donnelly, L. E. and P. J. Barnes (2002). "Expression and regulation of inducible nitric oxide synthase from human primary airway epithelial cells." Am J Respir Cell Mol Biol 26(1): 144-51.

Durrin, L. K., R. K. Mann, et al. (1991). "Yeast histone H4 N-terminal sequence is required for promoter activation in vivo." Cell 65(6): 1023-31.

Feelisch, M., J. Ostrowski, et al. (1989). "On the mechanism of NO release from sydnonimines." J Cardiovasc Pharmacol 14 Suppl 11: S13-22.

Forstermann, U., J. P. Boissel, et al. (1998). "Expressional control of the 'constitutive' isoforms of nitric oxide synthase (NOS I and NOS III)." Faseb J 12(10): 773-90.

Forstermann, U. and H. Kleinert (1995). "Nitric oxide synthase: expression and expressional control of the three isoforms." Naunyn Schmiedebergs Arch Pharmacol 352(4): 351-64.

Fujii, T., S. Hayashi, et al. (2002). "Interaction of alveolar macrophages and airway epithelial cells following exposure to particulate matter produces mediators that stimulate the bone marrow." Am J Respir Cell Mol Biol 27(1): 34-41.

Fujii, T., S. Hayashi, et al. (2001). "Particulate matter induces cytokine expression in human bronchial epithelial cells." Am J Respir Cell Mol Biol 25(3): 265-71.

Garg, A. K. and B. B. Aggarwal (2002). "Reactive oxygen intermediates in TNF signaling." Mol Immunol 39(9): 509-17.

Garvey, E. P., J. A. Oplinger, et al. (1997). "1400W is a slow, tight binding, and highly selective inhibitor of inducible nitric-oxide synthase in vitro and in vivo." J Biol Chem 272(8): 4959-63.

Garvey, E. P., J. A. Oplinger, et al. (1994). "Potent and selective inhibition of human nitric oxide synthases. Inhibition by non-amino acid isothioureas." J Biol Chem 269(43): 26669-76.

Glaser, K. B., M. J. Staver, et al. (2003). "Gene expression profiling of multiple histone deacetylase (HDAC) inhibitors: defining a common gene set produced by HDAC inhibition in T24 and MDA carcinoma cell lines." Mol Cancer Ther 2(2): 151-63.

Gray, S. G. and F. Dangond (2006). "Rationale for the use of histone deacetylase inhibitors as a dual therapeutic modality in multiple sclerosis." Epigenetics 1(2): 67-75.

Gronroos, E., U. Hellman, et al. (2002). "Control of Smad7 stability by competition between acetylation and ubiquitination." Mol Cell 10(3): 483-93.

Grozinger, C. M. and S. L. Schreiber (2002). "Deacetylase enzymes: biological functions and the use of small-molecule inhibitors." Chem Biol 9(1): 3-16.

Guo, F. H., H. R. De Raeve, et al. (1995). "Continuous nitric oxide synthesis by inducible nitric oxide synthase in normal human airway epithelium in vivo." Proc Natl Acad Sci U S A 92(17): 7809-13.

Guo, F. H., K. Uetani, et al. (1997). "Interferon gamma and interleukin 4 stimulate prolonged expression of inducible nitric oxide synthase in human airway epithelium through synthesis of soluble mediators." J Clin Invest 100(4): 829-38.

Haddad, I. Y., G. Pataki, et al. (1994). "Quantitation of nitrotyrosine levels in lung sections of patients and animals with acute lung injury." J Clin Invest 94(6): 2407-13.

Halliwell, B. and J. M. Gutteridge (1990). "Role of free radicals and catalytic metal ions in human disease: an overview." Methods Enzymol 186: 1-85.

Hammad, H., M. Chieppa, et al. (2009). "House dust mite allergen induces asthma via Toll-like receptor 4 triggering of airway structural cells." 15(4): 410-416.

Heid, C. A., J. Stevens, et al. (1996). "Real time quantitative PCR." Genome Res 6(10): 986-94.

Hellermann, G. R., S. B. Nagy, et al. (2002). "Mechanism of cigarette smoke condensate-induced acute inflammatory response in human bronchial epithelial cells." Respir Res 3: 22.

Heltweg, B., F. Dequiedt, et al. (2004). "Subtype Selective Substrates for Histone Deacetylases." Journal of Medicinal Chemistry 47(21): 5235-5243.

Hesslinger, C., M. D. Lehner, et al. (2008). "The highly selective iNOS inhibitor BYK402750 exerts potent anti-inflammatory effects in a mouse model of cigarette smoke-induced inflammation." Nitric Oxide 19(35).

Hesslinger, C., Strub, A., Boer, R., Ulrich, w. R., Lehner, M. D. and Braun, C. (2009). "Inhibition of inducible nitric oxide synthase in respiratory diseases." Biochemical Society Transactions 37(4).

Hibbs, J. B., Jr., R. R. Taintor, et al. (1988). "Nitric oxide: a cytotoxic activated macrophage effector molecule." Biochem Biophys Res Commun 157(1): 87-94.

Hildmann, C., D. Riester, et al. (2007). "Histone deacetylases--an important class of cellular regulators with a variety of functions." Appl Microbiol Biotechnol 75(3): 487-97.

Hoffmann, E., A. Thiefes, et al. (2005). "MEK1-dependent delayed expression of Fos-related antigen-1 counteracts c-Fos and p65 NF-kappaB-mediated interleukin-8 transcription in response to cytokines or growth factors." J Biol Chem 280(10): 9706-18.

Hogg, J. C., F. Chu, et al. (2004). "The nature of small-airway obstruction in chronic obstructive pulmonary disease." N Engl J Med 350(26): 2645-53.

Hogg, J. C. and W. Timens (2008). "The Pathology of Chronic Obstructive Pulmonary Disease." Annu Rev Pathol.

Hogg, J. C., J. L. Wright, et al. (1994). "Lung structure and function in cigarette smokers." Thorax 49(5): 473-8.

Hogg, N., V. M. Darley-Usmar, et al. (1992). "Production of hydroxyl radicals from the simultaneous generation of superoxide and nitric oxide." Biochem J 281 (Pt 2): 419-24.

Hong, L., G. P. Schroth, et al. (1993). "Studies of the DNA binding properties of histone H4 amino terminus. Thermal denaturation studies reveal that acetylation markedly reduces the binding constant of the H4 "tail" to DNA." J Biol Chem 268(1): 305-14.

Hoshimoto, A., Y. Suzuki, et al. (2002). "Caprylic acid and medium-chain triglycerides inhibit IL-8 gene transcription in Caco-2 cells: comparison with the potent histone deacetylase inhibitor trichostatin A." Br J Pharmacol 136(2): 280-6.

Huie, R. E. and S. Padmaja (1993). "The reaction of no with superoxide." Free Radic Res Commun 18(4): 195-9.

Hurley, J. H., A. M. Dean, et al. (1990). "Regulation of an enzyme by phosphorylation at the active site." Science 249(4972): 1012-6.

Ichinose, M., H. Sugiura, et al. (2000). "Increase in reactive nitrogen species production in chronic obstructive pulmonary disease airways." Am J Respir Crit Care Med 162(2 Pt 1): 701-6.

Ignarro, L. J., G. Cirino, et al. (1999). "Nitric oxide as a signaling molecule in the vascular system: an overview." J Cardiovasc Pharmacol 34(6): 879-86.

Imre, G., V. Gekeler, et al. (2006). "Histone deacetylase inhibitors suppress the inducibility of nuclear factor-kappaB by tumor necrosis factor-alpha receptor-1 down-regulation." Cancer Res 66(10): 5409-18.

Ischiropoulos, H. (2009). "Protein tyrosine nitration--an update." Arch Biochem Biophys 484(2): 117-21.

Ischiropoulos, H., L. Zhu, et al. (1992). "Peroxynitrite-mediated tyrosine nitration catalyzed by superoxide dismutase." Arch Biochem Biophys 298(2): 431-7.

Ito, K., P. J. Barnes, et al. (2000). "Glucocorticoid receptor recruitment of histone deacetylase 2 inhibits interleukin-1beta-induced histone H4 acetylation on lysines 8 and 12." Mol Cell Biol 20(18): 6891-903.

Ito, K., K. F. Chung, et al. (2006a). "Update on glucocorticoid action and resistance." J Allergy Clin Immunol 117(3): 522-43.

Ito, K., T. Hanazawa, et al. (2004). "Oxidative stress reduces histone deacetylase 2 activity and enhances IL-8 gene expression: role of tyrosine nitration." Biochem Biophys Res Commun 315(1): 240-5.

Ito, K., M. Ito, et al. (2005). "Decreased histone deacetylase activity in chronic obstructive pulmonary disease." N Engl J Med 352(19): 1967-76.

Ito, K., S. Lim, et al. (2001). "Cigarette smoking reduces histone deacetylase 2 expression, enhances cytokine expression, and inhibits glucocorticoid actions in alveolar macrophages." Faseb J 15(6): 1110-2.

Ito, K., S. Lim, et al. (2002). "A molecular mechanism of action of theophylline: Induction of histone deacetylase activity to decrease inflammatory gene expression." Proc Natl Acad Sci U S A 99(13): 8921-6.

Ito, K., S. Yamamura, et al. (2006b). "Histone deacetylase 2-mediated deacetylation of the glucocorticoid receptor enables NF-kappaB suppression." J Exp Med 203(1): 7-13.

Iwata, K., K. Tomita, et al. (2002). "Trichostatin A, a histone deacetylase inhibitor, down-regulates interleukin-12 transcription in SV-40-transformed lung epithelial cells." Cell Immunol 218(1-2): 26-33.

Jung, J. S., M. Y. Park, et al. (2000). "Protection against Hydrogen Peroxide Induced Injury in Renal Proximal Tubule Cell Lines by Inhibition of Poly(ADP--Ribose) Synthase." Kidney and Blood Pressure Research 23(1): 14-19.

Kamosinska, B., M. W. Radomski, et al. (1997). "Nitric oxide activates chloride currents in human lung epithelial cells." Am J Physiol Lung Cell Mol Physiol 272(6): L1098-1104.

Kent, L., L. Smyth, et al. (2008). "Cigarette smoke extract induced cytokine and chemokine gene expression changes in COPD macrophages." Cytokine 42(2): 205-16.

Khair, O. A., R. J. Davies, et al. (1996). "Bacterial-induced release of inflammatory mediators by bronchial epithelial cells." Eur Respir J 9(9): 1913-22.

Klampfer, L., J. Huang, et al. (2003). "Inhibition of interferon gamma signaling by the short chain fatty acid butyrate." Mol Cancer Res 1(11): 855-62.

Klampfer, L., J. Huang, et al. (2004). "Requirement of histone deacetylase activity for signaling by STAT1." J Biol Chem 279(29): 30358-68.

Kleinert, H., C. Euchenhofer, et al. (1996). "Glucocorticoids inhibit the induction of nitric oxide synthase II by down-regulating cytokine-induced activity of transcription factor nuclear factor-kappa B." Mol Pharmacol 49(1): 15-21.

Kleinert, H., A. Pautz, et al. (2004). "Regulation of the expression of inducible nitric oxide synthase." Eur J Pharmacol 500(1-3): 255-66.

Kleinert, H., T. Wallerath, et al. (1998). "Cytokine induction of NO synthase II in human DLD-1 cells: roles of the JAK-STAT, AP-1 and NF-kappaB-signaling pathways." Br J Pharmacol 125(1): 193-201.

Kong, S. K., M. B. Yim, et al. (1996). "Peroxynitrite disables the tyrosine phosphorylation regulatory mechanism: Lymphocyte-specific tyrosine kinase fails to phosphorylate nitrated cdc2(6-20)NH2 peptide." Proc Natl Acad Sci U S A 93(8): 3377-82.

Kouzarides, T. (1999). "Histone acetylases and deacetylases in cell proliferation." Curr Opin Genet Dev 9(1): 40-8.

Kraft, M., I. Striz, et al. (1998). "Expression of epithelial markers in nocturnal asthma." J Allergy Clin Immunol 102(3): 376-81.

Kroncke, K. D., K. Fehsel, et al. (1998). "Inducible nitric oxide synthase in human diseases." Clin Exp Immunol 113(2): 147-56.

Kuo, H. P., K. H. Hwang, et al. (1997). "Effect of endogenous nitric oxide on tumour necrosis factor-alpha-induced leukosequestration and IL-8 release in guinea-pigs airways in vivo." Br J Pharmacol 122(1): 103-11.

Kurdistani, S. K., S. Tavazoie, et al. (2004). "Mapping global histone acetylation patterns to gene expression." Cell 117(6): 721-33.

Laan, M., S. Bozinovski, et al. (2004). "Cigarette smoke inhibits lipopolysaccharide-induced production of inflammatory cytokines by suppressing the activation of activator protein-1 in bronchial epithelial cells." J Immunol 173(6): 4164-70.

Lannan, S., K. Donaldson, et al. (1994). "Effect of cigarette smoke and its condensates on alveolar epithelial cell injury in vitro." Am J Physiol 266(1 Pt 1): L92-100.

Lasa, M., M. Brook, et al. (2001). "Dexamethasone destabilizes cyclooxygenase 2 mRNA by inhibiting mitogen-activated protein kinase p38." Mol Cell Biol 21(3): 771-80.

Leoni, F., G. Fossati, et al. (2005). "The histone deacetylase inhibitor ITF2357 reduces production of pro-inflammatory cytokines in vitro and systemic inflammation in vivo." Mol Med 11(1-12): 1-15.

Leoni, F., A. Zaliani, et al. (2002). "The antitumor histone deacetylase inhibitor suberoylanilide hydroxamic acid exhibits antiinflammatory properties via suppression of cytokines
10.1073/pnas.052702999." Proceedings of the National Academy of Sciences: 052702999.

Leung, D. Y., R. J. Martin, et al. (1995). "Dysregulation of interleukin 4, interleukin 5, and interferon gamma gene expression in steroid-resistant asthma." J Exp Med 181(1): 33-40.

Lorsbach, R. B., W. J. Murphy, et al. (1993). "Expression of the nitric oxide synthase gene in mouse macrophages activated for tumor cell killing. Molecular basis for the synergy between interferon-gamma and lipopolysaccharide." J Biol Chem 268(3): 1908-13.

Luger, K., A. W. Mader, et al. (1997). "Crystal structure of the nucleosome core particle at 2.8 A resolution." Nature 389(6648): 251-60.

MacRedmond, R., C. Greene, et al. (2005). "Respiratory epithelial cells require Toll-like receptor 4 for induction of human beta-defensin 2 by lipopolysaccharide." Respir Res 6: 116.

Maestrelli, P., P. G. Calcagni, et al. (1996). "Integrin upregulation on sputum neutrophils in smokers with chronic airway obstruction." Am J Respir Crit Care Med 154(5): 1296-300.

Maestrelli, P., C. Paska, et al. (2003). "Decreased haem oxygenase-1 and increased inducible nitric oxide synthase in the lung of severe COPD patients." Eur Respir J 21(6): 971-6.

Mann, R. K. and M. Grunstein (1992). "Histone H3 N-terminal mutations allow hyperactivation of the yeast GAL1 gene in vivo." Embo J 11(9): 3297-306.

Mannino, D. M. and A. S. Buist (2007). "Global burden of COPD: risk factors, prevalence, and future trends." Lancet 370(9589): 765-73.

Marletta, M. A., A. R. Hurshman, et al. (1998). "Catalysis by nitric oxide synthase." Curr Opin Chem Biol 2(5): 656-63.

Martin, L. D., L. G. Rochelle, et al. (1997). "Airway epithelium as an effector of inflammation: molecular regulation of secondary mediators." Eur Respir J 10(9): 2139-46.

Marwick, J. A., G. Caramori, et al. (2009). "Inhibition of PI3Kdelta restores glucocorticoid function in smoking-induced airway inflammation in mice." Am J Respir Crit Care Med 179(7): 542-8.

Marwick, J. A., P. A. Kirkham, et al. (2004). "Cigarette smoke alters chromatin remodeling and induces proinflammatory genes in rat lungs." Am J Respir Cell Mol Biol 31(6): 633-42.

Meja, K. K., S. Rajendrasozhan, et al. (2008). "Curcumin restores corticosteroid function in monocytes exposed to oxidants by maintaining HDAC2." Am J Respir Cell Mol Biol 39(3): 312-23.

Migita, K., Y. Maeda, et al. (2005). "Peroxynitrite-mediated matrix metalloproteinase-2 activation in human hepatic stellate cells." FEBS Lett 579(14): 3119-25.

Miller, T. A., D. J. Witter, et al. (2003). "Histone deacetylase inhibitors." J Med Chem 46(24): 5097-116.

Minucci, S. and P. G. Pelicci (2006). "Histone deacetylase inhibitors and the promise of epigenetic (and more) treatments for cancer." Nat Rev Cancer 6(1): 38-51.

Mio, T., D. J. Romberger, et al. (1997). "Cigarette smoke induces interleukin-8 release from human bronchial epithelial cells." Am J Respir Crit Care Med 155(5): 1770-6.

Mishra, N., C. M. Reilly, et al. (2003). "Histone deacetylase inhibitors modulate renal disease in the MRL-lpr/lpr mouse." J Clin Invest 111(4): 539-52.

Mollace, V., C. Muscoli, et al. (2005). "Modulation of prostaglandin biosynthesis by nitric oxide and nitric oxide donors." Pharmacol Rev 57(2): 217-52.

Moncada, S., R. M. Palmer, et al. (1991). "Nitric oxide: physiology, pathophysiology, and pharmacology." Pharmacol Rev 43(2): 109-42.

Monick, M. M., T. O. Yarovinsky, et al. (2003). "Respiratory syncytial virus up-regulates TLR4 and sensitizes airway epithelial cells to endotoxin." J Biol Chem 278(52): 53035-44.

Mukae, H., J. C. Hogg, et al. (2000). "Phagocytosis of particulate air pollutants by human alveolar macrophages stimulates the bone marrow." Am J Physiol Lung Cell Mol Physiol 279(5): L924-31.

Mukaida, N., M. Morita, et al. (1994). "Novel mechanism of glucocorticoid-mediated gene repression. Nuclear factor-kappa B is target for glucocorticoid-mediated interleukin 8 gene repression." J Biol Chem 269(18): 13289-95.

Nakane, M., V. Klinghofer, et al. (1995). "Novel potent and selective inhibitors of inducible nitric oxide synthase." Mol Pharmacol 47(4): 831-4.

Nathan, C. (1992). "Nitric oxide as a secretory product of mammalian cells." Faseb J 6(12): 3051-64.

Nathan, C. (1997). "Inducible nitric oxide synthase: what difference does it make?" J Clin Invest 100(10): 2417-23.

Nusinzon, I. and C. M. Horvath (2006). "Positive and negative regulation of the innate antiviral response and beta interferon gene expression by deacetylation." Mol Cell Biol 26(8): 3106-13.

Ohtsuka, M., F. Konno, et al. (2002). "PPA250 [3-(2,4-difluorophenyl)-6-[2-[4-(1H-imidazol-1-ylmethyl) phenoxy]ethoxy]-2-phenylpyridine], a novel orally effective inhibitor of the dimerization of inducible nitric-oxide synthase, exhibits an anti-inflammatory effect in animal models of chronic arthritis." J Pharmacol Exp Ther 303(1): 52-7.

Osoata, G. O., T. Hanazawa, et al. (2009a). "Peroxynitrite elevation in exhaled breath condensate of COPD and its inhibition by fudosteine." Chest 135(6): 1513-20.

Osoata, G. O., S. Yamamura, et al. (2009b). "Nitration of distinct tyrosine residues causes inactivation of histone deacetylase 2." Biochem Biophys Res Commun.

Pauwels, R. A., A. S. Buist, et al. (2001). "Global strategy for the diagnosis, management, and prevention of chronic obstructive pulmonary disease. NHLBI/WHO Global Initiative for Chronic Obstructive Lung Disease (GOLD) Workshop summary." Am J Respir Crit Care Med 163(5): 1256-76.

Pechkovsky, D. V., G. Zissel, et al. (2002). "Pattern of NOS2 and NOS3 mRNA expression in human A549 cells and primary cultured AEC II." Am J Physiol Lung Cell Mol Physiol 282(4): L684-92.

Perry, M. and R. Chalkley (1982). "Histone acetylation increases the solubility of chromatin and occurs sequentially over most of the chromatin. A novel model for the biological role of histone acetylation." J Biol Chem 257(13): 7336-47.

Petros, A., G. Lamb, et al. (1994). "Effects of a nitric oxide synthase inhibitor in humans with septic shock." Cardiovasc Res 28(1): 34-9.

Pettersen, C. A. and K. B. Adler (2002). "Airways inflammation and COPD: epithelial-neutrophil interactions." Chest 121(5 Suppl): 142S-150S.

Poli, G., G. Leonarduzzi, et al. (2004). "Oxidative stress and cell signalling." Curr Med Chem 11(9): 1163-82.

Pryor, W. A. and K. Stone (1993). "Oxidants in cigarette smoke. Radicals, hydrogen peroxide, peroxynitrate, and peroxynitrite." Ann N Y Acad Sci 686: 12-27; discussion 27-8.

Qiagen (2002). "SuperFect Transfection Reagent Handbook."

Radi, R., J. S. Beckman, et al. (1991a). "Peroxynitrite oxidation of sulfhydryls. The cytotoxic potential of superoxide and nitric oxide." J Biol Chem 266(7): 4244-50.

Radi, R., J. S. Beckman, et al. (1991b). "Peroxynitrite-induced membrane lipid peroxidation: the cytotoxic potential of superoxide and nitric oxide." Arch Biochem Biophys 288(2): 481-7.

Radi, R., M. Rodriguez, et al. (1994). "Inhibition of mitochondrial electron transport by peroxynitrite." Arch Biochem Biophys 308(1): 89-95.

Rahman, I. and I. M. Adcock (2006). "Oxidative stress and redox regulation of lung inflammation in COPD." Eur Respir J 28(1): 219-42.

Rees, D. D., R. M. Palmer, et al. (1989). "Role of endothelium-derived nitric oxide in the regulation of blood pressure." Proc Natl Acad Sci U S A 86(9): 3375-8.

Reiter, C. D., R. J. Teng, et al. (2000). "Superoxide reacts with nitric oxide to nitrate tyrosine at physiological pH via peroxynitrite." J Biol Chem 275(42): 32460-6.

Remacle, J., M. Raes, et al. (1995). "Low levels of reactive oxygen species as modulators of cell function." Mutat Res 316(3): 103-22.

Retamales, I., W. M. Elliott, et al. (2001). "Amplification of inflammation in emphysema and its association with latent adenoviral infection." Am J Respir Crit Care Med 164(3): 469-73.

Ricciardolo, F. L., G. Caramori, et al. (2005). "Nitrosative stress in the bronchial mucosa of severe chronic obstructive pulmonary disease." J Allergy Clin Immunol 116(5): 1028-35.

Riffo-Vasquez, Y., S. Pitchford, et al. (2000). "Cytokines in airway inflammation." Int J Biochem Cell Biol 32(8): 833-53.

Robbins, R. A., K. J. Nelson, et al. (1991). "Complement activation by cigarette smoke." Am J Physiol 260(4 Pt 1): L254-9.

Robinson-Rechavi, M., A. S. Carpentier, et al. (2001). "How many nuclear hormone receptors are there in the human genome?" Trends Genet 17(10): 554-6.

Rochelle, L. G., B. M. Fischer, et al. (1998). "Concurrent production of reactive oxygen and nitrogen species by airway epithelial cells in vitro." Free Radic Biol Med 24(5): 863-8.

Rudd, B. D., E. Burstein, et al. (2005). "Differential role for TLR3 in respiratory syncytial virus-induced chemokine expression." J Virol 79(6): 3350-7.

Sakamoto, S., R. Potla, et al. (2004). "Histone deacetylase activity is required to recruit RNA polymerase II to the promoters of selected interferon-stimulated early response genes." J Biol Chem 279(39): 40362-7.

Sauty, A., M. Dziejman, et al. (1999). "The T cell-specific CXC chemokines IP-10, Mig, and I-TAC are expressed by activated human bronchial epithelial cells." J Immunol 162(6): 3549-58.

Schmeck, B., J. Lorenz, et al. (2008). "Histone acetylation and flagellin are essential for Legionella pneumophila-induced cytokine expression." J Immunol 181(2): 940-7.

Sengupta, N. and E. Seto (2004). "Regulation of histone deacetylase activities." J Cell Biochem 93(1): 57-67.

Senior, R. M., G. L. Griffin, et al. (1980). "Chemotactic activity of elastin-derived peptides." J Clin Invest 66(4): 859-62.

Singh, D., D. Richards, et al. (2007). "Selective inducible nitric oxide synthase inhibition has no effect on allergen challenge in asthma." Am J Respir Crit Care Med 176(10): 988-93.

Spange, S., T. Wagner, et al. (2009). "Acetylation of non-histone proteins modulates cellular signalling at multiple levels." Int J Biochem Cell Biol 41(1): 185-98.

Standiford, T. J., S. L. Kunkel, et al. (1990). "Interleukin-8 gene expression by a pulmonary epithelial cell line. A model for cytokine networks in the lung." J Clin Invest 86(6): 1945-53.

Strahl, B. D. and C. D. Allis (2000). "The language of covalent histone modifications." Nature 403(6765): 41-5.

Strub, A., W. R. Ulrich, et al. (2006). "The novel imidazopyridine 2-[2-(4-methoxy-pyridin-2-yl)-ethyl]-3H-imidazo[4,5-b]pyridine (BYK191023) is a highly selective inhibitor of the inducible nitric-oxide synthase." Mol Pharmacol 69(1): 328-37.

Struhl, K. (1998). "Histone acetylation and transcriptional regulatory mechanisms." Genes Dev 12(5): 599-606.

Stuehr, D., S. Pou, et al. (2001). "Oxygen reduction by nitric-oxide synthases." J Biol Chem 276(18): 14533-6.

Suuronen, T., J. Huuskonen, et al. (2006). "Characterization of the pro-inflammatory signaling induced by protein acetylation in microglia." Neurochem Int 49(6): 610-8.

Szabo, C. (1996). "DNA strand breakage and activation of poly-ADP ribosyltransferase: a cytotoxic pathway triggered by peroxynitrite." Free Radic Biol Med 21(6): 855-69.

Takizawa, H. (1998). "Airway epithelial cells as regulators of airway inflammation (Review)." Int J Mol Med 1(2): 367-78.

Titheradge, M. A. (1999). "Nitric oxide in septic shock." Biochim Biophys Acta 1411(2-3): 437-55.

Uetani, K., M. E. Arroliga, et al. (2001). "Double-stranded rna dependence of nitric oxide synthase 2 expression in human bronchial epithelial cell lines BET-1A and BEAS-2B." Am J Respir Cell Mol Biol 24(6): 720-6.

Vallance, P. and J. Leiper (2002). "Blocking NO synthesis: how, where and why?" Nat Rev Drug Discov 1(12): 939-50.

van Eeden, S. F. and J. C. Hogg (2000). "The response of human bone marrow to chronic cigarette smoking." Eur Respir J 15(5): 915-21.

Virag, L., E. Szabo, et al. (2003). "Peroxynitrite-induced cytotoxicity: mechanism and opportunities for intervention." Toxicol Lett 140-141: 113-24.

Walkinshaw, D. R., S. Tahmasebi, et al. (2008). "Histone deacetylases as transducers and targets of nuclear signaling." J Cell Biochem 104(5): 1541-52.

Walters, M. J., M. J. Paul-Clark, et al. (2005). "Cigarette smoke activates human monocytes by an oxidant-AP-1 signaling pathway: implications for steroid resistance." Mol Pharmacol 68(5): 1343-53.

Wegener, D., F. Wirsching, et al. (2003). "A fluorogenic histone deacetylase assay well suited for high-throughput activity screening." Chem Biol 10(1): 61-8.

Wei, X. M., H. S. Kim, et al. (2005). "Effects of cigarette smoke on degranulation and NO production by mast cells and epithelial cells." Respir Res 6: 108.

Weiss, S. T., M. R. Segal, et al. (1995). "Relation of FEV1 and peripheral blood leukocyte count to total mortality. The Normative Aging Study." Am J Epidemiol 142(5): 493-8; discussion 499-503.

Werner, E. R., A. C. Gorren, et al. (2003). "Tetrahydrobiopterin and nitric oxide: mechanistic and pharmacological aspects." Exp Biol Med (Maywood) 228(11): 1291-302.

Wetzler, C., H. Kampfer, et al. (2000). "Keratinocyte-derived chemotactic cytokines: expressional modulation by nitric oxide in vitro and during cutaneous wound repair in vivo." Biochem Biophys Res Commun 274(3): 689-96.

Wink, D. A. and J. B. Mitchell (1998). "Chemical biology of nitric oxide: Insights into regulatory, cytotoxic, and cytoprotective mechanisms of nitric oxide." Free Radic Biol Med 25(4-5): 434-56.

Wolffe, A. P. (1997). "Transcriptional control. Sinful repression." Nature 387(6628): 16-7.

Wolffe, A. P. and J. J. Hayes (1999). "Chromatin disruption and modification." Nucleic Acids Res 27(3): 711-20.

Workman, J. L. and A. R. Buchman (1993). "Multiple functions of nucleosomes and regulatory factors in transcription." Trends Biochem Sci 18(3): 90-5.

Wright, J. L., L. M. Lawson, et al. (1984). "The detection of small airways disease." Am Rev Respir Dis 129(6): 989-94.

Wu, R. S., H. T. Panusz, et al. (1986). "Histones and their modifications." CRC Crit Rev Biochem 20(2): 201-63.

Xu, W., S. Zheng, et al. (2006). "Role of epithelial nitric oxide in airway viral infection." Free Radic Biol Med 41(1): 19-28.

Xu, W. S., R. B. Parmigiani, et al. (2007). "Histone deacetylase inhibitors: molecular mechanisms of action." Oncogene 26(37): 5541-52.

Yang, S. R., A. S. Chida, et al. (2006). "Cigarette smoke induces proinflammatory cytokine release by activation of NF-kappaB and posttranslational modifications of histone deacetylase in macrophages." Am J Physiol Lung Cell Mol Physiol 291(1): L46-57.

Zang, L. Y., K. Stone, et al. (1995). "Detection of free radicals in aqueous extracts of cigarette tar by electron spin resonance." Free Radic Biol Med 19(2): 161-7.

Zhang, Z., R. Liu, et al. (2005). "Interaction of airway epithelial cells (A549) with spores and mycelium of Aspergillus fumigatus." J Infect 51(5): 375-82.

10 Supplement

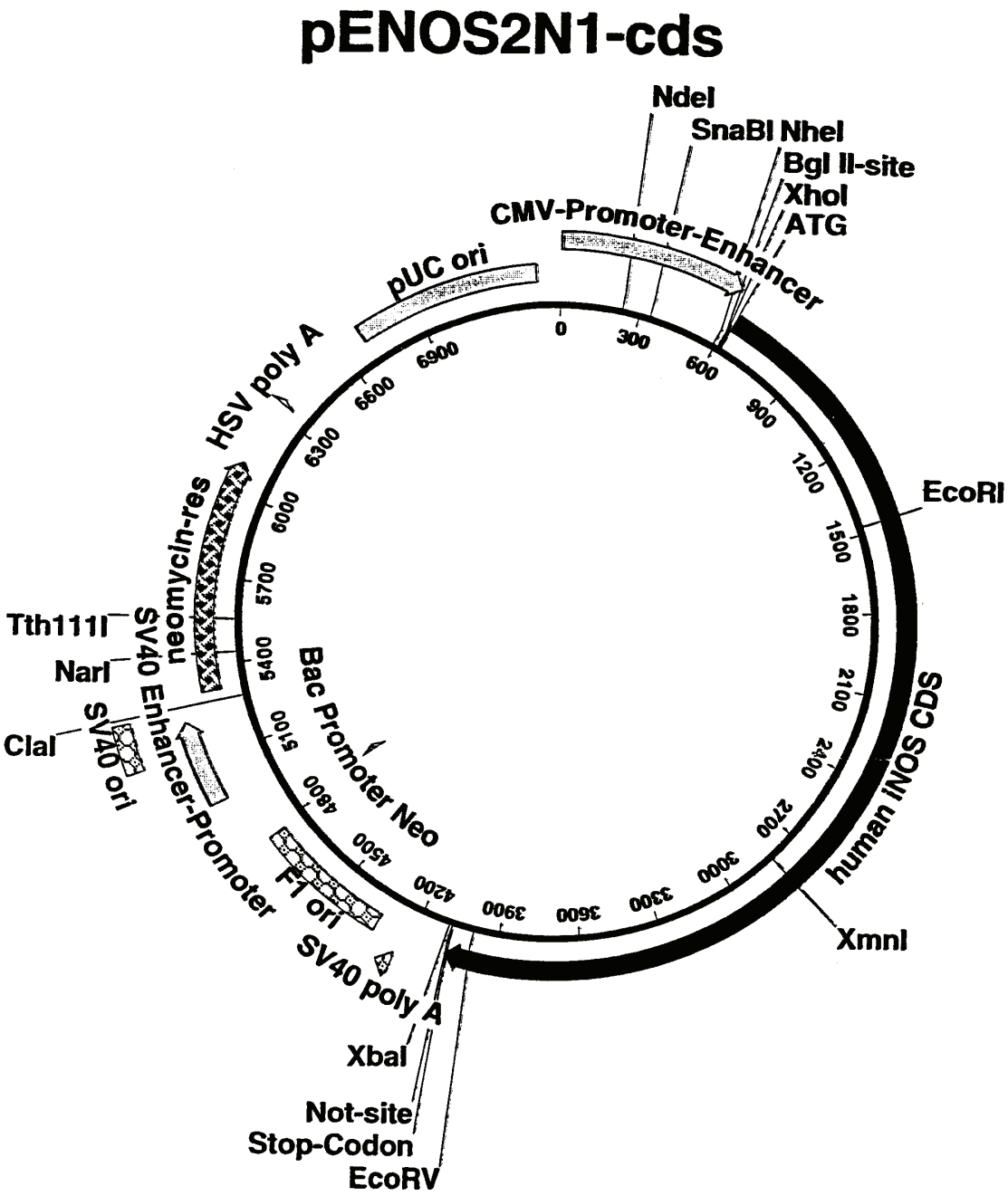

pEGFP-N1

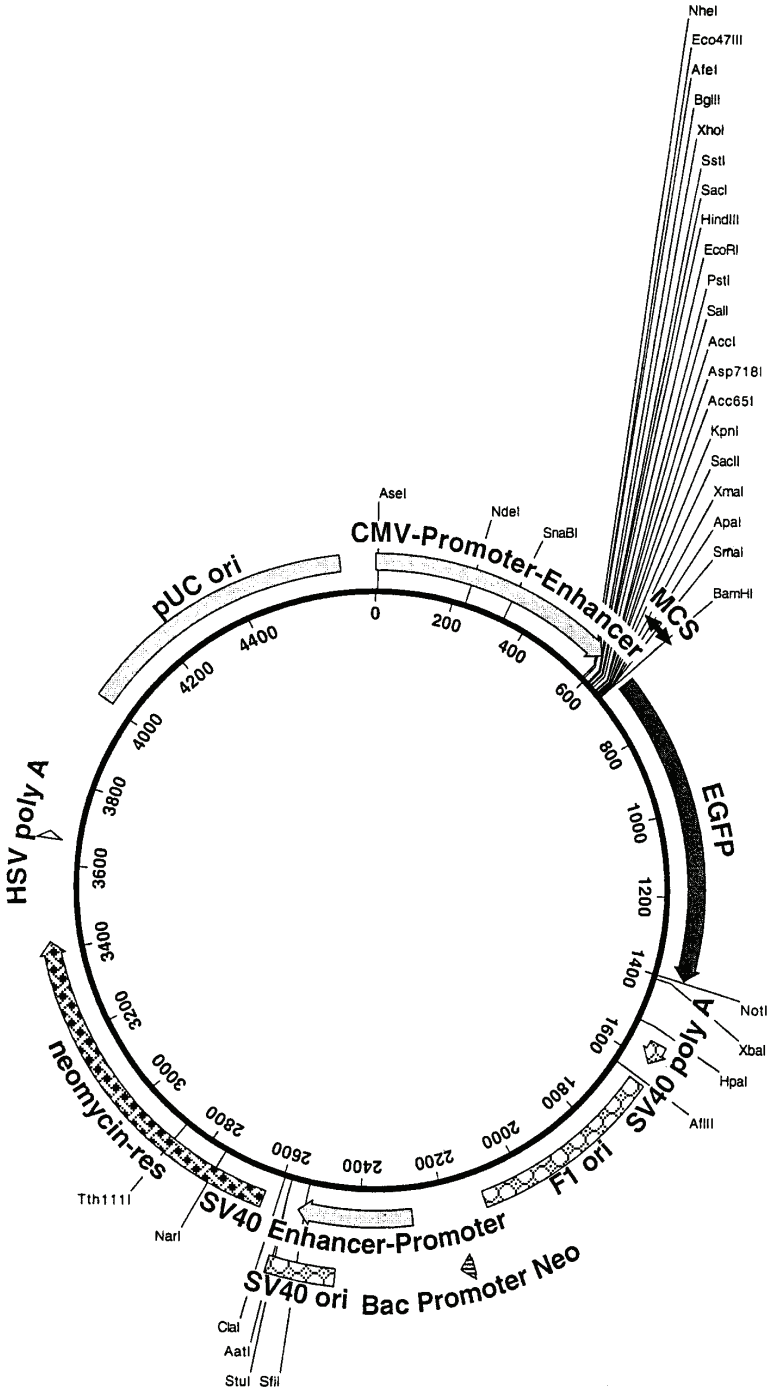
NheI
Eco47III
AfeI
BglII
XhoI
SstI
SacI
HindIII
EcoRI
PstI
SalI
AccI
Asp718I
Acc65I
KpnI
SacII
XmaI
ApaI
SmaI
BamHI
MCS
AseI
NdeI
SnaBI
CMV-Promoter-Enhancer
pUC ori
EGFP
HSV poly A
SV40 poly A
NotI
XbaI
HpaI
AflII
F1 ori
neomycin-res
Tth111I
NarI
SV40 Enhancer-Promoter
SV40 ori
Bac Promoter Neo
ClaI
AatI
StuI
SfiI
0
200
400
600
800
1000
1200
1400
1600
1800
2000
2200
2400
2600
2800
3000
3200
3400
3600
3800
4000
4200
4400